UNIVERSITAT DE BARCELONA

Avances en la Caracterización del Sustrato Arrítmico y Procedimientos de Ablación: Integración de Catéteres de Alta Densidad y Nuevas Aplicaciones de Resonancia Magnética Cardíaca

Sara Vázquez Calvo

Avances en la Caracterización del Sustrato Arrítmico y Procedimientos de Ablación: Integración de Catéteres de Alta Densidad y Nuevas Aplicaciones de Resonancia Magnética Cardíaca

Memoria de tesis doctoral presentada por

Sara Vázquez Calvo

para optar al grado de doctora por la Universitat de Barcelona

Directores de tesis:

Ivo Roca Luque

Jose Maria Tolosana Viu

Tutor:

Ivo Roca Luque

Universitat de Barcelona

Hospital Clinic de Barcelona

Septiembre 2024

AGRADECIMIENTOS

A mi familia, por su apoyo incondicional, por inculcarme los valores que me acompañan y regalarme una forma preciosa de ver el mundo.

A Leire, por la paciencia en estos años de entrega a este trabajo y de tiempo robado, gracias por la compresión y el apoyo.

A Ivo, por su orientación experta, paciencia y apoyo constante, por transmitirme su pasión por la investigación y la electrofisiología.

A Chema, mi guía en la metamorfosis de águila a topo, el consejero fiel.

A mis compañeros de la Sección de Arritmias, por acompañarme en esta etapa de crecimiento profesional y vital, por regalarme tantos buenos momentos de complicidad, por la confianza depositada en mí, por cuidarme en los momentos difíciles y arrancarme sonrisas siempre.

Especialmente gracias a mi pequeña familia de fellows, porque solo en equipo esto puede ser posible.

A mis amigos, por estar siempre ahí.

FINANCIACIÓN

Sara Vázquez Calvo ha recibido financiación a través de:

- Beca Emile Letang del Hospital Clinic de Barcelona

- Beca de Investigación en Centros Nacionales de la Sección del Ritmo de la Sociedad Española de Cardiología (SECARIT-FOR-NAC 22/008)

ÍNDICE

Lista de figuras

ABREVIATURAS

TV = Taquicardia ventricular

DAI = Desfibrilador automático implantable

WPW = Wolf Parkinson White

PPI = *Interval post pacing*

LAVA = *Local abnormal ventricular activity*

ATP = Terapia antitaquicardia

DEEP = Decrement-evoked potential

EGM = Electrogramas

ILAM = *Isochronal late activation mapping*

DZ = Zonas de deceleración

RMC = Resonancia magnética cardíaca

HCM= Miocardiopatía hipertrófica

DCM= Miocardiopatía dilatada

NDLVC= Miocardiopatía no dilatada de ventrículo izquierdo

ARVC= Miocardiopatía arritmogénica de ventrículo derecho

RCM= Miocardiopatía restrictiva

AHA = American Heart Association

ECG = Electrocardiograma

FEVI = Fracción de eyección del ventrículo izquierdo

RF = Radiofrecuencia

VPP = Valor predictivo positivo

VPN = Valor predictivo negativo

NIPS = Estimulación programada no invasiva

LGE = Late gadolinium-enhanced

ENUMERACIÓN DE LOS ARTÍCULOS DE LA TESIS

Tesis en formato de compendio de publicaciones. La tesis consta de 6 objetivos y 6 artículos:

Artículo 1

Orthogonal high-density mapping with ventricular tachycardia isthmus analysis vs. pure substrate ventricular tachycardia ablation: A case-control study

Vázquez-Calvo, S., Garre, P., Sanchez-Somonte, P., Borras, R., Quinto, L., Caixal, G., Pujol-Lopez, M., Althoff, T., Guasch, E., Arbelo, E., Tolosana, J. M., Brugada, J., Mont, L., & Roca-Luque, I.

Front Cardiovasc Med. 2022 Aug 1;9:912335. doi: 10.3389/fcvm.2022.912335. PMID: 35979023.

Impact Factor 3.6. Quartile Q1

Artículo 2

Personalized voltage maps guided by cardiac magnetic resonance in the era of high-density mapping

Vázquez-Calvo, S., Garre, P., Ferró, E., Sánchez-Somonte, P., Guichard, J. B., Falzone, P. V., Guasch, E., Porta-Sánchez, A., Tolosana, J. M., Borras, R., Arbelo, E., Ortiz-Pérez, J. T., Prats, S., Perea, R. J., Brugada, J., Mont, L., Roca-Luque, I.

Heart Rhythm. 2024 Apr 25:S1547-5271(24)02501-3, doi: 10.1016/j.hrthm.2024.04.074. PMID: 38670249.

Impact Factor 5.6. Quartile Q1

Artículo 3

Evolution of Deceleration Zones During Ventricular Tachycardia Ablation and Relation With Cardiac Magnetic Resonance

Vázquez-Calvo S, Casanovas JM, Garre P, Ferró E, Sánchez-Somonte P, Quinto L, Guasch E, Porta-Sanchez A, Tolosana JM, Borras R, Arbelo E, Ortiz-Pérez JT, Brugada J, Mont L, Roca-Luque I.

JACC Clin Electrophysiol. 2023 Jun;9(6):779-789. doi: 10.1016/j.jacep.2022.12.015. Epub 2023 Feb 22. PMID: 37380313.

Impact Factor 8. Quartile Q1

Artículo 4

Noninvasive Detection of Slow Conduction with Cardiac Magnetic Resonance Imaging for VT Ablation.

Vázquez-Calvo S, Mas Casanovas J, Garre P, Sánchez-Somonte P, Falzone PV, Uribe L, Guasch E, Tolosana JM, Borras R, Figueras I Ventura RM, Arbelo E, Ortiz-Pérez JT, Prats S, Perea RJ, Brugada J, Mont L, Porta-Sanchez A, Roca-Luque I.

Europace. 2024 Jan 23:euae025. doi: 10.1093/europace/euae025. PMID: 38262674.

Impact Factor 7.9. Quartile Q1

Artículo 5

Cardiac magnetic resonance to evaluate 3D ventricular substrate depth: Prognostic implications for VT ablation approach.

Vázquez-Calvo S, Frida Eulogio-Valenzuela, Pasquale Valerio Falzone, Paz Garre, Till Althoff, Eduard Guasch**.** José María Tolosana, Roger Borras, Elena Arbelo, José T. Ortiz-Pérez, Susana Prats, Rosario J. Perea, Josep Brugada, Lluís Mont, Andreu Porta-Sanchez and Ivo Roca-Luque.

Submitted

Artículo 6

Post-Ablation cardiac Magnetic resonance to assess Ventricular Tachycardia recurrence (PAM-VT study)

Roca-Luque I, **Vázquez-Calvo S**, Garre P, Ortiz-Perez JT, Prat-Gonzalez S, Sanchez-Somonte P, Ferro E, Quinto L, Alarcón F, Althoff T, Perea RJ, Figueras I Ventura RM, Guasch E, Tolosana JM, Lorenzatti D, Morr-Verenzuela CI, Porta-Sanchez A, Arbelo E, Sitges M, Brugada J, Mont L.

Eur Heart J Cardiovasc Imaging. 2024 Jan 29;25(2):188-198. doi: 10.1093/ehjci/jead261. 2023 Nov 21; PMID: 37819047.

Impact Factor 6.7. Quartile Q1

1. INTRODUCCIÓN

1.1. Arritmias ventriculares en pacientes con cardiopatía estructural

La muerte súbita es una causa de mortalidad muy relevante con una incidencia aproximada en España de 30.000 personas al año(1). Un 80% de ellas pueden atribuirse a arritmias ventriculares en pacientes con cardiopatía por lo que la correcta identificación de la población en riesgo es fundamental. En este sentido, el implante de desfibriladores, capaces de disminuir de forma drástica la muerte súbita arrítmica, ha supuesto un cambio de paradigma. El primer implante en un paciente se llevó a cabo en 1980 y desde entonces ha demostrado aumentar la supervivencia de pacientes seleccionados(2), por lo que el número de dispositivos implantados ha ido aumentando progresivamente, con más de 7500 implantes al año en nuestro país en 2022(3). Sin embargo, los desfibriladores no evitan la aparición de las arritmias, siendo éstas una causa de morbimortalidad muy importante, por lo que son necesarias estrategias complementarias. El tratamiento farmacológico con antiarrítmicos ha demostrado moderada eficacia en la prevención de arritmias ventriculares, pero sin lograr tener un impacto sobre la mortalidad, en gran parte debido a los efectos adversos. Algunos de los antiarrítmicos más habituales, como la flecainida(4), no pueden ser usados en pacientes con cardiopatía estructural por alto riesgo proarrítmico. Otros, como la amiodarona(5), son responsables de importantes efectos adversos, como alteraciones del tiroides, fibrosis pulmonar, depósitos corneales, prolongación del QT, etc. no siendo habitualmente tolerado a medio-largo plazo. El sotalol(6), otro de los antiarrítmicos más empleados, se suma a la lista de fármacos que potencialmente pueden alargar el QT, aumentando el riesgo de *Torsaide de Pointes*, lo que limita su uso. Como alternativa terapéutica en casos refractarios o donde la medicación antiarrítmica no era tolerada, nació la ablación por catéter. La evolución de esta técnica en las últimas décadas la ha llevado a ser considerada el tratamiento actual de elección para pacientes con taquicardias ventriculares (TVs) y cardiopatía estructural. Dos estudios principales respaldan actualmente la ablación por encima del tratamiento médico.

Por un lado, en 2016 se publicó el estudio multicéntrico VANISH(7) en el que se aleatorizaron a 259 pacientes que ya estaban bajo tratamiento antiarrítmico a ablación o a escalada terapéutica (aumentando la dosis de amiodarona o agregando mexiletina si la dosis ya era al menos de 300 mg al día). Tras un seguimiento de 27.9±17.1 meses, se observó una tasa significativamente más baja del endpoint primario compuesto de muerte, tormenta arrítmica o descarga apropiada en aquellos pacientes sometidos a ablación por catéter. Por otro lado, recientemente, en 2022, se publicó el estudio Survive VT(8), en el que 144 pacientes con cardiopatía isquémica fueron asignados aleatoriamente a ablación de sustrato endocárdico o terapia farmacológica antiarrítmica con un seguimiento de 24 meses. La ablación por catéter redujo el *endpoint* final compuesto por muerte cardiovascular, descarga apropiada del DAI, hospitalización por insuficiencia cardíaca o complicaciones graves relacionadas con el tratamiento en comparación con los fármacos antiarrítmicos (28.2% de los pacientes en el grupo de ablación vs. 46.6% de los del grupo de antiarrítmicos ([HR]: 0.52; IC del 95%: 0.30-0.90; P = 0.021).

Para obtener estos resultados la ablación por catéter ha evolucionado notablemente en las últimas décadas. A continuación, se realizará un breve resumen de la evolución de la ablación se hasta ser el tratamiento de elección de los pacientes con TVs y cardiopatía estructural, destacando los retos superados y los desafíos que aún debemos abordar.

1.2. Ablación de TV: los primeros avances

La ablación de TV mediante el uso de un catéter nació en la década de 1950 tras la observación de que pacientes con cardiopatía isquémica crónica y múltiples episodios de TVs quedaban libres de arritmias tras someterse a intervenciones quirúrgicas en las que se eliminaba el aneurisma secundario al infarto(9,10). En la década de los 70 se empezaron a realizar los primeros mapas

origen de la misma en la zona del borde de los aneurismas y se propuso la eliminación del endocardio a dicho nivel como una terapia más eficaz que la eliminación del aneurisma(11). Tras estos hallazgos, y con el auge global de la ablación por catéter en la década de los 80, especialmente aplicada a pacientes con Wolf-Parkinson-White (WPW) (12,13), el siguiente paso resultó obvio y, en la década de los 90, los pacientes con TVs refractarias ya no se trataban quirúrgicamente si no en el laboratorio de electrofisiología(14).

1.3. Entendiendo el origen y mantenimiento de las TV: la reentrada

En la década de los 70, con el inicio del mapeo de las TVs, se establecieron las bases para entender el mecanismo por el que se iniciaban y mantenían las mismas. Cabe destacar que en ese momento ya se habían definido los dos mecanismos más frecuentes de inicio de taquicardias: la actividad focal o *trigger* y la *reentrada*. Varios estudios demostraron que era posible inducir TV y terminarla mediante estimulación programada(15–17) lo que sugería ***la reentrada*** como principal mecanismo. Esta misma técnica de estimulación programada había sido usada con éxito para inducir y detener taquicardias supraventriculares en pacientes con WPW(18) en los que se sabía que existía un circuito de reentrada que utilizaba una vía accesoria y el propio nodo aurículo-ventricular. Tal y como fue estudiado en modelos animales(19), para que una taquicardia por reentrada ocurriese son necesarios cuatro elementos (Fig 1):

1. Bloqueo unidireccional.

2. Conducción por un circuito alternativo.

3. Retraso en la activación del tejido distal a la zona de bloqueo.

4. Reactivación del tejido proximal al sitio de bloqueo.

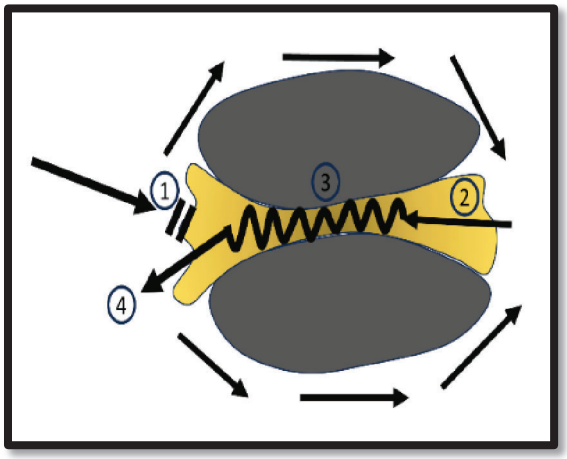

Fig 1**: Imagen ilustrativa de los elementos responsables de la reentrada (imagen propia).**

Para que la reentrada pudiera ocurrir se necesitaba por tanto alguna estructura con propiedades eléctricas diferentes o variables, hipotetizándose inicialmente que éstas podrían ser las fibras de Purkinje, las ramas izquierdas y derechas del Haz de His o las áreas fibróticas del tejido ventricular(15), donde se había demostrado que las velocidades de conducción disminuían notablemente(20). Distintas estrategias ayudaron a probar el mecanismo de reentrada como causa de la mayoría de las TVs en pacientes con cardiopatía estructural. El análisis de las señales eléctricas locales reveló la información más relevante. En varios estudios en modelos animales se observaron en ritmo sinusal señales muy fragmentadas y de larga duración en las zonas de cicatriz(21). En este mismo sentido, Josephson et al.(22) registró en humanos esta actividad continúa en el circuito arrítmico, cubriendo todo el ciclo de la taquicardia, lo que confirmaba su naturaleza reentrante. Además, demostró correlación con las señales fragmentadas y tardías que se observaban en ritmo sinusal, de forma que, cuando éstas se bloqueaban durante TV, la taquicardia cesaba.

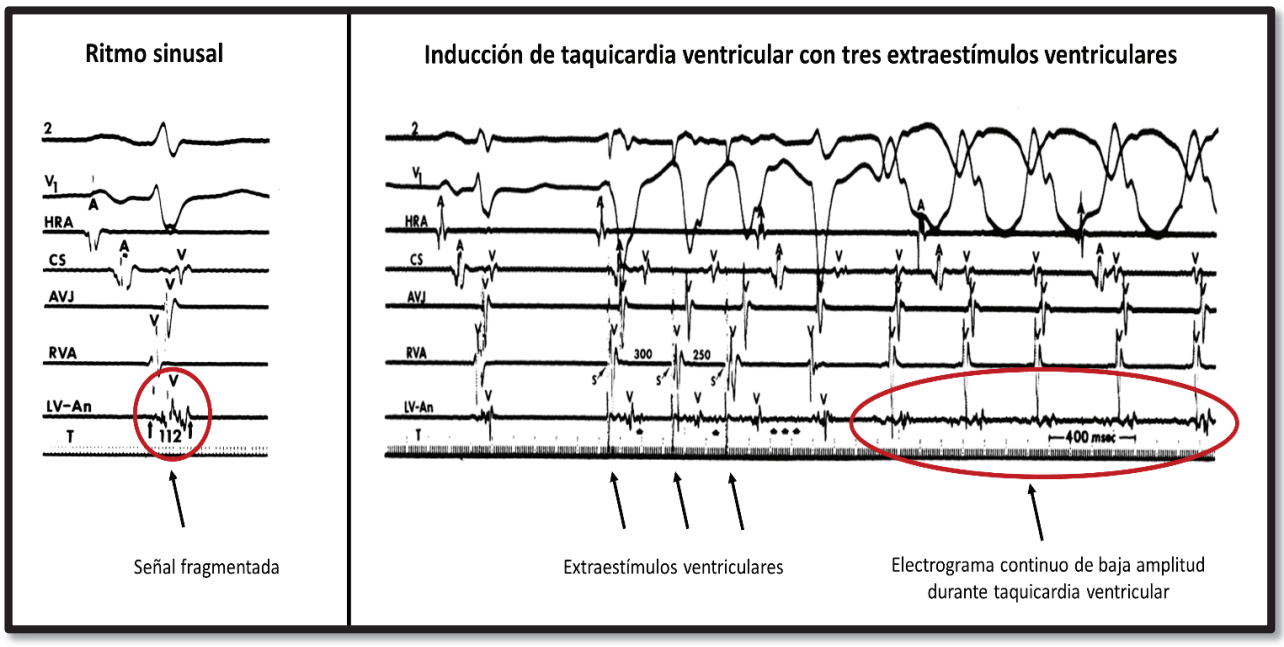

Fig. 2. **Electrogramas durante ritmo sinusal y taquicardia ventricular**. Imagen en la que se observa un potencial local fragmentado en ritmo sinusal en el borde del aneurisma. Al aplicar tres extraestímulos ventriculares sobre ritmo sinusal se induce una taquicardia ventricular observándose una señal local continua de muy baja amplitud que cubre prácticamente todo el ciclo de la taquicardia. Imagen modificada de Josephson et al. (15).

Por otro lado, múltiples estudios posteriores ayudaron a descartar el Haz de His, sus ramas y el sistema de Purkinje como responsables principales del circuito reentrante tras observar que extraestímulos supraventriculares, incluso consiguiendo despolarizar los ventrículos con un QRS igual al sinusal, no modificaban el ciclo de la taquicardia, lo que claramente sugería que el sistema de conducción no estaba implicado en el circuito y que éste debía de estar protegido en alguna zona relativamente pequeña en el miocárdico(23–26). Estos estudios pusieron el foco en la cicatriz como protagonista de estas arritmias, más concretamente, en una zona de cicatriz menos densa que presentaba miocitos viables y que parecía tener unas propiedades eléctricas específicas, llamada *border zone*. Modelos animales en la década de los 80 y 90 señalaron que el *border zone* presentaba un acoplamiento anormal de la unión entre las células, lo que generaba una conducción eléctrica lenta y no uniforme, viéndose estas áreas fuertemente relacionadas con el itsmo de las TVs(24–26). Estudios histológicos en pacientes confirmaron la correlación entre las señales patológicas obtenidas en procedimientos de ablación con la presencia de haces de miocitos viables (*border zone*) dentro o alrededor de la cicatriz densa lo que confirmó al concepto de circuito arrítmico con base anatómica en la cicatriz(27–29).

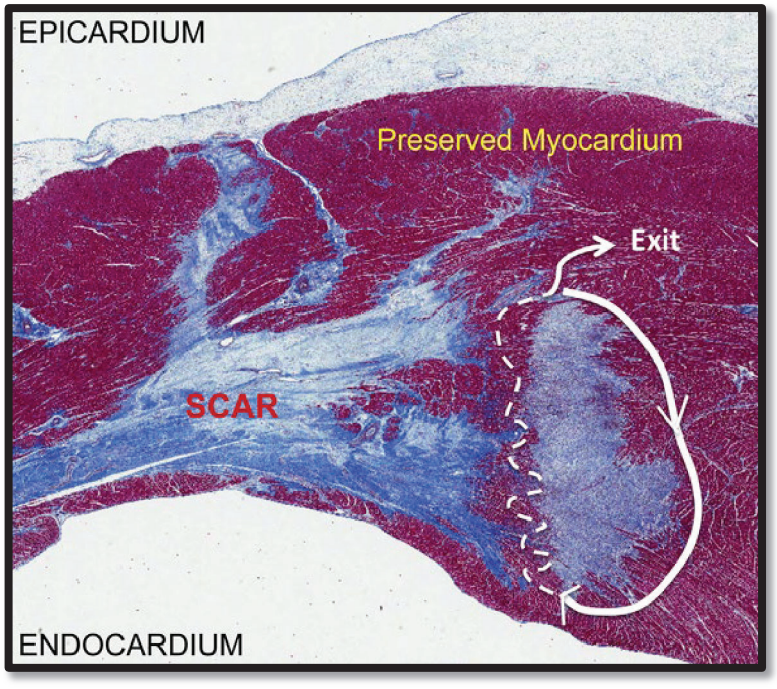

Fig. 3. **Bases anatómicas de la reentrada.** Imagen en la que se observa una muestra histológica teñida con tricrómico de Masson (miocardio sano en rojo, cicatriz en azul). Se aprecia dentro de la cicatriz un área con islotes de células miocárdicas viables (*border zone*) potencialmente responsables del circuito arrítmico. Este se dibuja en línea blanca discontinua en forma de zigzag para reproducir el enlentecimiento del frente de acción en dicha área. Imagen modificada de Ajijola et al.(29)

1.4. Mapa de activación de TV y encarrilamiento: el esbozo del circuito

Para identificar la localización de la TV durante los procedimientos de ablación en la década de los 90 era necesario inducir la TV mediante un protocolo de estimulación y realizar un mapa de activación de la misma. En aquellos pacientes en los que la TV era tolerada hemodinámicamente empezaron a realizarse los primeros estudios para entender la complejidad de los circuitos arrítmicos(30).

Para ello, durante taquicardia, se fijaba una referencia, habitualmente al inicio del QRS y se anotaba la precocidad de la señal local en diferentes localizaciones ventriculares con respecto a dicha referencia, de forma que las señales registradas justo antes del QRS se correspondían a la salida del canal arrítmico y las que estaban justo después del QRS se correspondían a la entrada del mismo, encontrándose las medio-diastólicas localizadas en el centro del circuito.

Sin embargo, algunas de estas señales aparecían en lugares que finalmente no constituían zonas críticas del circuito, por lo que el concepto de zonas de activación pasivas o *bystanders* cobró importancia. Para distinguir estas zonas era necesario realizar maniobras de **encarrilamiento**, consistentes en estimular el corazón de forma programada durante taquicardia, con un ciclo ligeramente menor al ciclo de la misma (habitualmente 30ms menos) para intentar "encarrilarla", es decir, intentar entrar dentro del circuito de la arritmia y observar su comportamiento. Diferentes parámetros, como la morfología del QRS obtenido al estimular, la distancia entre la espícula y el QRS, la duración desde el último latido estimulado hasta el siguiente latido postestimulación, etc. fueron descritos y extensamente empleados para entender el circuito de TV. En concreto, la ausencia de cambio de morfología del QRS al estimular se conoce como fusión oculta e implica que nos encontramos dentro del circuito arrítmico. Por contra, el cambio en la morfología del complejo capturado respecto al de la TV se conoce como fusión manifiesta e indica que estamos situados fuera del mismo. El *intervalo post-pacing* (PPI) desde el último latido estimulado hasta el siguiente latido de la TV nos aporta una información complementaria. Si estamos en una zona crítica del circuito, el tiempo que tardará el estímulo en volver a salir por el

mismo será corto (menos de 30ms añadido al ciclo de la TV) mientras que si estamos en un *bystander* (dentro del circuito pero en una parte no crítica) será largo.

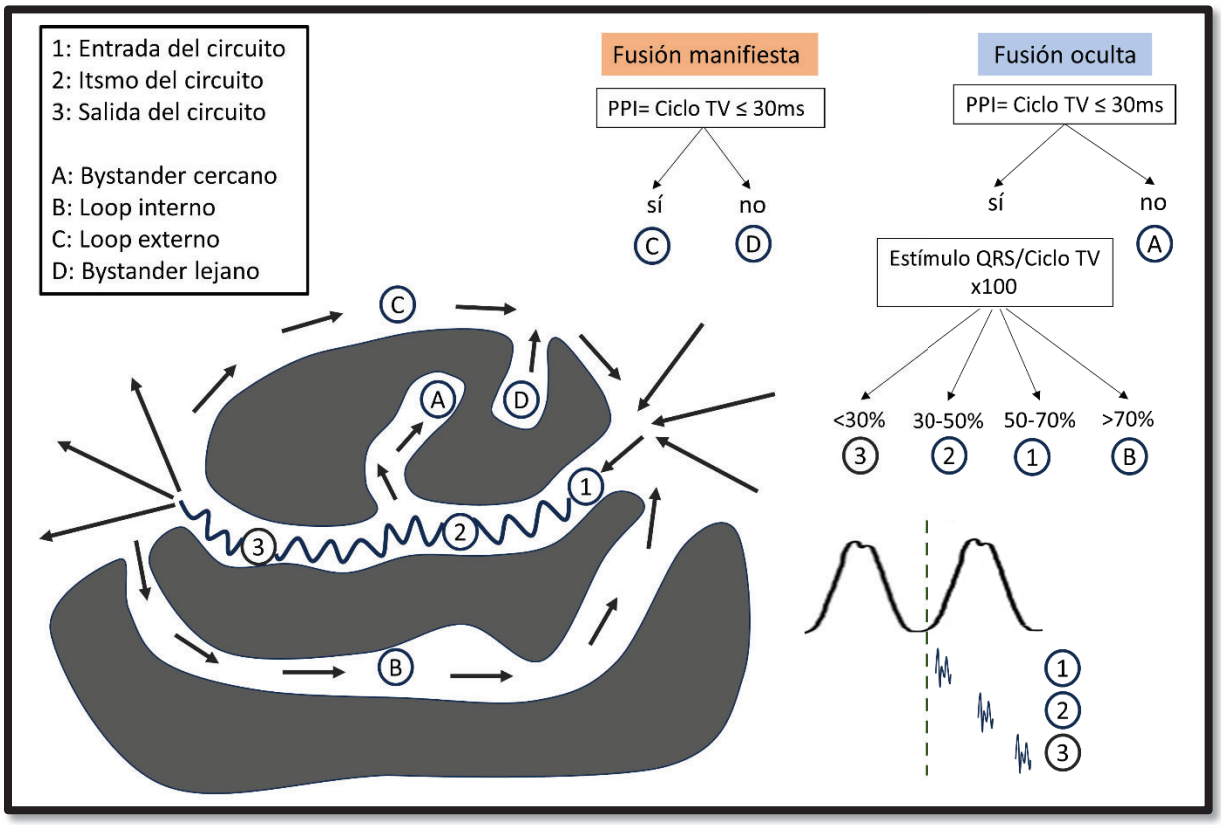

Fig. 4. **Descripción de circuito arrítmico y respuesta al encarrilamiento**. Se observa en gris tejido cicatricial y mediante flechas la dirección del frente de activación, que se enlentece en el canal arrítmico que atraviesa la cicatriz densa. Se señalizan con números y letras las distintas partes del circuito, así como su respuesta al encarrilamiento. Imagen modificada de Stevenson et al. (30).

Esto supuso un avance importantísimo para la comprensión del circuito y para el éxito de los procedimientos, pero presentaba importantes limitaciones. Principalmente, realizar un mapa de TV en taquicardia con encarrilamientos en distintas localizaciones requería que el paciente tolerase hemodinámicamente la misma durante un importante período de tiempo, lo cual era infrecuente(31). Segundo, solo se eliminaba la taquicardia inducida en el procedimiento, dejando

zonas de cicatriz que quizás pudieran ser responsables de nuevas arritmias en el futuro; y tercero, no se tenía en cuenta la tridimensionalidad del sustrato, por lo que circuitos epicárdicos o intramurales podían no ser detectados correctamente mediante encarrilamiento.

El otro mecanismo usado en esta época para localizar el circuito arrítmico era el ***pace-mapping o topoestimulación***, que consistía en intentar simular la morfología de la TV al estimular con el catéter el miocardio sobre ritmo sinusal, consiguiendo una concordancia mayor a medida que nos acercamos a la salida del circuito de reentrada(32). Las ventajas de esta técnica eran que permitía acotar la zona responsable de la taquicardia en paciente en los que la inducción de TV sostenida no era posible, bien por baja inducibilidad o por ausencia de tolerancia clínica.

Pese a la aparición de estas nuevas maniobras que permitían delimitar mejor el circuito arrítmico, la mayor parte de los procedimientos no eran efectivos. La eliminación de la TV clínica durante el procedimiento solo se lograba en un 50-65% de los casos, incluso en centros experimentados. Por otro lado, la tasa de recurrencia era muy alta, cercana al 30-40% solo un mes después de la ablación(33).

Eran necesarios, por tanto, nuevos abordajes que nos ayudasen a entender mejor, y a eliminar con mayor éxito, los circuitos arrítmicos.

1.5. Mapa de sustrato: una alternativa al mapa de activación

Debido a las dificultades para realizar mapas durante TV, principalmente debido a la mala tolerancia clínica, cobró mucha importancia identificar el circuito arrítmico y sus zonas críticas en ritmo basal del paciente, es decir, sin necesidad de inducir y mapear la taquicardia. Cassidi et al.(34,35) en la década de los 80 describieron realizando mapas en ritmo sinusal, las diferencias de los electrogramas (EGMs) en cuanto a amplitud de voltaje, duración y características de la señal entre sujetos sanos y pacientes con infarto crónico, encontrando importantes diferencias y sembrando las bases para establecer umbrales de voltaje que permitiesen diferenciar los tejidos. De esta forma, se establecieron amplitudes de voltaje de 0.5 y 1.5mV para identificar cicatriz

densa y tejido sano respectivamente, siendo considerado tejido intermedio o *border zone* aquel entre 0.5-1.5mV.

Además, las zonas responsables de las TVs tenían características morfológicas diferentes, habitualmente presentando potenciales fraccionados y de mayor duración (potenciales tardíos) o actividad anormal tardía ventricular (Local Abnormal Ventricular Activity, LAVA(34)).

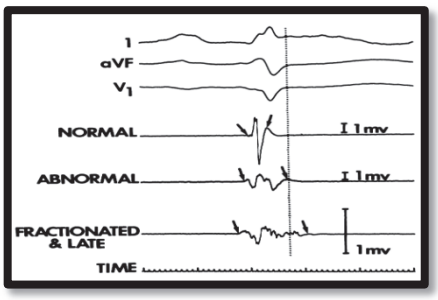

Fig. 5. **Descripción de electrogramas.** Registro y descripción de distintos potenciales obtenidos en distintos puntos del ventrículo izquierdo y clasificados como normales, anormales o fraccionados y tardíos según las características de los electrogramas en cuanto a amplitud y duración. Imagen procedente de Cassidi et al. (34,35)

En este momento, los procedimientos de ablación se realizaban exclusivamente guiados por la información de los electrogramas y la visualización en 2D que se generaba con el uso de fluoroscopia, con las limitaciones que ello conllevaba. En primer lugar, el guiado exclusivamente por fluoroscopia, suponía una cantidad importante de energía ionizante tanto para el paciente como para el operador. En segundo lugar, no era posible visualizar volumétricamente la superficie endocárdica por lo que la única forma de "recordar" zonas de interés era establecer relaciones visuales con estructuras cercanas (electrodo del DAI, costillas, etc). Finalmente, no era posible anotar las zonas en las que se había aplicado radiofrecuencia, lo que contribuía a administrar RF de forma innecesaria en la misma localización o a dejar gaps entre aplicaciones.

El desarrollo de **sistemas de navegación** permitió la representación tridimensional de las zonas que recorría el catéter generando un molde volumétrico de las estructuras cardíacas(36,37). Además, la representación de las características de los electrogramas (especialmente la amplitud) podía ser registrada de forma que el sistema automáticamente representaba de un color el tejido sano (con voltajes por encima de 1.5mv) y en otro el tejido cicatricial (0.5mv). Estos mapas de voltaje demostraron una muy buena correlación con muestras histológicas(38–40). Todo ello supuso un cambio de paradigma.

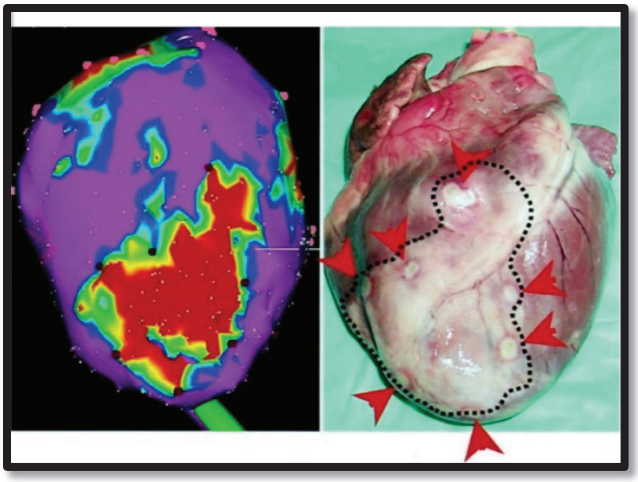

Fig. 6. **Correlación entre mapa de voltaje y muestra anatómica.** A la izquierda mapa de voltaje generado con sistema de navegación en el que se muestra tejido sano en violeta, cicatriz densa en rojo y *border zone* en una gama de colores intermedia (verde, amarillo, azul, etc). A la derecha muestra anatómica animal en la que se muestra la cicatriz rodeada por líneas discontinuas y señala con flechas. Obsérvese la clara correlación entre ambas imágenes. Imagen procedente de Tung et al. (38–40)

A raíz de dichos hallazgos, en la década de los 2000 empezaron a realizarse ablaciones de sustrato guiadas por escopia y sistemas de navegación. Distintas estrategias, que no precisaban la inducción de TV, fueron utilizadas. En este sentido, se desarrollaron métodos basados en las características patológicas de los electrogramas, ya sean potenciales tardíos(41) o LAVAS(42), y otros más basados puramente en voltaje, como la ablación de canales de voltaje(43), el aislamiento de la cicatriz(44) o la homogenización de la misma(45). Varias de estas técnicas demostraron mejores resultados que las ablaciones guiadas exclusivamente por mapa de activación durante la TV(46) en términos de menores tasas de recurrencia en el seguimiento.

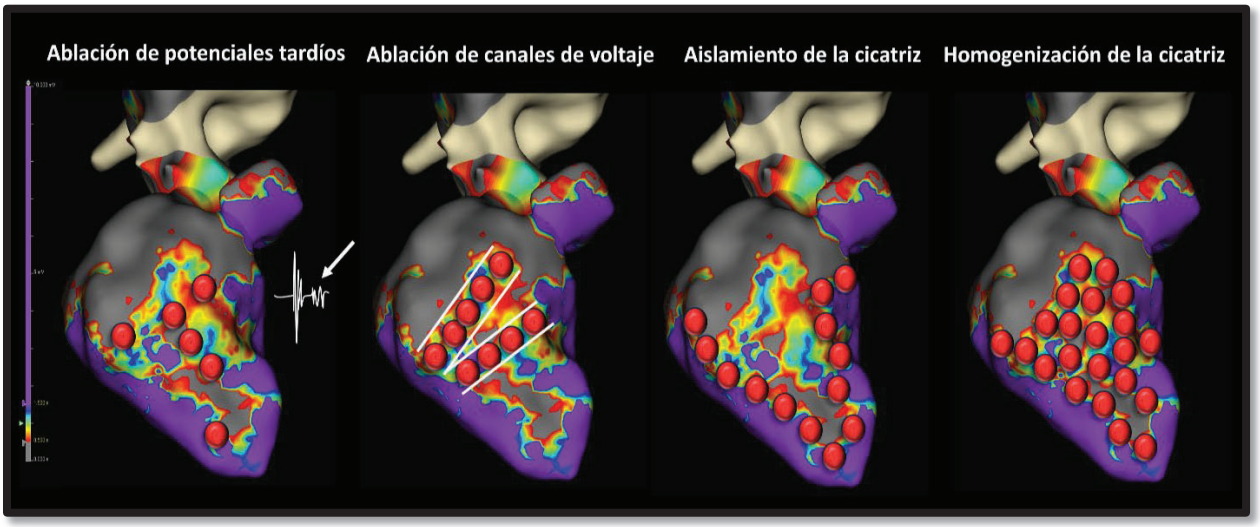

Fig. 7. **Estrategias de ablación por sustrato sobre mapa de voltaje**: ablación exclusiva de aquellos electrogramas que muestras características anormales (tardíos o fragmentados); aislamiento de la cicatriz o homogenización de la misma. Imagen propia.

1.5.1. Limitaciones del mapa de voltaje

La principal limitación del mapa de voltaje reside en que la identificación de la amplitud de las señales intracavitarias depende de muchos factores.

Por un lado, se requiere un **contacto** correcto del catéter con la superficie que se desea mapear. En este sentido, contactos débiles podrían llevar a detecciones de señales falsamente más pequeñas incrementando erróneamente la cantidad de cicatriz en el mapa electroanatómico. Para mejorar esta potencial limitación, los catéteres clásicos bipolares de ablación han incorporado sensor de fuerza consiguiendo una mejor representación del sustrato(47).

Además del contacto, la correcta interpretación de la señal depende de la **configuración del catéter**, o más concretamente, del número de electrodos del catéter, del tamaño de los mismos, de la distancia entre ellos y especialmente de la relación del ángulo del frente de onda respecto a la orientación de cada dipolo(48,49). Teniendo en cuenta que los primeros catéteres eran bipolares, es decir, tenían solo un dipolo, este último aspecto era crucial para una correcta identificación de la señal. En este sentido, el desarrollo de nuevos catéteres con más de un dipolo, llamados *catéteres de alta densidad*, ha constituido un paso importante para mejorar la definición de los mapas de sustrato. Distintos catéteres con diferente número de polos, distancia entre polos y distintas configuraciones de detección han sido desarrollados con el objetivo de la mejor detección de los electrogramas. Estos catéteres han demostrado lograr una mejor definición del sustrato, detectando señales patológicas no visibles con catéteres bipolares y también aumentando la amplitud de algunas señales previamente consideradas como cicatriz densa, pasando a ser identificadas como *border zone* o tejido sano, con las implicaciones consecuentes. El uso de estos catéteres ha sido especialmente importante en las zonas de bajo voltaje, donde se encuentran habitualmente las señales de mayor interés(50,51).

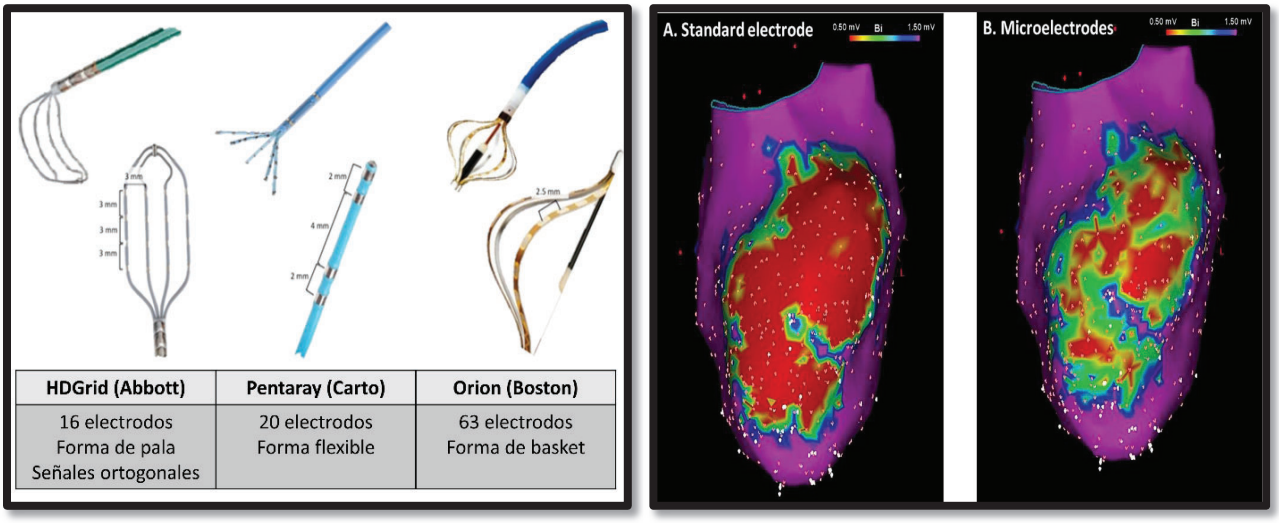

HDGrid (Abbott)	Pentaray (Carto)	Orion (Boston)
16 electrodos Forma de pala Señales ortogonales	20 electrodos Forma flexible	63 electrodos Forma de basket

Fig. 8. **Catéteres de alta densidad**. A la izquierda una representación de los principales catéteres de mapeo de alta densidad comercializados y sus principales características. A la derecha, imagen extraída de Leshem et al.(52) en el que se muestra la mejor definición del sustrato en el mapa generador con múltiples electrodos, en comparación con el generado con electrodo standard donde el tejido intermedio es falsamente identificado como cicatriz densa.

Dentro de este tipo de catéteres hay uno que ha conseguido resolver, al menos parcialmente, el conflicto de la orientación respecto al frente de onda gracias a una configuración en forma de cuadrícula o pala con 4x4 dipolos orientados perpendicularmente unos respecto a otros. De esta forma, si un dipolo recibe la señal en un ángulo de 90º ésta se infradetectará, pero será recibida con un ángulo de 180º en el bipolo perpendicular y por tanto detectándose aquí con su amplitud real(53) (Fig. 9).

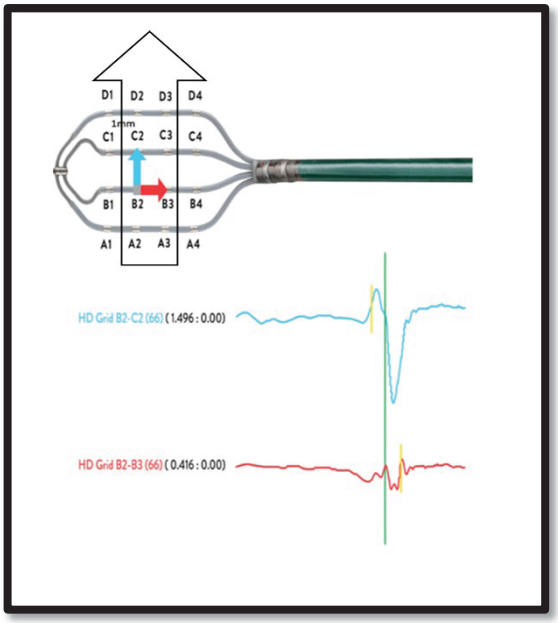

Fig. 9. **Catéter HDGrid**. En esta imagen puede observarse la diferente amplitud de señal según la orientación respecto al frente de onda. Imagen modificada de Papageorgiou et al.(54)

Varios estudios, tanto en modelo animal (55) como en humanos(56,57) han demostrado mejor definición del sustrato con este tipo de orientación de catéter. Es intuitivo pensar que la mejor definición del sustrato permitirá identificar mejor las zonas a ablacionar lo que podría llevar a una menor tasa de recidivas post procedimiento. De hecho, algunos estudios sugieren que el hecho de realizar los mapas electroanatómicos con catéteres de alta densidad podría llevar a mejores resultados clínicos, en concreto los catéteres con capacidad para detectar señales ortogonales podrían asociarse a menos terapia antitaquicardia (ATPs) y shocks en el seguimiento no solo comparado con catéteres bipolares si no con otros catéteres de alta densidad sin capacidad para detectar señales ortogonales(58).

Además, otro de los aspectos que añade complejidad a la anotación de señales es que la señal local (*near-field*) puede hallarse oculta dentro de una señal próxima de mayor voltaje (***far-field***), de forma que, al realizar el mapa de sustrato, el *far-field* nos impida visualizar zonas de interés. Esto es especialmente relevante en los bordes de la cicatriz debido a la proximidad del tejido sano que tiende a albergar señales de mucha más amplitud que pueden ocultar señales patológicas.

Sin embargo, otra de las limitaciones de los mapas de voltaje es la dificultad para establecer **umbrales**. Los clásicamente descritos (0.5-1.5mV) a partir de los cuales se definía el sustrato como sano o enfermo fueron realizados con catéteres bipolares sin sensor de fuerza. Roca-Luque et al.(59) estudiaron la influencia del sensor de fuerza en el cambio de los umbrales bipolares para identificar cicatriz, *border zone* y electrogramas patológicos observando una gran variabilidad individual: entre 0,02 y 2 mV (mediana 0.32 mV) para el umbral de cicatriz densa y de 0,3 a 6 mV (mediana 1,84 mV) para *border zone*. Por otro lado, dado que los catéteres de alta densidad permiten una mejor identificación del sustrato, "convirtiendo" en tejido sano o *border zone* zonas que aparentemente eran cicatriz densa, es lógico pensar que los umbrales con catéteres de alta densidad puedan ser diferentes a los establecidos para catéteres bipolares. Quizás en parte por ello varios estudios muestran que los canales de voltaje (*border zone* rodeado de cicatriz y conectado con tejido sano) presentan una baja especificidad (30%) respecto a los circuitos de TV (analizados con mapa de activación y encarrilamiento))(60). En el mismo sentido, los trabajos que han comparado el sustrato mediante cortes histológicos con mapas de voltaje

electroanatómicos han demostrado la ausencia de unos umbrales fijos que puedan aplicarse a pacientes con cardiopatía estructural(61) por lo que muchos autores han decido ajustar manualmente los umbrales(62,63) de forma individual aumentando con frecuencia el número de canales de voltaje (falsamente) detectados.

Por último, existen dudas razonables sobre si el sustrato que identificamos en un momento determinado representa realmente el total del sustrato arritmogénico o si, por la contra, existe un **sustrato latente** potencialmente responsable de eventos arrítmicos que no puede ser visualizado atendiendo de forma exclusiva a las señales electroanatómicas. Esto puede deberse bien a que éstas no presentan propiedades de conducción lenta en condiciones basales o porque estos potenciales tardíos están escondidos bajo las señales de alta amplitud del miocardio circundante (*far-field*). Con la idea de desenmascarar el sustrato arrítmico nace el concepto del análisis funcional del sustrato

1.6. Sustrato funcional: entendiendo el comportamiento de los canales arrítmicos

Se consideran mapeo de sustrato funcional a un grupo de estrategias de mapeo que no atienden exclusivamente a la amplitud de los electrogramas (voltaje) ni a las características morfológicas de las señales en situación basal, si no a cómo éstos responden a diferentes ciclos de estimulación o bien a sus patrones de activación eléctrica respecto a los electrogramas circundantes.

El sustrato funcional pretende enfatizar los condicionantes necesarios, además de un sustrato anatómico que ya es ampliamente conocido (*border zone* rodeado de cicatriz densa que comunica con tejido sano), para que se inicie una TV mediada por reentrada. En este sentido, múltiples estudios(64,65) han descrito que el mecanismo de inicio y mantenimiento de la TV se basa en un enlentecimiento de potenciales patológicos tras extraestímulos hasta que se produce un bloqueo unidireccional para posteriormente generarse una activación en sentido contrario (Fig. 10). Esto concuerda con el hecho de que las TVs clínicas parecen ser iniciadas en gran medida

por extrasístoles ventriculares(66,67) y con que la estimulación programada pueda inducir TV(15–17).

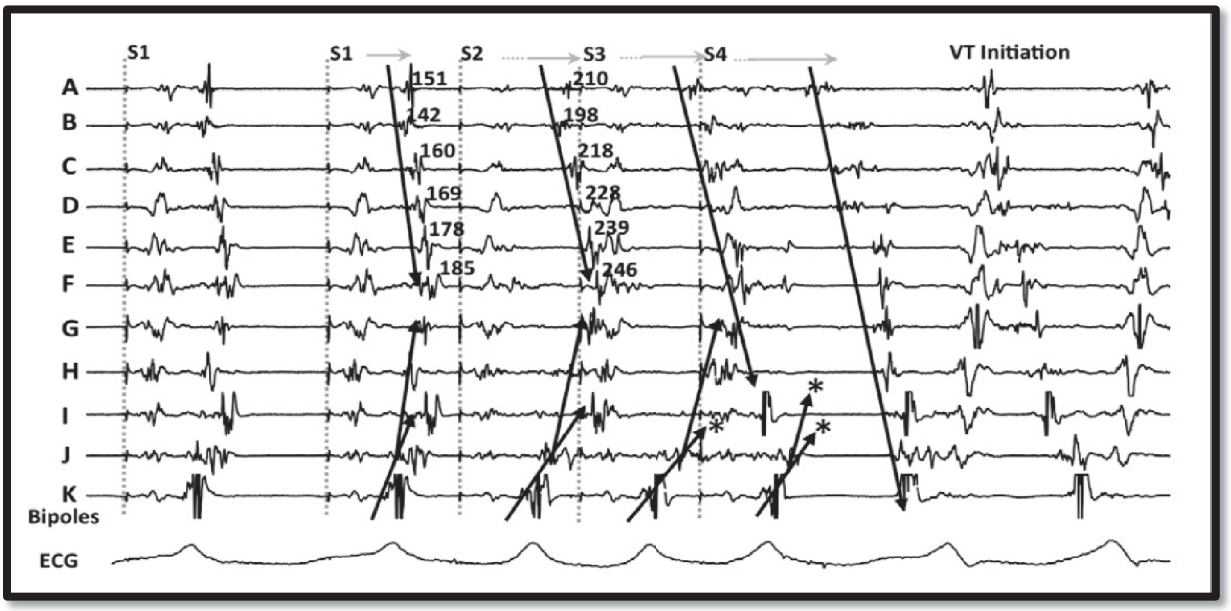

Fig. 10. **Inducción de TV tras decremento y bloqueo**. Imagen ejemplificando cómo aquellos electrogramas con capacidad de decremento y bloqueo inician el mecanismo de reentrada. Se observa la conducción decremental al estimular con intervalos de acoplamiento más cortos (S2) hasta producirse el bloqueo del electrograma I con S3 (mostrado en la figura con asterisco) para posteriormente con S4 iniciarse la TV tras el bloqueo de la salida del circuito. Imagen procedente de Jackson et al. (68)

Basado en este concepto, Jackson et al.(68) definió unos nuevos electrogramas con capacidad decremental que parecían identificar mejor el istmo de la TV que los potenciales tardíos sin conducción decremental. Estos electrogramas, llamados ***DEEP (DEcremental Evoked Potentials)***, incluían aquellos potenciales tardíos que se retrasaban más de 10 milisegundos después de un extraestímulo con acoplamiento fijo a 20ms por encima del período refractario ventricular sobre un ciclo de estimulación fijo a 600ms. De forma interesante, los potenciales que más decrementaban dentro de los DEEP (con una media de decremento de 27±13 ms) mostraban una especificidad del 95±1% (p=0.031) para el istmo de la TV, que seguía siendo ligeramente más alta que la encontrada para los potenciales tardíos situados dentro de la cicatriz (91.9%, p=0.1). Estos

resultados fueron confirmados en el ámbito clínico por Porta-Sanchez et al.(69) con 20 pacientes consecutivos con miocardiopatía isquémica en un estudio multicéntrico.

Uno de los inconvenientes de esta técnica en sus descripciones iniciales es que los extraestímulos para valorar conducción decremental solo se administraban en zonas ya identificadas como potenciales tardíos, por lo que si estos se encontraban dentro del *far-field* no eran visualizados. Acosta et al.(70) diseñó un estudio en el que administraban dos extraestímulos (+60ms y +40 o 20ms sobre el período refractario ventricular) en aquellos EGMs no patológicos que se encontraban dentro de la cicatriz o a su alrededor. Aquellos potenciales que se fraccionaban y se separaban del *far-field* eran definidos como ***electrogramas con conducción lenta oculta***, siendo identificados en un 56.7% de los pacientes, especialmente en aquellos con cicatrices pequeñas, hallazgos confirmados por estudios similares(71). Probablemente sea en las cicatrices pequeñas donde el tejido sano circundante esconda con mayor frecuencia las señales patológicas dada la proximidad de la cicatriz con el tejido sano en contraposición a cicatrices grandes. Es por ello que, basado en estos estudios, especialmente en pacientes con cicatrices pequeñas, realizar un protocolo de extraestímulos en la totalidad de la cicatriz y tejido circundante podría ayudar a desenmascarar sustrato arrítmico responsable de los circuitos críticos de la taquicardia.

En este sentido, de nuevo, la principal limitación de estos estudios era que dependían de la administración manual de los extraestímulos en las localizaciones que el operador eligiese, excluyendo zonas aparentemente sanas del protocolo de extraestímulos. No fue hasta el año 2020, con la publicación del Barts Sense Protocol(72), donde se realizó el primer **mapa automático de extraestímulos** en todo el ventrículo. En este trabajo, se compararon mapas en ritmo sinusal con mapas obtenidos automáticamente después de un extraestímulo desde ápex de ventrículo derecho, encontrando mayor área de potenciales tardíos en el mapa obtenido con extraestímulo (19.3 mm2 vs. 6.4 mm2, respectivamente, p=0.001). Este estudio ha abierto la puerta a nuevos protocolos de mapeo automático con extraestímulos, actualmente en desarrollo.

Además de los métodos descritos que consisten en desenmascarar potenciales tardíos no presentes (o al menos, no aparentemente presentes en el mapa de voltaje standard) o de

demostrar su condición decremental, el sustrato funcional también incluye un método que, desde su descripción en 2015(73), ha ganado adeptos en todo el mundo, sustituyendo en muchos casos a los mapas de voltaje. Se trata de **los mapas de isócronas de activación tardía** (ILAM). Estos mapas se basan en analizar la duración del potencial local respecto a los potenciales circundantes para identificar zonas de conducción lenta. Para ello, se anota automáticamente el final de cada electrograma y se crea una ventana con la duración del potencial más retrasado del total de la activación ventricular. Esta ventana se divide en ocho franjas simétricas de tiempo y se le otorga un color a cada franja. Aquellas zonas donde la actividad eléctrica se enlentezca presentarán varios colores en poca distancia, definiéndose una zona de deceleración (DZ) o enlentecimiento aquella con tres isócronas (tres colores) en menos de 1cm2.

Este método tiene grandes ventajas, la primera es que es completamente automático gracias al algoritmo Last Deflection (Abbott) o Late activation mapping (Biosense) consistentes en la anotación del último componente de la señal detectada. Además, puede hacerse de forma manual en cualquiera de los navegadores disponibles La segunda ventaja es que es fácilmente interpretable gracias a la representación gráfica en forma de isocronas de colores; y la tercera y más importante es que las DZs han demostrado una correlación del 95% con los istmos de la TV(74), lo que constituye el porcentaje más alto descrito hasta la fecha (en comparación con canales de voltaje, potenciales tardíos, *DEEPs*, etc)(68).

En cuanto a la estrategia de ablación utilizada, en el estudio pivotal de este método(74), dado que la media de DZs por paciente fue de 2±1, la DZ con señales más patológicos era elegida como DZ principal y ablacionada inicialmente. Solo si el paciente permanecía inducible después de ello se procedía a eliminar el resto de DZs. La tasa de recurrencia a los 12±10 meses post ablación fue del 30% (20% en pacientes con cardiopatía isquémica y 37% en pacientes con cardiopatía no isquémica). Un dato a destacar de dicho estudio es que, la tasa de recurrencia fue menor en aquellos pacientes en los que se realizó un segundo mapa (o *remap*) después de la primera ablación (24% vs. 47%; p=0,01). Este hecho abre la puerta a pensar que el sustrato no es estático y que puede variar después del primer set de lesiones de ablación. No solo eso si no que la eliminación de ese nuevo sustrato desenmascarado tiene relevancia clínica.

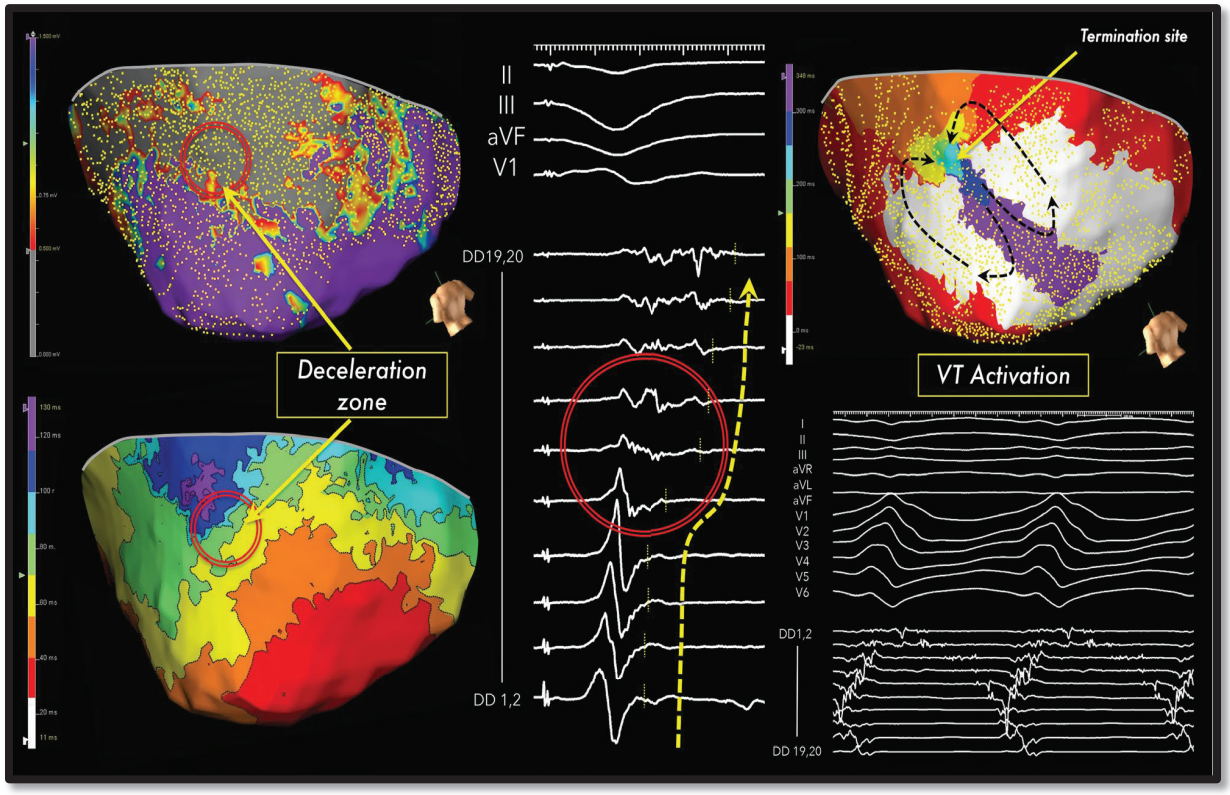

Fig. 11. **Mapa de isócronas: correlación entre DZ y TV.** Se observa a la izquierda el mapa de voltaje mostrando en gris cicatriz densa, en violeta tejido sano y en gana de colores intermedios (rojo, amarillo, verde, azul) *border zone*. En la parte inferior a la izquierda de la imagen se observa un mapa de isócronas con una zona en círculo con hasta cinco isócronas, lo que indica una zona de deceleración. A la derecha de la imagen un mapa extenso de activación de TV en la que se observa el circuito de la misma. Obsérvese la correlación entre el istmo de la TV y la zona de deceleración. Imagen procedente de Aziz et al. (74)

1.7. Resonancia magnética cardíaca (RMC): definición del sustrato y valor diagnóstico

Estudios realizados en la década de los 80-90(75,76) han sido fundamentales para ampliar nuestro conocimiento del sustrato arrítmico mediante pruebas no invasivas o mínimamente invasivas, como es la resonancia magnética. Esto se debe en gran parte a las secuencias de viabilidad que se obtienen tras la inyección de gadolinio. Este agente de contraste tiene la

capacidad de difundir libremente al intersticio, no consiguiendo penetrar a través de las membranas celulares, lo que conlleva a que se acumule en el tejido extracelular. El gadolinio se visualiza durante más tiempo en los tejidos cicatriciales debido a varios motivos. En primer lugar, la fibrosis produce una expansión del espacio extracelular que favorece su acumulación. Por otro lado, la fibrosis genera una disminución de la capilaridad de las zonas afectadas que impide su rápido lavado, promoviendo a su vez el retraso en su desaparición(77). El gadolinio reduce el tiempo de relajación en T1 del tejido adyacente, generando un aumento de la intensidad de la señal en las secuencias de RMC ponderadas en T1. De esta forma, el tejido cicatricial puede visualizarse en RMC con mayor intensidad (blanco) y el tejido sano con menor intensidad (negro), siendo la zona de *border zone* visualizada en una escala de grises(78). Para obtener imágenes de alta calidad, el tiempo entre la inyección de gadolinio y la toma de imágenes es fundamental. Existe un consenso general para utilizar unos tiempos alrededor de 7 a 15 minutos para conseguir un buen contraste en el ventrículo, es decir, conseguir que el tejido sano se visualice negro y el tejido cicatricial, blanco. Este tiempo de retraso hasta la adquisición de las imágenes debe ajustarse paciente a paciente según su función cardíaca, función renal, etc.(78). Es importante señalar que esta visualización diferencial de los tejidos puede excepcionalmente no cumplirse. Esto ocurre, por ejemplo, cuando existe obstrucción microvascular que impide la entrada de gadolinio generando, incluso dentro de cicatrices densas, una falsa imagen de tejido sano rodeado de tejido cicatricial que se ha llamado *dark core*(79).

Gracias al desarrollo de la RMC ha sido posible identificar patrones típicos de cicatriz (o realce tardío), que actualmente se utilizan no solo para diferenciar entre cardiopatía isquémica o no isquémica(80,81) si no para distinguir diversas entidades dentro de esta segunda categoría: miocardiopatía arritmogénica(82), sarcoidosis(83), miocarditis(84), laminopatías(85) etc. siendo una herramienta diagnóstica fundamental en nuestro día a día(86).

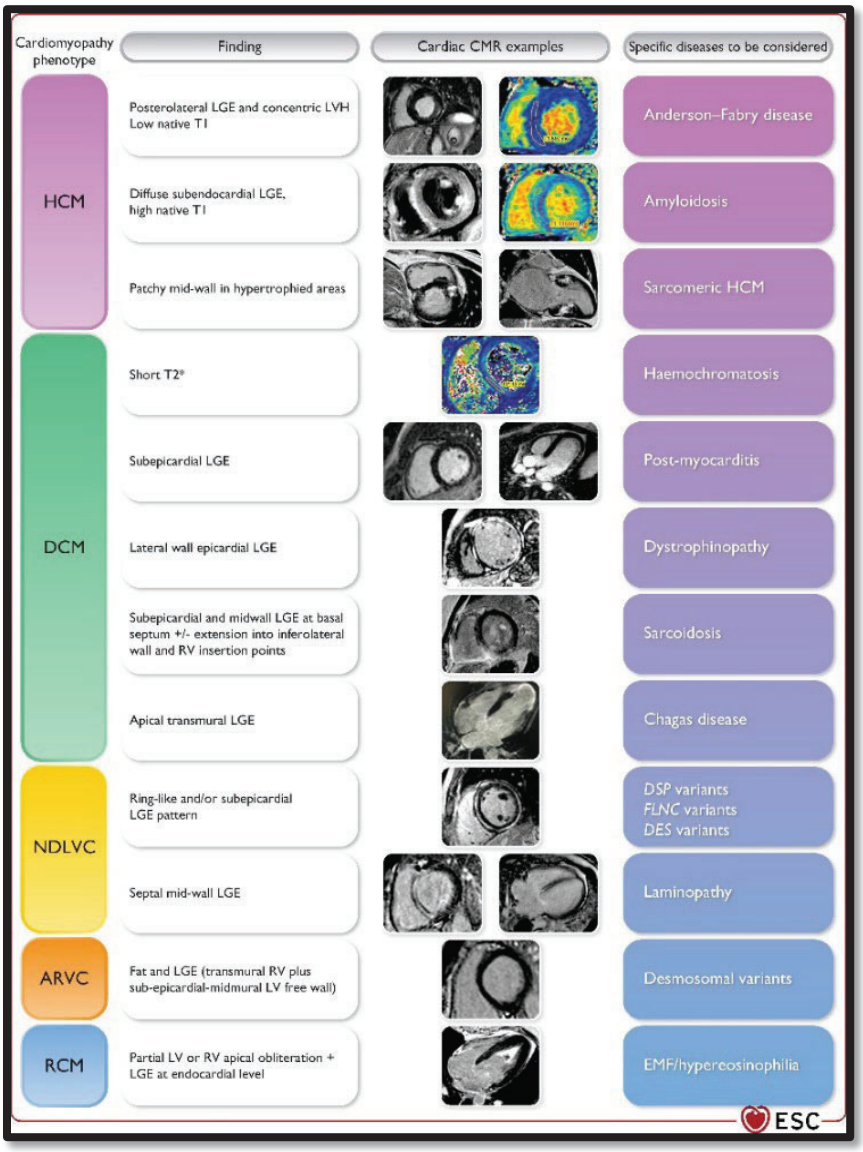

Fig. 12. **Valor diagnóstico de RMC**. Esquema procedente de las Guías de la Sociedad Europea de Cardiología para el manejo de miocardiopatías(86) en el que se muestran los hallazgos de RMC más característicos de los principales bloques de miocardiopatías, con ejemplos de cada una de ellas y el diagnóstico diferencial a tener en cuenta.

HCM= miocardiopatía hipertrófica

DCM= miocardiopatía dilatada

NDLVC= miocardiopatía no dilatada de ventrículo izquierdo

ARVC= miocardiopatía arritmogénica de ventrículo derecho

RCM= miocardiopatía restrictiva

1.7.1. RMC: post procesado con ADAS 3D software y otros sistemas

Para facilitar la interpretación del sustrato por RMC, algunas empresas han desarrollado softwares de postprocesado que han permitido no solo visualizar el sustrato de una forma más sencilla si no el cálculo automático de canales y la extracción de estadísticas sobre los parámetros

de la cicatriz. Existen varios softwares en el mercado (ADAS 3D, MUSIC, etc), con un funcionamiento relativamente similar entre ellos.

Primero se incorporan las imágenes crudas de RMC al software y se delinea la superficie endocárdica y epicárdica para definir la zona de interés, evitando estructuras anatómicas como el anillo mitral o los músculos papilares.

A continuación, el software realiza una codificación basada en la intensidad máxima de píxel de las imágenes de resonancia, adjudicándole un color determinado (por ejemplo rojo en el software ADAS3D) a aquellas regiones de miocardio con intensidad de pixel>60% (e identificándolas por tanto como cicatriz densa) y otro color (p.ej azul en el software ADAS 3D) para aquellas con <40% (codificadas por tanto como tejido sano). Aquellas regiones con intensidad de pixel entre 40 y 60% serán pintadas con una gama de colores intermedia e identificadas como *border zone*. Estos umbrales han sido seleccionados tras realizarse estudios de correlación con mapas de voltaje(87).

Posteriormente, para valorar de forma más sencilla la tridimensionalidad del sustrato, el espesor miocárdico se divide en nueve capas del mismo grosor que se pueden visualizar por separado, generándose nueve "mapas" de sustrato, los tres primeros correspondientes a capas endocárdicas, los tres siguientes a capas mesocárdicas, y los tres últimos a capas epicárdicas. Además, el sofware puede calcular de forma automática los segmentos de la American Heart Association (AHA) para facilitar la correcta localización del sustrato. Del mismo modo, se puede obtener de forma automática el espesor o grosor de cada segmento AHA.

Finalmente, el software calculará los canales buscando zonas de *border zone* (es decir, intensidades de pixel entre 40 y 60%) rodeadas por cicatriz densa y que conectan tejido sano, tal y como se ha descrito histológicamente(27–29,38).

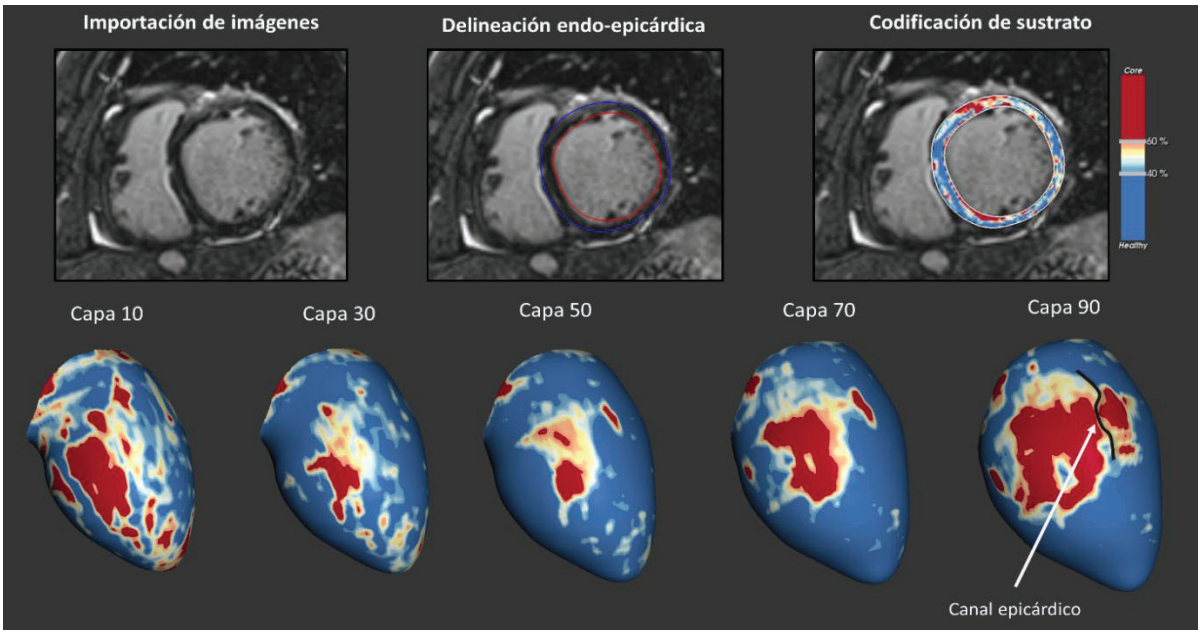

Fig. 13. **Imagen ejemplificando cómo funciona ADAS 3D Software**. Tras importar las imágenes de la RMC, se delinea el endocardio y el epicardio a través de los ejes cortos de la secuencia de gadolinio, siendo posteriormente codificada la intensidad del mismo en una escala de colores: intensidades de píxel superiores a 60% se colorean de rojo representando tejido cicatricial; intensidades por debajo de 40% de azul representando tejido sano e intensidades intermedias en una gana de colores alrededor del amarillo representando *border zone*. El software realiza una reconstrucción automática tridimensional dividiendo el espesor miocárdico en 9 capas iguales, desde el endocardio al epicardio. Las zonas de *border zone* rodeadas de tejido cicatricial que conectan con tejido sano son anotadas automáticamente como canales.

1.7.2. RMC: guiar la ablación de TV

Fruto del auge de la RMC y su capacidad para identificar el sustrato arrítmico, así como las limitaciones ya descritas del mapa de voltaje (altamente dependiente de las características del catéter, el contacto, así como la falta de umbrales de voltaje claros, etc.) pronto emergió la RMC como una herramienta potencialmente capaz de describir de forma fidedigna el sustrato arrítmico. Varios estudios comparando los hallazgos de la RMC con cortes histológicos y mapas de TV(88) demostraron el potencial papel de esta prueba de imagen para identificar las zonas críticas. Además de la identificación de los istmos de TV(89), estudios posteriores demostraron una buena correlación de la cicatriz (en términos de identificación de tejido sano, cicatriz densa

y *border zone*) por RMC con la obtenida en mapas de voltaje(90) y, además, la capacidad de la RMC para identificar correctamente los canales de voltaje(91–93) de los mapas electroanatómicos. Debido a la fuerte correlación entre ambas técnicas, muchos autores empezaron a utilizar la RMC para planificar la ablación de TV(94) obteniendo menores tiempos de radiofrecuencia, menor inducibilidad al final del procedimiento y mejores resultados en el seguimiento. El mayor ejemplo de una estrategia de ablación basada en RMC es la técnica "*scar dechanneling*" desarrollada por Berruezo et al.(95) que se describió inicialmente basada en la delineación de los canales de conducción lenta analizando los electrogramas típicos para eliminar la entrada de los mismos, y que posteriormente se convirtió en un protocolo basado exclusivamente en la eliminación de los canales observados en la RMC(96). En un estudio no randomizado(96) se compararó el resultado de tres grupos: un grupo al que se realizaba ablación sin resonancia previa, otro en el que se realizaba *scar dechanneling* clásico con información añadida de RMC y un tercero en el que se realizaba "*scar dechanneling* basado en RMC" consiguiendo de nuevo mejores resultados en cuanto a tiempo de procedimiento, fluoroescopia y radiofrecuencia así como menores tasas de inducibilidad al final del procedimiento y de recurrencia en los grupo en el que se usaba la RMC.

1.7.3. Limitaciones de la RMC

La mayoría de los pacientes remitidos para realización de RMC previa a ablación de sustrato son portadores de dispositivos intracardíacos, principalmente DAI, lo que supone varios retos.

Por un lado, el paciente se ve expuesto a un aumento de riesgo de daño del dispositivo. Éste altera sus propiedades al someterse a un fuerte campo magnético, principalmente por calentamiento del mismo, pudiendo presentar disfunción reversible o irreversible, llegando a administrar en ocasiones terapias inapropiadas al paciente.

En este sentido, en los últimos años, varios estudios han demostrado la seguridad de realizar RMC a pacientes con dispositivos. Inicialmente se demostró la seguridad en pacientes muy seleccionados con ritmo propio y sin cables abandonados tras realizar ciertas comprobaciones y

adaptar la configuración del mismo (97). Posteriormente estas recomendaciones se ampliaron a prácticamente todos los pacientes(98), incluso aquellos con electrodos abandonados (99), lo que ha permitido extender la aplicabilidad de la RMC en la ablación de TV de una manera muy importante(100).

Pese a la minimización de los riesgos relacionados con la seguridad, la presencia de artefactos generados por el DAI y, por tanto, la dificultad para lograr imágenes de alta calidad ha constituido el problema principal para la extensión del uso de la RMC. Los artefactos se generan por el cambio de frecuencia de los tejidos a 5-10cm de distancia del generador y aparecen en más de la mitad de los pacientes portadores de dispositivo en lado izquierdo(101), mostrándose como una imagen hiperintensa, habitualmente en cara anterior y apical, que pudiera semejar cicatriz densa en la secuencia de gadolinio, llevando a la mala interpretación de las características del sustrato. La aparición de una nueva secuencia llamada *wideband* ha permitido disminuir el riesgo de artefactos en prácticamente todos los pacientes(102) demostrando no solo una buena calidad de las imágenes si no una igual correlación entre los hallazgos de la RMN con los mapas electroanatómicos tanto en términos de correlación de cicatriz (103) como de canales(104).

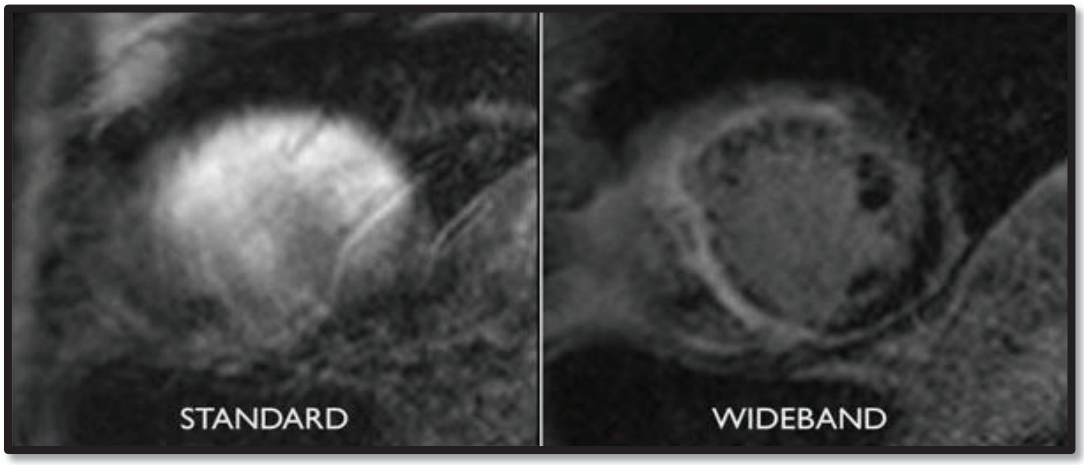

Fig. 14. **Comparación de secuencias de RMN en pacientes portadores de DAI**. Se observa a la izquierda una imagen de un eje corto ventricular de un paciente portador de un DAI sometido a una RMC mediante secuencias convencionales. A la derecha, el mismo paciente utilizándose una secuencia *wideband*, Tal y como se puede apreciar, la definición de endocardio y epicardio, así como las zonas hiperintensas correspondientes en este caso con una cicatriz septal extensa, solo pueden ser observadas en la secuencia *wideband*. Imagen adaptada de Stevens et al(103)

1.7.4. Retos de la RMC en la ablación de TV

Tal y como se ha comentado previamente, el desarrollo de la RMC en los últimos años ha llevado a la extensión de su uso, tanto por sus implicaciones diagnósticas, pronósticas, como por su capacidad para guiar la ablación de sustrato. Respecto a este último aspecto, múltiples estudios han demostrado una gran correlación con mapas de voltaje, siendo éste el motivo principal por el cual algunos grupos la utilizan como guía de los procedimientos de ablación. Sin embargo, la información que nos aporta la RMC va mucho más allá de la localización de la cicatriz o incluso los canales. A continuación, se citarán algunas de las aplicaciones que podrían derivar de un estudio más profundo de las imágenes de RMC.

1.7.4.1. RMC y Sustrato Funcional

Uno de los retos principales en la RMC es si será o no capaz de describir el **sustrato funcional** además del sustrato anatómico. ¿Es posible que mediante el análisis no invasivo del sustrato arrítmico por RMC se pueda valorar si unos canales tienen capacidad de generar arritmias y otros no?, ¿podrían algunos canales presentan capacidad de conducción lenta y otros no?, ¿se pueden predecir si esas arritmias serán o no rápidas, o si generarán episodios bien tolerados en el paciente o si éste presentará tormenta arrítmica o muerte súbita? En este sentido, un estudio recientemente publicado por Sánchez-Somonte et al.(105) describió que los canales de RMC que más se asociaban a la TV inducida durante los procedimientos de ablación eran aquellos que tenían mayor longitud, gramos y *protectedness* (cantidad de canal que está "protegido" por cicatriz densa).

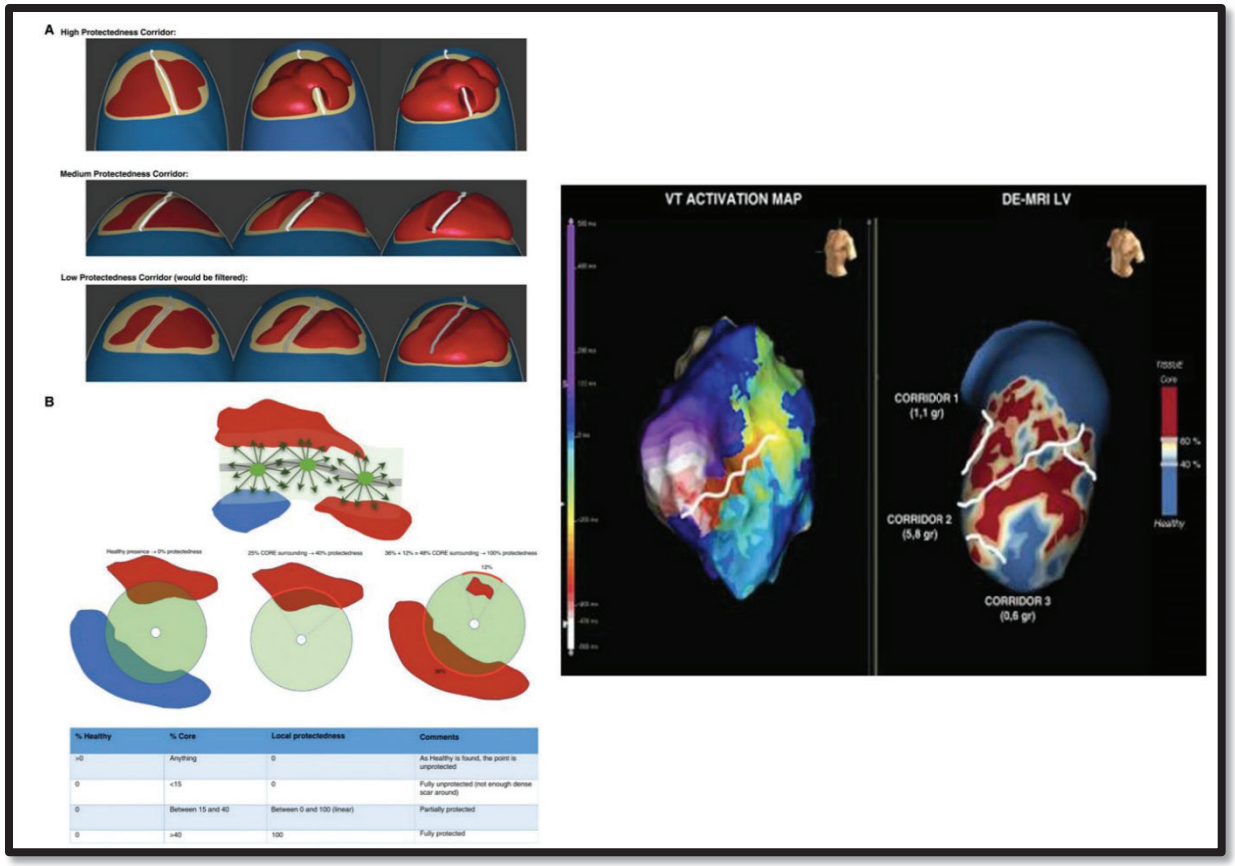

Fig. 15. **Definición de protectedness y correlación entre canales de RMC y TV**. A la izquierda (A) representación gráfica de tres canales, el superior con alta *protectedness*, es decir, muy rodeado tridimensionalmente por cicatriz densa; el del medio solo parcialmente *protegido*, y el inferior con baja *protectedness*. En el panel B se observa cómo se realiza el cálculo de la *protectedness* teniendo en cuenta el porcentaje de canal recubierto por cicatriz densa. A la derecha de la imagen se observa un mapa de activación de TV en un paciente con cardiopatía estructural que se ha sometido a una RMC pre-ablación. Se observa en la imagen la correlación entre el itsmo de la TV y el canal 2 de RMC. Nótese que existen otros dos canales, corridor 1 y corridor 3, que no se asocian con el circuito de la TV y que tienen menor longitud y masa. Imagen adaptada de Sánchez-Somonte et al. (105).

El hecho de que en este estudio se hayan descrito diferencias entre distintos canales que los hagan más o menos responsables de eventos arrítmicos, invita a continuar investigando el papel de la RMC en el comportamiento funcional del sustrato arrítmico.

1.7.4.2. RMC y Predictores de dificultad de ablación

Otro de los restos está en relación con la capacidad de la RMC **para predecir la dificultad para eliminar el sustrato arrítmico,** ya sea por permitir visualizar zonas de interés que pudieran pasar desapercibidas en los mapas de voltaje o por ayudar a planificar la aplicación de radiofrecuencia (RF) de forma diferente en zonas de más difícil acceso.

Respecto a la mejoría en la identificación de zonas de interés, ¿Podría la RMC ayudarnos a desenmascarar sustrato en zonas aparentemente normales en los mapas electroanatómicos? Tal y cómo hemos comentado previamente, una de las principales limitaciones de los mapas de voltaje es que dependen de la correcta interpretación de la señal, lo que varía según el contacto del catéter con el tejido y según las características del catéter principalmente, pero también según la presencia de sustrato funcional aparentemente normal en el mapa basal, señales de *far-field*, etc. Debido a la tridimensionalidad del sustrato, es muy probable, por ejemplo, que circuitos arrítmicos profundos no puedan ser detectados en la superficie endocárdica en su máxima amplitud debido a la distancia del catéter con el foco. Sin embargo, el sustrato arrítmico identificado por RMC no solo permite evitar los errores fruto de la interacción catéter-señal, sino que también nos aporta valiosa información tridimensional. Su aplicación en este sentido no ha sido estudiada.

Por otro lado, en caso de que algunas localizaciones de sustrato por RMC se asociasen a peores resultados de ablación, ¿podría la identificación de estas zonas mediante RMC llevarnos a aplicar energía de una manera diferente o a utilizar distintas técnicas de ablación en localizaciones concretas? Existen algunos estudios que sugieren que la presencia de algunos factores evaluables mediante técnicas de imagen puede suponer una menor probabilidad de éxito en la ablación. La presencia de calcificaciones dentro de la cicatriz en pacientes con cardiopatía isquémica, por ejemplo, parece asociarse a mayor tasa de recurrencias post ablación(106). Respecto a características de los canales, parece que aquellas cicatrices extensas con canales transmurales, especialmente si afectan a regiones septales donde existe con más frecuencia sustrato intramural profundo, podrían asociarse también a una mayor dificultad de ablación(107,108).

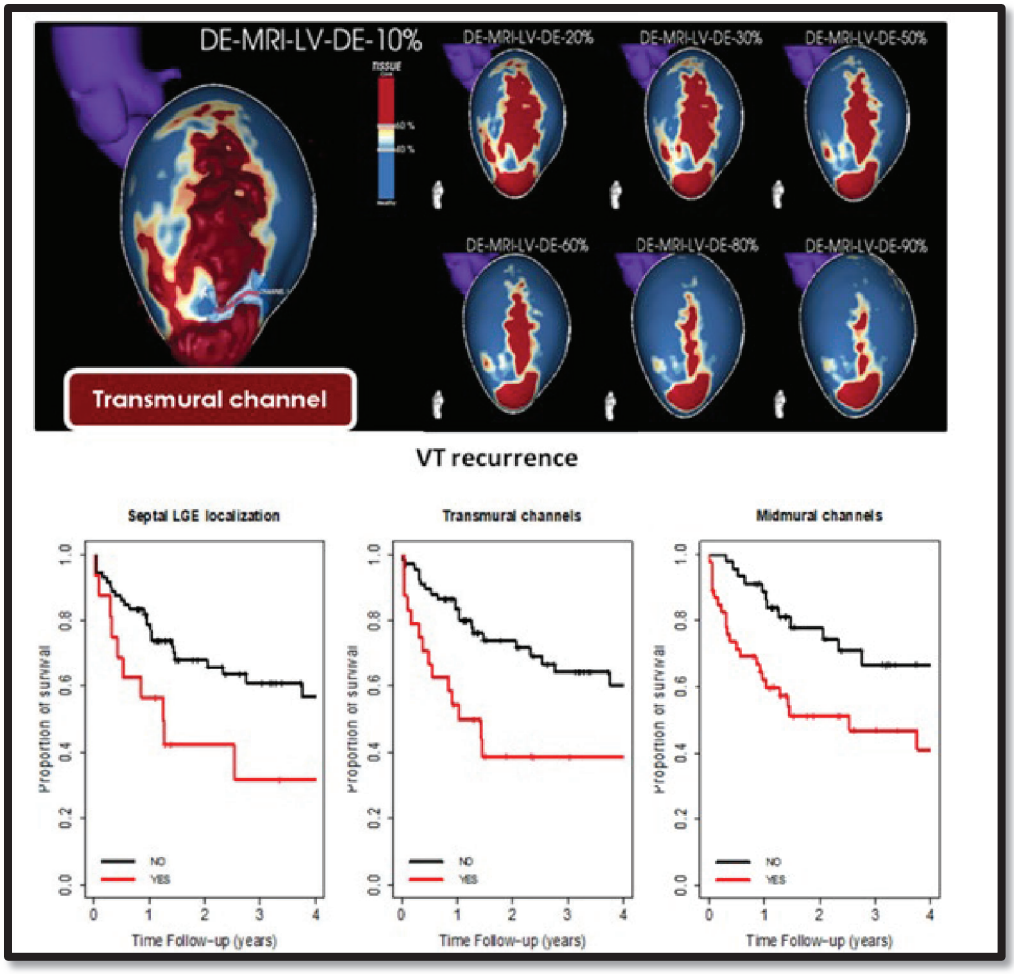

Fig. 16. **Predictores de recurrencia tras ablación de TV**. Imagen en la que se muestran las curvas de supervivencia (entendidas como probabilidad de recurrencia de TV post ablación) según la presencia de sustrato septal, canales transmurales o intramurales. Imagen adaptada de Quinto et al.(107).

Tal y como comentamos, la profundidad del sustrato podría ser fácilmente evaluable por RMC pudiendo llevarnos a cambiar la forma en la que aplicamos radiofrecuencia.

En este sentido, análisis histológicos de pacientes que fallecieron después de una ablación de TV muestran que, utilizando parámetros estándares de ablación (uso de catéter de ablación irrigado con sensor de fuerza con objetivo mínimo de 9 gramos, utilizando 45-50W, con una irrigación de 30mL/min con suero salino normal y una temperatura máxima de 43°C, con aplicaciones de 60 segundos), puede observarse una profundidad media de las lesiones de radiofrecuencia de

7.2mm (109). Además, esta profundidad analizada en muestras histológicas parece correlacionarse fuertemente con la profundidad de la lesión analizada por RMC(110).

Ajustar algunos de los parámetros de ablación, especialmente la duración de la aplicación de radiofrecuencia, la energía y la fuerza de contacto del catéter con el tejido, pueden modificar la profundidad de la lesión (111), permitiendo acceder a sustrato aparentemente inaccesible. Además del ajuste de parámetros, existen estrategias de ablación diferentes, como la ablación bipolar(112) o la ablación con catéteres irrigados usando como irrigación una solución salina baja en iones (al 50%) o irrigación con dextrosa al 5%(113), que han demostrado también generar lesiones más profundas.

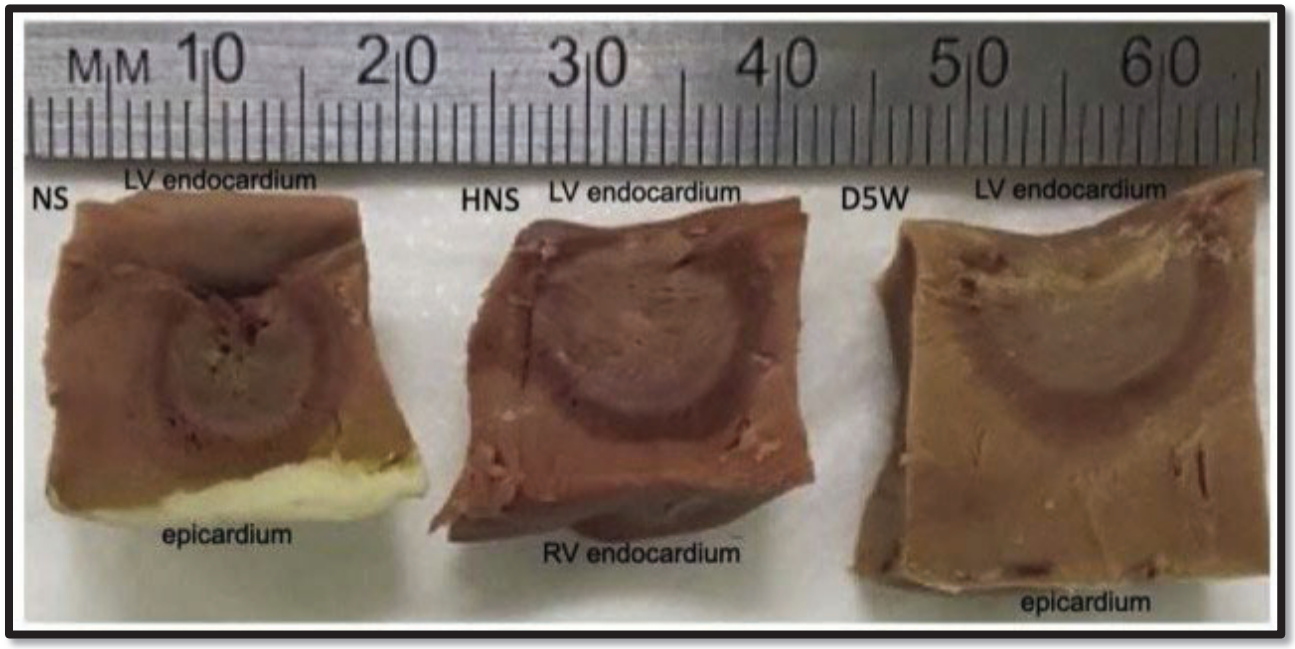

Fig. 17. **Efectos de la irrigación en la profundidad de la lesión por radiofrecuencia**. Imagen en la que se observan los cambios en la extensión de la lesión usando irrigación con suero normal (a la izquierda), suero salino al 50% (en la imagen del medio) y dextrosa al 5% (a la derecha). Imagen procedente de Bennett et al.(113)

Dado que existen diversas estrategias para abordar el sustrato más profundo, conocer antes del procedimiento la profundidad del sustrato puede permitirnos planificar mejor el procedimiento.

1.7.4.3. RMC para Elección de Abordaje

La **tercera** cuestión en la que la RMN puede tener un papel relevante está muy relacionada con el punto previo y hace referencia a la **elección del abordaje**. Actualmente existe un consenso general sobre usar el acceso epicárdico(114) tras el fallo de un procedimiento endocárdico previo, sin embargo, existe una gran controversia(115) entre distintos centros en el resto de las indicaciones de acceso epicárdico. Algunos grupos acceden directamente al epicardio en el primer procedimiento usando criterios electrocardiográficos de la TV(116), o la presencia de sustrato epicárdico en pruebas de imagen(91) o el tipo de cardiopatía (dado que se sabe que algunas cardiopatías no isquémicas presentan mayor probabilidad de cicatrices epicárdicas)(117). Algunos estudios muestran, de hecho, mejores resultados en pacientes no isquémicos cuando se utiliza el abordaje epicárdico(118) o incluso en pacientes isquémicos con cicatrices transmurales(107,119). Sin embargo, este abordaje no está exento de complicaciones, con un riesgo general en torno al 5% de complicaciones graves incluso en centros experimentados(120), por lo que una buena selección de los pacientes que van a beneficiarse del mismo resulta crucial. ¿Puede la RMC predecir qué pacientes van a requerir un abordaje epicárdico para la correcta eliminación del sustrato? Probablemente el estudio de la profundidad del sustrato pueda revelar información interesante al respecto, si bien este campo no ha sido estudiado.

1.7.4.4. RMC para evaluar los cambios en el sustrato post ablación

La cuarta cuestión guarda relación con el **análisis de los cambios secundarios a la radiofrecuencia**. Es importante recordar que las mejores tasas de no recurrencia post ablación se han logrado con estrategias de ablación muy extensas (homogeneización de la cicatriz(45)). Sin embargo, algunos grupos han planteado la hipótesis de que ablaciones largas puedan generar nuevas zonas de sustrato arrítmico. Por otro lado, ya se ha citado previamente que la aplicación de radiofrecuencia en zonas claramente arritmogénicas (potenciales tardíos en el mapa de

voltaje en un área que constituye una zona de deceleración en el mapa de isócronas y en el que se observan potenciales diastólicos en TV) usando parámetros estándares podría no ser suficiente para eliminar completamente el canal arrítmico. Se plantean pues varias cuestiones: ¿Podría este canal utilizar otras "ramas" que constituyan distintas salidas del circuito arrítmico? ¿Puede la RMN predecir si la lesión que se ha realizado ha sido o no suficiente, si se han creado o no zonas nuevas potencialmente arritmogénicas?

En este sentido, existen dudas acerca de cuáles son los motivos por los cuales los pacientes sometidos a ablación de sustrato presentan recurrencias. Todo indica que, en pacientes con cardiopatía isquémica, donde las zonas de sustrato se encuentran confinadas a las zonas del infarto previo, la no correcta eliminación del sustrato puede ser la causa principal. Existen más dudas acerca de cardiopatías no isquémicas, donde la progresión de la enfermedad puede jugar un papel muy relevante. Sin embargo, algunos estudios indican que, si bien la progresión de la enfermedad se puede observar en segundos procedimientos de ablación, la recurrencia se debe más a la no completa eliminación del sustrato que a la progresión de la enfermedad(121) en sí misma. Por tanto, la evaluación no invasiva de las lesiones realizadas podría ayudar a predecir si el procedimiento ha sido completo o no.

En la misma línea, existe muy poca información, sobre la valoración mediante RMC de cómo cambia el sustrato arrítmico post ablación. Algunos estudios en modelos animales(122,123) muestran que la apariencia de las lesiones de ablación es diferente en función del tiempo de evolución de la lesión (fase aguda vs. crónica). En la fase aguda, debido a hemorragia, necrosis coagulativa y obstrucción microvascular posterior, la apariencia es la de un área oscura rodeada por un borde periférico de realce (el mismo *dark core* descrito por obstrucción microvascular en pacientes que han sufrido un infarto de miocardio(79)). En la fase crónica, a medida que queda retenido el gadolinio, las lesiones de ablación se representan como áreas completamente brillantes mediante imágenes de RMC, asemejándose a la cicatriz que se observa en pacientes con un infarto crónico. Sin embargo, un estudio observacional retrospectivo reciente(124) sugiere que el *dark core* puede persistir en el seguimiento, principalmente cuando las lesiones de ablación se producen sobre tejido cicatricial, aunque dicho estudio no realizaba la RMC de forma sistemática a todos los pacientes tras la ablación. No existe hasta la fecha evidencia sobre

si de los hallazgos de las RMC post ablación se puede extraer predictores de recurrencia que permitan tomar estrategias precoces para evitar dicha recidiva y que, sobre todo, nos ayuden a entender cómo mejorar los procedimientos de ablación.

1.7.4.5. RMC: predictores de arritmogenicidad

Gracias al conocimiento adquirido en las últimas décadas, que nos ha permitido entender las bases de los circuitos de reentrada responsables de las taquicardias ventriculares, y sobre todo, gracias a los avances en el procesamiento de imágenes de RMC y a los múltiples estudios de validación que han demostrado una buena correlación del sustrato, hoy en día la RMC se ha consolidado no solo como una técnica diagnóstica si no como una técnica con un marcado carácter pronóstico. Teniendo en cuenta el conocimiento sobre la presencia de un circuito arrítmico anatómico (*border zone* rodeado de cicatriz) que se puede visualizar por RMC y que es responsable de las taquicardias ventriculares en pacientes con cardiopatía, parece lógico que la identificación de estos parámetros en RMC tenga un papel predictor de eventos, lo que podría ser especialmente relevante en paciente que aún no han tenido un primer episodio arrítmico.

Un metaanálisis publicado en 2016 por Disertori et al. (125) demostró que la presencia de cicatrices en la RMC era un potente predictor de riesgo de arritmias ventriculares (OR 5,62) tanto en pacientes isquémicos como no isquémicos. En el estudio GAUDI, Acosta et al.(126) realizaron un análisis detallado de las características de la cicatriz y observaron que la extensión y heterogeneidad de la misma eran predictores independientes de eventos arrítmicos. Establecieron un límite de 10 gramos de masa cicatricial para predecir eventos arrítmicos con una sensibilidad del 100 % y una especificidad del 72 %. Sánchez-Somonte et al.(127) en 2021 no solo confirmaron el valor potencial de este punto de corte, sino que también identificaron la ausencia de canales como una variable con un alto valor predictivo negativo, sugiriendo que aquellos pacientes con indicación de implante de DAI en prevención primaria, pero con menos de 10 g de tejido cicatricial y sin canales, tenían muy bajo riesgo de recibir terapias adecuadas (5,26% vs. 25,31% por año, p=0,034).

Por todo ello, continuar mejorando la capacidad de la RMC para definir el sustrato arrítmico, especialmente gracias a la comparación con mapas electroanatómicos generados con catéteres de alta densidad y, por tanto, que generen mapas más fidedignos, es uno de los principales retos actuales para entender mejor cómo se comporta dicho sustrato y cómo abordarlo. De forma consecuente, podremos aplicar esta mejora en la definición del sustrato por RMC a pacientes con cardiopatía, mejorando nuestra capacidad diagnóstica y pronóstica sobre una población en riesgo.

1.8. Revisiones relacionadas con el tema de autoría de la doctoranda

Revisión 1: Ventricular Tachycardia Ablation Guided by Functional Substrate Mapping: Practices and Outcomes

Vázquez-Calvo S, Roca-Luque I, Porta-Sánchez A.

J Cardiovasc Dev Dis. 2022;9(9):288. *doi:10.3390/jcdd9090288*

Impact Factor 2.4

Revisión 2: Management of Ventricular Arrhythmias in Heart Failure

Vázquez-Calvo S, Roca-Luque I, Althoff TF

Curr Heart Fail Rep. 2023;20(4):237-253. *doi:10.1007/s11897-023-00608-y*

Impact Factor 3.8

Revisión 3: Impact of LGE-MRI in Arrhythmia Ablation

Garre P, **Vázquez-Calvo S**, Ferro E, Althoff T, Roca-Luque I

Applied Sciences. 2023; 13(6):3862*. https://doi.org/10.3390/app13063862*

Impact Factor 2.5

Journal of
Cardiovascular
Development and Disease

MDPI

Review

Ventricular Tachycardia Ablation Guided by Functional Substrate Mapping: Practices and Outcomes

Sara Vázquez-Calvo, Ivo Roca-Luque and Andreu Porta-Sánchez *

Arrhythmia Unit, Cardiology Deparment of the Institut Clínic Cardiovascular (ICCV) at Hospital Clínic de Barcelona, Universitat de Barcelona and Institut d'Investigacions Biomédiques August Pi i Sunyer (IDIBAPS), C/Villarroel No 170, 08036 Barcelona, Spain
* Correspondence: APORTAS@clinic.cat or andreuportasanchez@gmail.com

Abstract: Catheter ablation of ventricular tachycardia has demonstrated its important role in the treatment of ventricular tachycardia in patients with structural cardiomyopathy. Conventional mapping techniques used to define the critical isthmus, such as activation mapping and entrainment, are limited by the non-inducibility of the clinical tachycardia or its poor hemodynamic tolerance. To overcome these limitations, a voltage mapping strategy based on bipolar electrograms peak to peak analysis was developed, but a low specificity (30%) for VT isthmus has been described with this approach. Functional mapping strategy relies on the analysis of the characteristics of the electrograms but also their propagation patterns and their response to extra-stimulus or alternative pacing wavefronts to define the targets for ablation. With this review, we aim to summarize the different functional mapping strategies described to date to identify ventricular arrhythmic substrate in patients with structural heart disease.

Keywords: ventricular tachycardia ablation; functional mapping; hidden substrate; decremental conduction; deceleration zones

Citation: Vázquez-Calvo, S.; Roca-Luque, I.; Porta-Sánchez, A. Ventricular Tachycardia Ablation Guided by Functional Substrate Mapping: Practices and Outcomes. *J. Cardiovasc. Dev. Dis.* **2022**, *9*, 288. https://doi.org/10.3390/jcdd9090288

Academic Editor: Shaojie Chen

Received: 21 July 2022
Accepted: 24 August 2022
Published: 30 August 2022

1. Introduction

Patients with structural heart disease that experience ventricular tachycardia (VT) have poorer outcomes compared to those who do not have VT [1,2]. Aiming to improve their prognosis has been a challenge over the last 30 years. Minimally invasive techniques for treating VT such as catheter ablation (CA) have an established role for such patients. Recent studies have shown as well favourable outcomes in terms of better prognosis and VT burden reduction [3–5]. Defining the critical regions sustaining VT had classically been performed by activation mapping and is considered the gold standard to identify the critical VT isthmus, but it is only tolerated in approximately 30% of patients. To overcome this problem, VT substrate mapping aiming to identify areas during stable rhythm (sinus rhythm or paced rhythm) that could be—but are not proven to be—involved in the VT circuit has gained widespread acceptance and some studies have shown superiority in terms of outcomes as compared to activation-mapping based VT ablation [6,7]. A simplistic way of depicting the VT substrate is by analyzing the peak-to-peak bipolar voltage amplitude, which has been correlated with the presence of myocardial scarring. By defining low-voltage areas (<0.5 mV), a border zone (0.5–1.5 mV), and healthy areas (>1.5 mV), several strategies were used to define the area to target with radiofrequency. Nevertheless, these thresholds have been obtained by conventional bipolar mapping catheters lacking contact sensors in the tip and validated in a small cohort of patients [8,9], so its application nowadays is controversial [10]. An alternative strategy is not just to quantify the peak-to-peak bipolar signal but to look for the qualities and timing of those signals, which have been described as late potentials [11] and their elimination shown to be useful in terms of decreasing episodes of VT during follow up [12–14]. Those RF targets are subject to some extent to interpretation and their assessment is limited by several factors: first, it depends

on the capability of the mapping catheter to correctly detect the EGMs according to the electrode size, interelectrode spacing, and angle of the incoming wavefront to the bipolar pairs [15,16]. Concerning this matter, some studies have compared traditional point-by-point catheters with new high-density (HD) catheters showing a better discrimination of abnormal electrograms and better clinical outcomes with the HD catheters [17–19]. Second, it is known that the abnormal EGMs can be hidden within the far-field signal and occur during the surface QRS and not after it. Several strategies based mainly in different settings of pacing have been designed to unmask the substrate. Third, even if we could identify all the abnormal EGMs, these could lead to ablate large areas of myocardium not always related with VT circuits. Additionally, this could potentially create new areas with a slow conduction capability and generate new potentially conducting channels.

The objective of this review is to analyze the different strategies to identify and unmask the arrhythmogenic substrate apart from the findings of peak-to-peak voltage mapping, in order to improve VT ablation outcomes.

2. Our Definition of Functional Mapping

We propose the definition of VT functional substrate mapping as a grouping term that uses not only the peak-to-peak voltage of the EGMs to analyze them but also their propagation patterns within the low-voltage areas and its response to either varying wavefronts of the activation or varying cycle lengths of pacing or extra-stimulation. Table 1 summarizes the different techniques.

Table 1. Comparation of different VT functional mapping strategies.

Strategy	Article	Population	Mapping System	Stimulation Setting	Measurement	Objective	RF Target	RF Time (min)	Results
DEEP	JACKSON 2015	6 ischemic.	Intraoperative mapping: custom-made 112 electrode ballon	If LP of fractionated EGM are identify: RV pacing 600 ms + VERP+20 ms	DEEP: delayed local potential after stimulation	To compare DEEP vs. LP mapping to identify VT isthmus (retrospectively)	VT critical sites based on activation mapping	N/A (surgical cryoablation)	DEEP mapping was more specific than LP mapping for identifying VT isthmus.
	PORTA-SÁNCHEZ 2018	20 ischemic.	CARTO: 9 Decanav 6 Pentarray 4 ablation cath.	For all LPs: RV pacing 600 ms + VERP+20 ms	DEEP: S2 local potential delayes or splits > 10 ms compared with S1	To compare DEEP vs. LP mapping to identify VT isthmus	DEEP area	30.6	Specificy of DEEP to detect VT isthmus was better than LPs
HIDDEN SUB-STRATE	ACOSTA 2015	37 patients: 75.7% ischemic.	CARTO	Identify potential HSC-EGM (>3 deflections and <133 ms) and double extra VERP+60 and VERP+40 to 20 ms	HSC-EGM: potential HSC-EGM that delays after stimulation	To analyses characteristics of patients with HSC-EGM	CCs (scar dechanneling) and HSC-EGM	Interv. group: 17.41 Hist. cohort: 23.11	Patients with HSC-EGM: More frequently ischaemic, smaller low voltage area, low number of LPs Location of HSC-EGM: EAM: 18.2% scar area vs. CMR: 92% scar area
	DE RIVA 2018	60 ischemic.	CARTO	RV pacing 500 ms + single extra VERP+50 ms	EDP: low amplitude (<1.5) near field potentials with conduction delay > 10 ms or block.	To compare patients with hidden vs. not hidden substrate	EDPs	Interv. group: 15 Matched cohort: 13	Hidden substrate group: Better FEVI, smaller scar and dense scar, higher 12 m VT free survival

Table 1. *Cont.*

Strategy	Article	Population	Mapping System	Stimulation Setting	Measurement	Objective	RF Target	RF Time (min)	Results
PEFA	REDFEARN 2018	(1) 14 ischemic. and 5 healthy controls (2) 10 ischemic	Ensite Precision	RV pacing 600 ms(x6) + VERP 150 RV pacing 600 ms(x6) + VERP 100 RV pacing 600 ms(x6) + VERP 50	4 types of response related to latency and EGM duration	(1) To compare different EGM responses after stimulation protocol (2) To validate PEFA method	(1) Operators were blinded to PEFA (2) Type I and II	Interv group: 39.47 Cohort: 39.88	(1) Type I and II responses: most frequently at VT termination sites (2) PEFA approach reduced VT inducibility
BARTS	SRINIVA-SAN 2018	30 ischemic.	Ensite Precision	Sinus rhythm (SR)(x5) + VERP 20 ms (SP)	Annotation of LP and LAVAs	To compare LP/LAVA with VT isthmus in two different maps: SR and SP	Total LPs and LAVAs	32	LP/LAVAs observed during SP were able to identify regions critical for VT ablation with a greater accuracy than SR mapping
PHYSIO VT	ANTER 2020	85 ischemic.	RHYTMIA 92.8% CARTO 7.2%	-SR and RV Pacing 600 ms and LV Pacing 600 ms	Area of activation maps (isochronal maps of 10 ms steps)	To compare areas of activation slowing and critical VT isthmus in three different maps (SR, RV and LV)	Acumulative area of activation slowing	27.7	The direction of LV activation is influenced by the magnitude and location of activation slowing: SR Mapping identify 66.2% of the entire area of activation slowing. RV and LV unmask an additional 33%
ILAMS	AZIZ 2019	120 patients: 50% ischemic	Ensite Precision	Annotation of last deflection and division of the total activation window in 8 equal isochrones	Deceleration zones (DZ): 3 isochrones in less than 1 cm.	To correlate DZ with VT isthmus	Primary DZs	29	DZs identify during SR are strongly predictive of critical sites for reentry.

3. Techniques for VT Functional Substrate Mapping

3.1. Decrement Evoked Potential (DEEP) Mapping

Voltage channels can be easily identified in patients with VT through voltage maps; adjusting the thresholds but a low specificity (30%) for VT isthmus has been described with this approach. The presence of LPs inside the CCs increases the specificity for identifying critical VT termination sites (85%) [20]. Despite strategies focusing on complete LP abolition, inducibility at the end of the procedure continues to be high (40%) and the VT recurrence still remains around 30% after one-year follow up [21,22].

Looking in depth into the mechanism of re-entry, which is the main mechanism of VT in patients with heart disease, conduction delay preceding unidirectional block has been demonstrated as essential for its initiation and maintenance [23,24] (Figure 1).

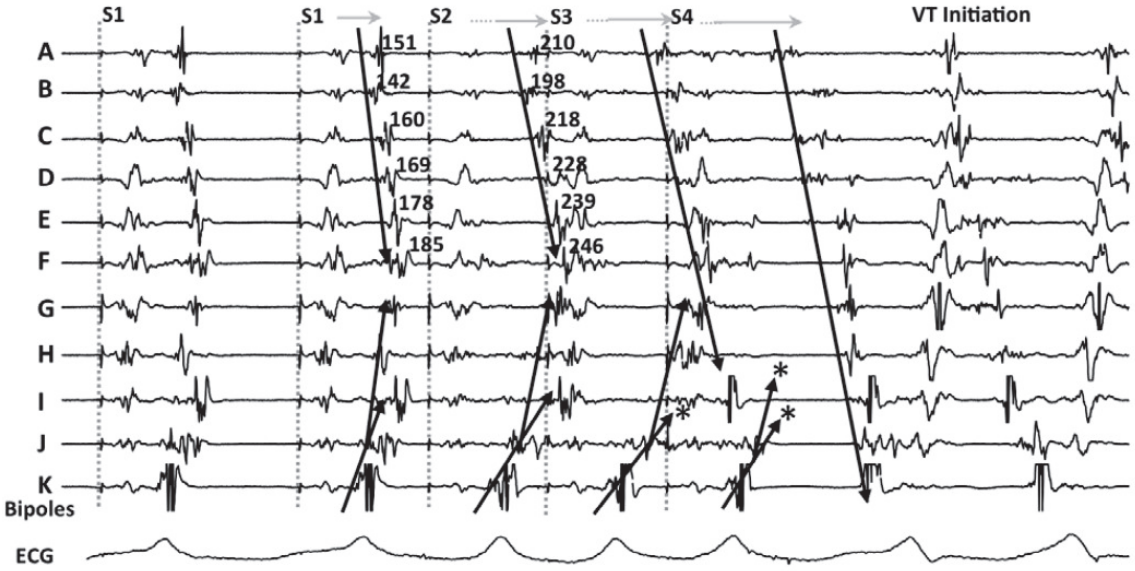

Figure 1. An example of decremental conduction, unidirectional block, and induction of ventricular tachycardia (VT) from Jackson et al. [25]. During right ventricular pacing, local abnormal potentials can be seen on bipoles A to K. With the introduction of the first extrastimulus (S2), an important delay in bipoles A to J is observed. With S3, there is a block (*) of the local potential on bipole I and subsequently with S4 there is block (*) at the VT exit site (bipole J). Block at the VT exit site and conduction delay through the entrance of the channel set the basis for re-entrance. The mechanistic study by Jackson et al. showed that those late potentials that had decremental properties were more frequently co-localized with the VT isthmus.

In their seminal paper, Jackson et al. [25] hypothesized that ventricular EGMs which showed decremental conduction (called decrement evoked potentials or DEEPs) could be more likely to colocalize with critical VT circuits than LPs without decremental conduction. They retrospectively analyzed the results of intraoperative mapping from six ischemic patients, and after that, used a human ventricular myocardium ionic model [26] to mathematically correlate DEEPs with the diastolic isthmus of VT. The mapping protocol consisted in performing a RV pacing train at 600 ms with a single extra-stimulus delivered at the ventricular effective refractory period (VERP)+20 ms whenever an LP or fractionated potential was identified. If the local potential delayed >10 ms, this would be annotated as a DEEP. In this setting, the use of DEEP mapping identified the diastolic pathway with greater specificity than LP mapping with similar sensitivity. Of note, only areas showing LP during baseline conditions were analyzed for the presence of DEEPs.

These results were confirmed in the clinical setting by Porta-Sanchez et al. [27] with 20 consecutive patients with ischemic cardiomyopathy in a multicentric study. They identified DEEPs as those LPs with decremental activity (>10 ms delay after pacing protocol).

The mean area with LPS was 16.8% of the myocardium mapped vs. 4.8% with DEEP ($p < 0.001$), but areas with DEEPs performed better than LPs at colocalizing within VT isthmus (ROC area under the curve of 0.86 vs. 0.79 with LPs). The ablation strategy consisted in ablation only of the DEEP regions and only expanded the ablation if the patient was still inducible (20%). Recurrence rates after DEEP-guided ablation were similar to what has been described in the literature (75% VT freedom at 6 months).

3.2. Hidden Slow Conduction (HSC) Mapping

Acosta et al. [28] described a new method to unmask EGMs showing hidden slow conduction (HSC-EGM) using a double ventricular extra-stimulus in 37 consecutive patients (with ischemic and non-ischemic myocardiopathy). They distinguished four different EGMs: normal (less than three sharp deflections with amplitude >3 mV and duration <70 ms; fractionated (multiple deflections, amplitude <0.5 mV and duration >133 ms; late (any EGM lasting beyond the QRS); and potential HSC-EGM (>3 deflections but <133 ms). Whenever a potential HSC-EGM was identified, a double extra-stimulus from the RV apex was delivered at VERP+60 ms and VERP+40 to 20 ms, respectively. When the EGM split and delayed from the far-field signal, it was annotated as HSC-EGM (Figure 2). These EGMs were found in 56.7% of patients. Ablation was delivered at conducting channels (scar dechannelling technique) and HSC-EGMs. Interestingly, patients showing HSC-EGM were more frequently ischemic with smaller and more heterogeneous scar areas and had less VT inducibility after ablation compared with an historic cohort. This study was enlarged by the same authors with a publication in 2020 including 70 patients and reproducing similar conclusions and potentially pointing towards a better outcome in terms of VT freedom [29].

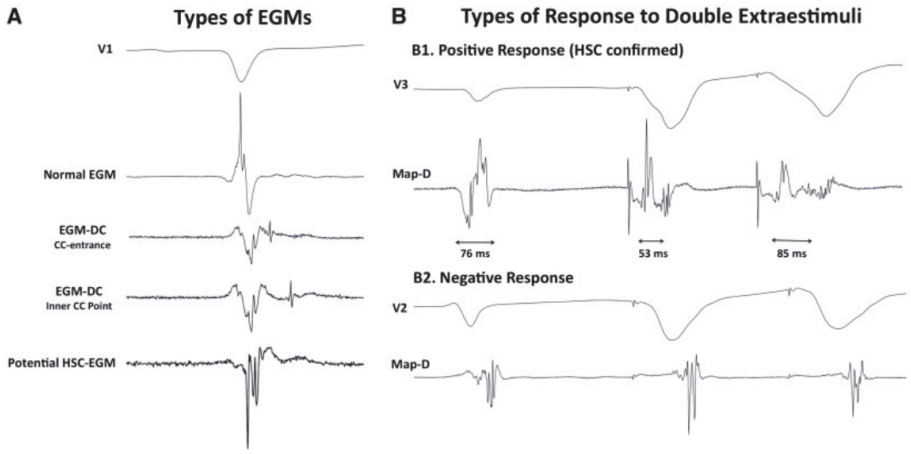

Figure 2. Electrogram classification and response to a double extraestimulus from Acosta et al. [28]. (**A**) different types of EGMs are shown: from normal through CC-EGMs to potential HSC. (**B**) the response of the potential HSC-EGM after a double extraestimulus is represented, considering a positive response if the local potential is delayed. Ablation was undertaken in those regions feeding the preserved voltage channels with the "scar dechanneling" technique.

3.3. Evoked Delayed Potential (EDP) Mapping

De Riva et al. [30] performed a similar study to Acosta's and Porta-Sánchez's including 60 consecutive ischemic patients and found that 62% of patients had hidden slow conduction (unmasked by pacing RV 500 ms + a single extra-stimulus VERP+50 ms and defined as conduction delay > 10 ms or block). These patients had better left ventricular function and smaller scar areas on the electroanatomical mapping system. The authors hypothesized that an ablation strategy based on the exclusive elimination of the EDPs can lead to a lower incidence of VT recurrence in the follow up (compared with an LVEF-matched historical cohort from their own institution).

In both Acosta's and De Riva's studies, the distribution of hidden substrate was analyzed and, when possible, compared not only with voltage maps but also cardiac magnetic resonance (CMR). Nearly 20–35% of these EGMs were located in healthy tissue (>1.5 mV bipolar peak to peak) as measured by mapping. This number clearly decreased when the analysis was made by CMR (8–9%), which emphasizes the possibility of a better definition of the VT substrate by CMR and functional substrate mapping as compared to the conventional voltage map. This is consistent with the study by Oduneye [31], in which a real-time CMR-guided electrophysiology system was used observing that abnormal EGMs were seen more often in BZ defined by CMR. One possible explanation for this inaccuracy of the voltage map is that far-field healthy-tissue signals can obscure the near field signals underestimating the scar and hiding the abnormal EGMs from conducting channels, especially in patients with small areas of scar. In those patients, trying to unmask the hidden substrate could be especially relevant but needs to be performed in a systematic way throughout the entire substrate.

3.4. Paced Electrogram Feature Analysis (PEFA)

A better characterization of the EGM response after a close-coupled extra-stimuli was studied by Redfearn et al. [32] both in ischemic and control subjects, defining four different types of response (type 0: no change in the characteristics of the EGM; type I: increased in duration and latency; type II: increase in duration; and type III: increase in latency) and correlated them with the VT isthmus. Programmed stimulation was performed using a RV stimulation 600 ms followed by an extra-stimulus applied every 7th beat: VERP+150 ms, VERP+100 ms, VERP+50 ms. So, three different maps were generated. They observed that the mean duration of the EGMs increased in all patients (significantly more in heart disease patients), but the latency behaved differently: it decreased with the first extra-stimuli (VERP+150 ms) and then (with VERP+100 and VERP+50 ms) increased in healthy patients, but continuously increased in all ischemic population. They also identified that latency (type III) was a common response in both LAVA and non-LAVA areas, type I and II responses found most frequently at VT termination sites.

The PEFA strategy was tested with 10 ischemic patients, targeting type I and II EGMs for radiofrequency, obtaining longer procedures but a lower VT inducibility rate at the end of the procedure in the interventional group as compared to the derivation cohort.

3.5. The Barts Sense Protocol

In an elegant study, focusing on a mechanistic and physiopathologically sound hypothesis, Srinivasan et al. designed an innovative strategy. It is based on the findings by Roelke et al. [33] that found that the VT was most often preceded by late-coupled premature depolarizations. Some years after that, Saeed confirmed these results showing that 66% of VTs were initiated after a single extrasystolic beat [34].

With the idea of closely reproducing this mechanism, the Barts Sense Protocol was designed [35]. A cohort of 30 ischemic patients were prospectively included for VT ablation in two UK centres. Two substrate maps were obtained, one during sinus rhythm and another after pacing the RV every fifth beat to simulate an extra-stimulus close to VERP. There were no significant differences in the scar area when comparing the intrinsic sinus rhythm map vs. the sensed extrasystole maps, but larger areas of late activation were identified after the extrasystole (Figure 3). In 21 patients, 75 VTs were analyzed with high-density activation mapping. This allowed to illustrate that, in 80% of cases, these abnormal EGMs were situated within 10 mm of the critical VT isthmus. Those stable and mappable VTs are not always the most common presentation of VTs in such advanced substrates, but it allowed to highlight that the main advantage of that strategy compared with DEEP mapping and hidden substrate mapping is that is could be slightly more automated, with less manual reannotation of EGMs with a reasonable balance of mean RF time (approximately 30 min).

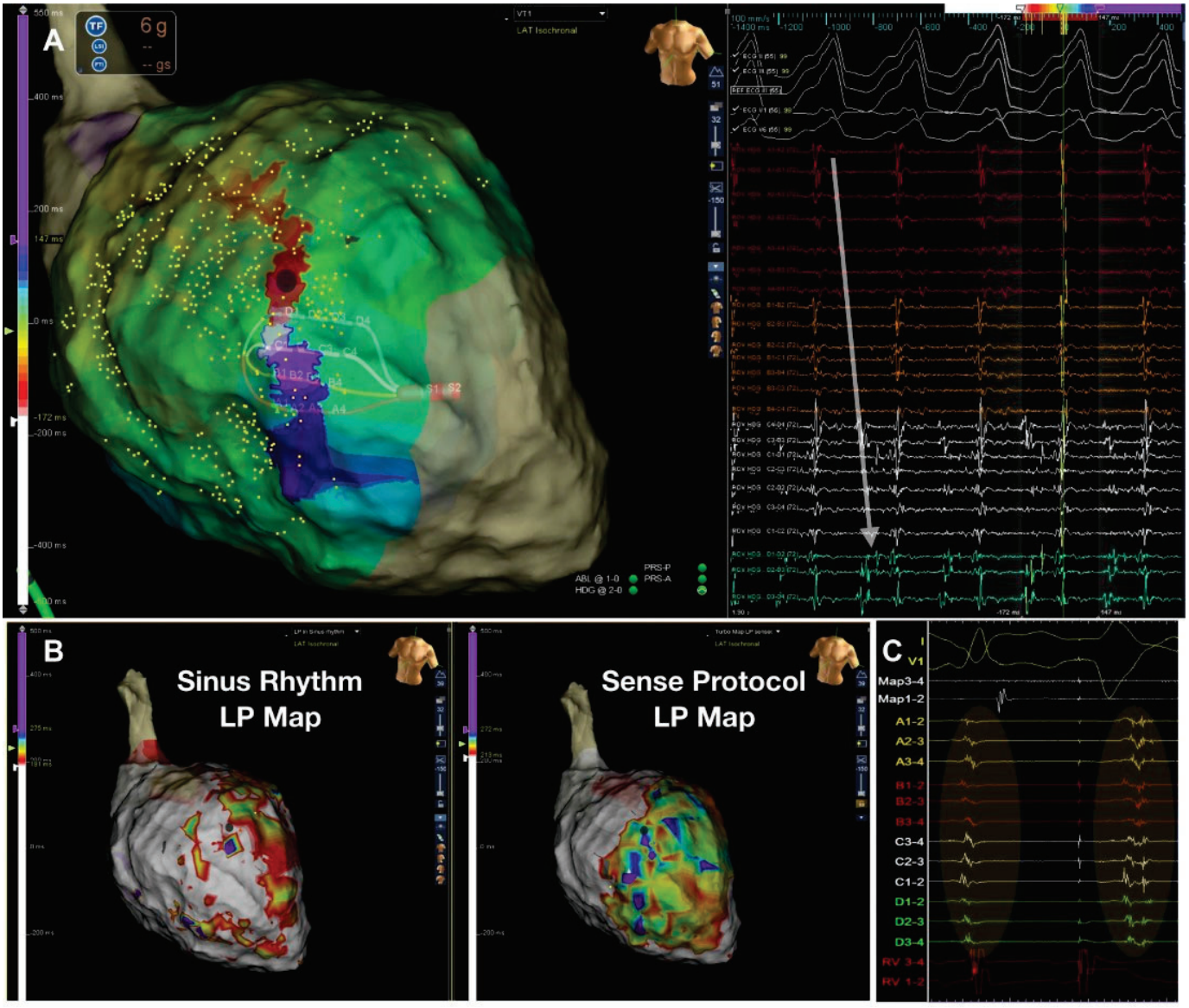

Figure 3. Figure adapted from Srinivasan et al. [35] illustrating the Barts' sensed protocol. (**A**) shows a high-density VT activation map. (**B**) illustrates the 2 activation maps during sinus rhythm (left) with a late potential (LP) color timing map and the activation time during the sensed RV pacing beat ((**B**) right) showing a greater region of LPs during Bart-sense-protocol colocalizing to a greater extent with the mapped isthmus of the induced VT (**A**). (**C**) shows delay and splitting of LPs during sense protocol (second beat) is observed within the region of the diastolic pathway of VT.

3.6. PHYSIO-VT

Conducting channels responsible for VT circuits are based mainly on anatomical features consisting of replacement of cardiomyocytes with fibrosis and persistence of viable cells inside the scar capable of slow conduction. However, the sole presence of scar is insufficient to produce the electroanatomical setting for re-entry. Several other factors, such as cellular coupling, gap junction distribution and function and fiber disarray, can lead to a nonuniform anisotropic conduction [36,37]; whether this is manifested and present independently of the rhythm that the patient presents was the main question for the PHYSIO-VT study. This study, led by Anter E et al., focused on analyzing the location of deceleration zones as assessed by the varying possible wavefronts and whether they identified overlapping areas to target with RF [38]. It was a multicenter study with 85 ischemic patients who underwent VT ablation. Ultra-high density left ventricular

mapping was performed during activation from 3 different wavefronts: SR, RV and LV pacing at 600 ms. Activation mapping during SR was performed in 90.5% patients, during RV or LV in 95.3% and from all 3 directions in 43.5%. In 43.7% patients with left bundle branch block, LV activation during SR was very similar to activation from RV, so in patient with left bundle branch block, an activation map was performed only from SR and LV. The main result was that activation from RV or LV allowed to unmask additional areas of activation slowing as compared with SR maps (mapping during SR identified only 66.2% of all activation slowing) (Figure 4). The total "accumulative slowing area" detected using the 3 different wavefronts was targeted for ablation and interestingly those patients in whom RV and LV mapping was performed in addition to SR mapping presented less incidence of appropriate ICD therapies in the follow up.

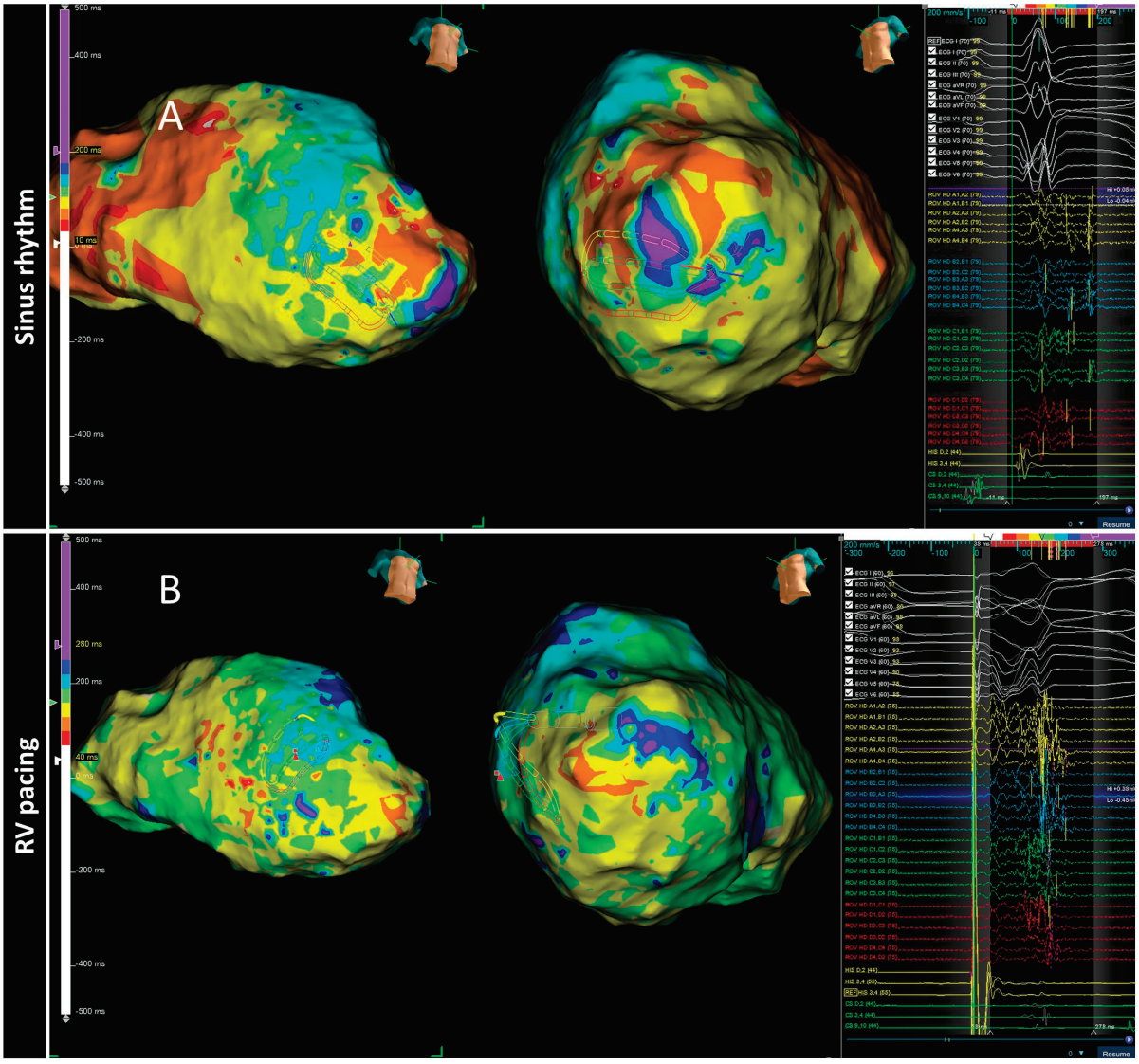

Figure 4. The spatial distribution of activation slowing is influenced by the direction of left ventricular activation. An example of two different maps performed in the same patient during two different ventricular activations: spontaneous sinus rhythm (**A**) and RV pacing (**B**). The general zone of activation slowing was similar between maps, similar to the signals shown on the right side of the panels obtained at each HD grid catheter location depicted, consequently, this area should be ablated according to the PHISIO-VT study [38].

3.7. Isochronal Late Activation Mapping (ILAM)

In 2015, a new substrate-based ablation strategy called ILAM (isochronal late activation mapping) was developed by Irie et al. [39]. These local activation time maps are performed during sinus rhythm (or RV pacing) and based their local activation time annotation on the latest part of the EGM, creating a map with a window starting at the earliest region of activation and ending at the latest site of activation. The overall activation time is divided into eight isochrones represented with 8 different colors, so the thickness of an isochrone is a graphical representation of the conduction velocity (distance/time). In the mechanistic study, Irie et al. [39] found that with that approach, the most likely regions to correlate with the VT isthmus were not the area with the latest activation but slow conduction regions propagating into the latest zone of activation using such an annotation criterion.

Subsequently, in 2019, Aziz et al. [40] presented a study with 120 patients who underwent VT ablation following ILAM approach and identified as relevant the deceleration zones (DZ) that were defined as regions with three different colors in less than 1 cm radius. In most instances (76%), mapping was performed during sinus rhythm and an average of 2 ± 1 DZ were identified. In cases of several DZs, the protocol encouraged to only ablate the primary DZ and check if the patient remained noninducible. In this study, DZs demonstrated a high correlation with VT isthmus, colocalized to successful VT termination sites in 95% of cases (Figure 5) and VT freedom at 12 ± 10 months of follow up was 70%, with ischemic patients having better VT-freedom (80%) than non-ischemic patients (63%).

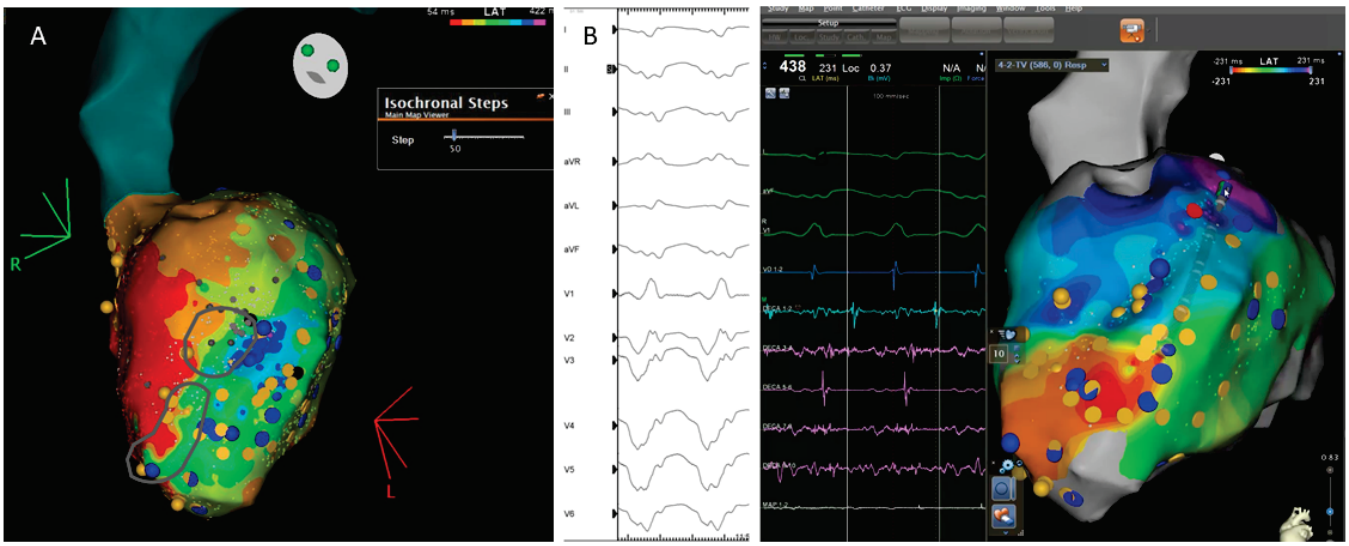

Figure 5. Correlation between the ventricular tachycardia (VT) circuit with critical diastolic pathway (**A**) and deceleration zone (DZ) location during sinus rhythm as depicted during ILAM mapping (**B**). Late isochronal activation map is shown in the left side of the panel (8 isochrones). Two deceleration zones are observed (more than 3 isochrones in less than 1 cm radius) in the anterior wall. The termination site of VT (on the right) colocalized to the DZs.

4. Discussion

VT ablation remains a challenging procedure due to the high recurrence rate and the complex subset of patients experiencing such a life-threatening condition. Voltage maps have initially constituted an alternative to the difficulty of mapping VT due to hemodynamic instability allowing, with the classic thresholds of 0.5–1.5 mV, to characterize the scar and "visualize" the surviving myocardium without the need to induce VT. The low specificity of these voltage channels to accurately identify the VT isthmuses [20] has led to an extensive study of EGMs, especially within the scar, identifying several patterns of so-called late potentials [41] and LAVAs. Elimination of these EGMs has been associated with less VT recurrences in the follow up [12]. Different substrate ablation approaches have been suggested since then, from extensive ablation (scar homogenization) [42] to a more limited

method as scar dechanneling [7], but recurrence rate continued to be non-neglegible [21]. In this sense, VT functional substrate mapping strategies based in the concept of a non-static behavior of the arrhythmic substrate have evolved with the aim to improve outcomes and identify targets for RF that could have been missed with previous "static" mapping. The main findings of the functional VT substrate mappping approaches can be summarized as follows:

1. The arrhythmic substrate is dynamic: its electric properties can change with different pacing settings and that help unmask regions that are critical for re-entry.
    - Late potentials showing decremental properties (DEEPs) seem to be more likely associated with VT isthmuses.
    - A pace protocol based in ventricular extra-stimulus has demonstrated to be able to change the shape and duration of selected EGMs, especially in patients with small scars. Targeting those electrograms that delay from the far field signal could lead to less VT recurrence in the follow up.
    - The direction of the wavefront also has an important impact in the arrhythmic substrate characterization and needs careful evaluation in some patients.
2. The analysis of the timing of the electrograms, not absolute and individually, but relative to the duration of all the ventricular electrograms and their pattern of propagation, has led to the development of a method for the identification of deceleration zones. These DZs have shown a good correlation with VT isthmus.

4.1. Additional Value as Compared to Historical VT Cohorts

VT functional substrate mapping strategies have let us increase the knowledge about the arrhythmic substrate, which in itself represents an important advance. Understanding the arrhythmic substrate as something not static but functional has been shown to be important to improve ablation results. Among the most outstanding findings, using different paced protocols and extra-stimulation, is the definition of new electrograms called DEEPs. These DEEPs have showed to have a greater specificity for identifying VT isthmus compared with conventional non-decremental LPs. The basis for pursuing those potentials with decremental conduction lies in how the ventricular tachycardias in scar-related patients are initiated [23,24]. Multiple studies have shown that this mechanism occurs after a conduction delay (or decrement) preceding unidirectional block and leading to reentry. It is reasonable, therefore, to think that those potentials with decremental capacity are responsible for the arrhythmic circuits.

Similarly, the main mechanism responsible for generating this decremental conduction and inducing VT is the extrastimuli [33,34], so performing map pacing with a stable rhythm might not be the most thorough way to identify all the potentially arrhythmogenic properties of the tissue. The different studies that have tried to define the behavior of the substrate after ventricular extra-stimuli have led to separation of the near-field signal from the far-field signal and the identification of hidden substrate that can potentially be ablated.

With regards to the direction of LV activation, several studies agreed on the greater accuracy to identify LP and LAVAs with an RV and/or LV pacing protocol compared with sinus rhythm. More specifically, it seems that the maximal activation slowing is achieved pacing close to the site where the wavefront first interacts with the infarcted area [38].

In this sense, one of the main messages behind functional VT mapping strategies is that by varying the speed and origin of the stimulation, we change the properties and characteristics of the substrate. Therefore, if we exclusively perform an electroanatomic map in sinus rhythm, without using extra-stimuli, we will have to assume a partial and not complete information about the substrate.

A second important message comes from the perspective of understanding the behavior of electrograms not only by themselves but relating them to neighboring electrograms. DZs are defined as areas not only with delay (that can importantly vary depending on pacing location, i.e., if we pace from the right ventricular apex, the most delayed activation will occur naturally in the lateral wall of the left ventricle) but deceleration. The ILAM has

emerged as a widespread method due to automatic annotation, visual representation of areas of interest and, of course, the higher correlation between DZs and VT isthmus [39], allowing more limited ablation targets.

Despite the important advances shown with functional VT substrate mapping, some limitations must be addressed. First, none of the previous studies focused specifically on the behavior of intramural substrates during functional mapping strategies. This could also be due to the lack of pre-procedural CMR to define the intramural substrate. Undoubtedly, identifying the septal arrhythmic substrate during mapping from both RV and LV endocardium is of importance, and functional mapping of the area and its comparison with a stable rhythm can help define targets for RF [43]. The role of systematic functional mapping in this setting remains unknown. Additionally, non-ischemic substrate tends to be located preferentially in anteroseptal locations, which is an area particularly refractory to RF delivery and substrate elimination. Most of the functional VT substrate studies have included ischemic patients, so the results cannot be readily extrapolated to the non-ischemic population, with a more patchy and non-confluent fibrosis that has always shown poorer outcomes after ablation [1].

4.2. Functional Substrate and High Density Mapping: Ablate More or Ablate Less?

The substrate approach strategy is based on the correct identification of the arrhythmic substrate. The bipolar signal depends on the electrode size, interelectrode spacing, and angle of the incoming wavefront to the mapping catheter, so areas of low-amplitude EGMs as LPs or LAVAs cannot be detected with classical bipolar catheters. High-density catheters have been shown to facilitate the discrimination of LAVAs/LPs, providing a more detailed characterization of the arrhythmic substrate, which is even more important in low-voltage areas [18,44].

Interestingly, less VT recurrence has been reported using this type of catheter [14,17], although the only randomized comparison failed to show an important difference in outcome [45].

Likewise, the functional substrate mapping can help us to unmask the hidden substrate both with extra-stimulus techniques and pacing from different locations, increasing the amount of potentially arrhythmic substrate. Furthermore, this strategy allows to better identify areas more specifically related with VT isthmus, such as DEEPs [27] or DZs [39].

The fact that we can visualize a greater amount of arrhythmic substrate but that at the same time we have tools to better delimit which zones are associated with critical VT circuits has led to some controversy nowadays regarding the preferred ablation strategy.

One possibility is based on performing limited ablation focused on identifying surrogates of the VT isthmus, either using activation mapping if possible, and/or targeting DZs or DEEPs (highly associated with critical isthmus). This could decrease the procedure and radiofrequency times at the expense of leaving an undetermined amount of arrhythmic substrate unablated, which could be responsible for events in the future.

The other perspective relies on a larger ablation approach involving all of the arrhythmic substrate. Techniques such as scar homogenization based on the elimination of the entire substrate have demonstrated less VT inducibility at the end of the procedure and possibly a decrease in VT recurrence rate during follow up [42].

4.3. Current Practice and Future Directions

Advancements in EAM systems and multielectrode catheters have allowed for a semi-automatization of the mapping process with different rhythms and thus have been instrumental in the description and analysis of such functional techniques. All of the most common mapping systems can be configured to allow for the creation in real time of several maps while the catheter is roving the chamber of interest or by replaying the movements and signals of the catheter afterwards and recreating a new map. Those features are present both in the CARTO v3 system (TM), Ensite X (TM) and Rhythmia HDX mapping systems (TM).

A unified and standardized VT ablation strategy has not yet been defined with total reproducibility such as in other standard EP procedures. The lack of randomized studies, the low number of patients included in them, the evolution of the substrate, the difficulty in creating transmural lesions, and several other factors make it difficult to draw clear conclusions about the different mapping methods, so there currently exists a great variability between centers and operators who perform VT ablation procedures.

A multicenter randomized study focused on performing the best possible analysis of the arrhythmic substrate (including the use of high-density mapping catheters, several pacing locations and an extra-stimulus protocol to identify hidden substrate with and without decremental properties and probably the image integration) and then test a more limited or more extensive ablation strategy could lead to clarification of the best approach for VT ablation and eventually improve clinical outcomes.

Author Contributions: Conceptualization, A.P.-S.; writing: S.V.-C.; supervision, A.P.-S. and I.R.-L. All authors have read and agreed to the published version of the manuscript.

Funding: This study was supported by Emile Letang Grant of Hospital Clinic de Barcelona/Instituto de Salud Carlos III (ISCIII) PI20/00693/CB16/11/00354, co-funded by the European Union/CIBERCV16-CB16/11/00354 of Instituto de Salud Carlos III, Madrid and CERCA Programme/Generalitat de Catalunya.

Institutional Review Board Statement: Not applicable.

Informed Consent Statement: Not applicable.

Data Availability Statement: Not applicable.

Conflicts of Interest: The authors declare no conflict of interest.

References

1. Trappe, H.-J.; Brugada, P.; Talajic, M.; Della Bella, P.; Lezaun, R.; Mulleneers, R.; Wellens, H.J. Prognosis of patients with ventricular tachycardia and ventricular fibrillation: Role of the underlying etiology. *J. Am. Coll. Cardiol.* **1988**, *12*, 166–174. [CrossRef]
2. Larsen, G.K.; Evans, J.; Lambert, W.E.; Chen, Y.; Raitt, M.H. Shocks burden and increased mortality in implantable cardioverter-defibrillator patients. *Heart Rhythm* **2011**, *8*, 1881–1886. [CrossRef] [PubMed]
3. Chen, M.; Wu, S.; Yao, Y.; Jiang, J.; Jiang, C.; Xue, Y.; Zhan, X.; Hu, H.; Fu, G.; Gu, K.; et al. Pan-Asia United States PrEvention of Sudden Cardiac Death Catheter Ablation Trial (PAUSE-SCD): Rationale and study design. *J. Interv. Card. Electrophysiol.* **2019**, *57*, 271–278. [CrossRef] [PubMed]
4. Bella, P.D.; Baratto, F.; Vergara, P.; Bertocchi, P.; Santamaria, M.; Notarstefano, P.; Calò, L.; Orsida, D.; Tomasi, L.; Piacenti, M.; et al. Does Timing of Ventricular Tachycardia Ablation Affect Prognosis in Patients With an Implantable Cardioverter Defibrillator? Results From the Multicenter Randomized PARTITA Trial. *Circulation* **2022**, *145*, 1829–1838. [CrossRef] [PubMed]
5. Arenal, A.; Ávila, P.; Jiménez-Candil, J.; Tercedor, L.; Calvo, D.; Arribas, F.; Fernández-Portales, J.; Merino, J.L.; Hernández-Madrid, A.; Fernández-Avilés, F.J.; et al. Substrate Ablation vs Antiarrhythmic Drug Therapy for Symptomatic Ventricular Tachycardia. *J. Am. Coll. Cardiol.* **2022**, *79*, 1441–1453. [CrossRef]
6. Biase, L.D.; Burkhardt, J.D.; Lakkireddy, D.; Carbucicchio, C.; Mohanty, S.; Mohanty, P.; Trivedi, C.; Santangeli, P.; Bai, R.; Forleo, G.; et al. Ablation of Stable VTs Versus Substrate Ablation in Ischemic Cardiomyopathy. *J. Am. Coll. Cardiol.* **2015**, *66*, 2872–2882. [CrossRef]
7. Berruezo, A.; Fernández-Armenta, J.; Andreu, D.; Penela, D.; Herczku, C.; Evertz, R.; Cipolletta, L.; Acosta, J.; Borràs, R.; Arbelo, E.; et al. Scar dechanneling. *Circ. Arrhythmia Elec.* **2015**, *8*, 326–336. [CrossRef]
8. Hsia, H.H.; Callans, D.J.; Marchlinski, F.E. Characterization of Endocardial Electrophysiological Substrate in Patients With Nonischemic Cardiomyopathy and Monomorphic Ventricular Tachycardia. *Circulation* **2003**, *108*, 704–710. [CrossRef]
9. Marchlinski, F.E.; Callans, D.J.; Gottlieb, C.D.; Zado, E. Linear Ablation Lesions for Control of Unmappable Ventricular Tachycardia in Patients with Ischemic and Nonischemic Cardiomyopathy. *Circulation* **2000**, *101*, 1288–1296. [CrossRef]
10. Roca-Luque, I.; Zaraket, F.; Garre, P.; Sanchez-Somonte, P.; Quinto, L.; Borras, R.; Guasch, E.; Arbelo, E.; Tolosana, J.M.; Brugada, J.; et al. Accuracy of standard bipolar amplitude voltage thresholds to identify late potential channels in ventricular tachycardia ablation. *J. Interv. Card. Electrophysiol.* **2022**, 1–11. [CrossRef]
11. Harada, T.; Stevenson, W.G.; Kocovic, D.Z.; Friedman, P.L. Catheter Ablation of Ventricular Tachycardia After Myocardial Infarction: Relation of Endocardial Sinus Rhythm Late Potentials to the Reentry Circuit. *J. Am. Coll. Cardiol.* **1997**, *30*, 1015–1023. [CrossRef]
12. Jaïs, P.; Maury, P.; Khairy, P.; Sacher, F.; Nault, I.; Komatsu, Y.; Hocini, M.; Forclaz, A.; Jadidi, A.S.; Weerasooryia, R.; et al. Elimination of Local Abnormal Ventricular Activities. *Circulation* **2012**, *125*, 2184–2196. [CrossRef]

13. Roca-Luque, I.; Quinto, L.; Sanchez-Somonte, P.; Garre, P.; Alarcón, F.; Zaraket, F.; Vazquez, S.; Prat-Gonzalez, S.; Ortiz-Perez, J.T.; Guasch, E.; et al. Late Potential Abolition in Ventricular Tachycardia Ablation. *Am. J. Cardiol.* **2022**, *174*, 53–60. [CrossRef]
14. Quinto, L.; Sanchez-Somonte, P.; Alarcón, F.; Garre, P.; Castillo, A.; Antonio, R.S.; Borras, R.; Guasch, E.; Arbelo, E.; Tolosana, J.M.; et al. Ventricular tachycardia burden reduction after substrate ablation: Predictors of recurrence. *Heart Rhythm* **2021**, *18*, 896–904. [CrossRef]
15. Anter, E.; Josephson, M.E. Bipolar voltage amplitude: What does it really mean? *Heart Rhythm* **2016**, *13*, 326–327. [CrossRef]
16. Takigawa, M.; Relan, J.; Martin, R.; Kim, S.; Kitamura, T.; Frontera, A.; Cheniti, G.; Vlachos, K.; Massoullié, G.; Martin, C.A.; et al. Effect of bipolar electrode orientation on local electrogram properties. *Heart Rhythm* **2018**, *15*, 1853–1861. [CrossRef]
17. Proietti, R.; Dowd, R.; Gee, L.V.; Yusuf, S.; Panikker, S.; Hayat, S.; Osman, F.; Patel, K.; Salim, H.; Aldhoon, B.; et al. Impact of a high-density grid catheter on long-term outcomes for structural heart disease ventricular tachycardia ablation. *J. Interv. Card. Electrophysiol.* **2021**, *62*, 519–529. [CrossRef]
18. Tschabrunn, C.M.; Roujol, S.; Dorman, N.C.; Nezafat, R.; Josephson, M.E.; Anter, E. High-Resolution Mapping of Ventricular Scar. *Circ. Arrhythmia Electrophysiol.* **2016**, *9*, e003841. [CrossRef] [PubMed]
19. Vázquez-Calvo, S.; Garre, P.; Sánchez-Somonte, P.; Borras, R.; Quinto, L.; Caixal, G.; Lopez, M.P.; Althoff, T.; Guasch, E.; Arbelo, E.; et al. Orthogonal high density mapping with VT isthmus analysis vs. pure substrate VT ablation: A case-control study. *Front. Cardiovasc. Med.* **2022**, *9*, 912335. [CrossRef]
20. Mountantonakis, S.E.; Park, R.E.; Frankel, D.S.; Hutchinson, M.D.; Dixit, S.; Cooper, J.; Callans, D.; Marchlinski, F.E.; Gerstenfeld, E.P. Relationship Between Voltage Map "Channels" and the Location of Critical Isthmus Sites in Patients with Post-Infarction Cardiomyopathy and Ventricular Tachycardia. *J. Am. Coll. Cardiol.* **2013**, *61*, 2088–2095. [CrossRef]
21. Tung, R.; Vaseghi, M.; Frankel, D.S.; Vergara, P.; Di Biase, L.; Nagashima, K.; Yu, R.; Vangala, S.; Tseng, C.-H.; Choi, E.-K.; et al. Freedom from recurrent ventricular tachycardia after catheter ablation is associated with improved survival in patients with structural heart disease: An International VT Ablation Center Collaborative Group study. *Heart Rhythm* **2015**, *12*, 1997–2007. [CrossRef]
22. Ghanbari, H.; Baser, K.; Yokokawa, M.; Stevenson, W.; Della Bella, P.; Vergara, P.; Deneke, T.; Kuck, K.-H.; Kottkamp, H.; Fei, S.; et al. Noninducibility in Postinfarction Ventricular Tachycardia as an End Point for Ventricular Tachycardia Ablation and Its Effects on Outcomes. *Circ. Arrhythmia Electrophysiol.* **2014**, *7*, 677–683. [CrossRef]
23. Lammers, W.J.; Kirchhof, C.; Bonke, F.I.; Allessie, M.A. Vulnerability of rabbit atrium to reentry by hypoxia. Role of inhomogeneity in conduction and wavelength. *Am. J. Physiol. Heart Circ. Physiol.* **1992**, *262*, H47–H55. [CrossRef]
24. Segal, O.R.; Chow, A.W.C.; Peters, N.S.; Davies, D.W. Mechanisms that initiate ventricular tachycardia in the infarcted human heart. *Heart Rhythm* **2010**, *7*, 57–64. [CrossRef]
25. Jackson, N.; Gizurarson, S.; Viswanathan, K.; King, B.; Massé, S.; Kusha, M.; Porta-Sanchez, A.; Jacob, J.R.; Khan, F.; Das, M.; et al. Decrement Evoked Potential Mapping: Basis of a Mechanistic Strategy for Ventricular Tachycardia Ablation. *Circ. Arrhythmia Electrophysiol.* **2015**, *8*, 1433–1442. [CrossRef]
26. Tusscher, K.H.W.J.T.; Noble, D.; Noble, P.J.; Panfilov, A.V. A model for human ventricular tissue. *Am. J. Physiol. Heart Circ. Physiol.* **2004**, *286*, H1573–H1589. [CrossRef]
27. Porta-Sanchez, A.; Jackson, N.; Lukac, P.; Kristiansen, S.B.; Nielsen, J.M.; Gizurarson, S.; Massé, S.; Labos, C.; Viswanathan, K.; King, B.; et al. Multicenter Study of Ischemic Ventricular Tachycardia Ablation with Decrement-Evoked Potential (DEEP) Mapping with Extra Stimulus. *JACC Clin. Electrophysiol.* **2018**, *4*, 307–315. [CrossRef]
28. Acosta, J.; Andreu, D.; Penela, D.; Cabrera, M.; Carlosena, A.; Korshunov, V.; Vassanelli, F.; Borras, R.; Martínez, M.; Fernández-Armenta, J.; et al. Elucidation of hidden slow conduction by double ventricular extrastimuli: A method for further arrhythmic substrate identification in ventricular tachycardia ablation procedures. *Europace* **2016**, *20*, 337–346. [CrossRef]
29. Acosta, J.; Soto-Iglesias, D.; Jáuregui, B.; Armenta, J.F.; Penela, D.; Frutos-López, M.; Arana-Rueda, E.; Pedrote, A.; Mont, L.; Berruezo, A. Long-term outcomes of ventricular tachycardia substrate ablation incorporating hidden slow conduction analysis. *Heart Rhythm* **2020**, *17*, 1696–1703. [CrossRef]
30. Riva, M.D.; Naruse, Y.; Ebert, M.; Androulakis, A.F.A.; Tao, Q.; Watanabe, M.; Wijnmaalen, A.P.; Venlet, J.; Brouwer, C.; Trines, S.A.; et al. Targeting the Hidden Substrate Unmasked by Right Ventricular Extrastimulation Improves Ventricular Tachycardia Ablation Outcome After Myocardial Infarction. *JACC Clin. Electrophysiol.* **2018**, *4*, 316–327.
31. Oduneye, S.O.; Pop, M.; Shurrab, M.; Biswas, L.; Ramanan, V.; Barry, J.; Crystal, E.; A Wright, G. Distribution of abnormal potentials in chronic myocardial infarction using a real time magnetic resonance guided electrophysiology system. *J. Cardiovasc. Magn. Reson.* **2015**, *17*, 27. [CrossRef] [PubMed]
32. Shariat, M.H.; Gupta, D.; E Gul, E.; Glover, B.; Hashemi, J.; Abdollah, H.; Baranchuk, A.; Simpson, C.; A Michael, K.; Redfearn, D.P.; et al. Ventricular substrate identification using close-coupled paced electrogram feature analysis. *Europace* **2018**, *21*, 492–501. [CrossRef] [PubMed]
33. Roelke, M.; Garan, H.; McGovern, B.A.; Ruskin, J.N. Analysis of the initiation of spontaneous monomorphic ventricular tachycardia by stored intracardiac electrograms. *J. Am. Coll. Cardiol.* **1994**, *23*, 117–122. [CrossRef]
34. Saeed, M.; Link, M.S.; Mahapatra, S.; Mouded, M.; Tzeng, D.; Jung, V.; Contreras, R.; Swygman, C.; Homoud, M.; Estes, N.; et al. Analysis of intracardiac electrograms showing monomorphic ventricular tachycardia in patients with implantable cardioverter-defibrillators. *Am. J. Cardiol.* **2000**, *85*, 580–587. [CrossRef]

35. Srinivasan, N.T.; Garcia, J.; Schilling, R.J.; Ahsan, S.; Babu, G.G.; Ang, R.; Dhinoja, M.B.; Hunter, R.J.; Lowe, M.; Chow, A.W.; et al. Multicenter Study of Dynamic High-Density Functional Substrate Mapping Improves Identification of Substrate Targets for Ischemic Ventricular Tachycardia Ablation. *JACC Clin. Electrophysiol.* **2020**, *6*, 1783–1793. [CrossRef]
36. Peters, N.S.; Coromilas, J.; Hanna, M.S.; Josephson, M.E.; Costeas, C.; Wit, A.L. Characteristics of the Temporal and Spatial Excitable Gap in Anisotropic Reentrant Circuits Causing Sustained Ventricular Tachycardia. *Circ. Res.* **1998**, *82*, 279–293. [CrossRef]
37. Rohr, S. Myofibroblasts in diseased hearts: New players in cardiac arrhythmias? *Heart Rhythm* **2009**, *6*, 848–856. [CrossRef]
38. Anter, E.; Neuzil, P.; Reddy, V.Y.; Petru, J.; Park, K.M.; Sroubek, J.; Leshem, E.; Zimetbaum, P.J.; Buxton, A.E.; Kleber, A.G.; et al. Ablation of Reentry-Vulnerable Zones Determined by Left Ventricular Activation from Multiple Directions: A Novel Approach for Ventricular Tachycardia Ablation: A Multicenter Study (PHYSIO-VT). *Circ. Arrhythmia Electrophysiol. Lippincott Williams Wilkins* **2020**, *13*, 539–550. [CrossRef]
39. Irie, T.; Yu, R.; Bradfield, J.S.; Vaseghi, M.; Buch, E.F.; Ajijola, O.; Macias, C.; Fujimura, O.; Mandapati, R.; Boyle, N.G.; et al. Relationship Between Sinus Rhythm Late Activation Zones and Critical Sites for Scar-Related Ventricular Tachycardia. *Circ. Arrhythmia Electrophysiol.* **2015**, *8*, 390–399. [CrossRef]
40. Aziz, Z.; Shatz, D.; Raiman, M.; Upadhyay, G.A.; Beaser, A.D.; Besser, S.A.; Shatz, N.A.; Fu, Z.; Jiang, R.; Nishimura, T.; et al. Targeted Ablation of Ventricular Tachycardia Guided by Wavefront Discontinuities during Sinus Rhythm: A New Functional Substrate Mapping Strategy. *Circulation* **2019**, *140*, 1383–1397.
41. Arenal, A.; Hernández, J.; Calvo, D.; Ceballos, C.; Atéa, L.; Datino, T.; Atienza, F.; González-Torrecilla, E.; Eidelman, G.; Miracle, A.; et al. Safety, Long-Term Results, and Predictors of Recurrence After Complete Endocardial Ventricular Tachycardia Substrate Ablation in Patients With Previous Myocardial Infarction. *Am. J. Cardiol.* **2013**, *111*, 499–505. [CrossRef] [PubMed]
42. Biase, L.D.; Santangeli, P.; Burkhardt, D.J.; Bai, R.; Mohanty, P.; Carbucicchio, C.; Dello Russo, A.; Casella, M.; Mohanty, S.; Pump, A.; et al. Endo-epicardial homogenization of the scar versus limited substrate ablation for the treatment of electrical storms in patients with ischemic cardiomyopathy. *J. Am. Coll. Cardiol.* **2012**, *60*, 132–141. [CrossRef] [PubMed]
43. Desjardins, B.; Yokokawa, M.; Good, E.; Crawford, T.; Latchamsetty, R.; Jongnarangsin, K.; Ghanbari, H.; Oral, H.; PelosiJr, F.; Chugh, A.; et al. Characteristics of Intramural Scar in Patients with Nonischemic Cardiomyopathy and Relation to Intramural Ventricular Arrhythmias. *Circ. Arrhythmia Electrophysiol.* **2013**, *6*, 891–897. [CrossRef]
44. Okubo, K.; Frontera, A.; Bisceglia, C.; Paglino, G.; Radinovic, A.; Foppoli, L.; Calore, F.; Della Bella, P. Grid Mapping Catheter for Ventricular Tachycardia Ablation. *Circ. Arrhythmia Electrophysiol.* **2019**, *12*, e007500. [CrossRef] [PubMed]
45. Acosta, J.; Penela, D.; Andreu, D.; Cabrera, M.; Carlosena, A.; Vassanelli, F.; Alarcón, F.; Soto-Iglesias, D.; Korshunov, V.; Borras, R.; et al. Multielectrode vs. point-by-point mapping for ventricular tachycardia substrate ablation: A randomized study. *Europace* **2017**, *20*, 512–519. [CrossRef] [PubMed]

Current Heart Failure Reports (2023) 20:237–253
https://doi.org/10.1007/s11897-023-00608-y

Management of Ventricular Arrhythmias in Heart Failure

Sara Vázquez-Calvo[1,2] · Ivo Roca-Luque[1,2] · Till F. Althoff[1,2]

Accepted: 8 May 2023 / Published online: 25 May 2023

Abstract

Purpose of Review Despite substantial progress in medical and device-based heart failure (HF) therapy, ventricular arrhythmias (VA) and sudden cardiac death (SCD) remain a major challenge. Here we review contemporary management of VA in the context of HF with one particular focus on recent advances in imaging and catheter ablation.

Recent Findings Besides limited efficacy of antiarrhythmic drugs (AADs), their potentially life-threatening side effects are increasingly acknowledged. On the other hand, with tremendous advances in catheter technology, electroanatomical mapping, imaging, and understanding of arrhythmia mechanisms, catheter ablation has evolved into a safe, efficacious therapy. In fact, recent randomized trials support early catheter ablation, demonstrating superiority over AAD. Importantly, CMR imaging with gadolinium contrast has emerged as a central tool for the management of VA complicating HF: CMR is not only essential for an accurate diagnosis of the underlying entity and subsequent treatment decisions, but also improves risk stratification for SCD prevention and patient selection for ICD therapy. Finally, 3-dimensional characterization of arrhythmogenic substrate by CMR and imaging-guided ablation approaches substantially enhance procedural safety and efficacy.

Summary VA management in HF patients is highly complex and should be addressed in a multidisciplinary approach, preferably at specialized centers. While recent evidence supports early catheter ablation of VA, an impact on mortality remains to be demonstrated. Moreover, risk stratification for ICD therapy may have to be reconsidered, taking into account imaging, genetic testing, and other parameters beyond left ventricular function.

Keywords Heart failure · Ventricular tachycardia · Sudden cardiac death · Catheter ablation · Imaging · Cardiac implantable electronic devices

Introduction

Irrespective of the underlying etiology, heart failure (HF) is frequently complicated by ventricular arrhythmias (VAs) that are associated with adverse outcome [1–2]. In fact, while advances in medical and device-based HF therapies have substantially reduced mortality over the last decades, VAs and sudden cardiac death (SCD) remain the main cause of death in HF patients [3–4].

Not infrequently, VAs are the first manifestation of a concealed structural heart disease that is only unmasked by comprehensive diagnostics including late gadolinium enhancement (LGE) cardiac magnetic resonance (CMR) imaging [5]. VAs and HF are tightly intertwined with a bidirectional causal relationship; while structural heart disease and HF constitute an arrhythmogenic substrate, VAs can in turn cause or aggravate HF [1, 2].

This review focuses on the diagnostic and therapeutic measures in patients with HF and VA, linking etiology and specific arrhythmia mechanisms to effective treatment approaches. Further, this review highlights the importance of imaging to guide management of VAs in the context of HF.

Epidemiology and Etiology

VAs are common in HF, with incremental prevalence in advanced disease stages [1]. The prevalence of non-sustained VAs, like frequent premature ventricular contractions (PVCs) or non-sustained ventricular tachycardias (VTs), among HF patients has been reported to be as high as 50%

✉ Till F. Althoff
althoff.tf@gmail.com

[1] Arrhythmia Section, Cardiovascular Institute (ICCV), CLÍNIC Barcelona University Hospital, C/Villarroel N° 170, 08036 Barcelona, Catalonia, Spain

[2] Institut d'Investigacions Biomèdiques August Pi I Sunyer (IDIBAPS), Barcelona, Catalonia, Spain

and above, whereas potentially life-threatening sustained VA are less frequent (< 2% per year). Of note, even non-sustained VTs are associated with accelerated disease progression and increased mortality [6, 7, 8•].

The high prevalence of VA among HF patients and their association with accelerated disease progression and increased mortality can (in part) be explained by a bidirectional causality: The structural and electrical myocardial remodeling processes in patients with HF include cardiomyocyte dysfunction or death and replacement fibrosis, as well as altered expression of ion channels and disturbed electrical properties. These changes in conjunction with metabolic dysbalance result in altered depolarization and repolarization properties as well as regionally abnormal propagation of the electrical wave-front (e.g., non-uniform anisotropy, slow conduction, or conduction block) that constitute the arrhythmogenic substrate for VAs. Vice versa, VAs can contribute to HF progression through hemodynamic impairment, with peripheral hypoperfusion resulting in neurohormonal as well as metabolic dysbalance and maladaptive adverse remodeling. These processes may generate a vicious circle that propels HF progression, further increasing susceptibility for Vas [2].

Against this background, it is not surprising that indicators of advanced HF such as NYHA functional class IV, severe impairment of left ventricular (LV) function (left ventricular ejection fraction, LVEF < 20–25%), or renal dysfunction are associated with higher risk of SCD [8•, 9, 10]. Likewise, the extent of myocardial fibrotic remodeling as assessed by LGE-CMR is predictive of VAs and SCD [11•, 12, 13•, 14•].

Diagnostic Evaluation

ECG

Obviously, an ECG-documentation of the VA is of utmost importance, and a 12-lead ECG must be persued for the correct diagnosis as well as the differentiation of distinct VA subtypes and localization of the mechanistic VA origin, as this has immense impact on risk stratification and therapeutic approaches. In the case of premature ventricular contractions, Holter ECG recordings should be performed at different time points for valid estimation of the arrhythmia burden. In patients with suspected but infrequent VAs or unexplained syncope, an implantable loop recorder may be considered to accomplish VA documentation [1, 15].

Specific Anamnesis and Genetic Testing

Diagnostic evaluation of HF patients with VA should include a thorough anamnesis with a special emphasis on family history, followed by genetic testing if first-degree relatives suffered from dilated cardiomyopathy or premature sudden cardiac death. In particular, mutations in the LMNA-gene coding for lamin A/C (5–10% of DCM patients) are associated with a substantially elevated risk of arrhythmias, conduction disease, and SCD as well as an accelerated progression to end-stage HF, thus warranting specific preventive measures [1, 15].

Imaging

Echocardiography Echocardiography plays a central role in the diagnosis and management of HF patients providing comprehensive structural and functional information. Serial echo-studies at follow-up visits can further help to evaluate disease progression and the effect of therapeutic measures.

Cardiac Magnetic Resonance CMR provides not only highly accurate functional and structural information but also characterizes myocardial tissue properties and therefore adds substantial diagnostic value. Using gadolinium-based contrast agents, CMR can detect and localize myocardial injury or inflammation as well as fibrotic remodeling in a 3-dimensional manner. These contrast agents diffuse freely into the intersitium, but they cannot cross intact cell membranes, and thus accumulate in the extracellular space. LGE-CMR makes use of the expansion of extracellular space and thus increased volume of distribution for the contrast agent that is associated with tissue fibrosis [16, 17]. As gadolinium-based contrast agents reduce the T1 relaxation time of adjacent tissue, LGE results in an increased signal intensity in T1-weighted MR sequences. It is noteworthy though that LGE is not specific for fibrotic tissue, but can also reflect other pathological processes associated with an expansion of the extracellular space like inflammation and edema [18].

Of note, different HF entities typically present with distinct patterns of regional distribution and transmural dispersion of LGE. LGE-CMR is therefore an important tool to specify the etiology and particular entity of HF, which commonly remains elusive after anamnestic and echocardiographic evaluation (Fig. 1). Thus, LGE-CMR is particularly useful in HF patients with non-ischemic etiology or concealed structural heart disease that may otherwise be overlooked [5, 19]. However, it is noteworthy that even with LGE-CMR, uncertainty may remain. In case of doubt, the diagnosis ought to be carefully reconsidered based on anamnestic re-evaluation and additional studies. In particular, inflammatory processes like sarcoidosis that is typically associated with VAs and may require specific therapy should be ruled out using PET-CT and biopsy [1].

Moreover, LGE-CMR has the capability to detect and precisely localize areas of fibrotic remodeling that harbor arrhythmogenic substrate. In fact, qualitative or quantitative assessment of LGE has consistently shown

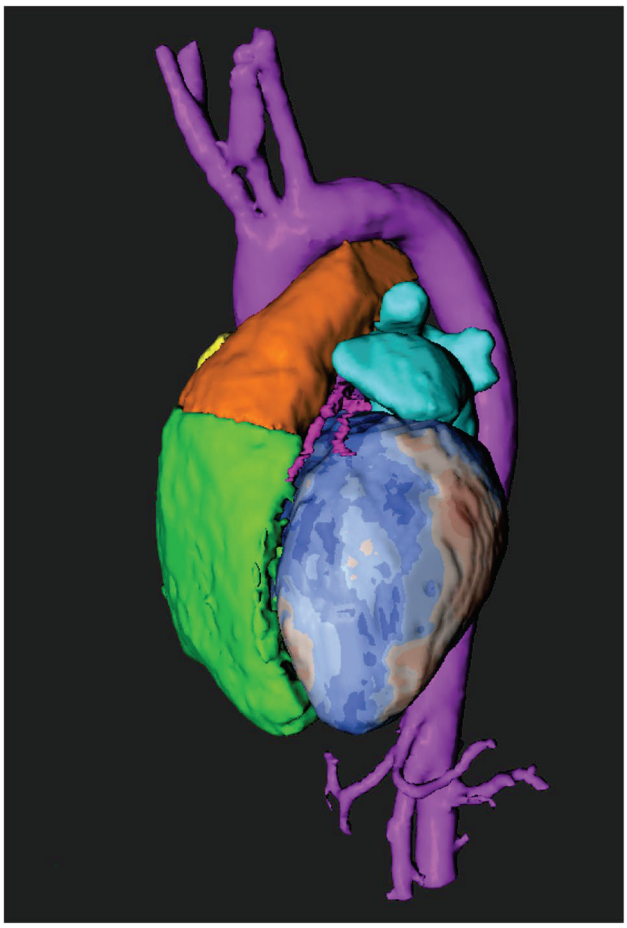

Fig. 1 CMR for the differential diagnosis of distinct cardiomyopathies. **A** Ischemic cardiomyopathy with inferior aneurysm of the left ventricle with LGE indicative of a previous transmural myocardial infarction. **B** Ischemic cardiomyopathy with typical subendocardial LGE indicative of a post-myocardial infarction scar. **C** Arrhythmogenic right ventricular cardiomyopathy (ARVC) with LGE indicating transmural fibrosis in the right ventricular outflow tract and the right ventricular free wall. Of note, the left ventricle is affected as well, with predominantly subepicardial LGE in the anteroseptal and anterior regions. **D** Constrictive pericarditis with pericardial thickening and hypointense areas reflecting pericardial calcification. Differential diagnosis of left ventricular hypertrophy (HCM vs. amyloidosis vs. M. Fabry). **E** Hypertrophic cardiomyopathy: asymmetric septal hypertrophy with a maximum thickness of 30 mm and heterogeneous fibrosis in the anteroseptal left ventricle. **F** Sarcoidosis with extensive LGE affecting the right ventricular diaphragmatic wall and the septum, extending subepicardially towards the left lateral wall (sparing the left ventricular subendocardium). **G** Fabry's disease with severe left ventricular hypertrophy most prominent in septal segments with inferolateral intramyocardial fibrosis and reduced native myocardial T1 (840 ms) reflecting decreased T1 longitudinal relaxation times due to glycosphingolipid deposition in T1 mapping (**H**)

to improve current predictive models for SCD and might play an important role in the risk stratification of HF patients [11•, 12, 13•, 14•, 20, 21, 22]. Finally, dedicated postprocessing software for 3-dimensional LGE quantification allows for accurate localization of arrhythmogenic substrate and definition of ablation targets, which is already used in clinical practice to plan and direct catheter ablation [23, 24, 25, 26, 27•, 28, 29, 30]. LGE-CMR has thus emerged as an invaluable tool for the management of VA in the context of HF.

Risk Stratification and Prevention of Sudden Cardiac Death

Epidemiology

VAs and SCD are responsible for a high proportion of deaths among patients with HF. In fact, SCD accounts for approximately 50% of all cardiovascular deaths. Both incidence and etiology of VAs and SCD are age-dependent. In the younger age group (< 50 years), the SCD incidence is below 50 per 100,000 patient years, and inherited electrical diseases and non-ischemic cardiomyopathies appear to be the predominant causes. The incidence of SCD is substantially higher in the elderly (100–200 per 100,000 patient years) with ischemic cardiomyopathy being the most common etiological factor [1, 2].

Primary Prevention

While general HF treatments including medical therapy and device-based cardiac resynchronization therapy have been shown to reduce SCD risk, ICDs were developed exclusively to prevent SCD by terminating potentially lethal VAs through direct current shocks or antitachycardic pacing [3]. Indeed, ICD therapy can effectively prevent SCD caused by VAs; however, both the relatively high number needed to treat in primary prevention and the risk of device-associated complications have to be considered [9, 10, 31, 32, 33, 34, 35]. Complications include inappropriate discharges, lead fractures, and device-related infections. Subcutaneous ICDs (S-ICD) obviate the risks associated with transvenous leads, but as they are devoid of pacing leads, they are obviously not capable of providing anti-bradycardic pacing, antitachycardic pacing, or cardiac resynchronization therapy [36•, 37]. Finally, the risk of SCD does not only have to be weighed against device-related complications, but also against the competing risk of non-arrhythmic death. Taken together, individual risk stratification for the numerous different HF sub-entities and distinct underlying etologies is complex, and we refer to recent guidelines for specific recommendations [1, 15].

Today, indication for ICD therapy is still largely based on LVEF and functional status (NYHA classification). Generally, ICD implantation for primary prophylaxis should be considered in symptomatic patients (NYHA II or III) with severe LV dysfunction (LVEF ≤ 35%). This recommendation applies to both patients with ischemic and non-ischemic

cardiomyopathy, although evidence is less robust in the context of non-ischemic cardiomyopathies [9, 10, 31, 32, 34, 35]. In the context of coronary artery disease (CAD) and ischemic cardiomyopathy, ICD therapy is also recommended in asymptomatic patients (NYHA I) if LVEF is ≤ 30%, based on a prognostic benefit demonstrated in the MADIT II trial [10]. It is important to note that, to avoid overtreatment, for risk stratification, LVEF should be determined after at least 3 months of optimal medical HF therapy and a minimum of 6 weeks after an acute myocardial infarction [4, 33]. Moreover, the need for pacing or a potential benefit from cardiac resynchronization therapy must be evaluated prior to implantation to choose the adequate type of device (single/dual chamber ICD, CRT-defibrillator, or S-ICD) [38].

In patients with non-ischemic cardiomyopathies, further diagnostic evaluation including LGE-CMR, electrophysiological studies (to test inducibility of sustained VTs), or implantable loop recorders may be warranted in cases of mildly or moderately reduced ejection fraction, particularly if they present with additional risk factors like non-sustained VTs or unexplained syncope [31].

While LVEF is a generally applicable and robust marker of increased SCD risk, its limited predictive capacity is also widely acknowledged. With a relatively low positive predictive value, LVEF as only criterion will inevitably lead to overtreatment in patients with severely reduced systolic function, and—perhaps even more worrisome—it will result in undertreatment of patients at risk for SCD despite preserved or only moderately reduced systolic function, because of the limited sensitivity. Against this background, immense research efforts are focusing on alternative or complementary predictors and models, and a growing body of evidence supports LGE-CMR for refined risk stratification [11•, 12, 13•, 14•, 20, 21, 22]. LGE-CMR-based assessment of arrhythmogenic substrate and the extent or pattern of LGE have consistently shown to improve predictive models and risk stratification for primary and secondary prevention of SCD throughout the different HF sub-entities and across a wide spectrum of LVEF. Both for ischemic and non-ischemic cardiomyopathies, LGE was demonstrated to be a strong and independent predictor of all-cause death and SCD [11•, 12, 14•, 20, 21, 22].

However, despite firm evidence establishing the predictive value of LGE-CMR in SCD risk stratification, LGE-CMR-based approaches to guide ICD treatment decisions have not been evaluated in randomized clinical trials (RCTs). Current guidelines recommend LGE-CMR to establish a diagnosis in patients with suspected non-ischemic cardiomyopathy, and they state that SCD risk stratification based on LGE can be useful [1, 15]. Moreover, a broad consensus on standardized LGE-CMR approaches and LGE-based parameters are lacking. The ongoing prospective randomized CMR–GUIDE trial and the PROFID trials are addressing some of these issues [39, 40].

It has become evident in contemporary HF trials that the considerable advances in HF therapy with novel drug classes and device-based cardiac resynchronization did not only reduce all-cause mortality, but also lead to a substantial decrease in SCD in HF patients over the last decades [3]. This will inevitably affect the balance between risk of SCD and competing risks of death, and we therefore have to assume that the risk–benefit-ratio of ICD therapy has considerably changed since the seminal RCTs (MADIT I and II, MUSTT, SCD-HFT, and DEFINITE) that established ICD therapy for primary prevention between 1996 and 2005 [9, 10, 31, 35]. The fact that in the more recent DANISH trial ICD therapy reduced SCD but not overall mortality likely reflects both the lower SCD incidence with contemporary medical therapy including CRT and the implicit increase in the relative weight of competing risks in terms of non-arrhythmic death [3, 21]. One might argue of course that contemporary trials found a lower SCD incidence, because they included patients with less severe disease, and indeed, this is evidenced by lower functional class or NTproBNP levels of the participants. But then, consequently, we must also not extrapolate data from early ICD trials like MADIT II or SCD-HeFT to contemporary populations with more moderate disease, as it is currently being performed [3, 41]. Against this background, reconsideration of our current practice and novel RCTs to re-evaluate the benefits of ICD therapy appear warranted.

Secondary Prevention

In SCD survivors, ICD therapy for secondary prevention is recommended. Outside special circumstances like acute myocardial infarction, ICD implantation is also recommended in patients with documented VF or hemodynamically not-tolerated VT and may even be considered in case of a putatively reversible cause [1, 15, 42, 43, 44, 45]. While ICD implantation may also be considered in patients with hemodynamically tolerated VT, evidence in this setting is scarce; in fact, randomized trials failed to demonstrate benefit from ICD therapy in patients with an LVEF ≥ 35% [44]. Of note, several smaller studies suggest that catheter ablation of sustained monomorphic VTs should be considered for SCD prevention in CAD patients with preserved or moderately reduced systolic function, even without ICD backup [1, 46, 47].

However, there is still a large degree of uncertainty and evidence gaps regarding ICD therapy in patients with hemodynamically tolerated VTs. While LGE-CMR can discriminate high-risk and low-risk patients in this setting, and may thus be useful for risk stratification, interventional trials testing such LGE-CMR-guided approaches are lacking [12, 48].

Acute Management of Ventricular Arrhythmias

In the acute setting, reversible causes of VA must be taken into account; in particular, ischemia should be ruled out. Further, electrolyte imbalances like hypokalemia that promote VA and are common among HF patients should be detected and corrected. Likewise, if drug-induced VA are suspected, agents that can cause electrolyte imbalance (e.g., thiazide and loop diuretics) and QT or QRS prolongation, respectively, should be avoided or withdrawn. In the case of torsade-de-point tachycardias, those measures are of particular importance, and it is noteworthy that intravenous magnesium is often effective even in the absence of hypomagnesemia [49]. In refractory cases, measures to elevate the basal heart rate and suppress the tachycardias, like isoproterenol (isoprenaline) or transvenous pacing, may be indicated.

In patients with structural heart disease, sustained monomorphic VTs are the most commonly encountered VA. Timely synchronized electric cardioversion and—if required—advanced life support should be performed. If hemodynamically tolerated, recording of a 12-lead ECG prior to cardioversion is critical for subsequent treatment decisions. Alternatively, pharmacological cardioversion with i.v. procainamide or i.v. amiodarone can be attempted in hemodynamically stable patients. While—if available—procainamide is the preferred choice in patients with advanced heart failure, both agents display negative inotropic effects. Thus, particularly, in patients with advanced heart failure, those hemodynamic effects must be balanced against the risk of anesthesia for electrical cardioversion [1, 15].

Electrical Storm

The term electrical storm describes incessantly recurring VA episodes or repetitive ICD discharges (by definition ≥ 3/24 h). In case of multiple ICD discharges, inadequate ICD therapies should be ruled out and ICD programmation optimized. In the absence of an appropriate programmer, ICD therapies can be disabled by posing a magnet over the device. In patients with repetitive ICD shocks, sympathetic activation plays an important role in arrhythmogenesis aggravating and perpetuating the condition. Therefore, sedation and i.v. betablocker therapy are recommended to lower sympathetic tone and its effects in order to interrupt the vicious circle [1]. In case of sustained monomorphic VTs, the most common cause of electrical storm, particularly in patients with structural heart disease, amiodarone is the antiarrhythmic drug (AAD) of choice, although different VA subtypes and specific underlying pathologies may warrant alternative AADs including procainamide, lidocaine, or quinidine [1, 15]. Patients with recurrent VA, refractory to antiarrhythmic therapy, may require deep sedation and intubation. If this is not sufficient, adjunct approaches to lower sympathetic tone including percutaneous blockade of the stellate ganglion, epidural anesthesia, or surgical cardiac sympathetic denervation may be considered as well [50, 51, 52, 53, 54].

Ultimately, if the abovementioned measures fail to achieve electrical stability, catheter ablation may provide a definite treatment, particularly for monomorphic VT, and should be considered even in the acute setting. Of note, mechanical circulatory support may be required if hemodynamic stabilization cannot be accomplished with conservative measures or to provide additional hemodynamic support during the ablation procedure [55, 56]. Finally, implantation of a left ventricular assist device (LVAD) or cardiac transplant can be a last resort if definite electrical and/or hemodynamic stability is not accomplished [1, 15, 4, 57].

Chronic Management of Ventricular Arrhythmias

General Considerations

Potentially life-threatening VAs in HF patients further complicate an already complex condition, which is why their management should ideally be reserved to specialized centers offering multidisciplinary care involving cardiac electrophysiologists, HF specialists, interventional cardiologists, cardiac surgeons, imaging specialists, and anesthesiologists where needed. Generally, in the absence of acute reversible causes, the primary objective should be an etiology-oriented treatment of the underlying disease, emphasizing the need for a comprehensive diagnostic evaluation—ideally including LGE-CMR [1, 15]. Further, all patients should receive optimal HF therapy, including the maximum tolerated dose of ACE-I/ARB/ARNIs, MRAs, beta-blockers, and SGLT2 inhibitors in those with reduced LV systolic function [4].

Antiarrhythmic Drugs

In theory, numerous AADs are available for chronic VA treatment (amiodarone, sotalol, propafenone, mexiletine, procainamide, or flecainide), but in the context of HF the repertoire is mostly limited to betablockers and amiodarone, because of potential proarrhythmic effects, particularly of class I sodium-channel–blocking drugs [58, 59, 60]. Of note, amiodarone can have proarrhythmic effects too, albeit less frequent. The use of amiodarone, on the other hand, is limited by its very specific and distinct profile of adverse effects (e.g., photosensitivity, corneal deposits, hypothyroidism, hyperthyroidism, pulmonary toxicity, hepatotoxicity, polyneuropathy, skin discoloration).

In patients with ICD, in whom proarrhythmic risk is less relevant, other AADs like sotalol or the class I sodium channel blocker mexiletine may be considered [61, 62, 63, 64]. Of note, mexiletine is also commonly used as an adjunct to class III

AADs like amiodarone or sotalol, although supporting evidence from RCTs is lacking [62]. However, both sotalol and mexiletine have been associated with worsening HF and should therefore be avoided in patients with severe ventricular dysfunction or decompensated HF [63, 65, 66]. In fact, most AADs share negative inotropic and chronotropic effects and should be used with caution in HF patients [63, 65, 66].

Betablockers are still the cornerstone of antiarrhythmic therapy in HF patients as they consistently reduced mortality in large RCTs while being relatively well tolerated [67, 68]. In contrast, while amiodarone was shown to prevent VAs and recurrent ICD shocks in patients with HF, there is no convincing data demonstrating prognostic benefits [9, 69, 70, 71]. In fact, mortality data on amiodarone are conflicting, and the beneficial antiarrhythmic effects may be offset by the risk of organ toxicity [7].

Against this background, AADs and particularly amiodarone can be considered in HF patients suffering from symptomatic VAs or ICD shocks to prevent recurrent episodes, but antiarrhythmic therapy should be reconsidered critically in case of clinical deterioration.

Catheter ablation

In the context of structural heart disease, the VA mechanism is typically scar-related reentry resulting in sustained monomorphic VT, which in principle is well amenable to catheter ablation. Polymorphic, irregular VAs may also occur, but they rather reflect acute myocardial ischemia or inflammation, whereas in chronic post-myocardial infarction or post-myocarditis stages VAs typically manifest as monomorphic VTs, as well.

Driven by technological achievements like multipolar high-resolution mapping and 3D imaging modalities accompanied by an incremental mechanistic understanding, VT ablation has seen immense progress in the last decade. In fact, standardized approaches targeting functional substrate based on high-resolution mapping, routinely and safely combining endo- and epicardial access, have substantially improved efficacy and safety of contemporary VT ablation. As a result, the significance of catheter ablation has grown considerably, particularly in patients with ischemic heart disease. Of note, in the context of CAD, the reentry circuit is often confined to the subendocardium and thus readily accessible by endocardial ablation, whereas non-ischemic etiologies are associated with more variable and complex substrates, commonly with intramural or epicardial distribution patterns, which may contribute to a less favorable outcome.

Evidence for Catheter Ablation Catheter ablation has consistently shown to prevent recurrent VT episodes and ICD discharges with several RCTs (VANISH, SMASH-VT, VTACH, SURVIVE VT) indicating superiority over AAD medical therapy (Table 1) [72•, 73, 74, 75]. However, for a long time, catheter ablation was only considered a last resort when AAD therapy failed, and to date, uncertainty remains regarding the optimal timing and prognostic benefit of ablation [76•]. Moreover, reported long-term success rates of VT ablation are highly variable between 30 and 70%, with more favorable results in ischemic cardiomyopathy compared to non-ischemic etiologies. Of note, the varying success rates may not only reflect different patient populations and underlying entities, but also quite distinct ablation and mapping approaches, many of which may not anymore be regarded state-of-the-art today. In fact, it was only in recent years that a broad consensus regarding standardized ablation strategies and endpoints, as well as specific high-resolution mapping approaches taking advantage of technological advances, has been reached [1].

Against this background, it is particularly noteworthy that evidence from three recent RCTs (PARTITA, PAUSE-SCD, and SURVIVE-VT) following current state-of-the-art consistently support catheter ablation as first-line therapy in patients with ischemic or non-ischemic cardiomyopathy and symptomatic VT [72•, 78•, 77•]. The PARTITA randomized trial even found an early ablation strategy to reduce all-cause mortality, although in light of very low event rates this result remains to be confirmed by sufficiently powered trials. The consistent positive results of the aforementioned trials, with very low complication rates, likely reflect the progress of catheter ablation in the last decade and may change our clinical practice towards an earlier consideration of ablation therapy. However, we also must not forget that patients were only ablated in highly specialized centers.

Ablation Procedure The first objective in ablation procedures for monomorphic VT is to define ablation targets by electroanatomical mapping using high-resolution multipolar mapping catheters. On one hand, ablation targets include so-called critical isthmuses, i.e., channels or corridors of slow conducting tissue protected by non-conducting scar tissue, that are the critical components of the reentry circuits maintaining the VT. Localization and definition of these critical VT isthmuses requires electroanatomical mapping during ongoing VTs that usually have to be induced by programmed electrical stimulation during the procedure. The critical VT isthmus is typically characterized by local diastolic potentials and confirmed by specific pacing maneuvers [79]. However, all other areas of slow conduction, even if unrelated to the induced VTs, are to be targeted as well, because they constitute an arrhythmogenic substrate potentially enabling future reentry circuits other than those of the inducible VTs. This potential arrhythmogenic substrate in terms of slow-conduction zones is mapped during sinus

Table 1 Evidence for catheter ablation

Trial	Inclusion	Randomization	Mapping/ablation	Entity	AAD use	Follow-up	Primary outcome	Secondary outcomes	Conclusion
SMASH-VT Reddy 2007 [75]	Post-MI patients undergoing ICD implant for secondary prevention, no AAD	ICD alone (64) vs. ICD + ablation (64)	Pace or substrate map, linear lesions	ICM Mean LVEF: 32% Mean age: 67 years	Abl: 0% Ctr.: 0%	23 months	**Appropriate ICD therapy** Ablation: 12% Control: 33% ($p=0.007$)	**Death** Abl:17% Ctr.: 9% ($p=0.29$)	Ablation reduced incidence of ICD therapy No impact on mortality
VANISH Sapp 2007 [73]	Post MI patients with ICD and VT under AAD (amiodarone or other class I or III AAD)	Ablation and AAD continuation (132) vs AAD escalation* (127)	VT mapping and ablation Substrate, if not inducible or not tolerated	ICM Mean LVEF: 31% Mean age: 69 years	n/a	28 months	**Composite of death, ≥ 3 VT/24 h, or appr. ICD shock** ablation: 59.1% AAD esc.: 68.5% ($p=0.04$) Driven by reduction of VT/ICD shocks No difference in ind. components	**Death** Abl: 27.3% Esc.: 27.6% ($p=0.86$) **VT below ICD detection** Abl: 3% Esc.: 14% ($p=0.02$)	Ablation better than AAD escalation in preventing VT 3 deaths from amiodarone-induced organ toxicity (2 pulmonary, 1 hepatic) in AAD escalation arm
VTACH Kuck 2010 [74]	Patients with 1st episode of stable VT, post-MI, and LVEF ≤ 50%	ICD alone (52) vs ICD + ablation (55)	VT mapping and ablation or pace/substrate map, linear lesions	ICM Mean LVEF: 34% Mean age: 66 years	Abl: 26% Ctr.: 31%	23 months	**Time to first VT/VF recurrence** Ablation: 19 months Control: 6 months ($p=0{\cdot}045$) **freedom from VT/VF:** Ablation: 47% Control: 29% ($p=0.045$)	**Appropriate ICD shocks:** Ablation: 27% Control: 47% ($p=0.045$) **Freedom from cardiac hosp.** Abl: 67% Ctr.: 45% ($p=0.044$) **Death at 24 months** Abl: 9% Ctr.: 9% ($p=0.677$)	Prophylactic VT ablation before ICD implant prolonged time to VT recurrence and reduced appropriate ICD shocks and hospital admissions No impact on mortality
Berlin VT Willems 2020 [76•]	Post-MI patients with LVEF 30–50%, sustained VT and ICD indication for secondary prevention	Ablation at the time of ICD (preventive, 76) vs Ablation after 3rd appropriate ICD shock (deferred, 83)	VT and substrate mapping/ablation	ICM mean LVEF: 41% mean age: 66 years	n/a	14 months	**Composite of death and hospitalization for VT or HF** preventive: 32.9% deferred: 27.7% ($p=0.77$) **Death** preventive: 7.9% deferred: 2.4% ($p=0.18$)	**Sustained VT** prev.: 39.7% def.: 48.2% ($p=0.050$) **Appropriate ICD therapy** prev.: 34.2% def.: 47.0% ($p=0.020$)	Ablation reduced appropriate ICD therapies, but did not impact mortality or the primary composite endpoint Premature termination for futility
Survive VT Arenal 2022 [72•]	ICD patients with previous MI and symptomatic sustained VT (ICD shocks or syncope) under OMT Amended criterion: VT necessitating ICD therapy Exclusion: Patients with concomitant AAD use	First-line ablation (71) vs AAD (73)	Substrate mapping/ablation	ICM Mean LVEF: 34% mean age: 72 years	Abl: 10% AAD: 96%	24 months	**CV death, appropriate ICD shock, HF hospitalization or severe treatment complications** Ablation: 28.2% AAD: 46.6% ($p=0.021$) **driven by severe treatment complications (including slow VT)** Ablation: 9.9% AAD: 28.8% ($p=0.006$) **Slow undetected VT** Ablation: 1.4% AAD: 13.7% ($p=0.028$)	**Death** Abl: 4.2 AAD: 5.5 ($p=0.624$) **Appropriate ICD therapies** Abl: 4.2% AAD: 5.5% ($p=0.624$) **Documented VT** Abl: 26.8% AAD: 28.8% ($p=0.417$)	Ablation reduced the primary endpoint This was driven by AAD-related complications including Bradycardia, slow VTs and hyper- or hypothyroidism No impact on mortality, HF hospitalizations, VT recurrence or ICD therapies

Table 1 (continued)

Trial	Inclusion	Randomization	Mapping/ablation	Entity	AAD use	Follow-up	Primary outcome	Secondary outcomes	Conclusion
PARTITA Della Bella 2022 [77•]	Patients with ischemic or nonischemic cardiomyopathy and primary or secondary prevention indication for ICD	Ablation after first ICD shock vs medical therapy (no AAD)	Substrate-based, VT mapping if necessary	78% ICM 22% NICM Mean LVEF 32% Mean age 68 years	Not allowed	24 months	**All-cause death or HF hospitalization** Ablation: 4% Control: 42% ($p=0.034$) **All-cause death** Ablation: 0 Control: 33% ($p=0.004$)	**ICD shocks** Abl: 9% control: 42% ($p=0.039$)	Ablation reduced the primary endpoint This was driven by a reduction in non-cardiac death
PAUSE-SCD Tung 2022 [78•]	Patients with cardiomyopathy and monomorphic VT with indication for ICD	Ablation + ICD vs Conventional therapy** + ICD	VT- & substrate-based mapping/ablation	35% ICM 30% NICM 35% ARVC Mean LVEF 40% Mean age 55 years	Abl.: 36% Ctr.: 43% ($p=0.45$)	31 months	**VT, CV hospitalization or death** Ablation: 49.3% Control: 65.5% ($p=0.04$) **VT recurrence** Ablation: 34.9% Control: 58.2% ($p=0.02$)	**ICD shocks** Abl: 10% control: 24% ($p=0.03$) **ATP** Abl: 16% control: 33% ($p=0.04$)	Ablation reduced the primary endpoint This was driven by a reduction in VT recurrence No difference in death or hospitalization

AAD antiarrhythmic drugs except beta-blockers, *ICM* ischemic cardiomyopathy, *NICM* non-ischemic dilated cardiomyopathy, *VT* ventricular tachycardia, *VF* ventricular fibrillation, *abl.* ablation, *ctr.* control, *esc.* escalation

*(a) Amio initiation if on other AAD (b) Amio increase to 300 mg if on amio < 300 mg or (c) addition of mexiletine if on amio ≥ 300 mg

**β-blockers and AAD at the discretion of the treating physician

rhythm and indicated by a temporal delay between adjacent bipolar electrograms or dispersion of local electrogram components [80•, 81]. In recent years, it has been increasingly acknowledged that we are dealing with 3-dimensional substrates that even combined endocardial and epicardial surface mapping may not fully capture [82•]. In fact, only imaging modalities like CMR have the potential to delineate the complete 3-dimensionality of the substrate (see section on imaging below). Finally, it is noteworthy that, while most sustained VAs in HF patients are monomorphic and based on reentry mechanisms, polymorphic VTs or ventricular fibrillation are less amenable to catheter ablation; however, the origin of putative trigger PVCs may be a promising ablation target here as well.

The second objective of the procedure is to address the defined targets by ablation (radiofrequency still constitutes the standard energy source) with the endpoints of (a) confirmed elimination of all arrhythmogenic substrate and (b) non-inducibility of any VT [1, 83]. As a consequence, extensive mapping and ablation both during sinus rhythm and—if tolerated—during induced VT is required, resulting in procedure times of several hours. Of note, even with a combined endocardial and epicardial access, the procedural endpoints cannot always be accomplished, particularly in the case of intramural and less accessible substrates [82•]. In that case alternative, less established ablation techniques like bipolar radiofrequency ablation, intramural needle ablation (under investigation), or non-invasive cardiac radiation with stereotactic radioablation may be considered [84, 85, 86, 87, 88, 89].

Imaging Recent guidelines highlight the value of preprocedural imaging to optimally plan and guide ablation procedures [1]. In that respect, CT imaging can provide high-resolution information on cardiac anatomy and localization of critical adjacent structures at risk, like coronary arteries or phrenic nerves. This information may be integrated in the 3D mapping system to facilitate electroanatomical mapping and to avoid collateral damage during ablation (Fig. 2). In addition, CT can be used to detect intracardiac thrombi that may prohibit endocardial ablation. While CT-guided identification and ablation of arrhythmogenic substrate based on local wall thickness has been proposed, data on such approaches are still scarce [25].

In contrast, LGE-CMR is already routinely employed in many centers for non-invasive localization and 3-dimensional delineation of arrhythmogenic substrate to be targeted by ablation, which is supported by a large body of evidence [23, 24, 25, 26, 27•, 28, 29, 30]. Of note, quantification of LGE in terms of relative signal intensities discriminates

surviving myocardium with residual viability from non-viable fibrotic tissue within areas of scar. Typically, it is scar-pervading channels of surviving myocardium with residual but slowed electrical conduction capacities that constitute the arrhythmogenic substrate, rather than the scar itself [23, 26, 27•, 28]. Dedicated postprocessing software allows for 3-dimensional image reconstructions to visualize the regional and transmural distributions of those potentially arrhythmogenic channels (Fig. 3). In combination with automatic measurement of local ventricular wall thicknesses, this enables an a priori estimation, whether an arrhythmogenic substrate will be accessible endocardially or whether an epicardial access, implicating an increased procedural risk, will indeed be required (Fig. 4) [29]. Moreover, during the procedure, 3D reconstructions of the scar and potentially arrhythmogenic channels can be integrated in the mapping system to efficiently direct electroanatomical mapping to the areas of interest (Fig. 5) [23, 27•, 30].

Taken together, CT and LGE-CMR are highly valuable tools to plan and guide complex VT ablation procedures, rendering them more efficient, safer, and possibly even more effective [30].

Periprocedural Management As VT ablation procedures are long and complex, and are being performed in often multimorbid, hemodynamically and electrically instable patients, they pose substantial demands on the full team, mandating thorough procedural planning and extensive interdisciplinary expertise including interventional electrophysiologists, cardiologists, HF specialists, cardiac anesthesiologists, and cardiac surgeons [1, 83]. Although procedural mortality is < 1%, there is a relevant risk of potentially life-threatening complications including pericardial tamponade, stroke, or acute periprocedural decompensation [73, 74, 76•].

Of note, as outlined above, VT ablation commonly requires extensive elimination of viable myocardium with unpredictable functional consequences, and the relative contribution of large-scale ablation to periprocedural aggravation of ventricular dysfunction is not well defined. Against this background, preprocedural management should include a thorough evaluation aiming at upfront identification of patients at risk and a hemodynamically guided optimization of cardiopulmonary status (e.g., decongestion with i.v. loop diuretics) to decrease the risk of acute periprocedural decompensation. Santangeli et al. have identified predictors of acute periprocedural decompensation that may be helpful in this respect. Those include chronic obstructive pulmonary disease, advanced age (> 60 years), general anesthesia, ischemic cardiomyopathy, NYHA functional class III or IV, LVEF < 25%, presentation with electrical storm, and diabetes mellitus [90]. In selected patients, periprocedural mechanical circulatory support may be considered for preemptive hemodynamic stabilization [55, 56]. Besides prevention of hemodynamic decompensation, mechanical circulatory support may also allow for comprehensive mapping

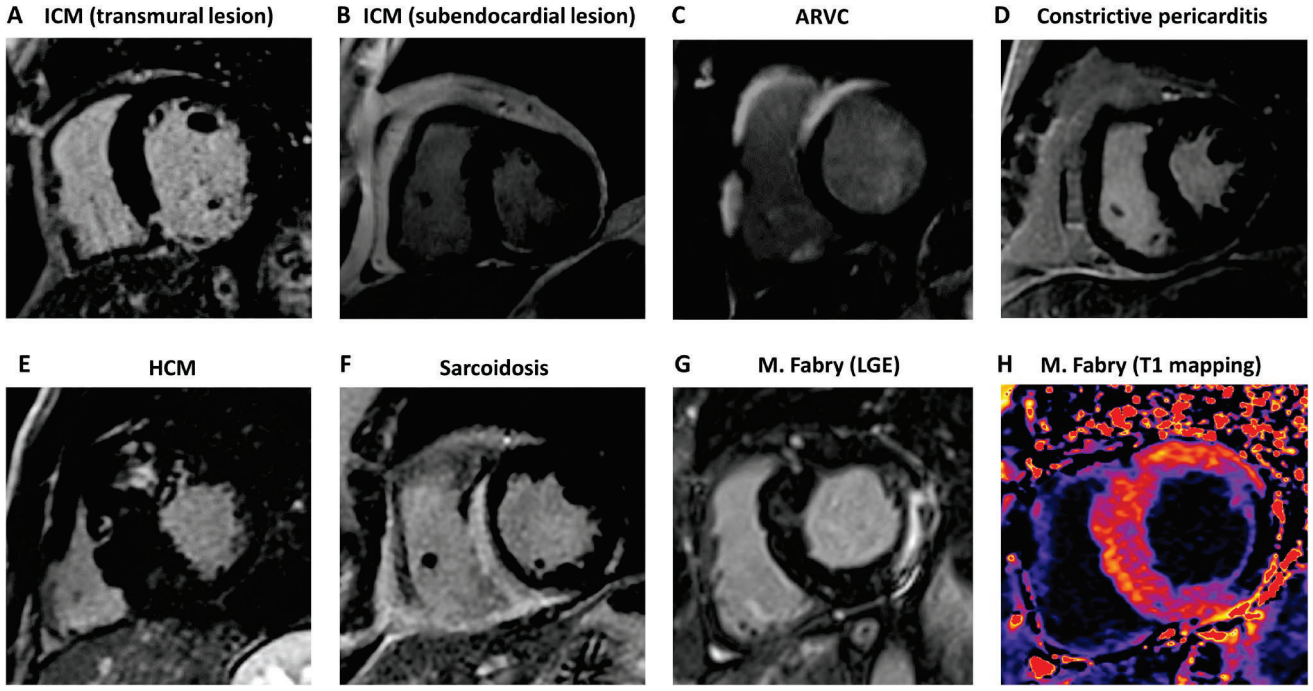

Fig. 2 3D reconstruction of CT scan. Shown are 3D reconstructions of the aorta with coronary arteries (purple), right ventricle (green), right ventricular outflow tract with pulmonary artery (orange), left atrium (cyan), and a wall thickness map of the left ventricle (color-coding according to local wall thickness as indicated)

of the reentry circuit and critical isthmus during ongoing VT that would otherwise not be tolerated hemodynamically. In fact, observational data suggest a benefit from preemptive mechanical circulatory support in patients at risk of hemodynamic decompensation according to the abovementioned predictors [55, 56].

However, it must be taken into account that mechanical circulatory support renders the ablation procedure more complex and more invasive, and indeed, studies found it to be associated with a higher risk of complications [91]. Thus, although the rationale for prophylactic mechanical circulatory support in selected patients at risk is appealing a priori, the benefits remain to be confirmed empirically in randomized trials.

Management of VA in Patients with Advanced or End-Stage HF

Patients with advanced or end-stage HF require specific considerations. AADs must be used even more cautiously; in fact, most AADs, apart from amiodarone, are contraindicated in advanced HF, and therapy with amiodarone, although to a lesser extent, can also result in myocardial depression and should therefore be monitored closely and reconsidered critically in case of worsening HF [61, 63].

In the context of catheter ablation, these patients require special considerations as well. Most importantly, patients with advanced or end-stage HF are at higher risk for acute periprocedural hemodynamic decompensation, and a hemodynamically guided optimization of cardiopulmonary status prior to ablation can be required [90]. Moreover, preemptive mechanical circulatory support may be considered in selected patients (see section on periprocedural management) [55, 56].

Patients with Left Ventricular Assist Devices

The incidence of VAs is particularly high among patients with advanced HF and LVAD in whom VAs typically manifest early upon LVAD implantation [57]. Today, LVADs are increasingly used as a bridge to transplant or destination therapy in patients with advanced or end-stage HF refractory to optimal medical management being evaluated or listed for cardiac transplantation [4]. Several observational studies reported an association between VAs and mortality in this setting, particularly when VAs occur in the early postoperative period [92, 93, 94, 95]. However, while frequent and/or sustained VAs can indeed cause functional deterioration, right ventricular failure, and hemodynamic decompensation

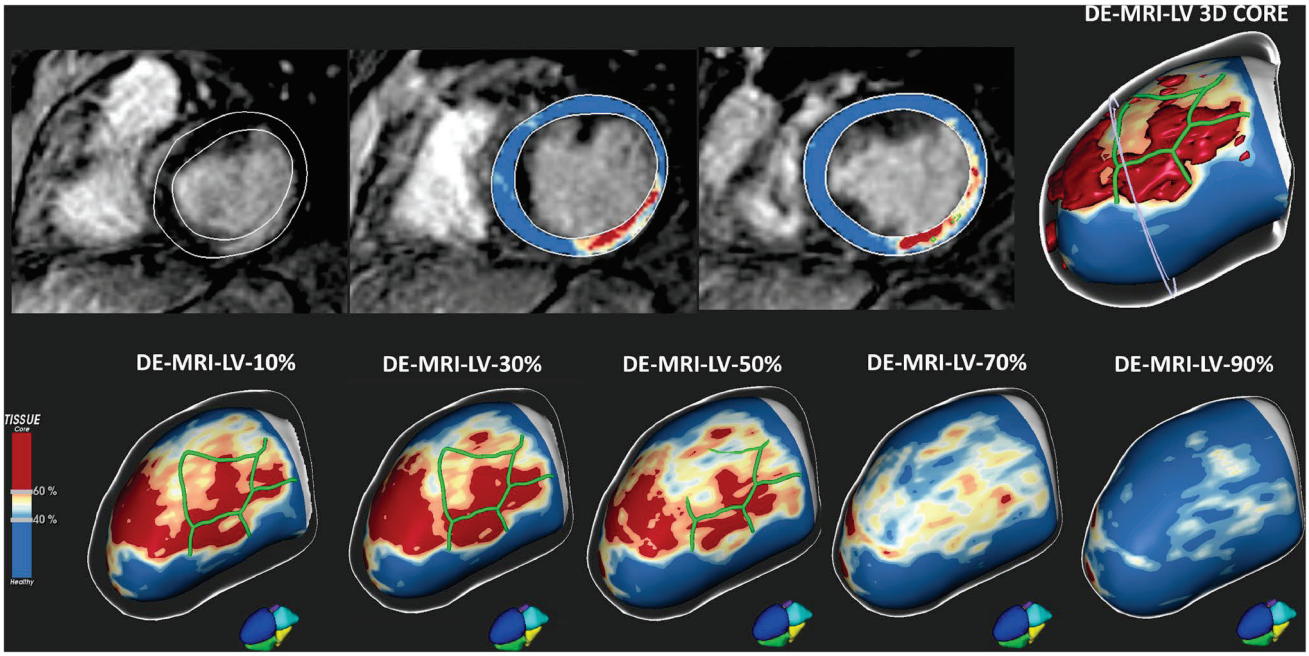

Fig. 3 3D visualization of arrhythmogenic substrate for CMR-guided ablation. Upper panel: T1 weighted short-axis LGE-CMR slices (left, middle) and 3D reconstruction (right) with LGE-based color-coding based on thresholds for dense scar (red, > 60% of the maximum signal intensity) and borderzone (yellow, 40–60% of the maximum signal intensity) (Adas3D Medical SL, Barcelona). The two middle images show constitute an overlay of the T1-weighted short-axis slices with the color-coding described above. In the 3D reconstruction software-predicted arrhythmogenic channels of slow conduction are displayed in green. Lower panel: Five distinct myocardial layers spanning the transmurality from endocardial (10% layer) to epicardial (90% layer) show the 3D distribution of the arrhythmogenic substrate and the course of the slow-conduction channels. In this example the arrhythmogenic substrate is predominantly located subendocardially

in LVAD patients, to some extent VA may simply reflect more severe myocardial disease and comorbidities that in turn imply a higher risk of death.

Regarding the management of VA in LVAD patients, there are a number of specific reversible causes related to the device itself that require consideration: Primarily, acute hemodynamic decompensation due to mechanical pump failure (e.g., pump thrombosis or technical problems) should be ruled out [57]. Further reversible causes include mechanical triggers due to wall contact of the inflow cannula or so-called suction events due to insufficient LV pre-load, which may require adaptation of pump speed and/or fluid status [96, 97].

In the absence of specific evidence from large RCTs, management of VAs in LVAD patients is mostly based on extrapolation from the general HF population. Thus, the pharmacological repertoire does not differ significantly, with similar considerations regarding proarrhythmic and hemodynamic side effects or organ toxicity. As AADs have not shown prognostic benefit and are mostly applied to reduce arrhythmia burden, they can be applied even more restrictively in LVAD patients, who generally tolerate VAs well. However, it has to be considered that sustained VAs can result in right ventricular failure and hemodynamic decompensation despite LV circulatory support [98, 99, 100]. Taken together, close monitoring and individual balancing of risks and benefits are warranted.

Despite the paucity of data from randomized trials, a number of studies have shown that catheter ablation can be performed safely and effectively in LVAD patients [99, 101]. However, due to the complexity of both the procedure and the patient condition, these ablations should be reserved to highly specialized centers [1, 83]. While the general concepts for VT ablation equally apply to LVAD patients, the trauma from ventriculotomy for the inflow cannula and subsequent fibrotic remodeling constitutes an LVAD-specific substrate in a considerable proportion of patients [99, 101]. Moreover, epicardial adhesions resulting from the LVAD implantation and other previous cardiac surgeries commonly render epicardial access difficult, requiring a surgical window. In light of these challenges, intra-operative ablation during LVAD implantation may be considered in patients with recurrent pre-implantation VTs [102, 103].

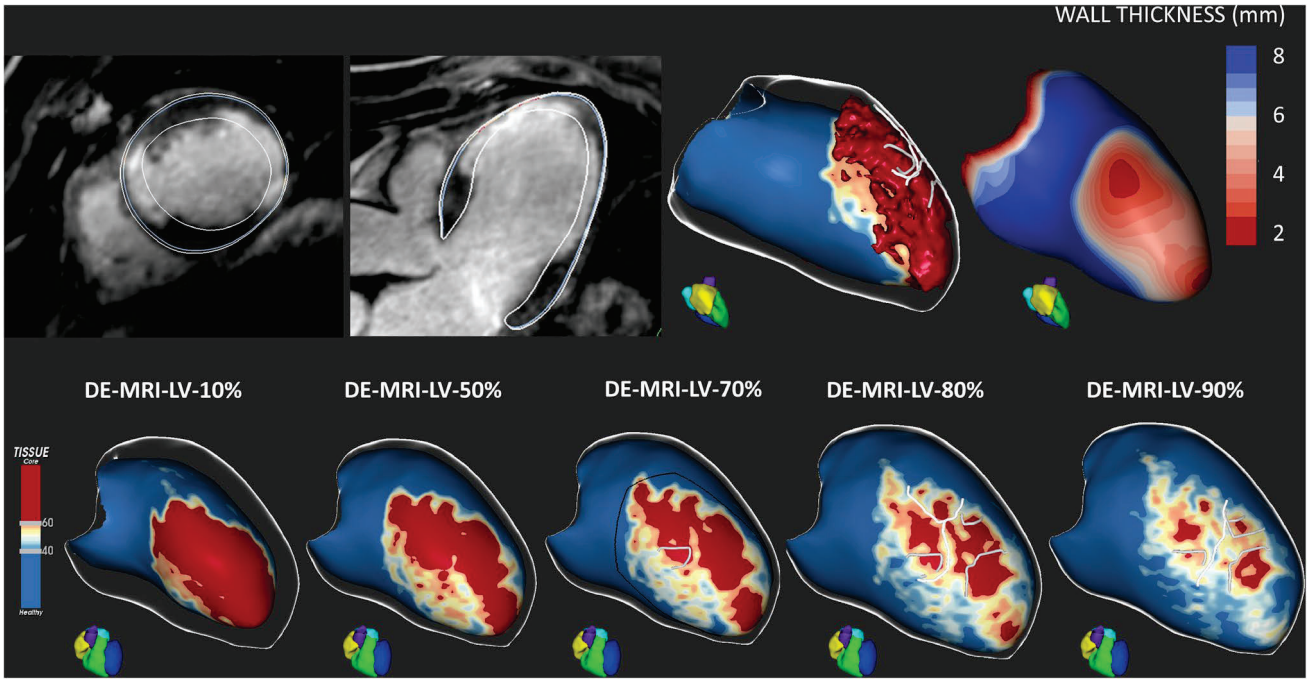

Fig. 4 CMR-guided procedural planning based on arrhythmogenic substrate and local wall thickness. Upper panel: T1 weighted short-axis LGE-CMR slices (2 images on the left) and the corresponding 3D-reconstructions (2 images on the right) are shown. The 3D reconstructions on the right are color-coded based on LGE as described in Fig. 3 and based on local wall thickness (far right), respectively. Lower panel: Five distinct myocardial layers spanning the transmurality from endocardial (10% layer) to epicardial (90% layer) show the 3D distribution of the arrhythmogenic substrate and the course of the slow-conduction channels. In this example, the putative slow-conduction channels are predominantly located epicardially, suggesting the necessity of an epicardial access. However, as indicated by the local wall thickness map, the tissue thickness in this area is consistently below 5 mm, suggesting that the epicardial arrhythmogenic substrate is accessible with an endocardial mapping/ablation approach. Indeed, endocardial mapping and ablation was successful without the need for an epicardial access in this case

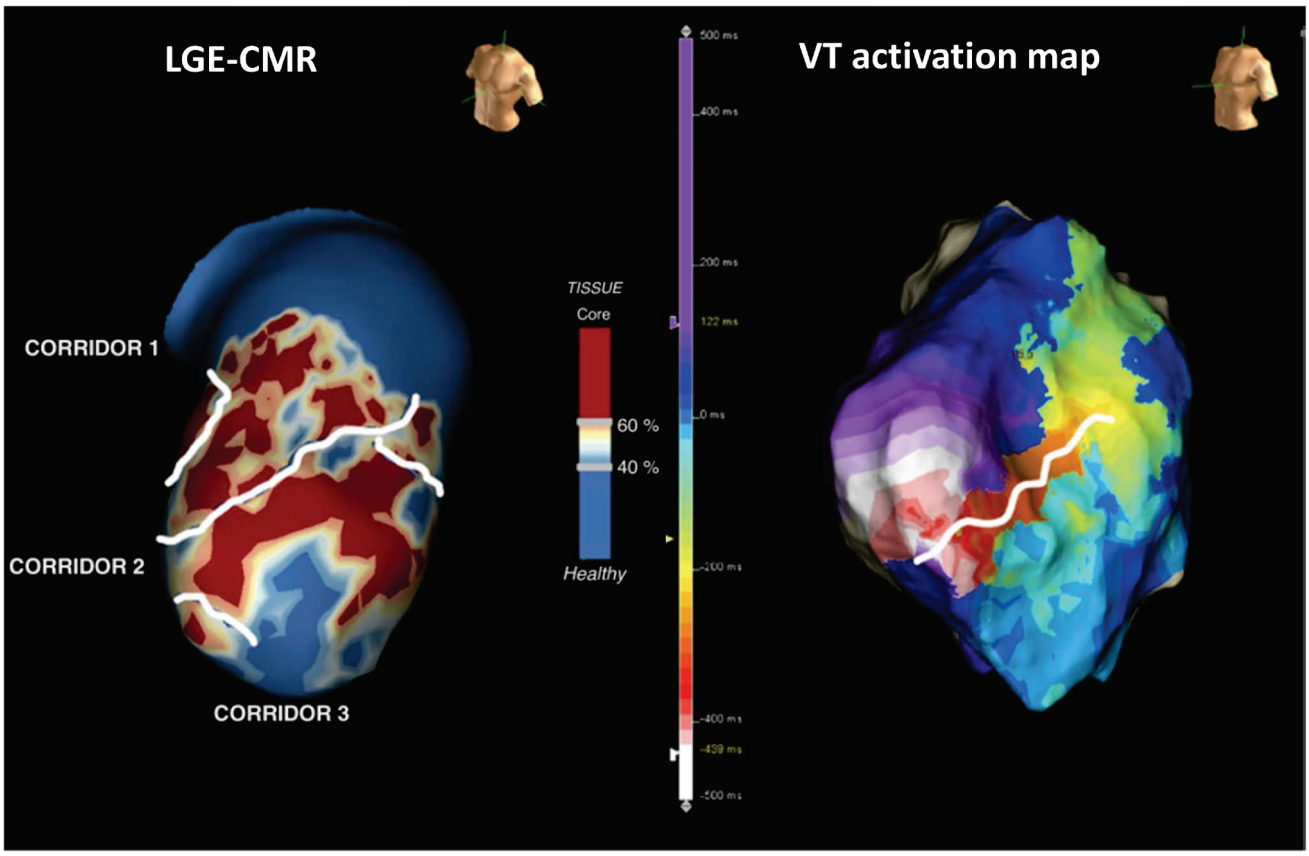

Fig. 5 LGE-CMR predicts critical VT isthmus. (Left) LGE-CMR 3D-reconstruction of the left ventricle, color-coded based on LGE as described in Fig. 3. Three putatively arrhythmogenic channels of slow conduction are predicted based on LGE-CMR (corridor 1–3, white color). (Right) Activation map created during VT. Color-coding indicates distinct local activation time delays relative to a fixed reference. The activation map reveals a VT isthmus of slow conduction (indicated by white color) that coincides with the LGE-CMR-detected corridor 2

Decision-making is equally complex regarding ICD therapy. While most patients already have an ICD in place prior to LVAD implantation, there is no evidence for benefit from ICD therapy in this population [104]. This is particularly noteworthy as due to the circulatory support most LVAD patients tolerate their VAs well and are fully conscious when they receive ICD shocks, which may lead to considerable psychological trauma. On the other hand, repetitive or sustained VA may promote right ventricular failure and cardiac decompensation despite LV circulatory support 98–100. Against this background, turning off ICD therapies should be considered on an individual basis involving shared decision-making [1, 15, 57].

Premature Ventricular Contractions

PVCs occur in virtually all HF patients and can be both cause and effect of HF. Frequent premature contractions can aggravate preexisting HF, but may also cause ventricular dysfunction in the absence of structural heart disease (PVC-induced cardiomyopathy). However, in patients with suspected PVC-induced cardiomyopathy, LGE-CMR should be performed in addition to echocardiography to rule out a concealed structural heart disease [105, 106, 107].

Although PVCs are considered a benign condition in the absence of structural heart disease, in HF patients, they have been statistically associated with adverse outcome, particularly if they manifest as consecutive beats or non-sustained VT [7, 108]. Still, neither PVCs nor non-sustained VTs warrant antiarrhythmic treatment per se. In fact, antiarrhythmic therapy reduces PVC burden and related symptoms in HF patients, but failed to prove prognostic benefit in large randomized trials [9, 70]. Thus, specific therapy is only warranted if PVCs lead to symptoms or aggravate ventricular dysfunction, although in clinical practice it may be challenging to establish such causal link in HF patients.

Patients with stable ventricular dysfunction sufficiently explained by the underlying structural heart disease may not require antiarrhythmic treatment, but should be followed

closely with regular echocardiographic assessment to detect LV functional deterioration timely. While evidence for a clear threshold is lacking, the risk of ventricular dysfunction is substantially increased with PVC burdens > 10% and further increases if PVC burden is higher than 20% [109, 110, 111, 112]. Against this background, HF patients with a PVC burden > 10% should receive antiarrhythmic therapy, if PVCs are suspected to aggravate ventricular dysfunction. Of note, in patients with extensive PVC burden (> 20%), even prophylactic antiarrhythmic treatment to prevent LV functional deterioration may be considered [109]. However, it is important to note that PVC burden is subject to a substantial temporal variability and should therefore be estimated based on multiple independent Holter ECG recordings.

Generally, in HF patients, antiarrhythmic treatment in terms of AAD or catheter ablation should be applied more generously, particularly if PVCs impede cardiac resynchronization therapy. Of note, catheter ablation consistently reduced PVC burden and improved ventricular function in patients with structural heart disease, irrespective of the underlying etiology or concomitant CRT, in numerous studies [113, 114, 115]. While catheter ablation appears to be more effective, AAD therapy may be considered too, particularly in HF patients with multifocal PVCs, or PVCs originating from areas that are not readily amenable to catheter ablation. In fact, there is evidence demonstrating successful PVC suppression and LV functional improvement with amiodarone or flecainide [70, 116, 117]. Although the generally more favorable adverse effect profile of flecainide compared to amiodarone must be weighed against potentially life-threatening pro-arrhythmic effects in the context of structural heart disease, particularly in patients with ICD, flecainide may be a valid option.

Conclusion

While progress in medical and device-based therapies has substantially reduced mortality of HF patients over the last decades, VAs and SCD remain a major concern. VA management in HF patients is highly complex and should be addressed in a multidisciplinary approach, preferably at specialized centers. In light of the limited efficacy and potentially life-threatening side effects of AADs, it is promising that with recent advances in electroanatomical mapping, imaging, and mechanistic understanding, catheter ablation has evolved as a standardized, safe, and efficacious treatment. Finally, while ICD therapy remains the cornerstone of SCD prevention, risk stratification and patient selection may need reconsideration and refinement, possibly taking into account imaging, genetic testing, and other predictors beyond LV systolic function.

Declarations

Conflict of Interest The authors declare no competing interests.

Human and Animal Rights and Informed Consent This article does not contain any studies with human or animal subjects performed by any of the authors.

References

Papers of particular interest, published recently, have been highlighted as:
• Of importance

1. Zeppenfeld K, Tfelt-Hansen J, de Riva M, Winkel BG, Behr ER, Blom NA, et al. 2022 ESC Guidelines for the management of patients with ventricular arrhythmias and the prevention of sudden cardiac death. Eur Heart J. 2022;43:3997–4126.
2. Lip GY, Heinzel FR, Gaita F, Juanatey JR, Le Heuzey JY, Potpara T, et al. European Heart Rhythm Association/Heart Failure Association joint consensus document on arrhythmias in heart failure, endorsed by the Heart Rhythm Society and the Asia Pacific Heart Rhythm Society. Europace. 2016;18:12–36.
3. Shen L, Jhund PS, Petrie MC, Claggett BL, Barlera S, Cleland JGF, et al. Declining risk of sudden death in heart failure. N Engl J Med. 2017;377:41–51.
4. McDonagh TA, Metra M, Adamo M, Gardner RS, Baumbach A, Böhm M, et al. 2021 ESC Guidelines for the diagnosis and treatment of acute and chronic heart failure. Eur Heart J. 2021;42:3599–726.
5. Hennig A, Salel M, Sacher F, Camaioni C, Sridi S, Denis A, et al. High-resolution three-dimensional late gadolinium-enhanced cardiac magnetic resonance imaging to identify the underlying substrate of ventricular arrhythmia. Europace. 2018;20:f179–91.
6. Chen J, Johnson G, Hellkamp AS, Anderson J, Mark DB, Lee KL, et al. Rapid-rate nonsustained ventricular tachycardia found on implantable cardioverter-defibrillator interrogation: relationship to outcomes in the SCD-HeFT (Sudden Cardiac Death in Heart Failure Trial). J Am Coll Cardiol. 2013;61:2161–8.
7. Packer DL, Prutkin JM, Hellkamp AS, Mitchell LB, Bernstein RC, Wood F, et al. Impact of implantable cardioverter-defibrillator, amiodarone, and placebo on the mode of death in stable patients with heart failure: analysis from the sudden cardiac death in heart failure trial. Circulation. 2009;120:2170–6.
8. • Younis A, Goldberger JJ, Kutyifa V, Zareba W, Polonsky B, Klein H, et al. Predicted benefit of an implantable cardioverter-defibrillator: the MADIT-ICD benefit score. Eur Heart J. 2021;42:1676–84. **This article established and validated a score that predicts the likelihood of benefit from prophylactic ICD implantation**
9. Bardy GH, Lee KL, Mark DB, Poole JE, Packer DL, Boineau R, et al. Amiodarone or an implantable cardioverter-defibrillator for congestive heart failure. N Engl J Med. 2005;352:225–37.
10. Moss AJ, Zareba W, Hall WJ, Klein H, Wilber DJ, Cannom DS, et al. Prophylactic implantation of a defibrillator in patients with myocardial infarction and reduced ejection fraction. N Engl J Med. 2002;346:877–83.
11. • Klem I, Klein M, Khan M, Yang EY, Nabi F, Ivanov A, et al. Relationship of LVEF and myocardial scar to long-term mortality risk and mode of death in patients with nonischemic

cardiomyopathy. Circulation. 2021;143:1343–58. **This study shows that the extent of LV fibrosis, as assessed by LGE-CMR, predicts all-cause mortality and cardiac death in patients with non-ischemic cardiomyopathy with a higher predictive value than LVEF.**

12. Klem I, Weinsaft JW, Bahnson TD, Hegland D, Kim HW, Hayes B, et al. Assessment of myocardial scarring improves risk stratification in patients evaluated for cardiac defibrillator implantation. J Am Coll Cardiol. 2012;60:408–20.
13.• Sánchez-Somonte P, Quinto L, Garre P, Zaraket F, Alarcón F, Borràs R, et al. Scar channels in cardiac magnetic resonance to predict appropriate therapies in primary prevention. Heart Rhythm. 2021;18:1336–43. **This article provides evidence that LGE-CMR-detected scar channels predict adequate ICD therapies and freedom from arrhythmia recurrence, respectively.**
14.• Zegard A, Okafor O, de Bono J, Kalla M, Lencioni M, Marshall H, et al. Myocardial fibrosis as a predictor of sudden death in patients with coronary artery disease. J Am Coll Cardiol. 2021;77:29–41. **In this study in patients with coronary artery disease, LV fibrosis as assessed by LGE-CMR was more strongly associated with ventricular arrhythmias and sudden cardiac death than LVEF.**
15. Al-Khatib SM, Stevenson WG, Ackerman MJ, Bryant WJ, Callans DJ, Curtis AB, et al. 2017 AHA/ACC/HRS Guideline for Management of Patients With Ventricular Arrhythmias and the Prevention of Sudden Cardiac Death: Executive Summary: A Report of the American College of Cardiology/American Heart Association Task Force on Clinical Practice Guidelines and the Heart Rhythm Society. Circulation. 2018;138:e210–71.
16. Bing R, Dweck MR. Myocardial fibrosis: why image, how to image and clinical implications. Heart. 2019;105:1832–40.
17. Mewton N, Liu CY, Croisille P, Bluemke D, Lima JA. Assessment of myocardial fibrosis with cardiovascular magnetic resonance. J Am Coll Cardiol. 2011;57:891–903.
18. Mont L, Roca-Luque I, Althoff TF. Ablation lesion assessment with MRI. Arrhythm Electrophysiol Rev. 2022;11:e02.
19. Rodrigues P, Joshi A, Williams H, Westwood M, Petersen SE, Zemrak F, et al. Diagnosis and prognosis in sudden cardiac arrest survivors without coronary artery disease: utility of a clinical approach using cardiac magnetic resonance imaging. Circ Cardiovasc Imaging. 2017;10:e006709.
20. Heidary S, Patel H, Chung J, Yokota H, Gupta SN, Bennett MV, et al. Quantitative tissue characterization of infarct core and border zone in patients with ischemic cardiomyopathy by magnetic resonance is associated with future cardiovascular events. J Am Coll Cardiol. 2010;55:2762–8.
21. Køber L, Thune JJ, Nielsen JC, Haarbo J, Videbæk L, Korup E, et al. Defibrillator implantation in patients with nonischemic systolic heart failure. N Engl J Med. 2016;375:1221–30.
22. Muser D, Nucifora G, Muser D, Nucifora G, Pieroni M, Castro SA, et al. Prognostic value of nonischemic ringlike left ventricular scar in patients with apparently idiopathic nonsustained ventricular arrhythmias. Circulation. 2021;143:1359–73.
23. Andreu D, Penela D, Acosta J, Fernández-Armenta J, Perea RJ, Soto-Iglesias D, et al. Cardiac magnetic resonance-aided scar dechanneling: influence on acute and long-term outcomes. Heart Rhythm. 2017;14:1121–8.
24. Falasconi G, Penela D, Soto-Iglesias D, Martí-Almor J, Berruezo A. Cardiac magnetic resonance and segment of origin identification algorithm streamline post-myocardial infarction ventricular tachycardia ablation. JACC Clin Electrophysiol. 2022;8:1603–8.
25. Jáuregui B, Soto-Iglesias D, Zucchelli G, Penela D, Ordóñez A, Terés C, et al. Arrhythmogenic substrate detection in chronic ischaemic patients undergoing ventricular tachycardia ablation using multidetector cardiac computed tomography: compared evaluation with cardiac magnetic resonance. Europace. 2021;23:82–90.
26. Quinto L, Sanchez P, Alarcón F, Garre P, Zaraket F, Prat-Gonzalez S, et al. Cardiac magnetic resonance to predict recurrences after ventricular tachycardia ablation: septal involvement, transmural channels, and left ventricular mass. Europace. 2021;23:1437–45.
27.• Roca-Luque I, Van Breukelen A, Alarcon F, Garre P, Tolosana JM, Borras R, et al. Ventricular scar channel entrances identified by new wideband cardiac magnetic resonance sequence to guide ventricular tachycardia ablation in patients with cardiac defibrillators. Europace. 2020;22:598–606. **This study shows that specific wideband sequences allow for high-quality and valid LGE-CMR without artefact in patients with cardiac implantable electronic devices to guide VT ablation.**
28. Sanchez-Somonte P, Garre P, Vázquez-Calvo S, Quinto L, Borràs R, Prat S, et al. Scar conducting channel characterization to predict arrhythmogenicity during ventricular tachycardia ablation. Europace. 2023;25:989.
29. Soto-Iglesias D, Acosta J, Penela D, Fernández-Armenta J, Cabrera M, Martínez M, et al. Image-based criteria to identify the presence of epicardial arrhythmogenic substrate in patients with transmural myocardial infarction. Heart Rhythm. 2018;15:814–21.
30. Soto-Iglesias D, Penela D, Jáuregui B, Acosta J, Fernández-Armenta J, Linhart M, et al. Cardiac magnetic resonance-guided ventricular tachycardia substrate ablation. JACC Clin Electrophysiol. 2020;6:436–47.
31. Buxton AE, Lee KL, Fisher JD, Josephson ME, Prystowsky EN, Hafley G. A randomized study of the prevention of sudden death in patients with coronary artery disease. Multicenter Unsustained Tachycardia Trial Investigators. N Engl J Med. 1999;341:1882–90.
32. Desai AS, Fang JC, Maisel WH, Baughman KL. Implantable defibrillators for the prevention of mortality in patients with nonischemic cardiomyopathy: a meta-analysis of randomized controlled trials. JAMA. 2004;292:2874–9.
33. Hohnloser SH, Kuck KH, Dorian P, Roberts RS, Hampton JR, Hatala R, et al. Prophylactic use of an implantable cardioverter-defibrillator after acute myocardial infarction. N Engl J Med. 2004;351:2481–8.
34. Kadish A, Dyer A, Daubert JP, Quigg R, Estes NA, Anderson KP, et al. Prophylactic defibrillator implantation in patients with nonischemic dilated cardiomyopathy. N Engl J Med. 2004;350:2151–8.
35. Moss AJ, Hall WJ, Cannom DS, Daubert JP, Higgins SL, Klein H, et al. Improved survival with an implanted defibrillator in patients with coronary disease at high risk for ventricular arrhythmia. Multicenter Automatic Defibrillator Implantation Trial Investigators. N Engl J Med. 1996;335:1933–40.
36.• Knops RE, Olde Nordkamp LRA, Delnoy PHM, Boersma LVA, Kuschyk J, El-Chami MF, et al. Subcutaneous or transvenous defibrillator therapy. N Engl J Med. 2020;383:526–36. **This study established non-inferiority of subcutaneous ICD compared to transvenous ICD with respect to device-related complications and inappropriate shocks. However, the capability for antitachycardic pacing of transvenous ICDs reduced the necessity of shocks.**
37. Lambiase PD, Theuns DA, Murgatroyd F, Barr C, Eckardt L, Neuzil P, et al. Subcutaneous implantable cardioverter-defibrillators: long-term results of the EFFORTLESS study. Eur Heart J. 2022;43:2037–50.
38. Moss AJ, Hall WJ, Cannom DS, Klein H, Brown MW, Daubert JP, et al. Cardiac-resynchronization therapy for the prevention of heart-failure events. N Engl J Med. 2009;361:1329–38.
39. Dagres N, Peek N, Leclercq C, Hindricks G. The PROFID project. Eur Heart J. 2020;41:3781–2.

40. Selvanayagam JB, Hartshorne T, Billot L, Grover S, Hillis GS, Jung W, et al. Cardiovascular magnetic resonance-GUIDEd management of mild to moderate left ventricular systolic dysfunction (CMR GUIDE): Study protocol for a randomized controlled trial. Ann Noninvasive Electrocardiol. 2017;22:e12420.
41. Leyva F, Israel CW, Singh J. Declining risk of sudden cardiac death in heart failure: fact or myth? Circulation. 2023;147:759–67.
42. A comparison of antiarrhythmic-drug therapy with implantable defibrillators in patients resuscitated from near-fatal ventricular arrhythmias. N Engl J Med. 1997;**337**:1576–1583.
43. Connolly SJ, Gent M, Roberts RS, Dorian P, Roy D, Sheldon RS, et al. Canadian implantable defibrillator study (CIDS): a randomized trial of the implantable cardioverter defibrillator against amiodarone. Circulation. 2000;101:1297–302.
44. Connolly SJ, Hallstrom AP, Cappato R, Schron EB, Kuck KH, Zipes DP, et al. Meta-analysis of the implantable cardioverter defibrillator secondary prevention trials. AVID, CASH and CIDS studies. Antiarrhythmics vs Implantable Defibrillator study. Cardiac Arrest Study Hamburg. Canadian Implantable Defibrillator Study. Eur Heart J. 2000;21:2071–8.
45. Kuck KH, Cappato R, Siebels J, Rüppel R. Randomized comparison of antiarrhythmic drug therapy with implantable defibrillators in patients resuscitated from cardiac arrest : the Cardiac Arrest Study Hamburg (CASH). Circulation. 2000;102:748–54.
46. Clemens M, Peichl P, Wichterle D, Pavlů L, Čihák R, Aldhoon B, et al. Catheter ablation of ventricular tachycardia as the first-line therapy in patients with coronary artery disease and preserved left ventricular systolic function: long-term results. J Cardiovasc Electrophysiol. 2015;26:1105–10.
47. Maury P, Baratto F, Zeppenfeld K, Klein G, Delacretaz E, Sacher F, et al. Radio-frequency ablation as primary management of well-tolerated sustained monomorphic ventricular tachycardia in patients with structural heart disease and left ventricular ejection fraction over 30%. Eur Heart J. 2014;35:1479–85.
48. Dawson DK, Hawlisch K, Prescott G, Roussin I, Di Pietro E, Deac M, et al. Prognostic role of CMR in patients presenting with ventricular arrhythmias. JACC Cardiovasc Imaging. 2013;6:335–44.
49. Tzivoni D, Banai S, Schuger C, Benhorin J, Keren A, Gottlieb S, et al. Treatment of torsade de pointes with magnesium sulfate. Circulation. 1988;77:392–7.
50. Do DH, Bradfield J, Ajijola OA, Vaseghi M, Le J, Rahman S, et al. Thoracic epidural anesthesia can be effective for the short-term management of ventricular tachycardia storm. J Am Heart Assoc. 2017;6. https://doi.org/10.1161/JAHA.117.007080
51. Fudim M, Qadri YJ, Waldron NH, Boortz-Marx RL, Ganesh A, Patel CB, et al. Stellate ganglion blockade for the treatment of refractory ventricular arrhythmias. JACC Clin Electrophysiol. 2020;6:562–71.
52. Savastano S, Dusi V, Baldi E, Rordorf R, Sanzo A, Camporotondo R, et al. Anatomical-based percutaneous left stellate ganglion block in patients with drug-refractory electrical storm and structural heart disease: a single-centre case series. Europace. 2021;23:581–6.
53. Tian Y, Wittwer ED, Kapa S, McLeod CJ, Xiao P, Noseworthy PA, et al. Effective use of percutaneous stellate ganglion blockade in patients with electrical storm. Circ Arrhythm Electrophysiol. 2019;12:e007118.
54. Vaseghi M, Barwad P, Malavassi Corrales FJ, Tandri H, Mathuria N, Shah R, et al. Cardiac sympathetic denervation for refractory ventricular arrhythmias. J Am Coll Cardiol. 2017;69:3070–80.
55. Muser D, Liang JJ, Castro SA, Hayashi T, Enriquez A, Troutman GS, et al. Outcomes with prophylactic use of percutaneous left ventricular assist devices in high-risk patients undergoing catheter ablation of scar-related ventricular tachycardia: a propensity-score matched analysis. Heart Rhythm. 2018;15:1500–6.
56. Mathuria N, Wu G, Rojas-Delgado F, Shuraih M, Razavi M, Civitello A, et al. Outcomes of pre-emptive and rescue use of percutaneous left ventricular assist device in patients with structural heart disease undergoing catheter ablation of ventricular tachycardia. J Interv Card Electrophysiol. 2017;48:27–34.
57. Gopinathannair R, Cornwell WK, Dukes JW, Ellis CR, Hickey KT, Joglar JA, et al. Device therapy and arrhythmia management in left ventricular assist device recipients: a scientific statement from the American Heart Association. Circulation. 2019;139:e967–89.
58. Preliminary report: effect of encainide and flecainide on mortality in a randomized trial of arrhythmia suppression after myocardial infarction. N Engl J Med. 1989;**321**:406–412.
59. Effect of the antiarrhythmic agent moricizine on survival after myocardial infarction. N Engl J Med. 1992;**327**:227–233.
60. Echt DS, Liebson PR, Mitchell LB, Peters RW, Obias-Manno D, Barker AH, et al. Mortality and morbidity in patients receiving encainide, flecainide, or placebo. The Cardiac Arrhythmia Suppression Trial. N Engl J Med. 1991;324:781–8.
61. Connolly SJ, Dorian P, Roberts RS, Gent M, Bailin S, Fain ES, et al. Comparison of beta-blockers, amiodarone plus beta-blockers, or sotalol for prevention of shocks from implantable cardioverter defibrillators: the OPTIC Study: a randomized trial. JAMA. 2006;295:165–71.
62. Lüderitz B, Mletzko R, Jung W, Manz M. Combination of antiarrhythmic drugs. J Cardiovasc Pharmacol. 1991;17(Suppl 6):S48-52.
63. Waldo AL, Camm AJ, deRuyter H, Friedman PL, MacNeil DJ, Pauls JF, et al. Effect of d-sotalol on mortality in patients with left ventricular dysfunction after recent and remote myocardial infarction. The SWORD Investigators. Survival With Oral d-Sotalol. Lancet. 1996;348:7–12.
64. Pacifico A, Hohnloser SH, Williams JH, Tao B, Saksena S, Henry PD, et al. Prevention of implantable-defibrillator shocks by treatment with sotalol. d, l-Sotalol Implantable Cardioverter-Defibrillator Study Group. N Engl J Med. 1999;340:1855–62.
65. Gottlieb SS, Weinberg M. Cardiodepressant effects of mexiletine in patients with severe left ventricular dysfunction. Eur Heart J. 1992;13:22–7.
66. Hoffmeister HM, Hepp A, Seipel L. Negative inotropic effect of class-I-antiarrhythmic drugs: comparison of flecainide with disopyramide and quinidine. Eur Heart J. 1987;8:1126–32.
67. The Cardiac Insufficiency Bisoprolol Study II (CIBIS-II): a randomised trial. Lancet. 1999;353:9–13.
68. Dargie HJ. Effect of carvedilol on outcome after myocardial infarction in patients with left-ventricular dysfunction: the CAPRICORN randomised trial. Lancet. 2001;357:1385–90.
69. Piccini JP, Berger JS, O'Connor CM. Amiodarone for the prevention of sudden cardiac death: a meta-analysis of randomized controlled trials. Eur Heart J. 2009;30:1245–53.
70. Singh SN, Fletcher RD, Fisher SG, Singh BN, Lewis HD, Deedwania PC, et al. Amiodarone in patients with congestive heart failure and asymptomatic ventricular arrhythmia. Survival Trial of Antiarrhythmic Therapy in Congestive Heart Failure. N Engl J Med. 1995;333:77–82.
71. Santangeli P, Muser D, Maeda S, Filtz A, Zado ES, Frankel DS, et al. Comparative effectiveness of antiarrhythmic drugs and catheter ablation for the prevention of recurrent ventricular tachycardia in patients with implantable cardioverter-defibrillators: a systematic review and meta-analysis of randomized controlled trials. Heart Rhythm. 2016;13:1552–9.
72.• Arenal Á, Ávila P, Jiménez-Candil J, Tercedor L, Calvo D, Arribas F, et al. Substrate ablation vs antiarrhythmic drug therapy for symptomatic ventricular tachycardia. J Am Coll Cardiol.

2022;79:1441–53. **This RCT demonstrated superiority of first-line VT ablation over AAD therapy, mostly driven by AAD-related adverse effects and incidence of slow VTs.**

73. Sapp JL, Wells GA, Parkash R, Stevenson WG, Blier L, Sarrazin JF, et al. Ventricular tachycardia ablation versus escalation of antiarrhythmic drugs. N Engl J Med. 2016;375:111–21.
74. Kuck KH, Schaumann A, Eckardt L, Willems S, Ventura R, Delacrétaz E, et al. Catheter ablation of stable ventricular tachycardia before defibrillator implantation in patients with coronary heart disease (VTACH): a multicentre randomised controlled trial. Lancet. 2010;375:31–40.
75. Reddy VY, Reynolds MR, Neuzil P, Richardson AW, Taborsky M, Jongnarangsin K, et al. Prophylactic catheter ablation for the prevention of defibrillator therapy. N Engl J Med. 2007;357:2657–65.
76.• Willems S, Tilz RR, Steven D, Kääb S, Wegscheider K, Gellér L, et al. Preventive or deferred ablation of ventricular tachycardia in patients with ischemic cardiomyopathy and implantable defibrillator (BERLIN VT): a multicenter randomized trial. Circulation. 2020;141:1057–67. **This RCT was stopped prematurely for futility and failed to prove prognostic benefit of an early VT ablation strategy compared to deferred ablation. However, early VT ablation reduced VT recurrence and appropriate ICD therapies.**
77.• Della Bella P, Baratto F, Vergara P, Bertocchi P, Santamaria M, Notarstefano P, et al. Does timing of ventricular tachycardia ablation affect prognosis in patients with an implantable cardioverter defibrillator? Results From the Multicenter Randomized PARTITA Trial. Circulation. 2022;145:1829–38. **This RCT found a decrease in ICD shocks and all-cause death with early VT ablation, albeit results remain to be confirmed in an adequately powered trial.**
78.• Tung R, Xue Y, Chen M, Jiang C, Shatz DY, Besser SA, et al. First-line catheter ablation of monomorphic ventricular tachycardia in cardiomyopathy concurrent with defibrillator implantation: the PAUSE-SCD randomized trial. Circulation. 2022;145:1839–49. **In this RCT, catheter ablation as first-line therapy for VT reduced the combined primary endpoint of death, cardiovascular hospitalisation, and recurrent VT in a mixed cohort of patients with ischemic (35%), non-ischemic (30%), and arrhythmogenic cardiomyopathy (35%). This was predominantly driven by a reduction in VT recurrence.**
79. Stevenson WG, Khan H, Sager P, Saxon LA, Middlekauff HR, Natterson PD, et al. Identification of reentry circuit sites during catheter mapping and radiofrequency ablation of ventricular tachycardia late after myocardial infarction. Circulation. 1993;88:1647–70.
80.• Aziz Z, Shatz D, Raiman M, Upadhyay GA, Beaser AD, Besser SA, et al. Targeted ablation of ventricular tachycardia guided by wavefront discontinuities during sinus rhythm: a new functional substrate mapping strategy. Circulation. 2019;140:1383–97. **This article introduces the concept of isochronal mapping for the identification of slow-conduction areas in sinus rhythm to be targeted by catheter ablation.**
81. Tung R. Substrate mapping in ventricular arrhythmias. Card Electrophysiol Clin. 2019;11:657–63.
82.• Tung R, Raiman M, Liao H, Zhan X, Chung FP, Nagel R, et al. Simultaneous endocardial and epicardial delineation of 3D reentrant ventricular tachycardia. J Am Coll Cardiol. 2020;75:884–97. **This work elaborates and highlights the 3-dimensionality of VT reentry circuits.**
83. Cronin EM, Bogun FM, Maury P, Peichl P, Chen M, Namboodiri N, et al. 2019 HRS/EHRA/APHRS/LAHRS expert consensus statement on catheter ablation of ventricular arrhythmias: executive summary. Europace. 2020;22:450–95.
84. Cuculich PS, Schill MR, Kashani R, Mutic S, Lang A, Cooper D, et al. Noninvasive Cardiac Radiation for Ablation of Ventricular Tachycardia. N Engl J Med. 2017;377:2325–36.
85. Futyma P, Sauer WH. Bipolar radiofrequency catheter ablation of left ventricular summit arrhythmias. Card Electrophysiol Clin. 2023;15:57–62.
86. Kany S, Alken FA, Schleberger R, Baran J, Luik A, Haas A, et al. Bipolar ablation of therapy-refractory ventricular arrhythmias: application of a dedicated approach. Europace. 2022;24:959–69.
87. Packer DL, Wilber DJ, Kapa S, Dyrda K, Nault I, Killu AM, et al. Ablation of refractory ventricular tachycardia using intramyocardial needle delivered heated saline-enhanced radiofrequency energy: a first-in-man feasibility trial. Circ Arrhythm Electrophysiol. 2022;15:e010347.
88. Stevenson WG, Tedrow UB, Reddy V, AbdelWahab A, Dukkipati S, John RM, et al. Infusion needle radiofrequency ablation for treatment of refractory ventricular arrhythmias. J Am Coll Cardiol. 2019;73:1413–25.
89. van der Ree MH, Blanck O, Limpens J, Lee CH, Balgobind BV, Dieleman EMT, et al. Cardiac radioablation-a systematic review. Heart Rhythm. 2020;17:1381–92.
90. Santangeli P, Muser D, Zado ES, Magnani S, Khetpal S, Hutchinson MD, et al. Acute hemodynamic decompensation during catheter ablation of scar-related ventricular tachycardia: incidence, predictors, and impact on mortality. Circ Arrhythm Electrophysiol. 2015;8:68–75.
91. Luni FK, Zungsontiporn N, Farid T, Malik SA, Khan S, Daniels J, et al. Percutaneous left ventricular assist device support during ablation of ventricular tachycardia: a meta-analysis of current evidence. J Cardiovasc Electrophysiol. 2019;30:886–95.
92. Cikes M, Jakus N, Claggett B, Brugts JJ, Timmermans P, Pouleur AC, et al. Cardiac implantable electronic devices with a defibrillator component and all-cause mortality in left ventricular assist device carriers: results from the PCHF-VAD registry. Eur J Heart Fail. 2019;21:1129–41.
93. Galand V, Flécher E, Auffret V, Boulé S, Vincentelli A, Dambrin C, et al. Predictors and clinical impact of late ventricular arrhythmias in patients with continuous-flow left ventricular assist devices. JACC Clin Electrophysiol. 2018;4:1166–75.
94. Greet BD, Pujara D, Burkland D, Pollet M, Sudhakar D, Rojas F, et al. Incidence, predictors, and significance of ventricular arrhythmias in patients with continuous-flow left ventricular assist devices: a 15-year institutional experience. JACC Clin Electrophysiol. 2018;4:257–64.
95. Makki N, Mesubi O, Steyers C, Olshansky B, Abraham WT. Meta-analysis of the relation of ventricular arrhythmias to all-cause mortality after implantation of a left ventricular assist device. Am J Cardiol. 2015;116:1385–90.
96. Hayward CS, Salamonsen R, Keogh AM, Woodard J, Ayre P, Prichard R, et al. Effect of alteration in pump speed on pump output and left ventricular filling with continuous-flow left ventricular assist device. Asaio j. 2011;57:495–500.
97. Vollkron M, Voitl P, Ta J, Wieselthaler G, Schima H. Suction events during left ventricular support and ventricular arrhythmias. J Heart Lung Transplant. 2007;26:819–25.
98. Andersen M, Videbaek R, Boesgaard S, Sander K, Hansen PB, Gustafsson F. Incidence of ventricular arrhythmias in patients on long-term support with a continuous-flow assist device (HeartMate II). J Heart Lung Transplant. 2009;28:733–5.
99. Cantillon DJ, Bianco C, Wazni OM, Kanj M, Smedira NG, Wilkoff BL, et al. Electrophysiologic characteristics and catheter ablation of ventricular tachyarrhythmias among patients with heart failure on ventricular assist device support. Heart Rhythm. 2012;9:859–64.
100. Ziv O, Dizon J, Thosani A, Naka Y, Magnano AR, Garan H. Effects of left ventricular assist device therapy on ventricular arrhythmias. J Am Coll Cardiol. 2005;45:1428–34.
101. Sacher F, Reichlin T, Zado ES, Field ME, Viles-Gonzalez JF, Peichl P, et al. Characteristics of ventricular tachycardia ablation

in patients with continuous flow left ventricular assist devices. Circ Arrhythm Electrophysiol. 2015;8:592–7.
102. Mulloy DP, Bhamidipati CM, Stone ML, Ailawadi G, Bergin JD, Mahapatra S, et al. Cryoablation during left ventricular assist device implantation reduces postoperative ventricular tachyarrhythmias. J Thorac Cardiovasc Surg. 2013;145:1207–13.
103. Patel M, Rojas F, Shabari FR, Simpson L, Cohn W, Frazier OH, et al. Safety and feasibility of open chest epicardial mapping and ablation of ventricular tachycardia during the period of left ventricular assist device implantation. J Cardiovasc Electrophysiol. 2016;27:95–101.
104. Clerkin KJ, Topkara VK, Demmer RT, Dizon JM, Yuzefpolskaya M, Fried JA, et al. Implantable cardioverter-defibrillators in patients with a continuous-flow left ventricular assist device: an analysis of the INTERMACS registry. JACC Heart Fail. 2017;5:916–26.
105. Aquaro GD, Pingitore A, Strata E, Di Bella G, Molinaro S, Lombardi M. Cardiac magnetic resonance predicts outcome in patients with premature ventricular complexes of left bundle branch block morphology. J Am Coll Cardiol. 2010;56:1235–43.
106. Muser D, Santangeli P, Castro SA, Casado Arroyo R, Maeda S, Benhayon DA, et al. Risk stratification of patients with apparently idiopathic premature ventricular contractions: a multicenter international CMR registry. JACC Clin Electrophysiol. 2020;6:722–35.
107. Yokokawa M, Siontis KC, Kim HM, Stojanovska J, Latchamsetty R, Crawford T, et al. Value of cardiac magnetic resonance imaging and programmed ventricular stimulation in patients with frequent premature ventricular complexes undergoing radiofrequency ablation. Heart Rhythm. 2017;14:1695–701.
108. Baldasseroni S, Opasich C, Gorini M, Lucci D, Marchionni N, Marini M, et al. Left bundle-branch block is associated with increased 1-year sudden and total mortality rate in 5517 outpatients with congestive heart failure: a report from the Italian network on congestive heart failure. Am Heart J. 2002;143:398–405.
109. Baman TS, Lange DC, Ilg KJ, Gupta SK, Liu TY, Alguire C, et al. Relationship between burden of premature ventricular complexes and left ventricular function. Heart Rhythm. 2010;7:865–9.
110. Latchamsetty R, Yokokawa M, Morady F, Kim HM, Mathew S, Tilz R, et al. Multicenter outcomes for catheter ablation of idiopathic premature ventricular complexes. JACC Clin Electrophysiol. 2015;1:116–23.
111. Lee AKY, Andrade J, Hawkins NM, Alexander G, Bennett MT, Chakrabarti S, et al. Outcomes of untreated frequent premature ventricular complexes with normal left ventricular function. Heart. 2019;105:1408–13.
112. Voskoboinik A, Hadjis A, Alhede C, Im SI, Park H, Moss J, et al. Predictors of adverse outcome in patients with frequent premature ventricular complexes: the ABC-VT risk score. Heart Rhythm. 2020;17:1066–74.
113. Berruezo A, Penela D, Jáuregui B, Soto-Iglesias D, Aguinaga L, Ordóñez A, et al. Mortality and morbidity reduction after frequent premature ventricular complexes ablation in patients with left ventricular systolic dysfunction. Europace. 2019;21:1079–87.
114. Penela D, Acosta J, Aguinaga L, Tercedor L, Ordoñez A, Fernández-Armenta J, et al. Ablation of frequent PVC in patients meeting criteria for primary prevention ICD implant: safety of withholding the implant. Heart Rhythm. 2015;12:2434–42.
115. Penela D, Van Huls Vans Taxis C, Aguinaga L, Fernández-Armenta J, Mont L, et al. Neurohormonal, structural, and functional recovery pattern after premature ventricular complex ablation is independent of structural heart disease status in patients with depressed left ventricular ejection fraction: a prospective multicenter study. J Am Coll Cardiol. 2013;62:1195–202.
116. Ling Z, Liu Z, Su L, Zipunnikov V, Wu J, Du H, et al. Radiofrequency ablation versus antiarrhythmic medication for treatment of ventricular premature beats from the right ventricular outflow tract: prospective randomized study. Circ Arrhythm Electrophysiol. 2014;7:237–43.
117. Hyman MC, Mustin D, Supple G, Schaller RD, Santangeli P, Arkles J, et al. Class IC antiarrhythmic drugs for suspected premature ventricular contraction-induced cardiomyopathy. Heart Rhythm. 2018;15:159–63.

applied sciences

MDPI

Review

Impact of LGE-MRI in Arrhythmia Ablation

Paz Garre [1,2], Sara Vázquez-Calvo [1,2], Elisenda Ferro [3,4], Till Althoff [1,2] and Ivo Roca-Luque [1,2,5,*]

1 Institut Clinic Cardiovascular, Hospital Clínic, Universitat de Barcelona, 08036 Barcelona, Spain
2 Institut d'Investigacions Biomèdiques August Pi i Sunyer (IDIBAPS), 08036 Barcelona, Spain
3 Medtronic Iberica, 08970 Sant Joan Despí, Spain
4 Fundació Clínic per a la Recerca Biomèdica (FCRB), 08036 Barcelona, Spain
5 Centro de Investigación Biomédica en Red de Enfermedades Cardiovasculares (CIBERCV), 28029 Madrid, Spain
* Correspondence: iroca@clinic.cat

Abstract: The use of late gadolinium enhancement magnetic resonance imaging (LGE-MRI) in arrhythmia ablation is increasing due to the capacity to detect, quantify and characterize cardiac fibrosis both in atrium and ventricle. Catheter ablation has become a standard treatment for arrhythmias, and LGE-MRI has demonstrated to be a useful tool to plan and guide ablation. Furthermore, recent studies have proved the usefulness in substrate analysis and postablation evaluation. This review will analyze the application and the current role of LGE-MRI to improve strategies for the two main cardiac arrhythmias: Atrial fibrillation and ventricular tachycardia.

Keywords: cardiac magnetic resonance; late gadolinium enhancement; atrial fibrillation; ventricular tachycardia; ablation; fibrosis; electroanatomical mapping

Citation: Garre, P.; Vázquez-Calvo, S.; Ferro, E.; Althoff, T.; Roca-Luque, I. Impact of LGE-MRI in Arrhythmia Ablation. *Appl. Sci.* **2023**, *13*, 3862. https://doi.org/10.3390/app13063862

Academic Editor: Julio Garcia Flores

Received: 31 January 2023
Revised: 6 March 2023
Accepted: 9 March 2023
Published: 17 March 2023

1. Introduction

Magnetic resonance imaging (MRI) has become a cornerstone of the diagnostic and prognostic evaluation of patients with cardiac arrhythmias. It is widely used for qualitative and quantitative evaluation of cardiac conditions and support diagnosis, monitoring disease progression and treatment planning [1]. Nowadays, late gadolinium enhancement (LGE) MRI is being used to detect and quantify cardiac fibrosis in both ventricular and atrial arrhythmias [2–6].

Atrial fibrillation (AF) is the most prevalent sustained cardiac arrhythmia, being observed in up to 2% of the general population and in over 5–10% of the elderly population (>70 years of age). In this sense, due to the ageing of society and demographic changes, the overall prevalence is expected to increase even further [7]. Atrial fibrillation is associated with a fivefold risk of stroke and a threefold incidence of congestive heart failure and doubles the risk of mortality and dementia [8]. Isolation of the pulmonary veins (PV) by catheter ablation has emerged as a first-line therapy for patients with symptomatic AF not responding to pharmaceutical treatment [9]. PVI has achieved high success in paroxysmal atrial fibrillation. Nevertheless, in persistent AF, there is still a high rate of recurrence. A very recent study (ERASE AF) demonstrated that ablation of extra PV areas with low voltage detected with mapping catheters is helpful in these patients. In this sense, MRI could play a role in detecting these areas with LGE.

Ventricular tachycardia (VT) is the most frequent etiology of sudden cardiovascular death (SCD) [10]. In patients with structural heart disease, VT is frequent and catheter ablation has become a standard treatment [11,12], being the main mechanism responsible for a re-entrant circuit [13–15]. In this sense, there is an area of slow conduction of intermediate tissue (so called border zone (BZ)) inside the core scar connecting regions of healthy tissue. These areas of slow conduction are referred to as conducting channels (CCs) which can be rigorously defined during ablation procedures using electroanatomical maps (EAMs) [15–18]. On the other hand, MRI allows the depiction of the BZ, healthy tissue and

core scar, identifying also CCs. A great concordance between EAMs and images obtained by MRI has been reported. Moreover, in a recent study [19] MRI has been carried out post mortem in cases of sudden cardiac death to research cardiac morphological alterations. Despite advancements in ablation technology and better understanding of arrhythmic substrates, VT recurrence rates are still high [20–23]. For this reason, there is a clinical need to improve the characterization of the VT substrate and the efficacy of VT ablation. In this context, LGE-MRI may play an important role.

The objective of this review is to analyse the application of LGE-MRI to improve ablation strategies for the two main cardiac arrhythmias: AF and VT.

2. Use of LGE-MRI for the Detection of Fibrosis

2.1. Principles of LGE

LGE-MRI for the detection of myocardial fibrosis was already described in the late 1990s. Its validation was firstly performed with a canine model with controlled myocardial infarction and LGE-MRI was compared with histology [24]. Contrast agents that use mainly gadolinium are able to diffuse freely into the interstitium but are unable to pass through intact cell membranes, leading to their accumulation in the extracellular space.

Fibrosis replacement produces an expansion of extracellular space so there is an increase in the volume of the distribution of gadolinium. More important, there is a prolonged washout of the gadolinium due the decreased number of capillary vessels in the scar tissue [25,26]. Regarding T1 sequence, gadolinium contrast agents decrease the T1 relaxation time of adjacent tissue. Therefore, LGE enhancement produces an increased signal intensity in T1-weighted MRI images. In addition, other diseases related to the expansion of the extracellular space can be shown by LGE, such as oedema and inflammation formation. Given the lack of specificity for fibrotic tissue detection, the lesion assessment can be challenging [27].

2.2. Protocol of Image Acquisition and LGE Analysis

To date, there is no agreement on the best standardized way to acquire MRI images for the detection of myocardial fibrosis [28–31]. Either 3T or 1.5 scanners can be used to acquire postcontrast images applying fast 3D gradient echo series with fat suppression and ECG gating. Subsequent inversion recovery sequences are used to nullify the signal of healthy myocardium and improve signal intensity and T1 contrast. The optimum inversion time (TI) that suppress healthy tissue (typically 250–300 ms) is initially determined empirically. Scar areas will thus appear hyperenhanced relative to healthy myocardium. Adjustment of TI values during acquisition may be necessary to accommodate incremental T1 values of the normal tissue owing to gadolinium washout. For this reason, ECG gating is important to limit motion artifacts and the MRI acquisition window is limited to less to 20% of the RR interval. For patients with AF, cardioversion is often recommended prior to the study to improve image quality [30,32]. Finally, in some patients another limiting factor could be the need for long breath-holds. To solve that limitation, free-breathing 3D navigators can be used that suppress respiratory artefacts through respiratory gating. Typical LGE-MRI sequences result in a voxel size of 1.25 × 1.25 × 2.5 mm with scan times of 10–15 min, depending on heart rate and breathing patterns.

Regarding myocardial fibrosis, to obtain high-quality LGE-MRI images to evaluate it, the time delay between contrast injection and image acquisition is crucial, as the LGE amount depends on wash-in and washout kinetics. Despite there being no official consensus, usually LGE-MRI acquisition is performed 15–25 min (atrium) or 7–15 min (ventricle) after gadolinium contrast agent injection. The time delay may even be adjusted for each patient due to individual perfusion (cardiovascular function) and washout kinetics (renal function).

In our centre, the acquisition of ventricle images is performed 10–15 min after an intravenous gadolinium injection, and 20 min in the atrium.

2.3. Image Acquisition for Patients with Cardiac Devices

Most patients scheduled for VT ablation are individuals with established cardiomyopathy who carry an implantable cardioverter defibrillator (ICD) implanted for primary or secondary prevention. This issue represents a major limitation for MRI because of security and also because of hyperintense image artefacts that can be caused by the device.

Regarding safety, several studies have shown an extremely low risk of device-related complications in patients who undergo cardiac MRI, not only in MRI conditional devices, but also in the case of theoretical MRI nonconditional devices. With adequate intraprocedural programming of the device, MRI is safe in patients with MRI nonconditional devices [33–35]. In this sense, the main issue with patients with cardiac devices is the quality of MRI images due to the possible artefacts related to the ICD. Artefacts can occur when metallic ICD components distort the magnetic field [36,37] making it difficult to obtain clear images using LGE-MRI. The effect of ICD artefacts are most prominent in the anterior wall, and in patients with left sided devices, in the anterior and apical left ventricle. Some studies have suggested that limited spectral bandwidth of the inversion pulse used in LGE-MRI is the primary cause of device-related artefacts [38,39]. To avoid those artefacts, particular wideband MRI sequences have been recently developed, increasing the bandwidth of the inversion and excitation pulses. Therefore, the use of wideband sequences can minimize device-related artefacts and, subsequently, overcome the image artefact, making LGE-MRI robust for myocardial characterization [33,40,41]. Many centres including ours are now applying these wideband sequences, avoiding device-related artefacts and achieving high quality images, even in areas closed to the ICD. In fact, our group has recently proved a strong correlation between wideband LGE-MRI and electroanatomical maps [42]. In this study [42] the accuracy of wideband sequences to detect CCs previously located in EAMs was analysed for 13 patients with an ICD and a wideband sequence. The accuracy of CCs identified was 85.1% and the positive predicting value was 92.5%.

3. Image Post-Processing (Pre-Procedural)

3.1. Image Processing: Segmentation and Fibrosis Detection

Post-processing is necessary to acquire a 3D anatomical reconstruction of the chamber of interest and to identify, analyse and evaluate the scarring tissue. To acquire this 3D anatomical segmentation, there is a great deal of established open-source and commercial software for image post-processing.

The two steps required to achieve this 3D anatomical structure are segmentation of the anatomical chamber (LA and/or RA and PPVV in the case of AF and LV and/or RV in the case of VT) and detection of fibrotic and scarring areas inside the segmented anatomical structure.

I. Segmentation of anatomical structures

Accurate segmentation is required for scar analysis and fibrosis visualization. The segmentation process was performed manually. Clinicians or engineers segment the atrial wall or the myocardium manually: An accurate slice-by-slice 2D tracing of the LA wall and endocardial and epicardial myocardium to confine the region of interest (ROI) while avoiding anatomical structures (aortic ring, valves, papillary muscles, etc.), the blood pool, fat, etc. Currently, the different segmentation software programs have semiautomatic tools available. Therefore, the manual process may be used after this automatic segmentation to refine the results.

II. Detection of fibrotic tissue

Once the anatomy is properly segmented, the fibrotic regions (LGE) can be assessed qualitatively by visual assessment or quantitatively by using different thresholding techniques. To apply thresholding techniques, different approaches with different algorithms have been improved for the detection of arrhythmogenic areas. To date, there is limited reproducibility across centres because there is no single standardized method for LGE image analysis.

Obtaining a consistent internal reference for normalization and validated signal intensity thresholds that can accurately differentiate between healthy and scar tissue are crucial for quantifying LGE. The reason is that T1-weighted imaging relies on signal intensity contrast instead of directly measured absolute values.

Different methods have been validated for atrial fibrosis quantification (Table 1) [29–31,43–47]. Each method uses distinct internal references and thresholds. As an internal reference, the mean signal intensity of the blood pool is used extensively by numerous groups. Our group has recently validated a method quantifying signal intensity ratios using the mean signal intensity of the left atrial (LA) blood pool as a reference (signal intensity of each given voxel/mean signal intensity of the blood) [29]. The atrium thresholds to characterize healthy myocardium (signal intensity ratio $\leq$ 1.2) and fibrotic tissue (signal intensity ratio > 1.32) were derived from distinct cohorts including both young healthy individuals and post-AF ablation patients. Subsequently these cut-offs were verified in various studies in comparison with voltage mapping during ablation procedures and they were correlated with clinical endpoints [6,48,49] (Figure 1).

Table 1. LGE-MRI post-processing defining thresholds for fibrosis analysis.

	Reference	Model	n	Reference for Normalization	Defined Thresholds
Atrial Fibrosis	Peters et al., 2007 [31]	Human	23	LA blood pool signal intensity	"Minimum threshold which eliminates most left atrial blood pool pixels"
	Oakes et al., 2009 [30]	Human	81	Normal tissue	Mean signal intensity (normal tissue) + (2–4) SD
	Khurram et al., 2014 [47]	Human	75	Mean LA blood pool signal intensity	Fixed IIR threshold: upper limit of normal > 0.97 and dense scar > 1.6
	Harrison et al., 2014 [43]	Animal	16	Mean LA blood pool signal intensity	"2.3 SD for LGE post ablation and 3.3 SD for LGE chronically"
	Dewire et al., 2014 [46]	Human	60	Mean LA blood pool signal intensity	Universal threshold (abnormal myocardium: IIR > 0.97 and <1.61; dense scar: IIR > 1.61)
	Harrison et al., 2015 [44]	Human	20	Mean LA blood pool signal intensity	No universal threshold. Visualization of signal intensities in SD from reference
	Benito el al., 2017 [29]	Human	40	Mean LA blood pool signal intensity	Fixed IIR threshold: upper limit of normal = 1.2 and dense scar > 1.32
	Kurose et al., 2020 [45]	Human	30	Healthy atrial wall	>2 SDs above the mean of healthy left atrium wall
LV Fibrosis	Amado et al., 2004 [50]	Animal	13	Healthy myocardial segment	Mean signal intensity (noninfarcted myocardium region) + (1–6 SD)
	Yan et al., 2006 [51]	Human	144	Healthy myocardial segment	BZ: 2–3 SDs and scar > 3 SDs above remote myocardium
	Andreu et al., 2011 [52]	Human	12	Maximal myocardial signal	Scar > 60% of maximal signal intensity
	Fernandez-Armenta et al., 2013 [53]	Human	21	Maximal myocardial signal	Healthy tissue < 40%, BZ: 40–60% and scar > 60% of maximal signal intensity
	Cochet et al., 2013 [54]	Human	9	Maximal myocardial signal	BZ: 35–50% and scar > 50% of maximal signal intensity

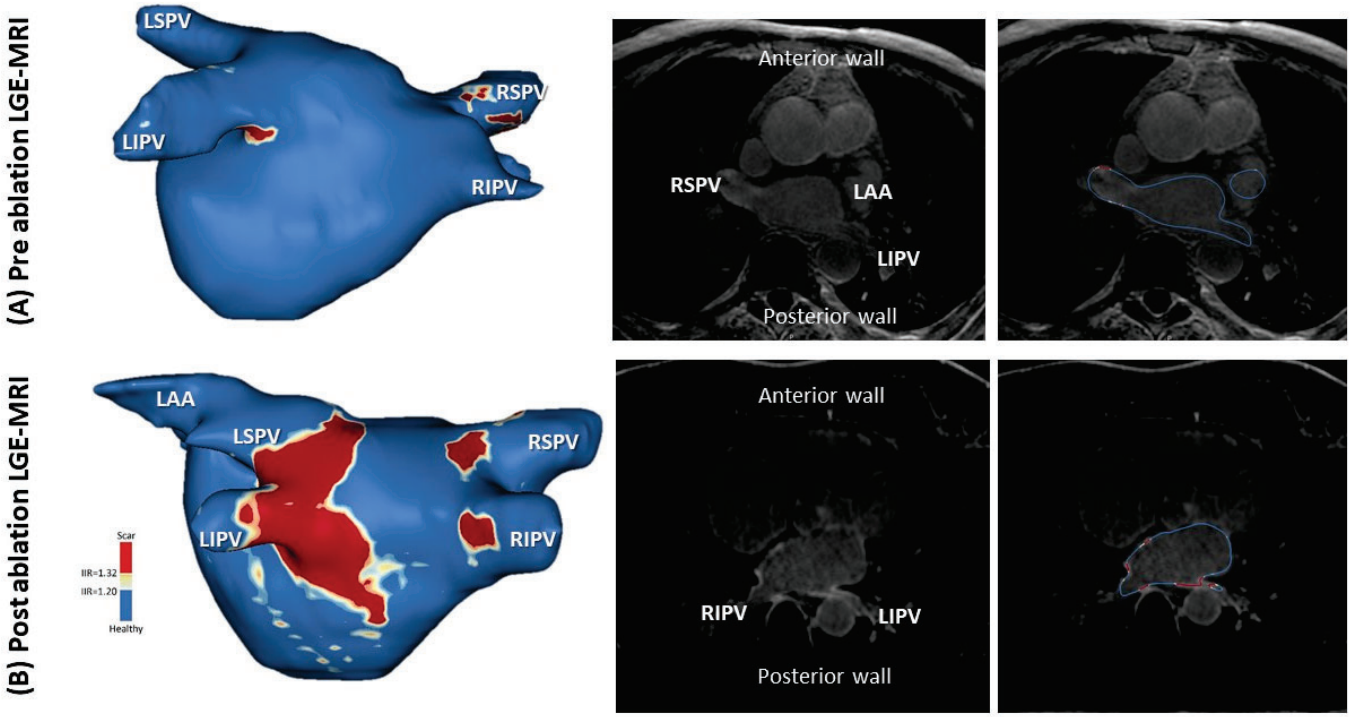

Figure 1. Postero-anterior view of three-dimensional left atrium reconstruction of LGE-MRI. 3D-LGE-LA reconstruction includes colour-coding based on image intensity ratios with thresholds for border zone (yellow 1.2–1.32) and dense scar (red > 1.32). (**A**) First line corresponds to preprocedural LGE-MRI and (**B**) second corresponds to a post-ablation LGE-MRI (3 months after PVI). LAA = left atrial appendage; LIPV = left inferior pulmonary vein; LSPV = left superior pulmonary vein; RIPV = right inferior pulmonary vein; RSPV = right superior pulmonary vein.

The most interesting approaches to detect and quantify fibrosis in LGE-MRI of the left atrial wall are carefully benchmarked by Pontecorboli et al. [2]. This review provides a critical analysis of the different methods to detect and quantify fibrosis in LGE-MRI, stating their advantages and limitations.

Likewise, for ventricular fibrosis quantification, various thresholds and methods have been verified (Table 1) [50–54]. Table 1 summarizes the main studies defining thresholds for LV. The most commonly used approach is the full width at half maximum (FWHM), which is a fixed thresholding method in which a fixed intensity threshold is defined as half of the maximum intensity of a user-selected hyperenhanced region. Another method is to define remote "healthy" myocardial segments as an internal reference for normalization. Another common method is the fixed-model approach, whereby intensities are thresholded to a fixed number of standard deviations (SD) from the mean intensity of the nulled myocardium or blood pool [55]. This is known as the n-SD method.

Our group study found that the correlation with EAM voltage mapping was reached with the thresholds of <40% as healthy tissue and >60% as a dense scar of the maximum signal intensity (Figure 2).

3.2. Deep Learning-Based Methods

With the development of artificial intelligence techniques, the application of deep learning to fibrosis and substrate visualization has also been studied, leading to the development of a fully automated key for LGE-MRI segmentation. An increasing number of various deep learning models using convolutional neural networks (for example, U-Net [56]) have demonstrated encouraging results in the segmentation of cardiac substructures. Goodfellow et al. 2016 [57] mathematically detail these deep neural networks.

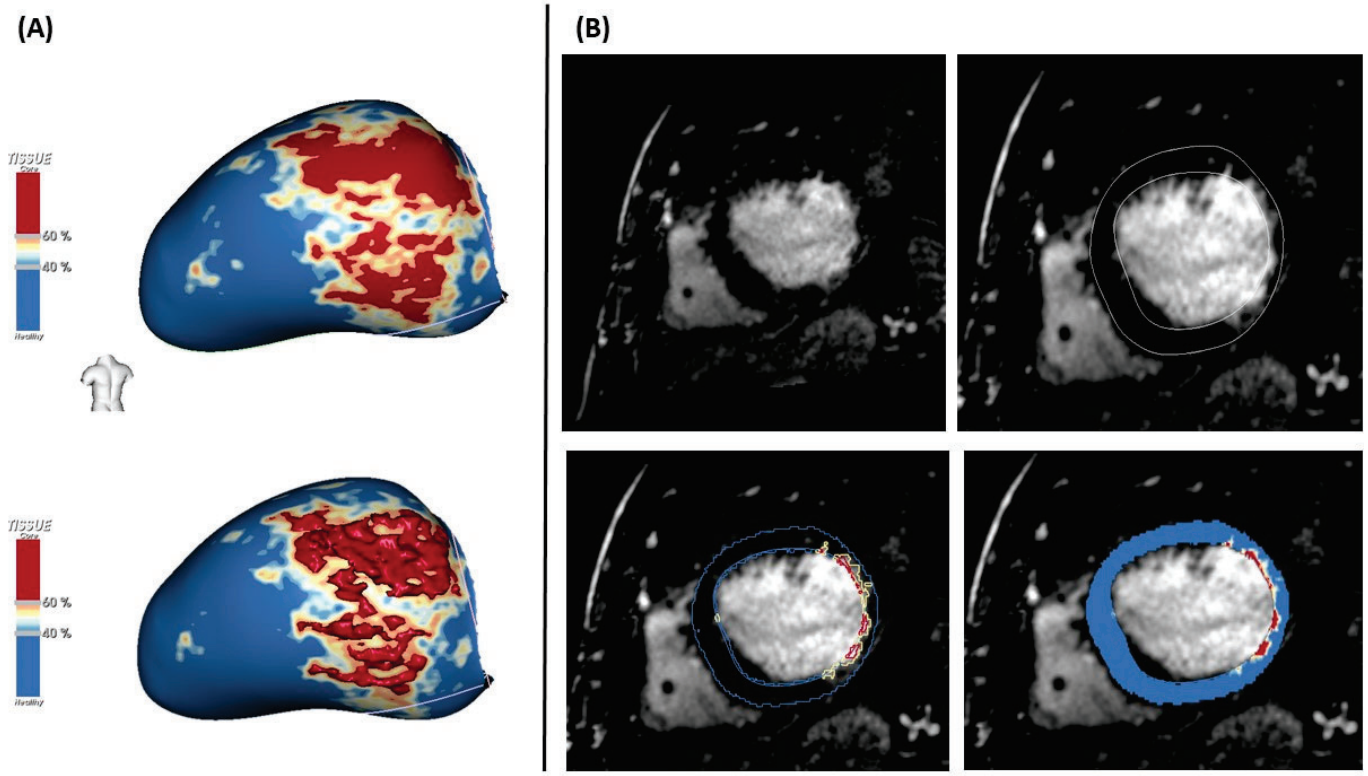

Figure 2. (**A**) Three-dimensional left ventricle reconstruction of LGE-MRI. LGE-based colour-coding is used to differentiate LV dense scar (red > 60% of maximum signal intensity) from border zone (yellow, 40–60% of maximum signal intensity) and healthy tissue (blue < 40%). (**B**) Raw images of LGE-MRI in a patient with chronic MI. Semiautomatic segmentation of epicardium and endocardium with detection of dense scar and border zone is shown.

4. Use of the Processed LGE-MRI for Ablation Procedures

LGE-MRI in VT or AF ablation procedures has proved to be an important tool to plan and guide ablation. Regarding planification, LGE-MRI allows us to perform a preprocedural assessment of cardiac anatomy and myocardial scar (location of conducting channels in the case of VT and PPVV gaps in AF), to decide the optimal access approach (especially in VT where both endocardial and epicardial approaches can be selected) and exclude intracardiac thrombus. In addition, 3D-LGE-MRI reconstruction can be visualized side by side or merged with electroanatomical maps during the procedure. In VT ablation, for example, MRI-aided ablation has demonstrated a lower need for RF delivery, higher noninducibility rates after substrate ablation, and a higher VT recurrence-free survival [58].

4.1. Determination of the Optimal Access Approach

In VT ablation, the location of the myocardial fibrosis is important for determining and designing ablation access: An epicardial approach for patients with epicardial or transmural scars and an endocardial approach for those without epicardial or transmural scars. In addition, LGE-MRI accurately defines intramural scarring, which is a major determinant of VT ablation failure [59]. For this specific case, ablation techniques such as septal alcholization [60], bipolar ablation or ablation using needle ablation catheters can be chosen to enhance outcomes [61].

4.2. Exclusion of Intracardiac Thrombus

In recent years, DE-MRI has been well validated as an accurate technique for the detection of left thrombi [62,63]. It is important in both VT and AF ablation to determine the presence of thrombus because patients with heart failure are at increased risk for thromboembolic events.

4.3. Integration of LGE-MRI and Electroanatomical Map (EAM) during Ablation

Several electroanatomical advanced mapping systems that display bipolar voltage maps and activation maps on a 3D reconstruction of the intracardiac chamber of interest have become available over the past few decades. Each system uses a different technology to generate a 3D image, record electrograms, and localize the electrode catheter in space. Current ablation techniques are heavily reliant on EAM systems (Carto (New York, NY, USA), Biosense Webster, Inc. (Irvine, CA, USA); NAVX (Paris, France), St Jude Medical (Saint Paul, MN, USA); Rhythmia Mapping, Boston Scientific Inc., (Boston, MA, USA).

Electroanatomical systems have been validated for anatomical and electrical accuracy in the atria as well as the ventricles [64–66]. However, there is an important limitation: the 3-dimensional reconstructions from catheters can provide inaccurate data on scar characteristics and could under- or overestimate the extent of scarring and arrhythmogenic substrate. This is due to different reasons: the influence of the electrode size, interelectrode spacing, angle of the incoming wavefront to the mapping catheter [60,67], and contact of the catheter with tissue (especially for those without a contact force sensor). Henceforth, EAMs can hardly be considered the gold standard of substrate definition. Moreover, it must be considered that low voltage detected in the EAM is not always equivalent to fibrosis and vice versa. Fibrosis distribution and fibrosis architecture and the possibility of far-field detection of the healthy tissue in the border of the fibrosis could affect the amplitude of the electrogram detected in the EAM.

Integration of imaging data into EAM systems provides more information about the arrhythmogenic substrate. Therefore, it is possible to merge the EAM with the 3D LGE-MRI reconstruction. Successful integration (with high accuracy) between EAM and MRI has been demonstrated in several studies [53,66,68].

For the merging process, landmarks in both the 3D reconstruction and EAM must be placed (one or more, depending on the system). The selected points to be used as the landmarks or fiducials must be in an identifiable and distinguishable place in the mapped anatomies (for example, the mitroaortic union, LV apex, the ostium of the pulmonary veins, etc.) with a certain angulation that enables them to be placed in the same direction. Once these points are selected, the estimated corresponding location of this endocardial point is marked on the imported 3D MRI surface reconstruction, thus creating a 'landmark pair'. At this point, the navigation system superimposes the 3D MRI surface reconstruction onto the real-time electroanatomic map with different algorithms, depending on each system (visual alignment, surface registration, etc.). Once the integration is completed, the user is able to navigate with the catheters over the 3D MRI reconstruction, visualizing and localizing the scar and the fibrotic tissue.

4.4. LGE-MRI for AF Ablation

The use of LGE-MRI for the assessment of fibrosis in the atrium has not become routine clinical practice. This is because the wall thickness of the atrium is lower than 1 mm, which is near the limit of spatial resolution of MRI, and due to less extensive and more diffuse fibrosis in comparison with the fibrosis in the ventricle. Nevertheless, recent improvements have been developed in MRI acquisition, including 3D navigated inversion recovery sequences to enhance signal-to-noise ratios and resolution, allowing valid atrium characterization [30,69]. These advances are now making LGE-MRI a widely accepted tool for assessing lesions, stratifying risks and selecting appropriate patients for AF ablation in many specialized centres [3].

Many other studies since then have tried to identify LGE-MRI predictors of recurrence after PVI ablation, and the degree of atrial fibrosis was confirmed to be an important predictor. In a retrospective study including patients undergoing AF ablation, there was an observed 45% increased risk of recurrence for each 10% increase in atrial fibrosis at the 5-year follow-up [70]. These data were supported by findings from another cohort of 165 patients. Patients with an amount of LGE less than 35% had favourable ablation outcomes regardless of AF persistence at baseline, whereas those with LGE greater than

35% had a higher rate of AF recurrence in the first year of follow-up after ablation [71]. In the DECAAF multicentre study [72], 260 patients who underwent PVI were included, and the extent of fibrosis in the LA was categorized as 1 (<10% of the atrial wall), 2 (>10% to <20%), 3 (>20% to <30%) and 4 (>30%). Recurrent arrhythmia during follow-up was direct and graded: from 15% in the stage I group to 51% in the stage IV group. In a subsequent randomized study, catheter ablation of left atrial fibrosis was proposed [73]. The benefit of ablation of these areas could not be demonstrated by this study. This result was supported by other randomized trials, where MRI fibrosis ablation plus PVI was not more effective than PVI alone [74].

Another important potential use of LGE-MRI is to guide repeated ablation procedures, as most cases of AF recurrence after PVI ablation are associated with areas of incomplete ablation or gaps around the pulmonary veins [49,75] (Figure 3). Some studies indicate that those gaps can be identified by LGE-MRI with high accuracy [6,48,49,76]. Badger et al. 2010 [75] demonstrated that LGE-MRI is able to confirm a PVI gap with very high predictive values. Bisbal et al. 2014 [6] showed for the first time that the elimination of gaps detected by LGE MRI generates a reisolation of PPVV in the majority of cases. In this particular study, the LGE-MRI reconstruction was merged with the EAM, so the operator was blinded to electrical information, only isolating gaps localized in the MRI. Reisolation was acquired in 95.6% of the reconnected PVs. In addition to guiding redo procedures, gap detection by LGE-MRI has been considered a predictor of AF recurrence. Linhart et al. 2018 [69] found that the relative gap length calculated as the absolute gap length divided by total length of the ablation line measured during MRI at 3 months of follow-up was a marker predicting AF recurrence 1 year after PVI.

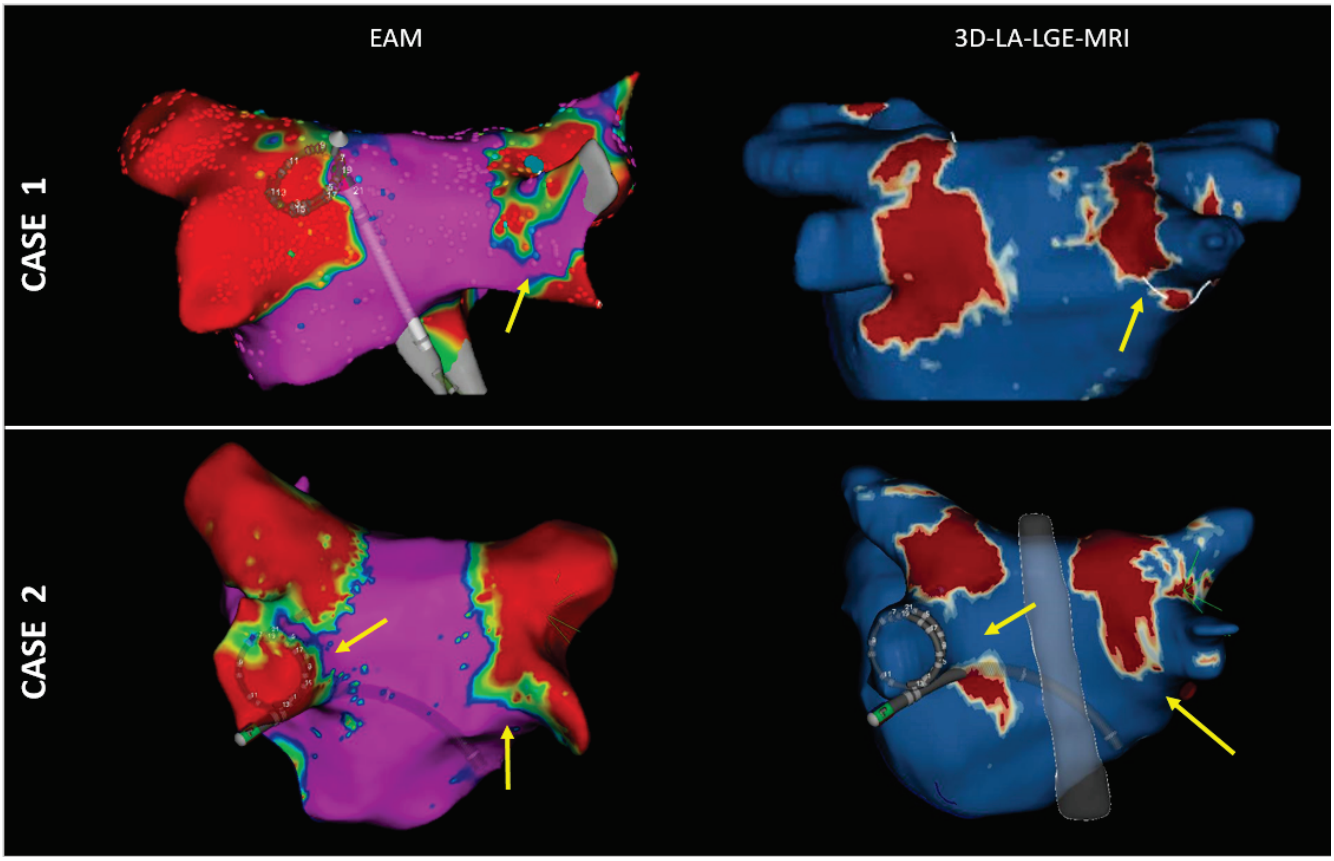

Figure 3. Agreement between EAM voltage map and LGE-MRI gap localisation. From (**left**) to (**right**), voltage map with gaps localised during a repeated ablation intervention. Right, gaps localised at the same region by prior LGE-MRI 3 months post first ablation. Yellow arrows indicate detected EAM gaps and LGE-MRI discontinuities, respectively.

4.5. LGE-MRI for VT Ablation

The use of LGE-MRI in patients undergoing VT ablation is increasing, especially for the preprocedural assessment of the cardiac anatomy and myocardial scarring and for intraprocedural integration.

On the one hand, the use of LGE-MRI provides accurate knowledge of the arrhythmic substrate, including the critical VT isthmuses, the BZ areas and CCs, supporting ablation strategies [52,54,58,77]. The identification of these specific areas has been very useful in cases of ischaemic cardiomyopathy [52,54,58,77]. Moreover, LGE-MRI is also very helpful in cases of nonischaemic cardiomyopathy (NICM). In this sense, some studies have demonstrated that the location of scar in NICM, is also useful for the ablation procedure [78]. This is because the ablation technique and the type of tachycardia is related to the location of scar tissue. Similarly, the effectiveness of using MRI for selecting the appropriate ablation technique was demonstrated in a study involving 80 patients with both NICM and ischemic cardiomyopathy (ICM). In that study, the epicardial or endocardial access was chosen based on MRI. In addition, in case of the intramural substrate, the distance of the scar to the right and left endocardium was used to decided how to approach this substrate [79]. Figure 4 shows an example of the correspondence of LGE-MRI 3D reconstruction with an EAM map.

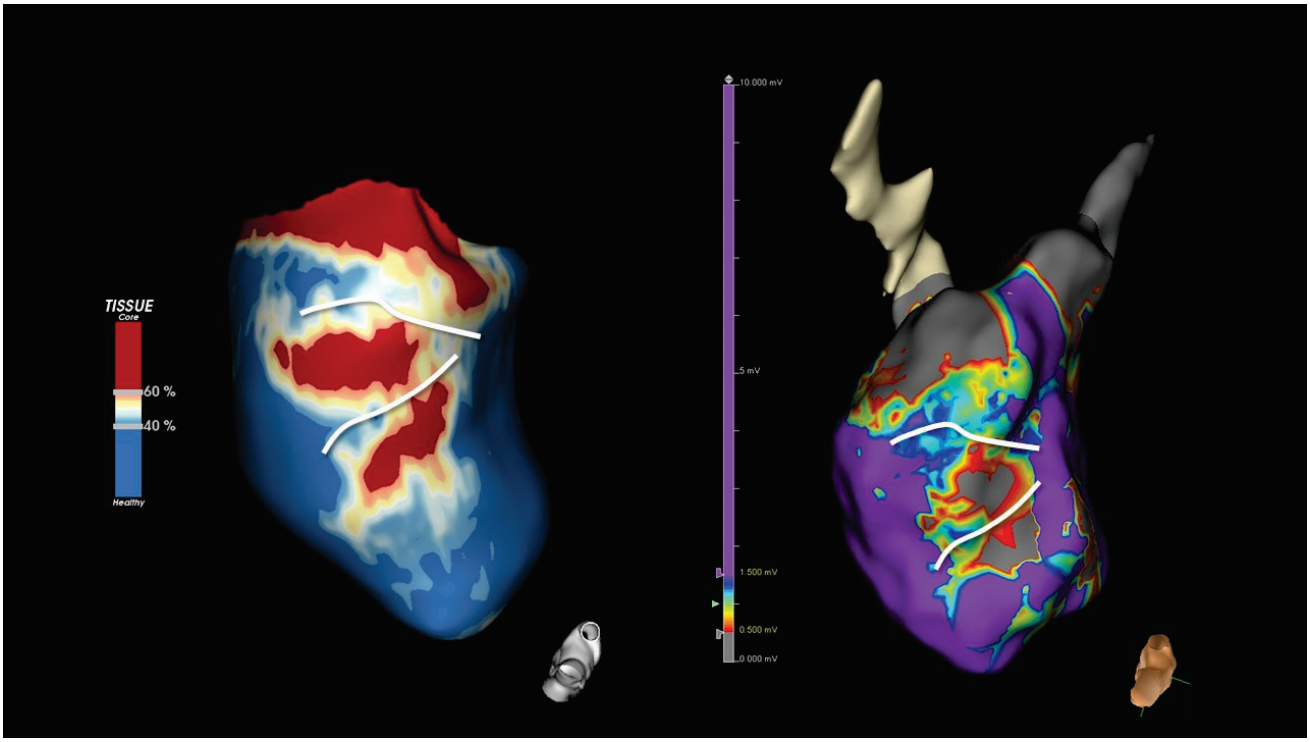

Figure 4. Example of correlation of the 3D-VI reconstruction from LGE-MRI with electroanatomical voltage map. From left to right: LGE-MRI map (colour-coding: blue: healthy tissue, yellow: border zone and red: core scar) with two clear conducting channels (white line); and electroanatomical map high density voltage map showing septal scar (colour-coding: purple: healthy tissue, red: border zone and grey: core scar), with conducting channels at the same region as compared to the LGE-MRI.

On the other hand, in relation to EAMs, studies have not only demonstrated the feasibility of integration during the ablation procedure and a good correlation between 3D-LV reconstruction and EAMs [52,79,80], but have also shown that the scars in MRI scans were larger compared to those detected by EAMs. Moreover, some VT isthmuses were found in regions identified as scar by MRI, but were nonvisible in EAMs [65]. These kinds of studies underscore the value of integrating LGE and EAM for comprehensive scar characterization, particularly in the context of defining infarct BZs, nontransmural scars, and small subepicardial scars [65]. This role of preprocedural MRI to aid procedural access

has also been related to a lower VT recurrence rate, improving the ablation results. A study in patients with ischemic heart disease and epicardial substrate identified prior to ablation by MRI showed that those patients that underwent ablation with epicardial access had better results in terms of VT recurrence, compared to patients who underwent exclusively the endocardial approach [80].

Finally, there is a clear role of MRI in predicting the risk of VT recurrence, even without integration images into the EAM. In a study by Quinto et al. [81], 110 patients who underwent VT ablation with preprocedural LGE-MRI were analysed, identifying MRI-related factors that were clearly linked to a higher rate of VT recurrence, such as mass of border zone and total scar, septal substrate or midmural and transmural CCs. Similarly, in a smaller study [82], scar area was also linked to clinical outcomes, such as VT recurrence. Another study [83] involving 25 non ischemic patients, also verified that the extension of septal LGE was associated with a higher rate of VT recurrence.

5. Conclusions

LGE-MRI constitutes the gold standard for noninvasive characterization of arrhythmogenic myocardial substrate in AF and VT. Its usefulness in both preprocedural planning, substrate analysis and post-ablation evaluation has been proved, even though more technological developments are needed to implement it into routine practice.

6. Limitations

Some limitations need to be addressed. First, consistent methodological and analytical standards defining fibrotic tissue characterization are needed to achieve reproducibility of results between centres. The use of the same values and methods to define fibrotic tissue, will promote the implementation in clinical practice. Second, there is also no homogenous method for integrating MRI-3D into the navigation system. Each group used different structures for merging (pulmonary veins, right ventricle, aortic roof, pulmonary artery, etc.). A more standardized method for using MRI to facilitate ablation would be beneficial for increasing its practical use. In the area of VT ablation, the assessment of ablation lesions has been investigated in small series [28,84,85]. More research is required to confirm and evaluate the usefulness of LGE-MRI in the evaluation of ventricular ablation lesions. Finally, despite new MRI scans, spatial resolution could be insufficient to detect small areas of fibrosis in the atrium wall due to its thickness. In the same line, some types of interstitial fibrosis could be underdetected with conventional LGE, and T1 mapping needs to be improved for clinical practice.

Author Contributions: Conceptualization: P.G., S.V.-C. and E.F., writing: P.G.; review: S.V.-C. and E.F.; and supervision: T.A. and I.R.-L. All authors have read and agreed to the published version of the manuscript.

Funding: This study was supported by Hospital Clinic de Barcelona/Instituto de Salud Carlos III (ISCIII) PI20/00693/CB16/11/00354.

Institutional Review Board Statement: Not applicable.

Informed Consent Statement: Not applicable.

Data Availability Statement: Not applicable.

Conflicts of Interest: I.R.-L. have served as consultants for Boston Scientific and Abbott Medical. T.A. has received research grants for investigator-initiated trials from Biosense Webster.

References

1. Kim, H.W.; Farzaneh-Far, A.; Kim, R.J. Cardiovascular magnetic resonance in patients with myocardial infarction. *J. Am. Coll. Cardiol.* **2009**, *55*, 1–16. [CrossRef] [PubMed]
2. Pontecorboli, G.; Figueras i Ventura, R.M.; Carlosena, A.; Benito, E.; Prat-Gonzales, S.; Padeletti, L.; Mont, L. Use of delayed-enhancement magnetic resonance imaging for fibrosis detection in the atria: A review. *Europace* **2017**, *19*, 180–189. [CrossRef] [PubMed]

3. Hindricks, G.; Potpara, T.; Dagres, N.; Arbelo, E.; Bax, J.J.; Blomstrom-Lundqvist, C.; Boriani, G.; Castella, M.; Dan, G.A.; Dilaveris, P.E.; et al. ESC guidelines for the diagnosis and management of atrial fibrillation developed in collaboration with the European Association of Cardio-Thoracic Surgery (EACTS). *Eur. Heart J.* **2021**, *42*, 373–498. [CrossRef] [PubMed]
4. Cronin, E.M.; Bogun, F.M.; Maury, P.; Peichl, P.; Chen, M.; Namboodiri, N.; Aguinaga, L.; Leite, L.R.; Al-Khatib, S.; Anter, E.; et al. 2019 HRS/EHRA/APHRS/LAHRS expert consensus statement on catheter ablation of ventricular arrhythmias: Executive summary. *Europace* **2020**, *22*, 450–495. [CrossRef]
5. Berruezo, A.; Penela, D.; Jáuregui, B.; Soto-Iglesias, D. The role of imaging in catheter ablation of ventricular arrhythmias. *Pacing Clin. Electrophysiol.* **2021**, *44*, 1115–1125. [CrossRef]
6. Bisbal, F.; Guiu, E.; Cabanas-Grandío, P.; Berruezo, A.; Prat-Gonzalez, S.; Vidal, B.; Garrido, C.; Andreu, D.; Fernandez-Armenta, J.; Tolosana, J.M.; et al. CMR-guided approach to localize and ablate gaps in repeat AF ablation procedure. *JACC Cardiovasc. Imaging* **2014**, *7*, 653–663. [CrossRef]
7. Feinberg, W.M.; Blackshear, J.L.; Laupacis, A.; Kronmal, R.; Hart, R.G. Prevalence, age distribution and gender of patients with atrial fibrillation: Analysis and implications. *Arch. Intern. Med.* **1995**, *155*, 469–473. [CrossRef]
8. January, C.T.; Wann, L.; Alpert, J.S.; Calkins, H.; Cigarroa, J.E.; Cleveland, J.C., Jr.; Conti, J.B.; Ellinor, P.T.; Ezekowitz, M.D.; Field, M.E.; et al. AHA/ACC/HRS guideline for the management of patients with atrial fibrillation: Executive summary: A report of the American College of Cardiology/American Heart Association Task Force on Practice Guidelines and the Heart Rhythm Society. *J. Am. Coll. Cardiol.* **2014**, *64*, 2246–2280. [CrossRef]
9. Calkins, H.; Kuck, K.H.; Cappato, R.; Brugada, J.; Camm, A.J.; Chen, S.A. 2012 HRS/EHRA/ECAS expert consensus statement on catheter and surgical ablation of atrial fibrillation: Recommendations for patient selection, procedural techniques, patient management and follow-up, definitions, endpoints, and research trial design. *Europace* **2012**, *14*, 528–606. [CrossRef]
10. John, R.M.; Tedrow, U.B.; Koplan, B.A.; Albert, C.M.; Epstein, L.M.; Sweeney, M.O.; Miller, A.L.; Michaud, G.; Stevenson, W. Ventricular arrhythmias and sudden cardiac death. *Lancet* **2012**, *380*, 1520–1529. [CrossRef]
11. Tung, R.; Vaseghi, M.; Frankel, D.S.; Vergara, P.; Di Biase, L.; Nagashima, K.; Yu, R.; Vangala, S.; Tseng, C.-H.; Choi, E.-K.; et al. Freedom from recurrent ventricular tachycardia after catheter ablation is associated with improved survival in patients with structural heart disease: An International VT Ablation Center Collaborative Group study. *Heart Rhythm* **2015**, *12*, 1997–2007. [CrossRef]
12. Dukkipati, S.R.; Koruth, J.S.; Chouddry, S.; Miller, M.A.; Whang, W.; Reddy, V.Y. Catheter ablation of ventricular. *J. Am. Coll. Cardiol.* **2017**, *70*, 2924–2941. [CrossRef]
13. De Bakker, J.M.T.; Van Capelle, F.J.L.; Janse, M.J.; Wilde, A.A.M.; Coronel, R.; Becker, A.E.; Dingemans, K.P.; van Hemel, N.M.; Hauer, R.N. Reentry as a cause of ventricular tachycardia in patients with chronic ischemic heart disease: Electrophysiologic and anatomic correlation. *Circulation* **1988**, *77*, 589–606. [CrossRef]
14. Harada, T.; Stevenson, W.G.; Kocovic, D.Z.; Friedman, P.L. Catheter ablation of ventricular tachycardia after myocardial infarction: Relation of endocardial sinus rhythm late potentials to the reentry circuit. *J. Am. Coll. Cardiol.* **1997**, *30*, 1015–1023. [CrossRef]
15. Mountantonakis, S.E.; Park, R.E.; Frankel, D.S.; Hutchinson, M.D.; Dixit, S.; Cooper, J.; Callans, D.; Marchlinski, F.E.; Gerstenfeld, E.P. Relationship between voltage map "channels" and the location of critical isthmus sites in patients with post-infarction cardiomyopathy and ventricular tachycardia. *J. Am. Coll. Cardiol.* **2013**, *61*, 2088–2095. [CrossRef]
16. Bogun, F.; Marine, J.E.; Oral, H.; Pelosi, F.; Morady, F. Relative timing of isolated potentials during post-infarction ventricular tachycardia and sinus rhythm. *J. Interv. Card. Electrophysiol.* **2004**, *10*, 65–72. [CrossRef]
17. Arenal, A.; Glez-Torrecilla, E.; Ortiz, M.; Villacastín, J.; Fdez-Portales, J.; Sousa, E.; del Castillo, S.; de Isla, L.P.; Jimenez, J.; Almendral, J. Ablation of electrograms with an isolated, delayed component as treatment of unmappable monomorphic ventricular tachycardias in patients with structural heart disease. *J. Am. Coll. Cardiol.* **2003**, *41*, 81–92. [CrossRef]
18. Bogun, F.; Good, E.; Reich, S.; Elmouchi, D.; Igic, P.; Lemola, K.; Tschopp, D.; Jongnarangsin, K.; Oral, H.; Chugh, A.; et al. Isolated potentials during sinus rhythm and pace-mapping within scars as guides for ablation of post-infarction ventricular tachycardia. *J. Am. Coll. Cardiol.* **2006**, *47*, 2013–2019. [CrossRef]
19. Bertozzi, G.; Cafarelli, F.P.; Ferrara, M.; Di Fazio, N.; Guglielmi, G.; Cipolloni, L.; Manetti, F.; La Russa, R.; Fineschi, V. Sudden Cardiac Death and Ex-Situ Post-Mortem Cardiac Magnetic Resonance Imaging: A Morphological Study Based on Diagnostic Correlation Methodology. *Diagnostics* **2022**, *12*, 218. [CrossRef]
20. Aziz, Z.; Shatz, D.; Raiman, M.; Upadhyay, G.A.; Beaser, A.D.; Besser, S.A. Targeted ablation of ventricular tachycardia guided by wavefront discontinuities during sinus rhythm: A new functional substrate mapping strategy. *Circulation* **2019**, *140*, 1383–1397. [CrossRef]
21. Willems, S.; Tilz, R.R.; Steven, D.; Kääb, S.; Wegscheider, K.; Gellér, L.; Meyer, C.; Heeger, C.-H.; Metzner, A.; Sinner, M.F.; et al. Preventive or deferred ablation of ventricular tachycardia in patients with ischemic cardiomyopathy and implantable defibrillator (Berlin VT): A multicenter randomized trial. *Circulation* **2020**, *2020*, 1057–1067. [CrossRef] [PubMed]
22. Hadjis, A.; Frontera, A.; Rosario, L.; Bisceglia, C.; Bognoni, L.; Foppoli, L.; Lipartiti, F.; Paglino, G.; Radinovic, A.; Tsitsinakis, G.; et al. Complete electroanatomic imaging of the diastolic pathway is associated with improved. *Circ. Arrhythm. Electrophysiol.* **2020**, *2020*, 927–937. [CrossRef]
23. Quinto, L.; Sanchez-Somonte, P.; Alarcón, F.; Garre, P.; Castillo, À.; San Antonio, R. Ventricular tachycardia burden reduction after substrate ablation: Predictors of recurrence. *Heart Rhythm* **2021**, *18*, 896–904. [CrossRef] [PubMed]

24. Kim, R.J.; Fieno, D.S.; Parrish, T.B.; Harris, K.; Chen, E.-L.; Simonetti, O.; Bundy, J.; Finn, J.P.; Klocke, F.J.; Judd, R.M. Relationship of MRI delayed contrast enhancement to irreversible injury, infarct age, and contractile function. *Circulation* **1999**, *100*, 1992–2002. [CrossRef]
25. Bing, R.; Dweck, M.R. Myocardial fibrosis: Why image, how to image and clinical implications. *Heart* **2019**, *105*, 1832–1840. [CrossRef]
26. Mewton, N.; Liu, C.Y.; Croisille, P. Assessment of myocardial fibrosis with cardiovascular magnetic resonance. *J. Am. Coll. Cardiol.* **2011**, *57*, 891–903. [CrossRef]
27. Kiuchi, K.; Fukuzawa, K.; Nogami, M.; Watanabe, Y.; Takami, M.; Izawa, Y.; Negi, N.; Kyotani, K.; Mori, S.; Hirata, K.-I. Visualization of intensive atrial inflammation and fibrosis after cryoballoon ablation: PET/MRI and LGE-MRI analysis. *J. Arrhythm.* **2021**, *37*, 52–59. [CrossRef]
28. Dickfeld, T.; Kato, R.; Zviman, M.; Lai, S.; Meininger, G.; Lardo, A.C.; Roguin, A.; Blumke, D.; Berger, R.; Calkins, H.; et al. Characterization of radiofrequency ablation lesions with gadolinium-enhanced cardiovascular magnetic resonance imaging. *J. Am. Coll. Cardiol.* **2006**, *47*, 370–378. [CrossRef]
29. Benito, E.M.; Carlosena-Remirez, A.; Guasch, E. Left atrial fibrosis quantification by late gadolinium-enhanced magnetic resonance: A new method to standardize the thresholds for reproducibility. *Europace* **2017**, *19*, 1272–1279. [CrossRef]
30. Oakes, R.S.; Badger, T.J.; Kholmovski, E.G. Detection and quantification of left atrial structural remodeling with delayed-enhancement magnetic resonance imaging in patients with atrial fibrillation. *Circulation* **2009**, *119*, 1758–1767. [CrossRef]
31. Peters, D.C.; Wylie, J.V.; Hauser, T.H.; Kissinger, K.V.; Botnar, R.M.; Essebag, V.; Josephson, M.E.; Manning, W.J. Detection of pulmonary vein and left atrial scar after catheter ablation with three-dimensional navigator-gated delayed enhancement MR imaging: Initial experience. *Radiology* **2007**, *243*, 690–695. [CrossRef]
32. Vijayakumar, S.; Kholmovski, E.; McGann, C.; Marrouche, N.F. Dependence of contrast to noise ratio between ablation scar and other tissues on patient heart rate and flip angle for late gadolinium enhancement imaging of the left atrium. *J. Cardiovasc. Magn. Reson.* **2012**, *14* (Suppl. S1), O107. [CrossRef]
33. Do, D.H.; Eyvazian, V.; Bayoneta, A.J.; Hu, P.; Finn, J.P.; Bradfield, J.S. Cardiac magnetic resonance imaging using wideband sequences in patients with non-conditional cardiac implanted electronic devices. *Heart Rhythm* **2018**, *15*, 218–225. [CrossRef]
34. Seewoster, T.; Lobe, S.; Hilbert, S.; Bollmann, A.; Sommer, P.; Lindemann, F.; Bacevičius, J.; Schöne, K.; Richter, S.; Döring, M.; et al. Cardiovascular magnetic resonance imaging in patients with cardiac implantable electronic devices: Best practice and real-world experience. *Europace* **2019**, *19*, 818–823. [CrossRef]
35. Flett, A.S.; Hasleton, J.; Cook, C.; Hausenloy, D.; Quarta, G.; Ariti, C.; Muthurangu, V.; Moon, J.C. Evaluation of techniques for the quantification of myocardial scar of differing etiology using cardiac magnetic resonance. *JACC Cardiovasc. Imaging* **2011**, *4*, 150–156. [CrossRef]
36. Dickfeld, T.; Tian, J.; Ahmad, G.; Jimenez, A.; Turgeman, A.; Kuk, R.; Peters, M.; Saliaris, A.; Saba, M.; Shorofsky, S.; et al. MRI-guided ventricular tachycardia ablation: Integration of late gadoliniumenhanced 3D scar in patients with implantable cardioverterdefibrillators. *Circ. Arrhythm. Electrophysiol.* **2011**, *4*, 172–184. [CrossRef]
37. Sasaki, T.; Hansford, R.; Zviman, M.M. Quantitative assessment of artifacts on cardiac magnetic resonance imaging of patients with pacemakers and implantable cardioverter-defibrillators. *Circ. Cardiovasc. Imaging* **2011**, *4*, 662–670. [CrossRef]
38. Rashid, S.; Rapacchi, S.; Shivkumar, K.; Plotnik, A.; Finn, J.P.; Hu, P. Modified wideband three-dimensional late gadolinium enhancement MRI for patients with implantable cardiac devices. *Magn. Reson. Med.* **2016**, *75*, 572–584. [CrossRef]
39. Rashid, S.; Rapacchi, S.; Vaseghi, M. Improved late gadolinium enhancement MR imaging for patients with implanted cardiac devices. *Radiology* **2014**, *270*, 269–274. [CrossRef]
40. Bhuva, A.N.; Kellman, P.; Graham, A.; Ramlall, M.; Boubertakh, R.; Feuchter, P.; Hawkins, A.; Lowe, M.; Lambiase, P.D.; Sekhri, N.; et al. Clinical impact of cardiovascular magnetic resonance with optimized myocardial scar detection in patients with cardiac implantable devices. *Int. J. Cardiol.* **2019**, *15*, 72–78. [CrossRef]
41. Hilbert, S.; Weber, A.; Nehrke, K.; Bornert, P.; Schnackenburg, B.; Oebel, S. Artefact-free late gadolinium enhancement imaging in patients with implanted cardiac devices using a modified broadband sequence: Current strategies and results from a real-world patient cohort. *Europace* **2018**, *20*, 801–807. [CrossRef] [PubMed]
42. Roca-Luque, I.; Van Breukelen, A.; Alarcon, F.; Garre, P.; Tolosana, J.M.; Borras, R. Ventricular scar channel entrances identified by new wideband cardiac magnetic resonance sequence to guide ventricular tachycardia ablation in patients with cardiac defibrillators. *Europace* **2020**, *22*, 598–606. [CrossRef] [PubMed]
43. James, L.H.; Henrik, K.J.; Sarah, A.P.; Amedeo, C.; Anne, K.G.; Lars, Ø.B.; Steen, F.; Pedersen, J.F.; Bentzon, C.K.; Rashed, K.; et al. Cardiac magnetic resonance and electroanatomical mapping of acute and chronic atrial ablation injury: A histological validation study. *Eur. Heart J.* **2014**, *35*, 1486–1495. [CrossRef]
44. Harrison, J.L.; Sohns, C.; Linton, N.W.; Karim, R.; Williams, S.E.; Rhode, K.S.; Gill, J.; Cooklin, M.; Rinaldi, C.A.; Wright, M.; et al. Repeat left atrial catheter ablation: Cardiac magnetic resonance prediction of endocardial voltage and gaps in ablation lesion sets. *Circ. Arrhythm. Electrophysiol.* **2015**, *8*, 270–278. [CrossRef] [PubMed]
45. Kurose, J.; Kiuchi, K.; Fukuzawa, K. Lesion characteristics between cryoballoon ablation and radiofrequency ablation with a contact-force sensing catheter: Late-gadolinium enhancement magnetic resonance imaging assessment. *J. Cardiovasc. Electrophysiol.* **2020**, *31*, 2572–2581. [CrossRef]

46. Dewire, J.; Khurram, I.M.; Pashakhanloo, F.; Spragg, D.; Marine, J.E.; Berger, R.D. The association of pre-existing left atrial fibrosis with clinical variables in patients referred for catheter ablation of atrial fibrillation. *Clin. Med. Insights Cardiol.* **2014**, *8* (Suppl. S1), 25–30. [CrossRef]
47. Khurram, I.M.; Beinart, R.; Zipunnikov, V.; Dewire, J.; Yarmohammadi, H.; Sasaki, T.; Spragg, D.D.; Marine, J.E.; Berger, R.D.; Halperin, H.R.; et al. Magnetic resonance image intensity ratio, a normalized measure to enable interpatient comparability of left atrial fibrosis. *Heart Rhythm* **2014**, *11*, 85–92. [CrossRef]
48. Quinto, L.; Cozzari, J.; Benito, E.; Alarcón, F.; Bisbal, F.; Trotta, O.; Caixal, G.; Antonio, R.S.; Garre, P.; Prat-Gonzalez, S.; et al. Magnetic resonance guided re-ablation for atrial fibrillation is associated with a lower recurrence rate: A case-control study. *Europace* **2020**, *22*, 1805–1811. [CrossRef]
49. Fochler, F.; Yamaguchi, T.; Kheirkahan, M. Late gadolinium enhancement magnetic resonance imaging guided treatment of post atrial fibrillation ablation recurrent arrhythmia. *Circ. Arrhythm. Electrophysiol.* **2019**, *12*, e007174. [CrossRef]
50. Amado, L.; Gerber, B.; Gupta, S.; Rettmann, D.; Szarf, G.; Schock, R.; Nasir, K.; Kraitchman, D.; Lima, J. Accurate and objective infarct sizing by contrastenhanced magnetic resonance imaging in a canine myocardial infarction model. *J. Am. Coll. Cardiol.* **2004**, *44*, 2383–2389. [CrossRef]
51. Yan, A.T.; Shayne, A.J.; Brown, K.A.; Gupta, S.N.; Chan, C.W.; Luu, T.M.; Di Carli, M.F.; Reynolds, H.G.; Stevenson, W.G.; Kwong, R.Y. Characterization of the peri-infarct zone by contrast-enhanced cardiac magnetic resonance imaging is a powerful predictor of postmyocardial infarction mortality. *Circulation* **2006**, *114*, 32–39. [CrossRef]
52. Andreu, D.; Berruezo, A.; Ortiz-Pérez, J.T.; Silva, E.; Mont, L.; Borràs, R.; de Caralt, T.M.; Perea, R.J.; Fernández-Armenta, J.; Zeljko, H.; et al. Integration of 3D electroanatomic maps and magnetic resonance scar characterization into the navigation system to guide ventricular tachycardia ablation. *Circ. Arrhythm. Electrophysiol.* **2011**, *4*, 674–683. [CrossRef]
53. Fernandez-Armenta, J.; Berruezo, A.; Andreu, D. Threedimensional architecture of scar and conducting channels based on high resolution ce-CMR: Insights for ventricular tachycardia ablation. *Circ. Arrhythm. Electrophysiol.* **2013**, *6*, 528–537. [CrossRef]
54. Cochet, H.; Komatsu, Y.; Sacher, F. Integration of merged delayed-enhanced magnetic resonance imaging and multidetector computed tomography for the guidance of ventricular tachycardia ablation: A pilot study. *J. Cardiovasc. Electrophysiol.* **2013**, *24*, 419–426. [CrossRef]
55. Roca-Luque, I.; Rivas-Gándara, N.; Francisco-Pascual, J.; Rodriguez-Sanchez, J.; Cuellar-Calabria, H.; Rodriguez-Palomares, J.; García-Del Blanco, B.; Pérez-Rodon, J.; Santos-Ortega, A.; Rosés-Noguer, F.; et al. Preprocedural imaging to guide transcoronary ethanol ablation for refractory septal ventricular tachycardia. *J. Cardiovasc. Electrophysiol.* **2019**, *30*, 448–456. [CrossRef]
56. Ronneberger, O.; Fischer, P.; Brox, T. U-Net: Convolutional networks for biomedical image segmentation. In *Medical Image Computing and Computer-Assisted Intervention—MICCAI 2015*; Lecture Notes in Computer Science; Navab, N., Hornegger, J., Wells, W., Frangi, A., Eds.; Springer: Cham, Switzerland, 2015; Volume 9351, pp. 234–241. [CrossRef]
57. Goodfellow, I.; Bengio, Y.; Courville, A. *Deep Learning*; MIT Press: Cambridge, MA, USA, 2016.
58. Gupta, S.; Desjardins, B.; Baman, T.; Ilg, K.; Good, E.; Crawford, T.; Oral, H.; Pelosi, F.; Chugh, A.; Morady, F.; et al. Delayed-enhanced MR scar imaging and intraprocedural registration into an electroanatomical mapping system in post-infarction patients. *JACC Cardiovasc. Imaging* **2012**, *5*, 207–210. [CrossRef]
59. Bogun, F.M.; Desjardins, B.; Good, E.; Gupta, S.; Crawford, T.; Oral, H.; Ebinger, M.; Pelosi, F.; Chugh, A.; Jongnarangsin, K.; et al. Delayed-enhanced magnetic resonance imaging in nonischemic cardiomyopathy: Utility for identifying the ventricular arrhythmia substrate. *J. Am. Coll. Cardiol.* **2009**, *53*, 1138–1145. [CrossRef]
60. Takigawa, M.; Relan, J.; Martin, R.; Kim, S.; Kitamura, T.; Frontera, A.; Cheniti, G.; Vlachos, K.; Massoullié, G.; Martin, C.A.; et al. Effect of bipolar electrode orientation on local electrogram properties. *Heart Rhythm* **2018**, *15*, 1853–1861. [CrossRef]
61. Kumar, S.; Tedrow, U.B.; Stevenson, W.G. Adjunctive interventional techniques when percutaneous catheter ablation for drug refractory ventricular arrhythmias fail: A contemporary review. *Circ. Arrhythm. Electrophysiol.* **2017**, *10*, e003676. [CrossRef]
62. Weinsaft, J.W.; Kim, H.W.; Shah, D.J.; Klem, I.; Crowley, A.L.; Brosnan, R.; James, O.G.; Patel, M.R.; Heitner, J.; Parker, M.; et al. Detection of left ventricular thrombus by delayed-enhancement cardiovascular magnetic resonance prevalence and markers in patients with systolic dysfunction. *J. Am. Coll. Cardiol.* **2008**, *52*, 148–157. [CrossRef]
63. Weinsaft, J.W.; Kim, R.J.; Ross, M.; Krauser, D.; Manoushagian, S.; LaBounty, T.M.; Cham, M.D.; Min, J.K.; Healy, K.; Wang, Y.; et al. Contrast-enhanced anatomic imaging as compared to contrast enhanced tissue characterization for detection of left ventricular thrombus. *JACC Cardiovasc. Imaging* **2009**, *2*, 969–979. [CrossRef] [PubMed]
64. Stevenson, W.G.; Delacretaz, E.; Friedman, P.L. Identification and ablation of macroreentrant ventricular tachycardia with the CARTO electroanatomical mapping system. *Pacing Clin. Electrophysiol.* **1998**, *21*, 1448. [CrossRef] [PubMed]
65. Marchlinski, F.E.; Callans, D.J.; Gottlieb, C.D.; Zado, E. Linear ablation lesions for control of un-mappable ventricular tachycardia in patients with ischemic and nonischemic cardiomyopathy. *Circulation* **2000**, *101*, 1288. [CrossRef] [PubMed]
66. Wijnmaalen, A.P.; van der Geest, R.J.; van Huls van Taxis, C.F.B.; Siebelink, H.M.J.; Kroft, L.J.M.; Bax, J.J.; Reiber, J.H.; Schalij, M.J.; Zeppenfeld, K. Head-to-head comparison of contrast-enhanced magnetic resonance imaging and electroanatomical voltage mapping to assess post-infarct scar characteristics in patients with ventricular tachycardias: Real-time image integration and reversed registration. *Eur. Heart J.* **2011**, *32*, 104–114. [CrossRef]
67. Vázquez-Calvo, S.; Garre, P.; Sánchez-Somonte, P. Orthogonal high density mapping with VT isthmus analysis vs. pure substrate VT ablation: A case-control study. *Front. Cardiovasc. Med.* **2022**, *9*, 912335. [CrossRef]

68. Yamashita, S.; Sacher, F.; Mahida, S.; Berte, B.; Lim, H.S.; Komatsu, Y.; Amraoui, S.; Denis, A.; Derval, N.; Laurent, F.; et al. Role of high-resolution image integration to visualize left phrenic nerve and coronary arteries during epicardial ventricular tachycardia ablation. *Circ. Arrhythm. Electrophysiol.* **2015**, *8*, 371–380. [CrossRef]
69. Linhart, M.; Alarcon, F.; Borras, R. Delayed gadolinium enhancement magnetic resonance imaging detected anatomic gap length in wide circumferential pulmonary vein ablation lesions is associated with recurrence of atrial fibrillation. *Circ. Arrhythm. Electrophysiol.* **2018**, *11*, e006659. [CrossRef]
70. Chelu, M.G.; King, J.B.; Kholmovski, E.G.; Ma, J.; Gal, P.; Marashly, Q.; AlJuaid, M.A.; Kaur, G.; Silver, M.A.; Johnson, K.A.; et al. Atrial fibrosis by late gadolinium enhancement magnetic resonance imaging and catheter ablation of atrial fibrillation: 5-year follow-up data. *J. Am. Heart Assoc.* **2018**, *7*, e006313. [CrossRef]
71. Khurram, I.M.; Habibi, M.; Gucuk Ipek, E.; Chrispin, J.; Yang, E.; Fukumoto, K.; Dewire, J.; Spragg, D.D.; Marine, J.E.; Berger, R.D.; et al. Left atrial LGE and arrhythmia recurrence following pulmonary vein isolation for paroxysmal and persistent AF. *JACC Cardiovasc. Imaging* **2016**, *9*, 142–148. [CrossRef]
72. Marrouche, N.F.; Wilber, D.; Hindricks, G.; Jais, P.; Akoum, N.; Marchlinski, F.; Kholmovski, E.; Burgon, N.; Hu, N.; Mont, L.; et al. Association of atrial tissue fibrosis identified by delayed enhancement MRI and atrial fibrillation catheter ablation: The DECAAF study. *JAMA* **2014**, *311*, 498–506. [CrossRef]
73. Marrouche, N.F.; Wazni, O.; McGann, C.; Greene, T.; Dean, J.M.; Dagher, L.; Kholmovski, E.; Mansour, M.; Marchlinski, F.; Wilber, D.; et al. Effect of MRI-Guided Fibrosis Ablation vs Conventional Catheter Ablation on Atrial Arrhythmia Recurrence in Patients with Persistent Atrial Fibrillation: The DECAAF II Randomized Clinical Trial. *JAMA* **2022**, *327*, 2296–2305. [CrossRef]
74. Bisbal, F.; Benito, E.; Teis, A.; Alarcón, F.; Sarrias, A.; Caixal, G.; Villuendas, R.; Garre, P.; Soto, N.; Cozzari, J.; et al. Magnetic Resonance Imaging-Guided Fibrosis Ablation for the Treatment of Atrial Fibrillation: The ALICIA Trial. *Circ. Arrhythm. Electrophysiol.* **2020**, *13*, e008707. [CrossRef]
75. Badger, T.J.; Daccarett, M.; Akoum, N.W. Evaluation of left atrial lesions after initial and repeat atrial fibrillation ablation: Lessons learned from delayed-enhancement MRI in repeat ablation procedures. *Circ. Arrhythm. Electrophysiol.* **2010**, *3*, 249–259. [CrossRef]
76. Chubb, H.; Aziz, S.; Karim, R. Optimization of late gadolinium enhancement cardiovascular magnetic resonance imaging of post-ablation atrial scar: A cross-over study. *J. Cardiovasc. Magn. Reson.* **2018**, *20*, 30. [CrossRef]
77. Desjardins, B.; Crawford, T.; Good, E.; Oral, H.; Chugh, A.; Pelosi, F.; Morady, F.; Bogun, F. Infarct architecture and characteristics on delayed enhanced magnetic resonance imaging and electroanatomic mapping in patients with postinfarction ventricular arrhythmia. *Heart Rhythm* **2009**, *6*, 644–651. [CrossRef]
78. Piers, S.R.D.; Tao, Q.; De Riva Silva, M.; Siebelink, H.M.; Schalij, M.J.; Van Der Geest, R.J.; Zeppenfeld, K. CMR-based identification of critical isthmus sites of ischemic and nonischemic ventricular tachycardia. *JACC Cardiovasc. Imaging* **2014**, *7*, 774–784. [CrossRef]
79. Andreu, D.; Ortiz-Perez, J.T.; Boussy, T.; Fernandez-Armenta, J.; Caralt, T.M.; Perea, R.J. Usefulness of contrast-enhanced cardiac magnetic resonance in identifying the ventricular arrhythmia substrate and the approach needed for ablation. *Eur. Heart. J.* **2014**, *35*, 1316–1326. [CrossRef]
80. Acosta, J.; Fernández-Armenta, J.; Penela, D.; Andreu, D.; Borras, R.; Vassanelli, F.; Korshunov, V.; Perea, R.J.; de Caralt, T.M.; Ortiz, J.T.; et al. Infarct transmurality as a criterion for first-line endo-epicardial substrate-guided ventricular tachycardia ablation in ischemic cardiomyopathy. *Heart Rhythm* **2016**, *13*, 85–95. [CrossRef]
81. Quinto, L.; Sanchez, P.; Alarco, F.; Garre, P.; Zaraket, F.; Prat-gonzalez, S. Cardiac magnetic resonance to predict recurrences after ventricular tachycardia ablation: Septal involvement, transmural channels, and left ventricular mass. *Europace* **2021**, *23*, 1437–1445. [CrossRef]
82. Ávila, P.; Pérez-David, E.; Izquierdo, M.; Rojas-González, A.; Sánchez-Gómez, J.M.; Ledesma-Carbayo, M.J. Scar extension measured by magnetic resonancebased nal intensity mapping predicts ventricular tachycardia recurrence after substrate ablation in patients with previous myocardial infarction. *JACC Clin. Electrophysiol.* **2015**, *1*, 353–365. [CrossRef]
83. Nishimura, T.; Patel, H.N.; Wang, S.; Upadhyay, G.A.; Smith, H.L.; Ozcan, C. Prognostic value of cardiac magnetic resonance septal late gadolinium enhancement patterns for periaortic ventricular tachycardia ablation: Heterogeneity of the anteroseptal substrate in nonischemic cardiomyopathy. *Heart Rhythm* **2021**, *18*, 579–588. [CrossRef] [PubMed]
84. Ghafoori, E.; Kholmovski, E.; Thomas, S.; Silvernagel, J.; Nathan, A.; Nan, H. Characterization of gadolinium contrast enhancement of radiofrequency ablation lesions in predicting edema and chronic lesion size. *Circ. Arrhythm. Electrophysiol.* **2017**, *10*, e005599. [CrossRef] [PubMed]
85. Dabbagh, G.S.; Ghannam, M.; Siontis, K.C.; Attili, A.; Cochet, H.; Jais, P.; Eng, M.J.; Latchamsetty, R.; Jongnarangsin, K.; Morady, F.; et al. Magnetic resonance mapping of cathter ablation lesions after postinfarction ventricular tachycardia ablation. *JACC Cardiovasc. Imaging* **2021**, *14*, 588–598. [CrossRef]

2. HIPÓTESIS

1. El uso de catéteres de mapeo de alta densidad con capacidad para detectar señales ortogonales permite una mejor identificación del sustrato arritmogénico y, por tanto, mejores resultados de la ablación de TV respecto a los procedimientos realizados con otros catéteres sin capacidad para detectar señales ortogonales.

2. Los umbrales de voltaje definidos con catéteres bipolares para la caracterización del sustrato (0.5mv-1.5mv) son diferentes a los realizados con nuevos catéteres de mapeo de alta densidad con evaluación de señal ortogonal.

3. El sustrato arrítmico visualizado en los mapas electroanatómicos no es estático ni representa de forma absoluta el sustrato total. El análisis de canales por RMC puede ayudarnos a desenmascarar sustrato arrítmico en los mapas electroanatómicos.

4. Los canales anatómicos (es decir, *border zone* rodeada de cicatriz densa que comunica con tejido sano) detectados mediante RMC presentan características diferentes que se relacionan con su potencial arritmogenicidad.

5. La profundidad de los canales medidos mediante RMC se relaciona con la posibilidad de su correcta eliminación cuando se realizan aplicaciones endocárdicas. La evaluación de dicha profundidad, por tanto, puede ayudarnos a planificar adecuadamente el abordaje (endocárdico, epicárdico o mixto).

6. La RMC post ablación de TV permite identificar pacientes con mayor probabilidad de recidiva mediante la detección de canales de conducción lenta residuales no ablacionados o la creación de nuevos canales.

3. OBJETIVOS

1. Evaluar la efectividad a 12 meses de la ablación de TV con el uso de una estrategia de ablación basada en un mapeo detallado del sustrato mediante catéteres con evaluación de señales ortogonales.

2. Definir nuevos voltajes de cicatriz, *border zone* y tejido sano con catéteres de alta densidad y señales ortogonales.

3. Estudiar la evolución de las zonas de deceleración observadas en mapas de isócronas a lo largo del procedimiento de ablación (mapa basal y *remaps*) y su relación con canales de RMC.

4. Identificar las características de los canales de RMC que están relacionados con zonas de deceleración en los mapas electroanatómicos.

5. Definir un punto de corte de profundidad de canal que permita elegir el abordaje en la ablación de TV (endocárdico o epicárdico)

6. Evaluar mediante RMC los predictores de recurrencia post ablación de TV.

4. Material, métodos y resultados

Artículo 1: Mapeo de alta densidad con señales ortogonales y análisis del istmo de la taquicardia ventricular vs. Ablación de taquicardia ventricular basada puramente en sustrato: un estudio casos-controles

El objetivo de este estudio fue comparar los resultados clínicos después de utilizar dos estrategias de ablación de TV diferentes: una basada en un mapeo extenso con un catéter de mapeo de alta densidad capaz de analizar señales ortogonales, que incluye un mapa electroanatómico extenso incluyendo el análisis del istmo de la TV, y la otra basada en ablación de sustrato puro ("*scar dechaneling*") con el uso de catéter de alta densidad sin capacidad de analizar señales ortogonales.

Para ello, se incluyeron 40 pacientes consecutivos sometidos a ablación de TV con el método de mapeo extenso de alta densidad en el Hospital Clinic de Barcelona (noviembre de 2018 a noviembre de 2019). Los resultados clínicos se compararon con una cohorte histórica de 26 pacientes consecutivos que se sometieron a ablación utilizando una técnica de *scar dechanneling* previa a 2018 con catéter de alta densidad sin capacidad de mapeo ortogonal. La densidad de puntos de mapeo fue mayor en el grupo de mapeo extenso (2370.24 ± 920.78 vs. 576.45 ± 294.46; $p < 0.001$). Después de 1 año de seguimiento, la TV recidivó en el 18.4% de los pacientes en el grupo de mapeo extenso frente al 34.6% de los pacientes en el grupo de control histórico ($p = 0.14$), con una reducción significativamente mayor de la carga de TV: episodios de TV (81.7 ± 7.79 vs. 43.4 ± 19.9%, $p < 0.05$), estimulación anti-taquicardia (99.45 ± 2.29 vs. 33.9 ± 102.5%, $p < 0.001$), y descargas del DAI (99 ± 4.5 vs. 64.7 ± 59.9%, $p = 0.02$).

Como conclusión, el uso de un método basado en un mapeo extenso con catéteres de alta densidad con capacidad de detectar señales ortogonales permite una mejor discriminación del sustrato arrítmico y podría estar asociado con una mayor disminución de la carga de TV.

frontiers | Frontiers in Cardiovascular Medicine

TYPE Original Research
PUBLISHED 01 August 2022
DOI 10.3389/fcvm.2022.912335

OPEN ACCESS

EDITED BY
Harilaos Bogossian,
Evangelisches Krankenhaus Hagen-Haspe, Germany

REVIEWED BY
Jose Francisco Huizar,
Hunter Holmes McGuire VA Medical Center, United States
Dimitris Tsiachris,
Athens Medical Center, Greece
Johannes Steinfurt,
University Heart Center Freiburg, Germany

*CORRESPONDENCE
Ivo Roca-Luque
iroca@clinic.cat

SPECIALTY SECTION
This article was submitted to Cardiac Rhythmology, a section of the journal Frontiers in Cardiovascular Medicine

RECEIVED 04 April 2022
ACCEPTED 04 July 2022
PUBLISHED 01 August 2022

CITATION
Vázquez-Calvo S, Garre P, Sanchez-Somonte P, Borras R, Quinto L, Caixal G, Pujol-Lopez M, Althoff T, Guasch E, Arbelo E, Tolosana JM, Brugada J, Mont L and Roca-Luque I (2022) Orthogonal high-density mapping with ventricular tachycardia isthmus analysis vs. pure substrate ventricular tachycardia ablation: A case–control study. *Front. Cardiovasc. Med.* 9:912335. doi: 10.3389/fcvm.2022.912335

Orthogonal high-density mapping with ventricular tachycardia isthmus analysis vs. pure substrate ventricular tachycardia ablation: A case–control study

Sara Vázquez-Calvo[1,2], Paz Garre[1,2], Paula Sanchez-Somonte[1,2,3], Roger Borras[1,2], Levio Quinto[1,2], Gala Caixal[1,2], Margarida Pujol-Lopez[1,2], Till Althoff[1,2], Eduard Guasch[1,2,3], Elena Arbelo[1,2,3], José Maria Tolosana[1,2,3], Josep Brugada[1,2,3], Lluís Mont[1,2,3] and Ivo Roca-Luque[1,2,3]*

[1]Department of Cardiology, Cardiovascular Clinical Institute, Arrythmia Section, Hospital Clínic, Universitat de Barcelona, Barcelona, Spain, [2]Institut d'Investigacions Biomèdiques August Pi i Sunyer (IDIBAPS), Barcelona, Spain, [3]Centro de Investigación Biomédica en Red de Enfermedades Cardiovasculares (CIBERCV), Madrid, Spain

Background: Substrate-based ablation has become a successful technique for ventricular tachycardia (VT) ablation. High-density (HD) mapping catheters provide high-resolution electroanatomical maps and better discrimination of local abnormal electrograms. The HD Grid Mapping Catheter is an HD catheter with the ability to map orthogonal signals on top of conventional bipolar signals, which could provide better discrimination of the arrhythmic substrate. On the other hand, conventional mapping techniques, such as activation mapping, when possible, help to identify the isthmus of the tachycardia.

Aim: The purpose of this study was to compare clinical outcomes after using two different VT ablation strategies: one based on extensive mapping with the HD Grid Mapping Catheter, including VT isthmus analysis, and the other based on pure substrate ablation.

Methods: Forty consecutive patients undergoing VT ablation with extensive HD mapping method in the hospital clinic (November 2018–November 2019) were included. Clinical outcomes were compared with a historical cohort of 26 consecutive patients who underwent ablation using a scar dechanneling technique before 2018.

Results: The density of mapping points was higher in the extensive mapping group (2370.24 ± 920.78 vs. 576.45 ± 294.46; $p < 0.001$). After 1 year of follow-up, VT recurred in 18.4% of patients in the extensive mapping group vs. 34.6% of patients in the historical control group ($p = 0.14$), with a significantly greater reduction of VT burden: VT episodes (81.7 ± 7.79

vs. 43.4 ± 19.9%, $p < 0.05$), antitachycardia pacing (99.45 ± 2.29 vs. 33.9 ± 102.5%, $p < 0.001$), and implantable cardioverter defibrillator (ICD) shocks (99 ± 4.5 vs. 64.7 ± 59.9%, $p = 0.02$).

Conclusion: The use of a method based on extensive mapping with the HD Grid Mapping Catheter and VT isthmus analysis allows better discrimination of the arrhythmic substrate and could be associated with a greater decrease in VT burden.

KEYWORDS

ventricular tachycardia ablation, high-density mapping catheters, activation mapping, cardiac magnetic resonance, arrhythmic burden

Introduction

Catheter ablation has become a standard treatment for ventricular tachycardia (VT) in patients with structural heart disease (1). Activation and entrainment mapping can be performed in only 30–40% of cases due to hemodynamically untolerated VTs. Substrate-based ablation based on the identification of the arrhythmic substrate through mapping during sinus or paced rhythm has been developed in recent years, initially to treat poorly tolerated infarct-related VT (2, 3). Nowadays, it has become established as the cornerstone for VT ablation in patients with structural heart disease. The main mechanism behind scar-related VT is the re-entrant circuit. This circuit is caused by the presence of a channel of border zone tissue with slow conduction surrounded by core scar tissue that connects to healthy tissue, leading to re-entry. These regions are also called conducting channels (CCs). These CCs can be accurately identified with the aid of electroanatomical maps (EAMs) obtained during ablation (2, 3). In these areas, reduced conduction velocity produces areas of delayed, fractionated electrical activity that can persist even after the inscription of the QRS complex (3, 4). Several studies have demonstrated the relation of these electrograms, so-called late potentials (LPs) or local abnormal ventricular activity (LAVA), with VT (5). Indeed, many authors have suggested that complete elimination of the VT substrate results not only in tachycardia non-inducibility, but also results in fewer VT recurrences on long-term follow-up (1, 6, 7).

This substrate approach strategy is based on the correct identification and posterior elimination of the entire arrhythmic substrate. The bipolar signal, especially in cases of fractioned and/or low-amplitude electrograms (EGMs) as LPs or LAVAs, depends on the electrode size, interelectrode spacing, and angle of the incoming wavefront to the mapping catheter (8, 9). Multielectrode high-density (HD) catheters have been developed to increase mapping resolution, allowing detailed anatomical characterization of the endocardial substrate (10). To overcome the dependence of the EGM amplitude on the wavefront orientation, a new high-density catheter with a grip shape was designed. This catheter (the Advisor^{TM} HD Grid Mapping Catheter, Abbott Medical, United States) receives bipolar signals between each of its 16 electrodes, forming an extensive network of orthogonal signals. Through a dedicated algorithm (HD Wave Solution algorithm, Abbott Medical, United States), the highest peak-to-peak voltage among the two orthogonal signals of every dipole is selected. This grid catheter has been shown to facilitate the discrimination of LAVAs/LPs, providing a more detailed characterization of the arrhythmic substrate (11, 12), which is even more important in low-voltage areas.

This study aimed to compare the clinical outcomes of VT ablation guided by two different strategies: one based on high-density mapping with the HD Grid Mapping Catheter and induction and the other based on a scar dechanneling technique using the conventional bipolar HD Grid Mapping Catheter.

Materials and methods

Study population

This was a single-center, observational, prospective study that included all the consecutive patients who underwent VT catheter ablation with an extensive mapping method with the HD Grid Mapping Catheter in our center from October 2018 to December 2019 (group 1). This cohort was compared with a historical cohort of 26 consecutive patients who underwent ablation for VT from January 2013 to November 2018 using a scar dechanneling technique with an HD catheter without the ability to detect orthogonal signals (PENTARAY, Biosense Webster, Diamond Bar, California, United States) (group 2). The inclusion criteria were the presence of structural heart disease and episodes of sustained monomorphic VT. This study was carried out according to the guidelines of the Declaration

of Helsinki and the deontological code of our institution. This study protocol was approved by the ethics committee of the hospital.

Preprocedural evaluation

The number of events before the procedure was collected, as well as other clinical aspects, including the type of heart disease, antiarrhythmic treatment, and the New York Heart Association (NYHA) functional class. A cardiac ultrasound was performed on all the patients. Cardiac MR (CMR) with late gadolinium enhancement (LGE) was performed, if there were no contraindications [3 T scan in patients without an implantable cardioverter defibrillator (ICD) or 1.5 T with a wideband sequence in patients with ICD]. Manual segmentation of the left ventricle and right ventricle was performed. Automatic quantitative analysis of the substrate was executed using ADAS 3D software (ADAS 3D, ADAS 3D Medical SL) following a previously described protocol (13). In brief, the analysis was performed in 9 layers from the endocardium to the epicardium. A three-dimensional map was obtained for each layer. The LGE pixel signal intensity maps obtained from the CMR were projected onto each layer according to a trilinear interpolation algorithm and were color-coded. To identify the areas of scarring, an algorithm based on the intensity of the pixel signal was applied to characterize the areas of hyperenhancement, such as the core of the scar or the border zone, using 40 $\pm$ 5% and 60 $\pm$ 5% of the maximum intensity as a threshold, respectively.

Ablation procedure

Procedures were performed under general anesthesia. Access to the left ventricle was achieved with a transseptal and/or retrograde aortic approach. Epicardial mapping was performed in cases when an epicardial origin of VT was suspected and in cases of failed endocardial ablation.

A substrate voltage map of the left ventricle was obtained during right ventricular (RV) pacing for better stability of the cardiac cycle using the HD Grid Mapping Catheter and the EnSite Precision Cardiac Mapping System (Abbott Medical, United States) in group 1 and the PENTARAY Catheter and the CARTO® 3 system (Biosense Webster, Diamond Bar, California, United States) in group 2. Peak-to-peak amplitudes of 0.5–1.5 and $<$ 0.5 mV were used to define the low-voltage zone and the dense scar zone, respectively. Abnormal electrogram features, such as "LAVA" (defined as local EGMs with split, fractionated, or high-frequency components) and LPs, were manually tagged. In both the groups, areas of scarring were confirmed with a contact-sensor ablation catheter (TactiCath SE, Abbott Medical in group 1 and SmartTouch, Biosense Webster in group 2) using 4 gr of contact as the cutoff point to avoid the overdetection of low-voltage areas (14). In both the groups, LGE-CMR postprocessed images (when available) were used to aid the ablation. In group 1, persistent scatterer interferometry (PSI) maps were visualized by the navigation system side by side. In group 2, PSI maps were merged with the substrate map as previously described (2).

Group 1

After voltage mapping and tagging of LAVAs and LPs, analysis of deceleration zones was performed by activation mapping during RV pacing. Automated annotation was performed at the offset of the latest local EGM component (last deflection algorithm, Abbott Medical, United States). After the delineation of slow conduction areas, the HD Grid Mapping Catheter was positioned in a potential area of the VT isthmus (slow conduction area and/or channel isthmus according to LGE-CMR images). VT was induced by programmed electrical stimulation (drive cycles of 600, 500, and 430 ms, up to triple extrastimuli to refractoriness or 200 ms). When VT was hemodynamically tolerated, activation mapping for diastolic and presystolic activities was performed. Entrainment mapping was performed at sites that demonstrated diastolic activity. In cases in which VT was not hemodynamically tolerated, the VT isthmus was defined as the area with a fast transition from good pace mapping (suggesting VT exit site) to poor pace mapping (suggesting VT entrance site), as described previously (15). Radiofrequency (RF) was delivered using an externally irrigated 3.5-mm tip ablation catheter with 45°C temperature control (irrigation rate of 26–30 ml/min), and a power limit of 40–50 W (60 W in septal areas and/or in cases of a deep substrate according to LGE-CMR PSI maps). The primary target for ablation was the central isthmus of VT according to activation mapping and/or pacemap mapping. After the VT isthmuses were targeted, substrate ablation was performed. The main targets were the deceleration zones and the entrances and exits of the defined conducting channels. Remapping with the HD Grid Mapping Catheter was performed to detect residual substrate. Additional RF lesions were delivered in areas with persistent LAVA and/or isolated LPs. The procedural endpoint was the abolition of LAVA and LPs, as well as the lack of VT inducibility at the end of the procedure.

Group 2

Substrate ablation was performed following a 4-step scar dechanneling technique, as previously described (2). The workflow involved the identification of CCs by EAM (and/or by LGE-CMR postprocessing model reconstruction) during sinus rhythm or RV stimulation. Isolated late potentials (ILPs) were manually tagged during mapping to define CCs inside the scar. Radiofrequency was delivered using an irrigated 3.5-mm tip ablation catheter with 45°C temperature control, power limit of 40–50 W, and irrigation rate of 26–30 ml/min (40 W and

TABLE 1 Demographic and clinical baseline characteristics of the population.

	Group 1	Group 2	*P*-value
Age, years	64.42 ± 12.00	66.12 ± 12.19	0.583
Male	94.7%	88.5%	0.358
Hypertension	68.4%	80.8%	0.272
Diabetes mellitus	42.1%	34.6%	0.546
Dyslipidemia	64.9%	73.1%	0.491
COPD	12.1%	19.2%	0.451
CKD (< 60)	17.9%	34.6%	0.160
Permanent AF	13.2%	3.8%	0.209
LVEF (%)	34.38 ± 11.02	35.64 ± 12.00	0.681
LVEDD (mm)	61.35 ± 11.15	59.00 ± 8.60	0.457
LVESD (mm)	45.24 ± 16.65	42.86 ± 12.77	0.664
NYHA-I	27.3%	38.5%	0.218
NYHA-II	69.7%	50.0%	0.218
NYHA-III/IV	3.0%	11.5%	0.218
Ischemic cardiomyopathy	68.4%	88.5%	0.063
Beta blockers	72.2%	92.3%	0.048
ACE inhibitor	61.1%	53.8%	0.567
Sotalol	19.4%	11.5%	0.404
Amiodarone	72.2%	65.4%	0.564
CMR preintervention	76.3%	76.0%	0.977
Total Scar by CMR (g)	9.19 ± 5.93	10.17 ± 6.59	0.631
Total BZ by CMR (g)	22.16 ± 8.43	20.64 ± 11.17	0.646
Epicardial scar by CMR (cm^2)	91.30 ± 61.28	89.34 ± 60.35	0.922
Arrhythmic storm	26.3%	26.9%	0.957
Incessant VT	16.2%	7.7%	0.317
Episodes 1 year preablation	4.97 ± 8.96	2.31 ± 2.02	0.142
ATP 1 year preablation	5.89 ± 9.77	4.54 ± 8.15	0.582
Shocks 1 year preablation	2.64 ± 4.84	2.54 ± 4.32	0.933

COPD, Chronic obstructive pulmonary disease; CKD, Chronic kidney disease; LVEF, Left ventricular ejection fraction; LVEDD, Left ventricular end-diastolic diameter; LVESD, Left ventricular end-systolic diameter; NYHA, New York Heart Association; ACE, Angiotensin-converting enzyme; ATP, Antitachycardia pacing.

17 ml/min at epicardium) at the CC entrance during sinus rhythm. Remapping was used to confirm the elimination of all the CCs and to check for residual ILPs. Residual ILPs identified by remapping were completely eliminated when possible. Programmed electrical stimulation (drive cycles of 600 and 400 ms, up to triple extrastimuli to refractoriness or 200 ms) was performed after substrate ablation, and any residual-induced VT was targeted. The procedural endpoint comprised the entrance of CC abolition, late potential abolition, and no VT inducibility at the end of the procedure.

Ventricular tachycardia burden

The preprocedural burden of VT was defined as the number of VT episodes and ICD therapies within the last year until the day of the ablation procedure. The postprocedural burden of VT was established as the number of VT events during the 12 months after ablation.

A VT episode was defined as continuous VT for 30 s and/or a syncopal event or as VT that required an appropriate intervention for termination.

Implantable cardioverter defibrillator therapies were qualified and quantified by remote monitoring and outpatient device monitoring.

TABLE 2 Procedural characteristics.

	Group 1	Group 2	*P*-value
Transeptal puncture	78.4%	96.0%	0.053
Epicardial access	8.1%	32.0%	0.021
Retroaortic access	68.6%	28.0%	0.002
Endocardial mapping points	**2370.24 ± 920.78**	**576.45 ± 294.46**	**0.000**
Epicardial mapping points	**1509.00**	**846.29 ± 536.60**	**0.000**
Procedure duration, min	**255.06 ± 46.67**	**195.55 ± 67.07**	**0.000**
RF application time, sec	**1791.48 ± 780.70**	**1073.27 ± 605.40**	**0.001**
RF application, *n*	**63.28 ± 25.11**	**31.59 ± 14.05**	**0.000**
Fluoroscopy duration, min	**37.59 ± 15.1427**	**20.30 ± 8.4769**	**0.000**
Number of induced VT	**1.68 ± 1.165**	**0.79 ± 1.062**	**0.004**
Number of VT target	**1.63 ± 1.060**	**0.38 ± 0.647**	**0.000**
Number of VT ablated	**1.53 ± 1.082**	**0.25 ± 0.532**	**0.000**
Complete LAVA abolition	77.4%	84.0%	0.538
No VT inducibility postablation	74.7%	72.4%	0.226

RF, Radiofrequency.

Follow-up

The primary endpoint was VT burden reduction. The arrhythmic load was evaluated by analyzing the number of VT events (previously defined) and ICD therapies. Death during follow-up was categorized as either cardiovascular or non-cardiovascular. Among cardiovascular deaths, sudden deaths attributed to ventricular arrhythmia were recorded.

Statistical analysis

Continuous variables are presented as the mean ± *SD* or median with an interquartile range, as appropriate. A *t*-test was used to compare the means of two variables. Categorical variables are expressed as the total number or percentage and were compared between groups using the chi-squared test

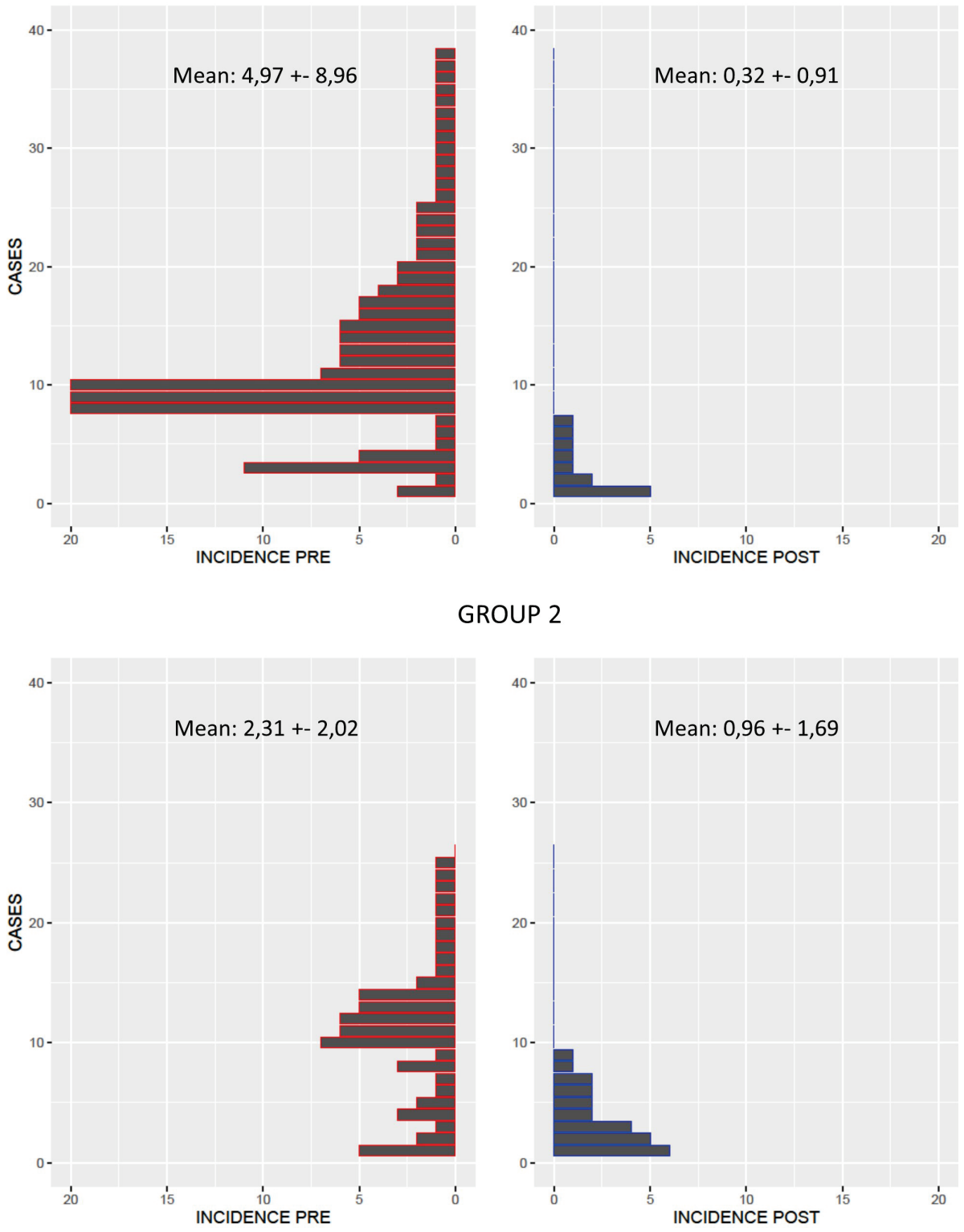

FIGURE 1
VT burden before (red) and after ablation (blue) in group 1 (extensive mapping) and group 2 (scar dechanneling). A reduction in VT was observed in both the groups, but the reduction was larger in the extensive HD mapping group.

or Fisher's exact test to compare the VT burden before and after the procedure; we used the non-parametric Wilcoxon test for paired data.

Recurrence-free survival over time was calculated by the Kaplan–Meier method, and comparisons between the groups were performed with the log-rank test. All the analyses were performed with SPSS version 18.0 (SPSS, United States) and R software version 3.6.1 (R project for Statistical Computing; Austria). All the statistical tests were two-sided, and $p < 0.05$ was considered statistically significant.

Results

Baseline characteristics

During this period, 40 patients undergoing VT ablation met the inclusion criteria. Two patients were excluded due to complications related to the epicardial approach in which no mapping was performed. Therefore, 38 patients were prospectively included (group 1). This cohort was compared with a historical cohort of 26 consecutive patients. Both the groups were similar with respect to age and sex distribution, baseline left ventricular ejection fraction (LVEF), and antiarrhythmic therapy before ablation. The baseline characteristics of the patients are shown in **Table 1**.

Mapping and ablation procedure

Ventricular tachycardia ablation was performed with an epicardial or endoepicardial approach in 8.1% of patients in group 1 and 32.0% of patients in group 2 ($p = 0.021$) and exclusively by an endocardial approach in the remaining patients. The average mapping points were higher in group 1 than in group 2 (endocardium: 2370.24 ± 920.78 vs. 576.45 ± 294.46, epicardium: 1509.00 vs. 846.29 ± 536.60, $p < 0.001$). The percentage of induced VTs in which the diastolic isthmus was confirmed (by activation mapping and/or pace mapping) was higher in group 1 (92.17 vs. 57.05%, $p < 0.001$). The duration of the procedure (255.06 ± 46.67 vs. 195.55 ± 67.07 min, $p < 0.001$), fluoroscopy exposure (37.591 ± 15.14 vs. 20.304 ± 8.48 min, $p = 0.000$), radiofrequency exposure (1791.48 ± 780.70 vs. 1073.27 ± 605.40 s, $p < 0.001$), and the number of radiofrequency applications (63.28 ± 25.10 vs. 31.59 ± 14.05, $p = 0.000$) were greater in group 1.

Regarding the acute procedural endpoint of ablation, there was no difference between the groups. Major complications occurred in 2 patients in group 1 (pericardial effusion and femoral pseudoaneurysm) vs. 3 patients in group 2 [femoral hematoma, complete atrioventricular (AV) block, and ischemic stroke]. The ablation procedure parameters are given in **Table 2**.

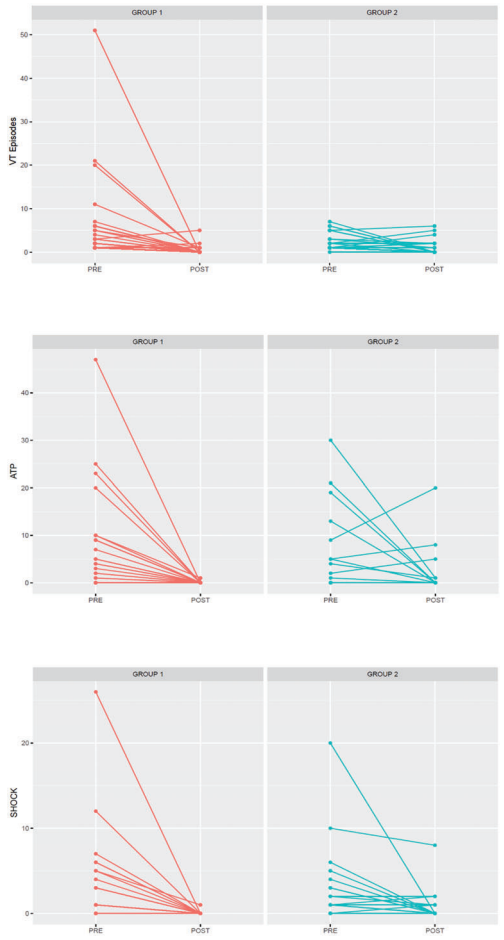

FIGURE 2
Differences in arrhythmic burden (VT episodes, ATP, and shocks) between pre- and postablation by group (group 1, extensive HD mapping, red; group 2, scar dechanneling, blue).

Follow-up

After 1 year of follow-up, a significantly higher reduction in the arrhythmic burden was observed in the extensive mapping group in terms of VT episode reduction (81.69 ± 7.79 vs. 43.46 ± 19.97%, $p < 0.05$), antitachycardia pacing (ATP) therapy reduction (99.47 ± 2.29 vs. 33.94 ± 102.46%, $p < 0.001$), and ICD shock reduction (99.00 ± 4.47 vs. 64.67 ± 59.87%, $p = 0.02$). **Figures 1**, **2** show the decrease in the VT burden in both the groups. In addition, a non-significant tendency toward a lower rate of VT recurrence (**Figure 3**) was also observed (18.4 vs. 34.6%, $p = 0.142$), with a hazard ratio of 2.032 (0.76–5.46) ($p = 0.16$). Only one patient from group 2 underwent a second VT ablation procedure. No patients from group 1 underwent a second VT ablation procedure. Death from any cause occurred in 3 patients in the HD mapping group and none in the historical cohort ($p = 0.26$). No deaths from a cardiac cause were observed.

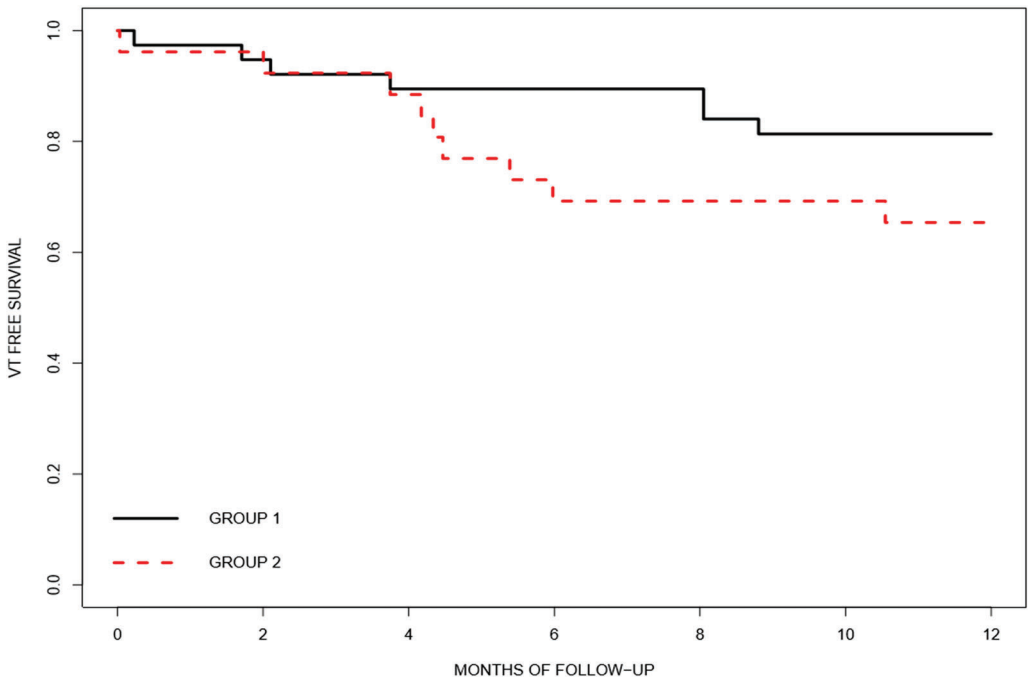

FIGURE 3
The Kaplan–Meier curve showing ventricular tachycardia-free survival after ablation by group (group 1, extensive HD mapping, black; group 2, scar dechanneling, red).

Discussion

We assessed the clinical efficacy of VT ablation with a method based on extensive HD mapping with catheters with the ability to analyze orthogonal signals (HD Grid Mapping Catheter) and induction vs. a scar dechanneling method with HD catheters that map only bipolar signals (PENTARAY). The major study findings were a higher substrate map density, a higher proportion of mapped VT, and a significantly larger reduction in VT burden (VT episodes and ICD therapies) in group 1.

Successful elimination of the arrhythmic substrate is based on the ability to create a detailed substrate map with identification of all the abnormal EGMs suggesting slow conduction. The resolution of electroanatomical mapping is determined by multiple parameters, including the mapping rhythm, vector of propagation, electrode size, interelectrode spacing, and filtering (8, 9). In this sense, several studies have shown that the use of multielectrode mapping catheters with smaller electrodes and interelectrode spacing can increase map resolution, enhancing the identification of surviving channels and macrore-entrant circuits (10, 16, 17). However, there is another key factor that determines the amplitude and shape of EGMs, i.e., the activation wavefront relative to the catheter orientation (18). Some studies have demonstrated, not only in animal models (19), but also in patients who underwent VT ablation (11), higher accuracy in scar detection with the use of catheters that are able to analyze orthogonal signals, with less beat-to-beat variation and better correspondence with histology (10).

In the present study, there was a clear difference in terms of HD mapping points in the HD mapping group in both the endocardium and epicardium, not only because of the different strategies. Higher-density mapping points have also been shown in other studies that compared the HD Grid Mapping Catheter with other HD mapping catheters (PENTARAY, Duo-Decapolar Catheter, etc.) (12). The HD Grid Mapping Catheter acquires simultaneous signals across orthogonal planes, achieving higher-density maps and providing a more thorough evaluation of the electrogram amplitude and direction. Therefore, by analyzing orthogonal signals at every single point, this catheter and its automatic algorithm enhance the identification of border zones and slow conduction areas (12, 16).

Similarly, more VTs were mapped in group 1. Detection of the diastolic isthmus in VT has recently been related to better long-term success (17). Currently, VT mapping is limited by poor tolerance of arrhythmia in many patients. However, the highly detailed substrate maps enabled the careful identification of potential slow conduction areas with the HD Grid Mapping Catheter before VT induction, which allowed us to perform limited VT mapping of the potential culprit areas in most of the patients. Because the map was limited to the region of interest,

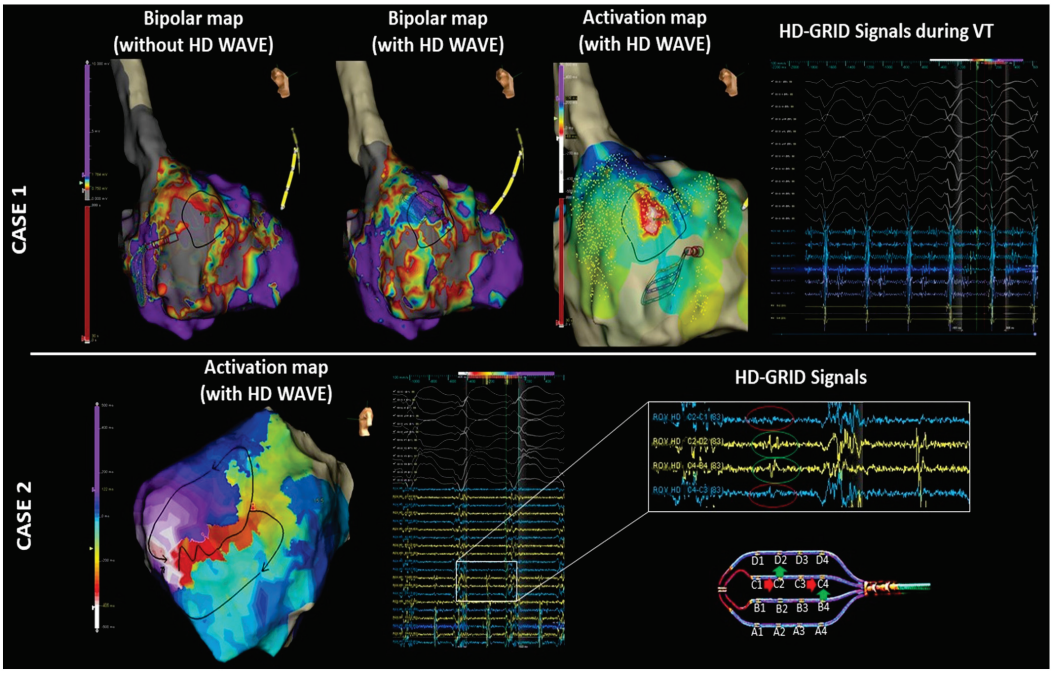

FIGURE 4
Electroanatomical maps (EAMs) of the left ventricle in 2 representative examples. Case 1: Left panel: high-density voltage map using only bipolar signals showing an extensive septal scar. Middle panel: the same map obtained using both the bipolar and orthogonal signals (HD Wave algorithm) shows "hidden" viable tissue in the upper part of this septal scar. Right panel: activation map obtained with the HD Grid Mapping Catheter and HD Wave algorithm shows mid-diastolic signals during VT. These mid-diastolic signals were located in the viable tissue only identified by the orthogonal signals during substrate mapping. Case 2: Activation map of VT obtained with the HD Grid Mapping Catheter and HD Wave algorithm. The importance of the orthogonal signals in relation to the activation wavefront is clearly illustrated: The conventional bipolar C1-C2 and C3-C4 (blue tracings) do not show any notable mid-diastolic potentials (red circles). In contrast, orthogonal signals in the same place (C2-D2 and B4-C4, yellow tracing) show clear mid-diastolic EGMs in the isthmus of VT (green circles). The VT activation map is shown in the left panel.

activation mapping could be performed in a short period of time, overcoming the problem of hemodynamic tolerance. In addition, the ability to detect orthogonal signals at every point increases the ability to detect diastolic low-voltage signals during tachycardia, as the wavefront direction is even more critical during tachycardia than during basal rhythm. A clear example of the relevance of orthogonal signals both in the substrate sinus map and VT activation map is shown in **Figure 4**.

Many studies have demonstrated that substrate ablation with the elimination of slow conduction areas (LAVAs, LPs, deceleration zones, etc.) is associated with better clinical outcomes (6, 12, 20, 21). As stated before, the properties of the HD Grid Mapping Catheter, including the capability of orthogonal signal detection, as well as the use of a specific algorithm (HD Wave Solution), reduce variability in electrogram characteristics associated with differential orientations relative to the propagating wavefront and allow selection of the highest-amplitude signal in each location. Concerning this matter, a small study (20) compared traditional point-by-point catheters vs. high-density catheters (PENTARAY) and found that the PENTARAY provided better discrimination of abnormal electrograms, without significant differences in VT inducibility after substrate ablation, but with a shorter radiofrequency time. Indeed, Proietti et al. (12) analyzed clinical outcomes after the use of different mapping catheters (HD Grid, PENTARAY, Duo-Decapolar, and point-by-point catheters) and found a reduction in ATP and/or significant appropriate shocks with HD catheters.

In our study, an ablation based on an extensive mapping with the HD Grid Mapping Catheter, compared to a scar dechanneling strategy with PENTARAY, resulted in a significant reduction in the overall VT burden at 1 year postprocedure, not only in ATP and appropriate ICD shocks but also in overall VT episodes. As mentioned above, due to the orthogonal signal mapping, more accurate substrate mapping and better discrimination of the VT diastolic isthmus can explain the better results obtained. Further larger and randomized controlled trials are needed to confirm these results.

Limitations

This was an observational single-center study with the inherent limitations of such a study design. The retrospective

cohort included a set of patients referred for ablation up to 5 years earlier than patients in the prospective cohort. During this time, some aspects, in addition to the use of a different mapping catheter, could have potentially contributed to the differences observed.

Another potential limitation is that although the main difference between the two groups was the use of different high-density mapping catheters, the ablation strategy was modified; in the PENTARAY group, a scar dechanneling technique was used in every patient, and in the HD Grid Mapping Catheter group, deceleration zone and VT isthmus analysis and ablation were included in the ablation strategy.

Epicardial access was more frequent in the historical group. In that period, any patient with some epicardial scar in the CMR, even patients with ischemic heart disease and also endocardial scar, underwent endoepicardial ablation. However, in the group with the extensive HD Grid Substrate Mapping Catheter, only epicardial access was performed in case of extensive epicardial scar or ECG suggestive of epicardial VT origin. To overcome some influence of larger epicardial scars in some of the groups with recurrence rate (as epicardial substrates are known to have higher recurrence rate), we have analyzed the amount of scar both in the endocardium and epicardium founding no differences between the groups; so, despite the lack of matching analysis, recurrence rate does not seem to be related with differences in scar amount.

Finally, the radiofrequency duration was also longer in patients treated with the HD Grid Mapping Catheter. However, the RF duration is similar to that in other published studies of the HD Grid Mapping Catheter (12) and could be related to the identification of slower conduction areas that ultimately need to be targeted.

Conclusion

Ventricular tachycardia ablation strategy based on extensive mapping with the use of the HD Mapping Catheter with the ability to map orthogonal signals allows better definition of the arrhythmogenic substrate and better identification of the diastolic VT isthmus and may be associated with a lower arrhythmic burden on follow-up compared with conventional pure substrate-based strategy using the conventional bipolar HD Grid Mapping Catheter.

Data availability statement

The raw data supporting the conclusions of this article will be made available by the authors, without undue reservation.

Ethics statement

The studies involving human participants were reviewed and approved by the Ethical Committee of Hospital Clinic (CEIm). The patients/participants provided their written informed consent to participate in this study.

Author contributions

IR-L and LM: study concept and design. SV-C, PS-S, LQ, MP-L, and GC: acquisition of data. SV-C and PG: analysis and interpretation of data. RB and TA: statistical analysis. SV-C and IR-L: drafting of the manuscript. EG, EA, JT, and JB: critical revision of the manuscript for important intellectual content. All authors have contributed to the article and approved the submitted version of the manuscript.

Funding

This study was supported by the Emile Letang Grand of Hospital Clinic de Barcelona/Instituto de Salud Carlos III (ISCIII) PI20/00693/CB16/11/00354, co-funded by the European Union.

Acknowledgments

We thank Neus Portella for her assistance in editing this manuscript.

Conflict of interest

LM, EA, JB, IR-L, and JT report activities as consultant, lecturer, and advisory board member for Abbott Medical, Boston Scientific, Biosense Webster, Medtronic, and Biotronik. MP-L has received honoraria from Medtronic.

The remaining authors declare that the research was conducted in the absence of any commercial or financial relationships that could be construed as a potential conflict of interest.

Publisher's note

References

1. Tung R, Vaseghi M, Frankel DS, Vergara P, di Biase L, Nagashima K, et al. Freedom from recurrent ventricular tachycardia after catheter ablation is associated with improved survival in patients with structural heart disease: an international VT ablation center collaborative group study. *Heart Rhythm.* (2015) 12:1997–2007. doi: 10.1016/j.hrthm.2015.05.036

2. Berruezo A, Fernández-Armenta J, Andreu D, Penela D, Herczku C, Evertz R, et al. Scar dechanneling: new method for scar-related left ventricular tachycardia substrate ablation. *Circ Arrhythmia Electrophysiol.* (2015) 8:326–36. doi: 10.1161/CIRCEP.114.002386

3. Arenal A, Glez-Torrecilla E, Ortiz M, Villacastín J, Fdez-Portales J, Sousa E, et al. Ablation of electrograms with an isolated, delayed component as treatment of unmappable monomorphic ventricular tachycardias in patients with structural heart disease. *J Am Coll Cardiol.* (2003) 41:81–92. doi: 10.1016/S0735-1097(02)02623-2

4. Josephson ME, Anter E. Substrate mapping for ventricular tachycardia: assumptions and misconceptions. *JACC Clin Electrophysiol.* (2015) 1:341–52. doi: 10.1016/j.jacep.2015.09.001

5. Pierre J, Philippe M, Paul K, Frédéric S, Isabelle N, Yuki K, et al. Elimination of local abnormal ventricular activities. *Circulation.* (2012) 125:2184–96. doi: 10.1161/CIRCULATIONAHA.111.043216

6. Quinto L, Sanchez-Somonte P, Alarcón F, Garre P, Castillo A, San Antonio R, et al. Ventricular tachycardia burden reduction after substrate ablation: predictors of recurrence. *Heart Rhythm.* (2021) 18:896–904. doi: 10.1016/j.hrthm.2021.02.016

7. Roca-Luque I, Quinto L, Sanchez-Somonte P, Garre P, Alarcón F, Zaraket F, et al. Late potential abolition in ventricular tachycardia ablation. *Am J Cardiol.* (2022) 174:53–60. doi: 10.1016/j.amjcard.2022.02.053

8. Takigawa M, Relan J, Martin R, Kim S, Kitamura T, Frontera A, et al. Effect of bipolar electrode orientation on local electrogram properties. *Heart Rhythm.* (2018) 15:1853–61. doi: 10.1016/j.hrthm.2018.07.020

9. Anter E, Josephson ME. Bipolar voltage amplitude: what does it really mean? *Heart Rhythm.* (2016) 13:326–7. doi: 10.1016/j.hrthm.2015.09.033

10. Tschabrunn CM, Roujol S, Dorman NC, Nezafat R, Josephson ME, Anter E. High-resolution mapping of ventricular scar: comparison between single and multielectrode catheters. *Circ Arrhythm Electrophysiol.* (2016) 9:10.1161/CIRCE115.003841. doi: 10.1161/CIRCEP.115.003841

11. Kenji O, Antonio F, Caterina B, Gabriele P, Andrea R, Luca F, et al. Grid mapping catheter for ventricular tachycardia ablation. *Circ Arrhythmia Electrophysiol.* (2019) 12:e007500. doi: 10.1161/CIRCEP.119.007500

12. Proietti R, Dowd R, Gee LV, Yusuf S, Panikker S, Hayat S, et al. Impact of a high-density grid catheter on long-term outcomes for structural heart disease ventricular tachycardia ablation. *J Interv Cardiac Electrophysiology Int J Arrhythmias Pacing.* (2021) 62:519–29. doi: 10.1007/s10840-020-00918-4

13. Andreu D, Penela D, Acosta J, Fernández-Armenta J, Perea RJ, Soto-Iglesias D, et al. Cardiac magnetic resonance–aided scar dechanneling: influence on acute and long-term outcomes. *Heart Rhythm.* (2017) 14:1121–8. doi: 10.1016/j.hrthm.2017.05.018

14. Sánchez Muñoz JJ, Peñafiel Verdú P, Martínez Sánchez J, Salar Alcaraz M, Valdés Chavarri M, García Alberola A. Usefulness of the contact force sensing catheter to assess the areas of myocardial scar in patients with ventricular tachycardia. *Rev Espanola Cardiol (English ed).* (2015) 68:159–60. doi: 10.1016/j.rec.2014.09.011

15. de Chillou C, Groben L, Magnin-Poull I, Andronache M, MagdiAbbas M, Zhang N, et al. Localizing the critical isthmus of postinfarct ventricular tachycardia: the value of pace-mapping during sinus rhythm. *Heart Rhythm.* (2014) 11:175–81. doi: 10.1016/j.hrthm.2013.10.042

16. Jiang R, Beaser AD, Aziz Z, Upadhyay GA, Nayak HM, Tung R. High-density grid catheter for detailed mapping of sinus rhythm and scar-related ventricular tachycardia: comparison with a linear duodecapolar catheter. *JACC Clin Electrophysiol.* (2020) 6:311–23. doi: 10.1016/j.jacep.2019.11.007

17. Hadjis A, Frontera A, Limite LR, Bisceglia C, Bognoni L, Foppoli L, et al. Complete electroanatomic imaging of the diastolic pathway is associated with improved freedom from ventricular tachycardia recurrence. *Circ Arrhythm Electrophysiol.* (2020) 13:e008651. doi: 10.1161/CIRCEP.120.008651

18. Proietti R, Adlan AM, Dowd R, Assadullah S, Aldhoon B, Panikker S, et al. Enhanced ventricular tachycardia substrate resolution with a novel omnipolar high-density mapping catheter: the omnimapping study. *J Interv Cardiac Electrophysiology.* (2020) 58:355–62. doi: 10.1007/s10840-019-00625-9

19. Porta-Sánchez A, Magtibay K, Nayyar S, Bhaskaran A, Lai PFH, Massé S, et al. Omnipolarity applied to equi-spaced electrode array for ventricular tachycardia substrate mapping. *Europace Eur Pacing Arrhythmias Cardiac Electrophysiology : Journal of the Working Groups Cardiac Pacing Arrhythmias Cardiac Cell Electrophysiol Eur Soc Cardiol.* (2019) 21:813–21. doi: 10.1093/europace/euy304

20. Acosta J, Penela D, Andreu D, Cabrera M, Carlosena A, Vassanelli F, et al. Multielectrode vs. point-by-point mapping for ventricular tachycardia substrate ablation: a randomized study. *Europace Eur Pacing Arrhythmias Cardiac Electrophysiology : Journal of the Working Groups Cardiac Pacing Arrhythmias Cardiac Cell Electrophysiol Eur Soc Cardiol.* (2018) 20:512–9. doi: 10.1093/europace/euw406

21. Maagh P, Christoph A, Dopp H, Mueller MS, Plehn G, Meissner A. High-density mapping in ventricular tachycardia ablation: a PentaRay(®) study. *Cardiol Res.* (2017) 8:293–303. doi: 10.14740/cr636w

Artículo 2: Mapas de voltaje personalizados guiados por resonancia magnética cardíaca en la era del mapeo de alta densidad

El objetivo de este estudio fue crear mapas de voltaje personalizados utilizando RMC para guiar el ajuste de los umbrales de voltaje.

Para ello, se incluyeron todos los pacientes consecutivos con TV relacionada con cicatriz sometidos a ablación después de RMC (octubre de 2018 a diciembre de 2020). En primer lugar, se definieron umbrales de voltaje personalizados de manera sistemática guiados por RMC según la distribución de la cicatriz y la ubicación de los canales. En segundo lugar, para validar estos nuevos umbrales, se realizó una comparación con umbrales estándar (0.5-1.5mV). Se registraron las características del tejido de las áreas identificadas como zonas de deceleración (DZ) para cada par de umbrales. Además, se analizó la relación de los circuitos de TV con los canales de voltaje para ambos mapas.

Resultados: Se incluyeron 32 pacientes (edad media 66.6±11.2 años; 93.8% hombres; 78.1% miocardiopatía isquémica). Se observaron 52 DZs: el 44.2% se identificaron como tejido *border zone* con los umbrales estándar vs. el 75.0% utilizando umbrales de voltaje personalizados (p=0.003). De los 31 istmos de TV detectados, solo el 35.5% se correlacionó con un canal de voltaje con umbrales estándar frente al 74.2% utilizando umbrales ajustados (p=0.005). Los voltajes bipolares ajustados que coincidían mejor con las imágenes de RMC fueron de 0.51±0.32 y 1.79±0.71mV con una variabilidad interindividual muy alta (desde 0.14-1.68mV hasta 0.7-3.21mV).

Como conclusión, los mapas de voltaje personalizados basados en imágenes de RMC permiten una identificación más clara del sustrato con una mayor correlación tanto con las DZ como con los istmos de TV comparado con los mapas de voltaje convencionales que utilizan umbrales fijos.

HeartRhythm

The Official Journal of the Heart Rhythm Society, The Cardiac Electrophysiology Society, and The Pediatric & Congenital Electrophysiology Society

Heart Rhythm Society SM

Personalized voltage maps guided by cardiac magnetic resonance in the era of high-density mapping

Sara Vázquez-Calvo, MD,[1,2] Paz Garre, BEng,[1,2] Elisenda Ferró, BEng,[1,2] Paula Sánchez-Somonte, MD,[1,2] Jean-Baptiste Guichard, MD, PhD,[1,2] Pasquale Valerio Falzone, MD,[1,2] Eduard Guasch, MD, PhD,[1,2,3] Andreu Porta-Sánchez, MD, PhD,[1,2] José Maria Tolosana, MD, PhD,[1,2,3] Roger Borras, MSc,[2,4] Elena Arbelo, MD, PhD,[1,2,3] José T. Ortiz-Pérez, MD, PhD,[1,2,3] Susana Prats, MD, PhD,[1,2] Rosario J. Perea, MD, PhD,[1,2] Josep Brugada, MD, PhD,[1,2,3] Lluís Mont, MD, PhD,[1,2,3] Ivo Roca-Luque, MD, PhD[1,2,3]

ABSTRACT

BACKGROUND Voltage mapping could identify the conducting channels potentially responsible for ventricular tachycardia (VT). Standard thresholds (0.5–1.5 mV) were established using bipolar catheters. No thresholds have been analyzed with high-density mapping catheters. In addition, channels identified by cardiac magnetic resonance (CMR) has been proven to be related with VT.

OBJECTIVE The purpose of this study was to analyze the diagnostic yield of a personalized voltage map using CMR to guide the adjustment of voltage thresholds.

METHODS All consecutive patients with scar-related VT undergoing ablation after CMR (from October 2018 to December 2020) were included. First, personalized CMR-guided voltage thresholds were defined systematically according to the distribution of the scar and channels. Second, to validate these new thresholds, a comparison with standard thresholds (0.5–1.5 mV) was performed. Tissue characteristics of areas identified as deceleration zones (DZs) were recorded for each pair of thresholds. In addition, the relation of VT circuits with voltage channels was analyzed for both maps.

RESULTS Thirty-two patients were included [mean age 66.6 ± 11.2 years; 25 (78.1%) ischemic cardiomyopathy]. Overall, 52 DZs were observed: 44.2% were identified as border zone tissue with standard cutoffs vs 75.0% using personalized voltage thresholds ($P = .003$). Of the 31 VT isthmuses detected, only 35.5% correlated with a voltage channel with standard thresholds vs 74.2% using adjusted thresholds ($P = .005$). Adjusted cutoff bipolar voltages that better matched CMR images were 0.51 ± 0.32 and 1.79 ± 0.71 mV with high interindividual variability (from 0.14–1.68 to 0.7–3.21 mV).

CONCLUSION Personalized voltage CMR-guided personalized voltage maps enable a better identification of the substrate with a higher correlation with both DZs and VT isthmuses than do conventional voltage maps using fixed thresholds.

KEYWORDS Ventricular tachycardia ablation; Cardiac magnetic resonance; Voltage mapping; Voltage thresholds; High-density mapping

(Heart Rhythm 2024;■:1–9)

Introduction

Substrate-based ventricular tachycardia (VT) methods have been developed to identify ablation target sites during sinus rhythm, especially to guide ablation when VT is noninducible or hemodynamically nontolerated. Initially, voltage mapping was the principal strategy to define the abnormal arrhythmic substrate because of its potential ability to distinguish dense scar, border zone (BZ), and healthy tissue as well as its ability

From the [1]Institut Clinic Cardiovascular, Hospital Clínic, Universitat de Barcelona, Barcelona, Spain, [2]Institut d'Investigacions Biomèdiques August Pi i Sunyer (IDIBAPS), Barcelona, Spain, [3]Centro de Investigación Biomédica en Red de Enfermedades Cardiovasculares (CIBERCV), Madrid, Spain, and [4]Centro de Investigación Biomédica en Red de Salud Mental, CIBERSAM, Instituto de Salud Carlos III, Madrid, Spain.

https://doi.org/10.1016/j.hrthm.2024.04.074

to delimit the conducting channels (CCs) responsible for the clinical/induced VT. However, thresholds are needed to distinguish the different characteristics of the tissue. In the 1980s, important studies tried to define the characteristics of the abnormal electrograms observed in sinus rhythm, concluding that they had similar peak-to-peak voltages, that is, <0.5 mV.[1] In parallel, studies in healthy subjects established a value for healthy tissue above 1.5 mV.[2] Therefore, cutoffs of 0.5–1.5 mV were proposed initially for patients with ischemic cardiomyopathy and later for patients with nonischemic cardiomyopathy.[3] These thresholds were validated in a porcine model with transmural scar.[4]

Over the next few years, a comparison between the characteristics of the electroanatomic maps based on these thresholds and cardiac magnetic resonance (CMR) was performed in both ischemic[5–7] and nonischemic[8] cardiomyopathy and the findings revealed that voltage maps had important limitations. Wijnmaalen et al[6] studied this correlation in a small cohort of 15 patients with ischemic cardiomyopathy and observed the substantial variability of median bipolar voltage for segments with different transmurality, finding that endocardial bipolar electrograms amplitudes for the core infarct and BZ decreased significantly with increasing scar transmurality, thus yielding an acceptable correlation (using the classically defined thresholds) only in regions of transmural scars. Spears et al[8] also evaluated the cutoffs based on CMR analysis and transmurality of the scar in patients with nonischemic cardiomyopathy, and they obtained similar results.

One of the main limitations of the current thresholds is that they have been defined in a small cohort of patients using bipolar catheters without a contact sensor in the tip. Sánchez Muñoz et al[9] compared the scar areas of 11 patients with and without contact force catheters (using a minimum of 5 g) and observed important differences (both underestimation and overestimation) in the extent of the scar. In contrast, high-density (HD) catheters have been developed to increase mapping resolution, thus allowing the creation of a detailed anatomical characterization of the endocardial substrate, which turned out to be especially important in low-voltage areas.[10] In addition, some of the new HD catheter designs, such as the HD Grid (Abbott Medical, Green Oaks, IL), could have the capability to map orthogonal signals for every single point and by software analysis to select the largest of the 2 recorded bipolar signals, creating maps that are inherently less dependent on the wavefront direction.[11] The fact that the VT recurrence outcomes after ablation have improved over time may be partially due to the implementation of HD mapping strategies.[12,13]

Abbreviations

BZ: border zone

CC: conducting channel

CMR: cardiac magnetic resonance

DZ: deceleration zone

HD: high-density

ILAM: isochronal late activation mapping

LAVA: local abnormal ventricular activity

LGE: late gadolinium enhancement

VT: ventricular tachycardia

WT: wall thickness

In parallel, mapping strategies that highlight not only the peak-to-peak voltage but also the propagation patterns of the entire chamber, such as isochronal late activation mapping (ILAM), also performed during sinus rhythm or stable right ventricular apical pacing, have been described in recent years to identify deceleration zones (DZs).[12,13] Despite this strategy based on targeting DZs, whether aided by CMR or not, have demonstrated to be effective in terms of relatively low rates of VT ablation recurrence, the potential additional role of voltage mapping should not be overlooked. Moreover, this technique is still being used by many groups and considered an alternative in VT guidelines.[14] The present study aimed to define the role of CMR in creating new personalized voltage HD maps and to evaluate their usefulness in comparison with traditional voltage maps with fixed thresholds in relation to DZs and the VT isthmuses.

Methods

Study population

This was a prospective observational study of all consecutive patients with structural heart disease and preprocedural CMR who underwent VT ablation in a single center (Hospital Clinic, University of Barcelona) from October 2018 to December 2020. Late gadolinium enhancement (LGE)–CMR was performed within 6–12 months before ablation. The exclusion criteria of the study were the absence of preprocedural CMR. Patients without an LGE-detected scar or with an exclusive epicardial scar were also excluded. All patients provided written informed consent. The study was conducted according to the Declaration of Helsinki guidelines and the deontological code of our institution. The study protocol was approved by the ethics committee of the hospital.

Preprocedural CMR

LGE-CMR was performed if there were no contraindications for a 3 T scan in patients without implantable cardioverter-defibrillator and a 1.5 T scan with a wideband sequence in patients with ICD to abolish artifacts as described.[15] After manual segmentation of the left ventricle, a quantitative analysis of the substrate was executed using ADAS 3D software (ADAS 3D Medical S.L.) following a standardized and widely validated protocol.[16] In brief, ADAS 3D creates a total of 9 3-dimensional layers from the endocardium (layer 10–30) to the epicardium (layer 60–90). The LGE pixel signal intensity maps obtained from CMR are projected onto each layer according to a trilinear interpolation algorithm and were color coded using 40% ± 5% and 60% ± 5% of the maximum intensity as thresholds. Therefore, dense scar areas with high LGE enhancement (≥60%) are colored red, healthy tissue (LGE enhancement ≤40%) is colored blue, and BZs with a percentage of LGE enhancement between 40% ± 5% and 60% ± 5% are colored in an intermediate color range. *Channels*, defined as BZ tissue surrounded by a dense scar and connected to healthy tissue, were detected automatically by the system.[16]

HD mapping: Substrate mapping and ILAM

Procedures were performed under general anesthesia. Access to the left ventricle was achieved with a transseptal and/or retrograde aortic approach.

A substrate voltage map of the left ventricle was obtained during right ventricular pacing for better stability of the cardiac cycle using an HD Grid catheter and EnSite Precision system (Abbott Medical). Points were obtained with the last duplicate algorithm and the HD wave solution with all possible bipoles of the HD Grid catheter. The peak-to-peak bipolar voltage was recorded. Abnormal electrogram features, such as LAVA (local abnormal ventricular activity) and late potentials, were manually tagged. *Local activation time* was defined as the latest deflection of electrograms (last deflection algorithm, Abbott Medical). The whole activation of the chamber was then divided into 8 equally distributed isochrones of activation, with white being the earliest and purple being the latest. *DZs* were defined as regions with isochronal crowding with >3 isochrones within a 1 cm radius, as previously described.[12] LGE-CMR postprocessed images were visualized into the navigation system side by side at the time of mapping.

Localized induction, ablation strategy, and remapping

After delineation of the DZs, the HD Grid catheter was positioned in a potential area for a VT isthmus (slow conduction area and/or middle segment channel according to CMR-detected CC images). VT was induced by programmed electrical stimulation (drive cycles of 600, 500, and 430 ms, up to triple extrastimuli to refractoriness or 200 ms). When VT was hemodynamically tolerated, activation mapping for diastolic and presystolic activities was performed. In cases in which induced VT permitted activation mapping, the initial target for ablation was the central VT isthmus. After the VT isthmuses were targeted, substrate ablation was performed by strictly targeting the DZs. Remapping with an HD Grid catheter was performed to detect DZs, and additional radiofrequency lesions were delivered if DZs were still present. Radiofrequency was delivered using an externally irrigated 3.5-mm-tip ablation catheter (TactiCath SE, Abbott Medical) with a temperature control of 45 °C, a power limit of 40–50 W (60 W in septal areas and/or in cases of a deep substrate according to CMR), and an irrigation rate of 26–30 mL/min. The procedural end point was the abolition of DZs, LAVA, and late potentials as well as the lack of VT inducibility at the end of the procedure.

Threshold personalization and substrate analysis

Step 1

To define the new thresholds in a systematic way, for each patient, the HD bipolar voltage map was compared with CMR segmented endocardial layers (10–30) attending to the distribution of the scar and CMR channels. Alignment of the CMR images and voltage maps was strictly conducted side by side to ensure the same orientation with both techniques. Initially, the lower threshold was set to 0.05 mV and increased in 0.05 mV intervals until the best correlation was achieved. After that, the upper threshold was set to obtain a voltage map that was as close as possible to the CMR endocardial reconstruction. This fine-tuning began with the minimal threshold value previously set and progressed in 0.05 mV intervals. This adjustment was conducted by an expert electrophysiologist blinded to ablation details, and in cases of uncertainty, a second expert operator was available for discussion.

Step 2

Once the new thresholds were defined, the corresponding characteristics of the tissue (dense scar, BZ, or healthy tissue) of those areas identified as DZs in the ILAM were identified. This analysis was repeated for the conventional 0.5–1.5 mV bipolar voltage thresholds. Finally, if VT activation mapping was performed during the case, the concordance between the voltage channels identified by conventional and personalized maps and the VT isthmus was analyzed.

CMR characteristics and correlation with personalized thresholds

Characteristics of the CMR scar, including total mass, scar mass, location of the scar, transmurality of the scar, and wall thickness (WT) of the scar regions, were collected using ADAS 3D. Endocardial scar was considered when more than two-thirds of the scar was observed in the first 3 layers. *Transmural scar* was defined as the presence of the scar from endocardial to epicardial layers. *Epicardial scar* was defined as the presence of scar exclusively in the last outer 3 layers. After the definition of personalized thresholds, the correlation between these thresholds and all the parameters described were determined.

Clinical follow-up

Patients underwent 1-year follow-up. Arrhythmic recurrence was evaluated by analyzing the presence of VT events detected by implantable cardioverter-defibrillator (with or without therapies) or requiring medical attention. Death during follow-up was categorized as either cardiovascular or noncardiovascular.

Statistical analysis

Continuous variables are presented as mean ± SD. To compare the means of 2 variables, we used the Student *t* test and the Mann-Whitney *U* test, as appropriate. Categorical variables are expressed as the total number (percentage) and were compared between groups using the χ^2 test. To assess the correlation between minimum and maximum thresholds and CMR characteristics, Spearman ρ and linear correlation analysis reporting β with standard error were used. A 2-sided type I error of 5% was used for all tests. Statistical analysis was performed using R software for Windows version 4.2.2 (R Project for Statistical Computing, Vienna, Austria).

Results

Baseline and procedural characteristics

During the study period, a total of 40 patients underwent VT ablation. Of those, 7 were excluded because of the clinical impossibility of undergoing CMR (severe renal dysfunction or arrhythmic storm). One patient was excluded because of an exclusive epicardial scar. Therefore, 32 patients were finally analyzed. The most prevalent cardiomyopathy etiology was ischemic heart disease (78.1%). Most patients were male (93.8%), with a mean age of 66.6 ± 11.2 years. The mean ejection fraction was 33.3% ± 6.7%. The main indication for VT ablation was implantable cardioverter-defibrillator therapy in 65.6% of patients, and 21.9% underwent ablation because of an arrhythmic storm. The mean number of shocks 1 year before the ablation procedure was 3.14 ± 6.27 shocks per patient, with a mean of 8 ± 8.99 antitachycardia pacing therapies per patient. The clinical characteristics of the population are summarized in Table 1.

VT ablation was performed with an exclusively endocardial approach in 93.5% of cases. All patients underwent VT ablation procedures using HD mapping catheters. The average mapping points was 2253.9 ± 741.2 in baseline maps. Noninducibility at the end of the procedure was achieved in 76.7% of patients, with a total abolition of DZs in 80.0%. The characteristics of the ablation procedure are summarized in Table 2. One-year VT recurrence was 21.9%.

Correlation between voltage thresholds and electroanatomic maps

The analysis was exclusively performed by 1 operator in 90.6% of cases, with the opinion of a second expert operator being necessary in 9.4% of cases. Overall, 52 DZs were observed. Only 44.2% of these DZs identified as BZs with fixed threshold voltage maps vs 75.0% using CMR-guided personalized voltage maps ($P = .003$). Similarly, of the 31 VT isthmuses mapped, only 35.5% correlated with a voltage channel with the standard cutoffs vs 74.2% using personalized thresholds ($P = .005$). Personalized voltage cutoffs that better matched with CMR images were 0.50 ± 0.32 and 1.79 ± 0.71 mV with high interindividual variability: bottom threshold in all patients, 0.14–1.68 mV; upper threshold in all patients, 0.7–3.21 mV. An illustrative example of the better correlation with the personalized voltage maps is shown in Figure 1. No differences were observed regarding the location of the scar in CMR (Table 3).

Table 1 Clinical characteristics of the patients studied (N = 32)

Characteristic	Value
Age (y)	66.6 ± 11.2
Male sex	30 (93.8)
Hypertension	21 (65.6)
Diabetes	17 (53.1)
Dyslipidemia	22 (71.0)
COPD	5 (16.7)
CKD	10 (35.7)
NYHA class	I: 5 (19.2)
	II: 18 (69.2)
	III–IV: 3 (11.5)
Ischemic cardiomyopathy	25 (78.1)
Permanent AF	5 (16.1)
ACE inhibitors	18 (64.3)
β-Blocker therapy	21 (75.0)
Sotalol therapy	4 (14.3)
Amiodarone therapy	23 (82.1)
VT storm	7 (21.9)
LVEF (%)	33.3 ± 6.7
LVEDD (mm)	60.8 ± 9.6

Values are presented as mean ± SD or n (%).
ACE inhibitors = angiotensin-converting enzyme inhibitors; AF = atrial fibrillation; CKD = chronic kidney disease; COPD = chronic obstructive pulmonary disease; LVEDD = left ventricular end-diastolic diameter; LVEF = left ventricular ejection fraction; NYHA = New York Heart Association; VT = ventricular tachycardia.

Table 2 Procedural characteristics (N = 32)

Characteristic	Value
Endocardial approach	29 (93.5)
Arterial access	17 (58.6)
Transeptal access	30 (96.8)
Agilis	18 (60.0)
Number of mapping points	2253.9 ± 741.2
Number of VT inductions per patient	1.97 ± 1.8
Number of targeted VTs per patient	1.79 ± 1.7
Procedural time (min)	246.3 ± 43.3
X-ray time (min)	37.3 ± 13.2
Number of RF applications	64.8 ± 22.2
RF time (s)	1964.4 ± 772.3
Final noninducibility	23 (76.7) (n = 30)
Abolition of DZs	24 (80.0) (n = 30)

Values are presented as mean ± SD or n (%).
DZ = deceleration zone; VT = ventricular tachycardia.

CMR characteristics and correlation with voltage thresholds

Because of the presence of an implantable cardioverter-defibrillator, 1.5 T CMR was performed in 71.4% of patients, and 28.6% underwent 3 T CMR before implantable cardioverter-defibrillator implantation. The median number of CMR channels per patient was 3.23 ± 2.0. Most patients presented endocardial (46.9%) or transmural (53.1%) scar, with a mean total scar (including BZ and dense scar) of 37.44 ± 16.7 g. The mean WT of scar segments per patient was 7.80 ± 1.85 mm.

Regarding the correlation between the characteristics of the scar measured by CMR and voltage thresholds, an inverse relation between the amount of scar and the value of cutoffs was observed for all the studied parameters: total dense scar, total BZ, and total scar (BZ and dense scar). The total scar mass (BZ + dense core) was the parameter with the best correlation with the individualized voltage threshold (Table 3). WT was not correlated with thresholds in our study. No significant differences were observed between patients with ischemic cardiomyopathy and those with nonischemic cardiomyopathy.

Discussion

The present study compares 2 different voltage maps with HD catheters: the standard voltage map with fixed

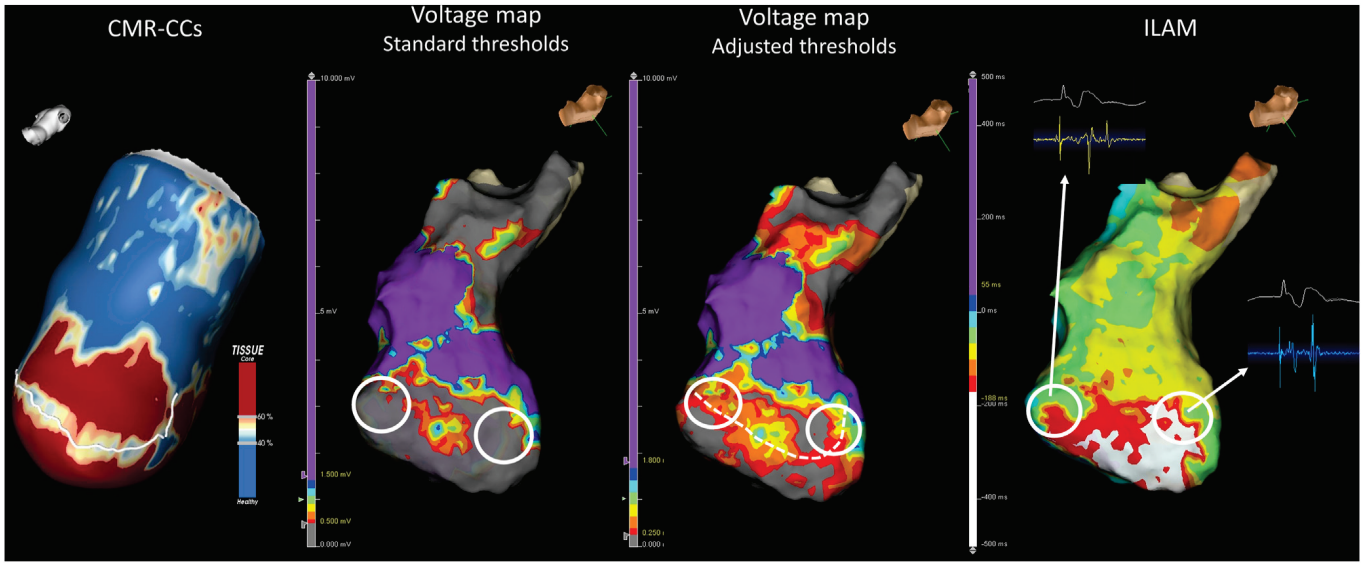

Figure 1
Example of the personalized voltage map guided by CMR. A septal-apical channel is observed in the CMR scan that is not observed in the initial voltage map with standard cutoffs (0.5–1.5 mV), but that clearly corresponds to a voltage channel using personalized thresholds (in this specific case: 0.25–1.80 mV). ILAM shows 2 DZs (*circles*) in the same area. CC = conducting channel; CMR = cardiac magnetic resonance; DZ = deceleration zone; ILAM = isochronal late activation mapping.

thresholds (0.5–1.5 mV) vs a new personalized CMR-guided voltage map. The diagnostic yield of both maps to localize slow conduction areas and VT isthmuses has been analyzed. Two main findings arise from our study. First, personalized voltage maps guided by CMR allow a better characterization of the VT substrate with a greater identification of DZs and channels responsible for VT circuits during ablation. Second, high individual variability regarding minimal and maximal thresholds to depict scar, BZ, and healthy tissue has been identified.

Substrate mapping: A need to improve voltage mapping

Voltage mapping based on bipolar electrogram peak-to-peak analysis has been initially used for patients with nontolerated or noninducible VT in whom ablation based on activation mapping during tachycardia was not feasible. The current cut-off values of 0.5–1.5 mV were established on the basis of studies with a small number of patients using a healthy population,[2,17] analyzing the characteristics of abnormal electrograms in patients with ischemic cardiomyopathy[1] and, more recently, in patients with nonischemic cardiomyopathy.[3]

Table 3 CMR characteristics and correlation with voltage thresholds

Scar location	Minimal threshold	*P*	Maximal threshold	*P*
Anterior	0.48 ± 0.27	.88	1.79 ± 0.67	.90
Inferior	0.49 ± 0.25		1.87 ± 0.68	
Septal	0.48 ± 0.23	.77	1.76 ± 0.72	.78
Lateral	0.51 ± 0.34		1.78 ± 0.62	
Basal-medio	0.62 ± 0.36	.25	1.95 ± 0.81	.18
Medio-apical	0.32 ± 0.11		1.10 ± 0.28	
Basal-medio-apical	0.45 ± 0.25		1.79 ± 0.68	
Endocardial	0.53 ± 0.22	.17	1.67 ± 0.52	.38
Transmural	0.46 ± 0.34		1.90 ± 0.85	

CMR	N = 32	*R*: minimal threshold	*P*	*R*: maximal threshold	*P*
Total tissue (gr)	171.25 ± 48.4	−0.19	.312	−0.11	.555
Dense scar (g)	10.96 ± 6.2	−0.52	.003	−0.22	.238
BZ (g)	26.47 ± 11.87	−0.40	.048	−0.34	.059
Core (BZ + dense scar) (g)	37.44 ± 16.7	−0.47	.008	−0.38	.033
Wall thickness of the scar (mm)	7.80 ± 1.85	0.09	.628	0.05	.788
Location of the scar	15/32 (46.9)	−0.25	.165	0.16	.374
Endocardial	17/32 (53.1)				
Transmural					

Values are presented as mean ± SD or n/N (%) unless stated otherwise.
BZ = border zone.

Several studies since then have confirmed the limitations of voltage channels in identifying the VT isthmus. Mountantonakis et al[18] performed a study comparing voltage channels obtained using standard thresholds with VT channels (confirmed by entrainment) in a population with ischemic cardiomyopathy, observing a low specificity (30%) between them. Glashan et al[19] failed as well in finding a generalized voltage cutoff to identify fibrosis in patients with nonischemic cardiomyopathy using whole heart histological sizes. In this sense, some groups have decided to manually adjust thresholds until a meaningful voltage map is generated,[20,21] thus increasing the number of voltage channels detected. However, this manual adjustment of voltage thresholds has not been validated with electrical end points as DZ or LAVA/LPs. In the same line, the specificity of this manual voltage channels with VT isthmus has not been studied. In contrast, several attempts to better define new thresholds have been executed in the last few years. Roca-Luque et al[22] studied bipolar cutoffs with bipolar catheters with contact sensors that better identified scars and BZs in terms of the detection of abnormal EGMs, observing high individual variability: 0.32 mV (0.02–2 mV) and 1.84 mV (0.3–6 mV). Our study examines the role of CMR in defining more specific voltage thresholds in the era of HD mapping and the potential value of these personalized voltage maps to guide ablation. To our knowledge, this is the first method to personalize voltage values using CMR and with validation with electrical parameters such as DZ and VT isthmus. Therefore, it could be an additional substrate mapping technique alongside ILAM and the rest of the available methods.

HD mapping: Improving the definition of the arrhythmic substrate

In recent years, HD mapping catheters have replaced conventional bipolar mapping catheters after demonstrating a greater capability to define the VT substrate. It is well known that the amplitude of the registered electrogram depends on the electrode size, interelectrode spacing, and especially the angle of the incoming wavefront in relation to the catheter.[23,24] In this sense, HD catheters with a higher density of electrodes in several orientations enable a more accurate identification of the true electrograms, which is especially important in areas of low voltage where the distinction between the dense scar and the BZ can be crucial to identify voltage channels.[10] Because of the better characterization of the substrate, a lower VT recurrence rate has been achieved recently using HD mapping.[25,26] Nevertheless, for the identification of substrates (channels) in voltage maps, there are no defined voltage thresholds. Our study apparently reflects a similar mean threshold compared with the standard thresholds (0.50 ± 0.32 and 1.79 ± 0.71 mV). However, even more importantly, there was high variability between patients: bottom thresholds from 0.14 to 1.68 mV and upper thresholds from 0.7 to 3.21 mV (Figure 2). Therefore, the establishment of a fixed mean threshold for all patients does have a limited value. In this sense, our most important result (with potential clinical implications in substrate mapping) is the personalization of voltage thresholds according to CMR. By using these individualized voltage thresholds guided by CMR, the diagnostic yield of voltage maps to detect slow conduction areas in basal rhythm (75% vs 44,2%; $P < .0001$; Figure 3) and VT isthmuses during activation mapping (74.2% vs 35.5%; $P < .001$; Figure 4) was higher than that obtained with conventional voltage maps with fixed thresholds. Therefore, CMR seems to be an appropriate instrument to guide threshold adjustment.

CMR: An important tool to plan and guide VT ablation

CMR has been widely used to evaluate VT substrate, demonstrating a high accuracy in identifying dense scar, BZ, and

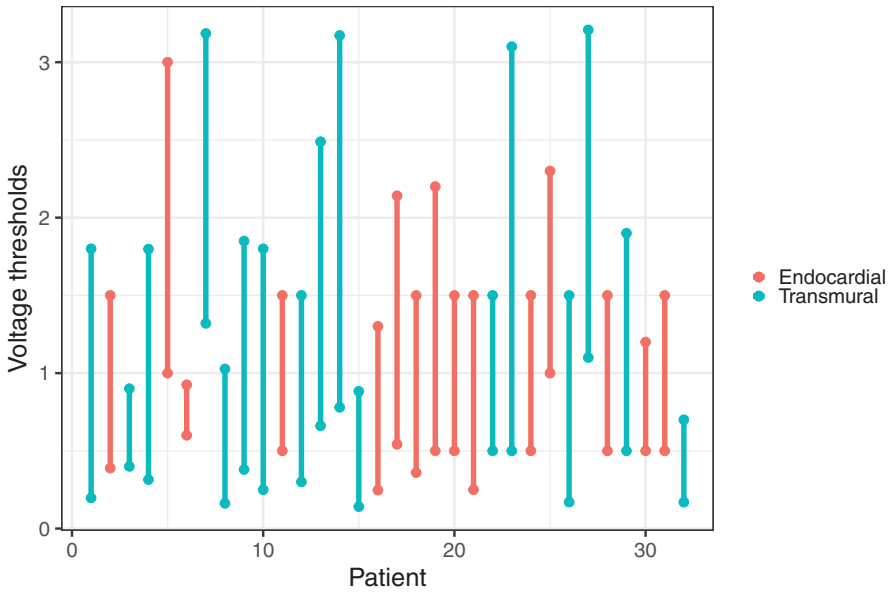

Figure 2
Distribution of bipolar voltage thresholds per individual patient in the cardiac magnetic resonance–detected endocardial (*red*) and transmural (*blue*) scars.

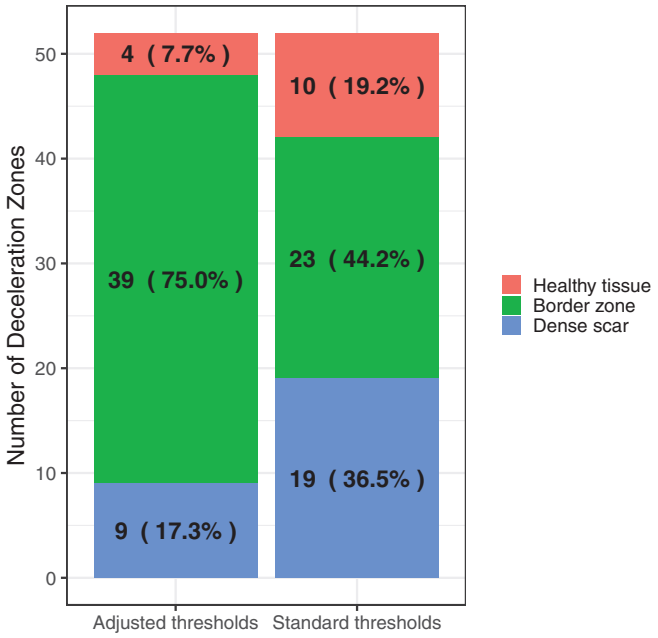

Figure 3
Substrate identification of DZ areas with adjusted and standard thresholds for all patients. DZ = deceleration zone.

healthy tissue (and consequently locate potential CCs) in a 3D model,[27] distinguishing endocardial from epicardial scars. Our group has evaluated its use with a 2D sequence called wideband that allows a decrease in implantable cardioverter-defibrillator-related artifacts, showing a similar concordance between CMR images and voltage maps compared with 3D sequences.[15] In addition to the capability to identify CCs, a recent study has shown not only a strong correlation between CMR-detected CCs and DZs but also a higher capability of CMR to recognize those areas with slow conduction activity compared with baseline electroanatomic maps (EAMs), suggesting an important role of CMR in obtaining a more comprehensive arrhythmic map.[28]

As stated previously, the standard cutoffs of 0.5–1.5 mV have been established in patients with transmural scar and are less accurate for patients with other scar characteristics.[6,8] A recent study has explored how these cutoffs vary in patients with ischemic cardiomyopathy and transmural scar, also considering the WT of the scar by cardiac computerized tomography, observing that 0.5 mV was the best threshold to identify dense scars only for those areas with a WT of 3 mm, changing for those patients with thinner areas (0.2 mV for a WT of 2 mm and 0.1 mV for a WT of 5 mm).[29]

In our study, we separately analyzed the amount of scar, the transmurality of the scar and the WT of the scar regions, observing a tendency for both minimal and maximal thresholds to decrease when the amount of scar increased (Figure 5). Transmurality and WT of the scar segments using CMR seemed not to be related to changes in the thresholds. At first sight, WT should be related with voltage. However, in our study, we focused on personalizing the voltage area according to CMR scar, with most patients presenting with either endocardial or transmural scar. In this sense, voltage could have been highly influenced by the scar on the endocardial surface, masking the potential effect of the deeper healthy tissue.

Limitations

There are some limitations of our study that must be addressed. The main limitation is that the comparison between CMR images and EAMs was performed side by side and not by merging. The merging process, especially with the EnSite Precision system, requires time-consuming postprocessing. Although merging would be essential for a quantitative comparison, in our study, any quantitative parameter of the voltage map, such as low voltage area, was analyzed. In this sense, we believe that a side-by-side comparison between CMR images and voltage maps can be a suitable and reproducible method. In contrast to other studies of our group in

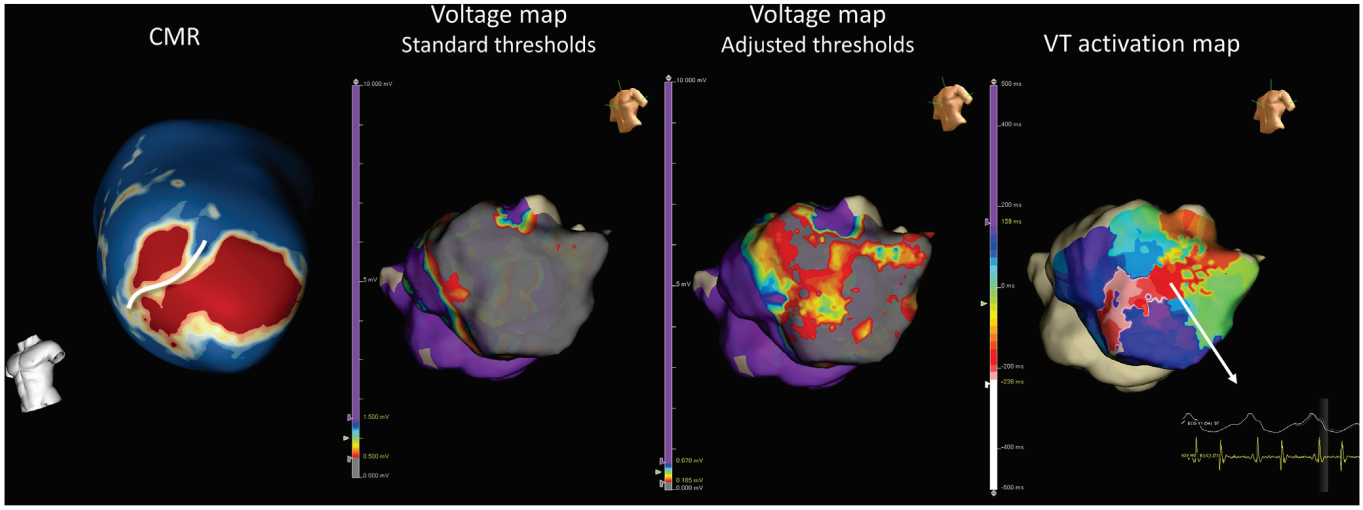

Figure 4
Example of how a voltage map based on personalized thresholds guided by CMR is able to better identify the arrhythmic substrate. In this case, an anterior-apical channel of a patient with ischemic cardiomyopathy is shown in CMR and in the voltage map only after adjusting the thresholds (0.185–0.870 mV). The VT isthmus of the induced VT correlated with the channel. CMR = cardiac magnetic resonance; VT = ventricular tachycardia.

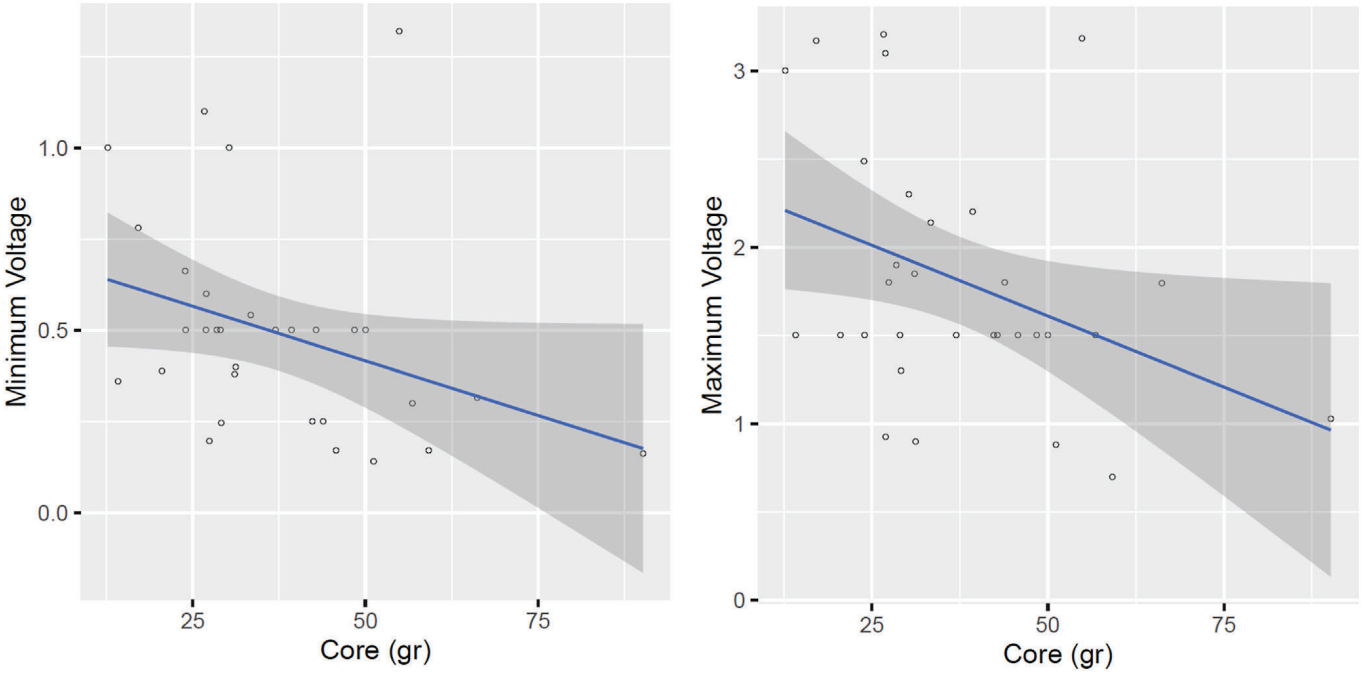

Figure 5
Correlation between the minimum and maximum voltage thresholds (in millivolts) and core (border zone + dense scar).

which American Heart Association segments were used to enable a side-by-side comparison between structures (such as CMR conducing channels and DZs), this study was not designed to assess the special coregistration between EAM and CMR. Indeed, the objective of the comparison was to generate the more resembling voltage map using CMR scar/BZ and CMR channels, so this visual correlation was more important than an accurate localization of the relevant area (which was not a primary concern). Another potential limitation is based on the low number of patients included. This applies especially to the population of patients with nonischemic cardiomyopathy. Many of the CMR parameters studied could have been nonsignificant because of the small size of the population, so these results should be considered cautiously in patients with nonischemic cardiomyopathy. In the same line, no patients with exclusive intramural scar were analyzed in our study, so our results could not be extrapolated to this population. In contrast, the WT of the scar has been validated in computerized tomography and not in CMR, so we believe that the lack of association between WT and thresholds should be analyzed with caution. In addition, as commented in the Discussion section, the high influence of endocardial scar could have masked the potential effect of WT. Finally, some comments must be made about the use of 1.5 T and 3 T CMR. Even though 3 T has higher spatial resolution, which could hypothetically influence the detection of CCs, our group[15] demonstrated that the diagnostic yield of 1.5 T CMR using a wideband sequence was similar to that of 3 T CMR in detecting CCs. In addition, we are aware that not all centers have the capability to perform CMR with a wideband sequence, which adds another limitation to the applicability of our results.

Conclusion

Personalized cutoffs guided by CMR images allow a better characterization of the VT substrate with a greater identification of DZs and VT isthmuses during ablation. Finally, there is high individual variability in both patients with ischemic cardiomyopathy and those with nonischemic cardiomyopathy regarding optimal thresholds with HD mapping catheters, so the use of CMR is extremely helpful in overcoming this problem.

Funding Sources: This study was supported by the Instituto de Salud Carlos III PI20/00693/CB16/11/00354, cofunded by the European Union and grant 2021_SGR_01350, SGR21/GENCAT, Spain.

Disclosures: Drs Mont and Brugada report activities as a consultant, lecturer, and advisory board member for Abbott Medical, Boston Scientific, Biosense Webster, Medtronic, and Biotronik. They are also shareholders of ADAS 3D Medical. Drs Roca-Luque, Tolosana, and Porta-Sánchez report activities as a consultant and lecturer for Biosense Webster, Medtronic, Boston Scientific, and Abbott Medical. All other authors report that they have no relationships relevant to the contents of this paper to disclose.

Address reprint requests and correspondence: Dr Ivo Roca-Luque, Cardiovascular Institute, Arrhythmia Section, Hospital Clinic, Villarroel, 170, 08036 Barcelona, Spain. E-mail address: iroca@clinic.cat

References

1. Cassidy DM, Vassallo JA, Buxton AE, et al. The value of catheter mapping during sinus rhythm to localize site of origin of ventricular tachycardia. Circulation 1984; 69:1103–1110.

2. Cassidy DM, Vassallo JA, Marchlinski FE, et al. Endocardial mapping in humans in sinus rhythm with normal left ventricles: activation patterns and characteristics of electrograms. Circulation 1984;70:37–42.
3. Hsia HH, Callans DJ, Marchlinski FE. Characterization of endocardial electrophysiological substrate in patients with nonischemic cardiomyopathy and monomorphic ventricular tachycardia. Circulation 2003;108:704–710.
4. Reddy VY, Wrobleski D, Houghtaling C, et al. Combined epicardial and endocardial electroanatomic mapping in a porcine model of healed myocardial infarction. Circulation 2003;107:3236–3242.
5. Codreanu A, Odille F, Aliot E, et al. Electroanatomic characterization of post-infarct scars: comparison with 3-dimensional myocardial scar reconstruction based on magnetic resonance imaging. J Am Coll Cardiol 2008;52:839–842.
6. Wijnmaalen AP, van der Geest RJ, van Huls van Taxis CF, et al. Head-to-head comparison of contrast-enhanced magnetic resonance imaging and electroanatomical voltage mapping to assess post-infarct scar characteristics in patients with ventricular tachycardias: real-time image integration and reversed registration. Eur Heart J 2011;32:104–114.
7. Perez-David E, Arenal Á, Rubio-Guivernau JL, et al. Noninvasive identification of ventricular tachycardia-related conducting channels using contrast-enhanced magnetic resonance imaging in patients with chronic myocardial infarction: comparison of signal intensity scar mapping and endocardial voltage mapping. J Am Coll Cardiol 2011;57:184–194.
8. Spears DA, Suszko AM, Dalvi R, et al. Relationship of bipolar and unipolar electrogram voltage to scar transmurality and composition derived by magnetic resonance imaging in patients with nonischemic cardiomyopathy undergoing VT ablation. Heart Rhythm 2012;9:1837–1846.
9. Sánchez Muñoz JJ, Peñafiel Verdú P, Martínez Sánchez J, et al. Usefulness of the contact force sensing catheter to assess the areas of myocardial scar in patients with ventricular tachycardia. Rev Esp Cardio (Engl Ed) 2015;68:159–160.
10. Tschabrunn CM, Roujol S, Dorman NC, et al. High-resolution mapping of ventricular scar: comparison between single and multielectrode catheters. Circ Arrhythm Electrophysiol 2016;9:e003841.
11. Okubo K, Frontera A, Bisceglia C, et al. Grid mapping catheter for ventricular tachycardia ablation. Circ Arrhythm Electrophysiol 2019;12:e007500.
12. Aziz Z, Shatz D, Raiman M, et al. Targeted ablation of ventricular tachycardia guided by wavefront discontinuities during sinus rhythm: a new functional substrate mapping strategy. Circulation 2019;140:1383–1397.
13. Irie T, Yu R, Bradfield JS, et al. Relationship between sinus rhythm late activation zones and critical sites for scar-related ventricular tachycardia. Circ Arrhythm Electrophysiol 2015;8:390–399.
14. Zeppenfeld K, Tfelt-Hansen J, de Riva M, et al. 2022 ESC Guidelines for the management of patients with ventricular arrhythmias and the prevention of sudden cardiac death. Eur Heart J 2022;43:3997–4126.
15. Roca-Luque I, Van Breukelen A, Alarcon F, et al. Ventricular scar channel entrances identified by new wideband cardiac magnetic resonance sequence to guide ventricular tachycardia ablation in patients with cardiac defibrillators. Europace 2020;22:598–606.
16. Andreu D, Penela D, Acosta J, et al. Cardiac magnetic resonance–aided scar dechanneling: influence on acute and long-term outcomes. Heart Rhythm 2017;14:1121–1128.
17. Sramko M, Abdel-Kafi S, van der Geest RJ, et al. New adjusted cutoffs for "normal" endocardial voltages in patients with post-infarct LV remodeling. JACC Clin Electrophysiol 2019;5:1115–1126.
18. Mountantonakis SE, Park RE, Frankel DS, et al. Relationship between voltage map "channels" and the location of critical isthmus sites in patients with post-infarction cardiomyopathy and ventricular tachycardia. J Am Coll Cardiol 2013;61:2088–2095.
19. Glashan CA, Androulakis AFA, Tao Q, et al. Whole human heart histology to validate electroanatomical voltage mapping in patients with non-ischaemic cardiomyopathy and ventricular tachycardia. Eur Heart J 2018;39:2867–2875.
20. Arenal A, del Castillo S, Gonzalez-Torrecilla E, et al. Tachycardia-related channel in the scar tissue in patients with sustained monomorphic ventricular tachycardias. Circulation 2004;110:2568–2574.
21. Hsia HH, Lin D, Sauer WH, et al. Anatomic characterization of endocardial substrate for hemodynamically stable reentrant ventricular tachycardia: identification of endocardial conducting channels. Heart Rhythm 2006;3:503–512.
22. Roca-Luque I, Zaraket F, Garre P, et al. Accuracy of standard bipolar amplitude voltage thresholds to identify late potential channels in ventricular tachycardia ablation. J Interv Card Electrophysiol 2023;66:15–25.
23. Takigawa M, Relan J, Martin R, et al. Effect of bipolar electrode orientation on local electrogram properties. Heart Rhythm 2018;15:1853–1861.
24. Anter E, Josephson ME. Bipolar voltage amplitude: what does it really mean? Heart Rhythm 2016;13:326–327.
25. Proietti R, Dowd R, Gee LV, et al. Impact of a high-density grid catheter on long-term outcomes for structural heart disease ventricular tachycardia ablation. J Interv Card Electrophysiol 2021;62:519–529.
26. Vázquez-Calvo S, Garre P, Sánchez-Somonte P, et al. Orthogonal high density mapping with VT isthmus analysis vs. pure substrate VT ablation: a case-control study. Front Cardiovasc Med 2022;9:912335.
27. Andreu D, Ortiz-Pérez JT, Fernández-Armenta J, et al. 3D delayed-enhanced magnetic resonance sequences improve conducting channel delineation prior to ventricular tachycardia ablation. Europace 2015;17:938–945.
28. Vázquez-Calvo S, Casanovas JM, Garre P, et al. Evolution of deceleration zones during ventricular tachycardia ablation and relation with cardiac magnetic resonance. JACC Clin Electrophysiol 2023;9:779–789.
29. Ene E, Halbfaß P, Nentwich K, et al. Optimal cut-off value for endocardial bipolar voltage mapping using a multipoint mapping catheter to characterize the scar regions described in cardio—CT with myocardial thinning. J Cardiovasc Electrophysiol 2022;33:2174–2180.

Artículo 3: Evolución de las Zonas de Desaceleración Durante la Ablación de Taquicardia Ventricular y su Relación con la Resonancia Magnética Cardíaca

El propósito de este estudio fue analizar la evolución de las zonas de deceleración (DZs) durante la ablación y su correlación con la RMC.

Para ello, se incluyeron 42 pacientes consecutivos con TV relacionada con cicatriz sometidos a ablación después de la RMC en el Hospital Clínic (octubre de 2018-diciembre de 2020) (edad mediana 65.3 ± 11.8 años; 94.7% hombres; 73.7% enfermedad cardíaca isquémica). Se analizaron las DZs basales y su evolución en *remaps* en mapas de isocronas de activación tardía. Se realizó una comparación entre las DZs y los canales de conducción de la RMC.

En total, se analizaron 95 DZs, el 93.68% de las cuales se correlacionaron con los canales de RMC: el 44.8% ubicado en el segmento medio y el 55.2% ubicado en la entrada/salida del canal. Se realizó *remap* en el 91.7% de los pacientes (1 *remap*: 33.3%, 2 *remaps*: 55.6%, y 3 *remaps:* 2.8%). Con respecto a la evolución de las DZs, el 72.2% desapareció después del primer bloque de ablación, con un 14.13% de DZs no siendo eliminadas al final del procedimiento. Un total del 32.5% de las DZs en los *remaps* se correlacionaron con un canal de RMC ya asociado a DZ en el primer mapa, pero un 17.5% se correspondían a nuevas zonas de DZ no visualizadas en el mapa basal pero sí relacionadas con un canal de RMC. La recurrencia de TV a un año fue del 22.9%.

Como conclusión, las DZs son dinámicas y están altamente correlacionadas con los canales de RMC. Además, el *remap* puede conducir a la identificación de sustrato oculto inicialmente no identificado por el mapeo electroanatómico, pero sí detectado por RMC.

JACC: CLINICAL ELECTROPHYSIOLOGY VOL. 9, NO. 6, 2023

ORIGINAL RESEARCH

Evolution of Deceleration Zones During Ventricular Tachycardia Ablation and Relation With Cardiac Magnetic Resonance

Sara Vázquez-Calvo, MD,[a,b] Judit Mas Casanovas, BEng,[a] Paz Garre, BEng,[a,b] Elisenda Ferró, BEng,[a,b] Paula Sánchez-Somonte, MD,[a,b] Levio Quinto, MD,[a,b] Eduard Guasch, MD, PhD,[a,b,c] Andreu Porta-Sanchez, MD, PhD,[a,b] José Maria Tolosana, MD, PhD,[a,b,c] Roger Borras, MSc,[a,b] Elena Arbelo, MD, PhD,[a,b,c] José T. Ortiz-Pérez, MD, PhD,[a,b,c] Josep Brugada, MD, PhD,[a,b,c] Lluís Mont, MD, PhD,[a,b,c] Ivo Roca-Luque, MD, PhD[a,b,c]

ABSTRACT

BACKGROUND A new functional mapping strategy based on targeting deceleration zones (DZs) has become one of the most commonly used strategies within the armamentarium of substrate-based ablation methods for ventricular tachycardia (VT) in patients with structural heart disease. The classic conduction channels detected by voltage mapping can be accurately determined by cardiac magnetic resonance (CMR).

OBJECTIVES The purpose of this study was to analyze the evolution of DZs during ablation and their correlation with CMR.

METHODS Forty-two consecutive patients with scar-related VT undergoing ablation after CMR in Hospital Clinic (October 2018-December 2020) were included (median age 65.3 ± 11.8 years; 94.7% male; 73.7% ischemic heart disease). Baseline DZs and their evolution in isochronal late activation remaps were analyzed. A comparison between DZs and CMR conducting channels (CMR-CCs) was realized. Patients were prospectively followed for VT recurrence for 1 year.

RESULTS Overall, 95 DZs were analyzed, 93.68% of which were correlated with CMR-CCs: 44.8% located in the middle segment and 55.2% located in the entrance/exit of the channel. Remapping was performed in 91.7% of patients (1 remap: 33.3%, 2 remaps: 55.6%, and 3 remaps: 2.8%). Regarding the evolution of DZs, 72.2% disappeared after the first ablation set, with 14.13% not ablated at the end of the procedure. A total of 32.5% of DZs in remaps correlated with a CMR-CCs already detected, and 17.5% were associated with an unmasked CMR-CCs. One-year VT recurrence was 22.9%.

CONCLUSIONS DZs are highly correlated with CMR-CCs. In addition, remapping can lead to the identification of hidden substrate initially not identified by electroanatomic mapping but detected by CMR. (J Am Coll Cardiol EP 2023;9:779–789)

From the [a]Institut Clinic Cardiovascular, Hospital Clínic, Universitat de Barcelona, Spain; [b]Institut d'Investigacions Biomèdiques August Pi i Sunyer (IDIBAPS), Barcelona, Spain; and the [c]Centro de Investigación Biomédica en Red de Enfermedades Cardiovasculares (CIBERCV), Madrid, Spain.
The authors attest they are in compliance with human studies committees and animal welfare regulations of the authors' institutions and Food and Drug Administration guidelines, including patient consent where appropriate. For more information, visit the Author Center.

Manuscript received August 3, 2022; revised manuscript received December 2, 2022, accepted December 14, 2022.

ISSN 2405-500X https://doi.org/10.1016/j.jacep.2022.12.015

JACC: CLINICAL ELECTROPHYSIOLOGY VOL. 9, NO. 6, 2023
JUNE 2023:779–789

ABBREVIATIONS AND ACRONYMS

3D = 3 dimensional

BZ = border zone

CCs = conducting channels

DZ = deceleration zone

EGM = electrograms

ICD = implantable cardioverter-defibrillator

ILAM = isochronal late activation mapping

LAVA = local abnormal ventricular activity

LGE-CMR = late gadolinium-enhanced cardiac magnetic resonance

LP = late potentials

VT = ventricular tachycardia

Classic ventricular tachycardia (VT) ablation techniques, such as VT activation mapping or entrainment, are established methods of isthmus identification but are limited by hemodynamic instability during VT.[1] Substrate mapping during sinus or paced rhythm was initially developed as an alternative method and is currently a cornerstone of ablation in scar-related VT.[2] This method is based on the concept of conducting channels (CCs), which are areas of border zone (BZ) surrounded by dense scars and connected to healthy tissue with slow conduction properties. The BZ area is classically defined as those regions with voltages between 0.5 and 1.5 mV in voltage maps. However, these voltage cutoff values have moderate sensitivity and specificity that enable the identification of areas with slow conduction properties,[3] so ablation targets are currently identified mainly by electrogram (EGM) characteristics on top of voltage. In addition, not all BZ tissue has slow conduction properties, and consequently, not all BZs are associated with reentry. Areas of slow conduction can be identified in sinus or paced rhythm with different types of abnormal electrical activity. These EGMs are characteristically with voltage <1.5 mV and have delayed activation with components after the end of QRS (so-called late potentials [LPs]) and/or have abnormal fragmentation despite not being so delayed (so-called LAVAs [local abnormal ventricular activity]: defined as local EGMs with split, fractionated, or high-frequency components). These types of abnormal EGMs have been related to VT circuits, although with variable sensitivity and specificity for the detection of the VT isthmus.[4] Therefore, most substrate ablation strategies use activation maps in sinus or paced rhythm to automatically identify areas with LPs, identifying LAVAs manually in these maps with no such late activation. The complete elimination of these abnormal EGMs is one of the most accepted ablation endpoints and has been associated with better outcomes regarding less appropriate implantable cardioverter-defibrillator (ICD) therapies and a decrease in VT burden.[5-7] Finally, in 2015, a new substrate-based ablation strategy based on slow conduction was developed[8]: isochronal late activation mapping (ILAM). These maps are conventional activation maps with annotation at the latest part of the EGM, creating a map with a window starting at the earliest region of activation and ending at the latest site of activation. The overall activation time is divided into 8 isochrones, so the thickness of an isochrone is a graphical simplified representation of the conduction velocity (distance/time). A deceleration zone (DZ) was defined as the region with 3 different colors in <1 cm. Since this advance, many studies have shown a high correlation between DZs and VT circuits, with higher specificity than conventional LP maps.[4,8-10]

In parallel, late gadolinium-enhanced cardiac magnetic resonance (LGE-CMR) can accurately define healthy tissue, dense scars, and BZs. The identification of these CCs by CMR allows not only planning the procedure but also generating a noninvasive map of the arrhythmogenic substrate, with important clinical implications.[11] A great correlation between CCs defined by CMR and voltage maps has been demonstrated,[12,13] but no study, to our knowledge, has analyzed the relation of CMR channels and DZs.

The main objective of this study was to analyze the correlation between CMR-detected CCs and DZs identified with the ILAM approach and their evolution during ablation and remapping.

METHODS

STUDY POPULATION. This was a prospective observational study of all consecutive patients with structural heart disease who underwent VT ablation in a single center (Hospital Clinic, University of Barcelona) from October 2018 to December 2020. LGE-CMR was performed within 6 to 12 months before ablation. The exclusion criteria of the study were the absence of a preprocedure CMR. All patients provided written informed consent. The study was carried out according to the Declaration of Helsinki guidelines and the deontological code of our institution. The study protocol was approved by the ethics committee of the hospital.

PREPROCEDURAL CMR. LGE-CMR was performed if there were no contraindications at 3.0-T scan in patients without an ICD, 1.5-T with a wideband sequence in patients with an ICD to abolish artifacts as described.[14] After manual segmentation of the left ventricle, a quantitative analysis of the substrate was executed using ADAS 3-dimensional (3D) software (ADAS 3D, Galgo Medical S.L.) following a standardized and widely validated protocol.[13] In brief, ADAS 3D creates a total of 9 3D maps from the endocardium to the epicardium. The LGE pixel signal intensity maps obtained from the CMR were projected onto each layer according to a trilinear interpolation algorithm and were color coded using 40% ± 5% and 60% ± 5% of the maximum intensity as thresholds. Therefore, dense scar areas with high LGE (≥60%) are colored red, healthy tissue (LGE ≤40%) is colored

blue, and BZs with a percentage of LGE between 40% ± 5% and 60% ± 5% are colored in an intermediate color range. Channels were detected automatically by the system.[13]

HIGH-DENSITY MAPPING: SUBSTRATE AND ILAM. Procedures were performed under general anesthesia. Access to the left ventricle was achieved with a transseptal and/or retrograde aortic approach. Epicardial mapping was performed in cases when an epicardial origin of VT was suspected and in cases of failed endocardial ablation.

A substrate voltage map of the left ventricle was obtained during right ventricular pacing for better stability of the cardiac cycle using an HDGrid catheter and EnSite Precision system (Abbott Medical, USA). Abnormal EGM features, such as LAVA and LPs, were manually tagged. Local activation time was defined as the latest deflection of EGM (Last Deflection algorithm, Abbott Medical, USA). The whole activation of the chamber was then divided in 8 equally distributed isochrones of activation, with white being the earliest and purple being the latest. DZs were defined as regions with isochronal crowding with >3 isochrones within a 1-cm radius, as previously described.[8] LGE-CMR postprocessed images were visualized into the navigation system side by side.

ABLATION STRATEGY AND REMAPPING. After delineation of the DZs, the HDGrid catheter was positioned in a potential area for a VT isthmus (slow conduction area and/or middle segment channel according to CMR-detected CC images). VT was induced by programmed electrical stimulation (drive cycles of 600, 500, and 430 ms, up to triple extrastimuli to refractoriness or 200 ms). When VT was hemodynamically tolerated, activation mapping for diastolic and presystolic activity was performed. In cases in which VT was not hemodynamically tolerated, the VT isthmus was defined as the area with a fast transition from good pace mapping (suggesting VT exit site) to poor pace mapping (suggesting VT entrance site).[15] In cases in which induced VT permitted activation mapping, the initial target for ablation was the central VT isthmus. After the VT isthmuses were targeted, substrate ablation was performed by strictly targeting the DZs. Remapping with an HDGrid catheter was performed to detect DZs, and additional radiofrequency lesions were delivered if DZs were still present. Radiofrequency was delivered using an externally irrigated 3.5-mm-tip ablation catheter (Tacticath SE, Abbott Medical) with 45°C temperature control, a power limit of 40 to 50 W (60 W in septal areas and/or in cases of a deep substrate according CMR), and an irrigation rate of 26 to 30 mL/min. The procedural endpoint was the abolition of DZs, LAVA, and LPs as well as the lack of VT inducibility at the end of the procedure.

POST HOC OFFLINE ANALYSIS. CMR-defined CCs were automatically annotated in CMR as described in the Methods section by ADAs 3D software. The entrance/exit or middle segment of the CMR channel was defined anatomically (**Figure 1**).

During the procedure, DZs were identified on the electroanatomic mapping (EAM) as described (3 isochrones in <1-cm radius). The characteristics of the DZs, including the number of basal DZs, correlation with CMR channels, position inside the channels, location according to 17 American Heart Association (AHA) segment classifications, and so forth, were annotated post hoc. This systematic analysis performed in every remap, attending specifically to the relative position change inside the CMR channel. The evolution of DZ after the first ablation set was analyzed (**Figure 2**). The difficulty of ablating a DZ was defined as the persistence of a DZ after the first ablation set.

CLINICAL FOLLOW-UP. Patients underwent 1-year follow-up. Arrhythmic recurrence was evaluated by analyzing the presence of VT events detected by ICD (with or without therapies) or requiring medical attention. Death during follow-up was categorized as either cardiovascular or noncardiovascular.

STATISTICAL ANALYSIS. Continuous variables are presented as the mean ± SD and minimum and maximum values. Categorical variables are expressed as the total number or percentage and compared with chi-squared test. Predictors of DZ elimination were assessed using generalized linear mixed-effects models for binary response. To predict VT recurrence at 1-year follow-up, logistic regression analysis was used. Odds ratios were computed for both models. All analyses were performed with SPSS version 18.0 and R software version 3.6.1 (R project for Statistical Computing). All statistical tests were 2-sided, and a P value <0.05 was considered statistically significant.

RESULTS

BASELINE CHARACTERISTICS. A total of 42 patients with structural heart disease underwent VT ablation during the study period. Four patients were excluded due to poor-quality preprocedural CMR. Therefore, 38 patients (94.7% male, median age 65.3 ± 11.8 years) were finally included in the analysis. The most frequent substrate was ischemic heart disease (73.7%). The mean left ventricular ejection fraction

FIGURE 1 Example of Evolution of DZ Within the Same CMR Channel

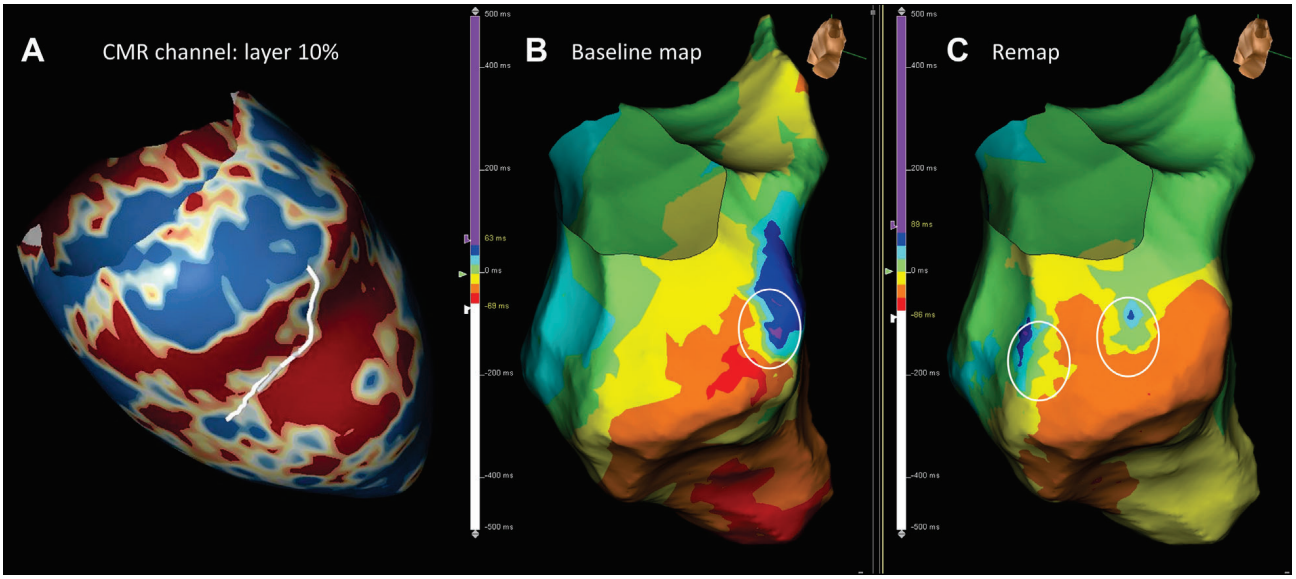

A posteroseptal cardiac magnetic resonance (CMR) channel **(in white)** is observed (**blue**, healthy tissue; **red**, dense scar; **yellow**, border zone [BZ]) in **A**. In **B**, the baseline isochronal late activation mapping (ILAM) shows a deceleration zone (DZ) that correlates with the entrance of the CMR channel. In **C**, the first remap is shown with a change in the position of the DZ from the entrance to the isthmus and exit within the same CMR channel.

FIGURE 2 Methods

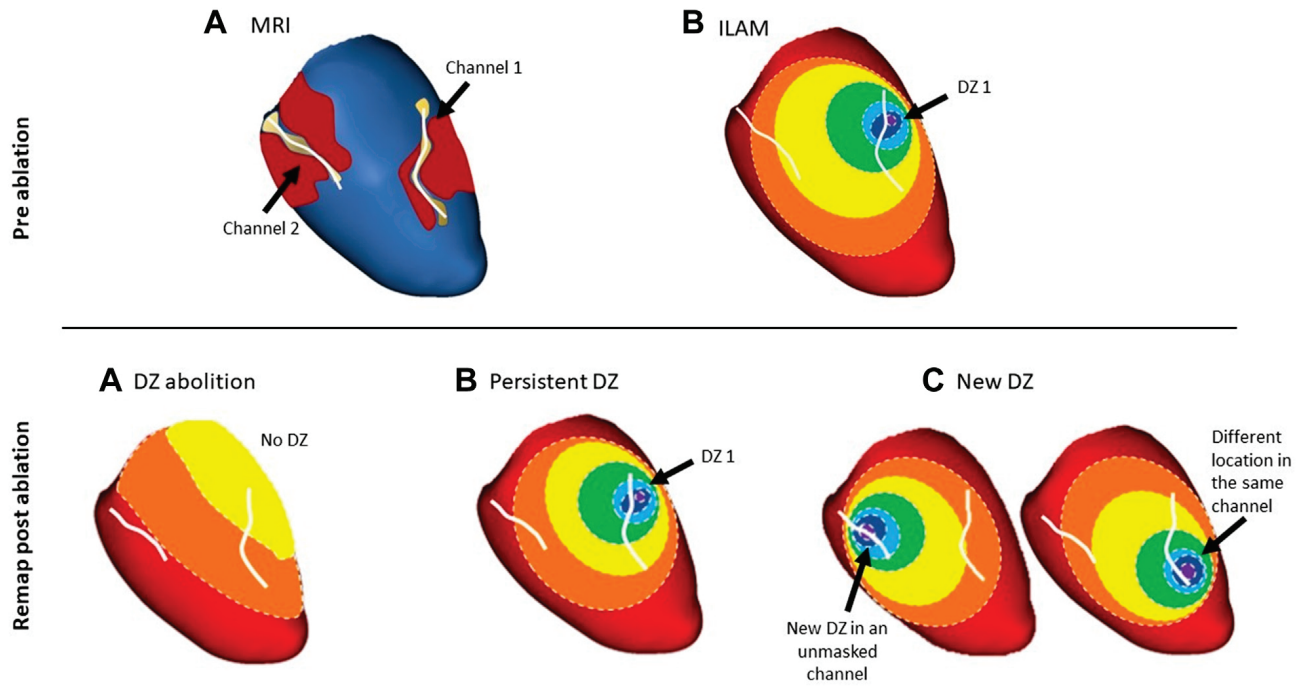

The analysis of the CCs is performed in CMR. DZs are drawn in the EAM, and the correlation with channels is annotated. The location inside the channel (entrance/exit vs middle segment) is also registered. After the first remap, DZs were reevaluated. As the figure shows, DZs can disappear **(A)**, can persist in the same position **(B)**, or can move to another position in the same channel or unmask a new channel **(C)**. CCs = conducting channels; other abbreviations as in Figure 1.

TABLE 1 Clinical Characteristics (N = 38)

Age (y)	65.3 ± 11.8 (26-82)
Male	36 (94.7)
Hypertension	26 (68.4)
Diabetes	20 (52.6)
Dyslipidemia	25 (67.6)
COPD	6 (17.1)
CKD	11 (33.3)
NYHA functional class	
I	7 (21.9)
II	21 (65.6)
III-IV	4 (12.5)
Ischemic cardiomyopathy	28 (73.7)
Permanent AF	7 (18.9)
ACE inhibitors	21 (63.6)
Beta-blocker therapy	25 (75.8)
Sotalol therapy	4 (12.1)
Amiodarone therapy	26 (78.8)
VT storm	7 (18.4)
LVEF (%)	33.3 ± 7.7 (20-48)
LVEDD (mm)	61.5 ± 9.8 (40-77)

Values are mean ± SD (range) or n (%).

ACE inhibitors = angiotensin-converting enzyme inhibitors; AF = atrial fibrillation; CKD = chronic kidney disease; COPD = chronic obstructive pulmonary disease; LVEDD = left ventricular end-diastolic diameter; LVEF = left ventricular ejection fraction; NYHA = New York Heart Association; VT = ventricular tachycardia.

TABLE 2 Procedural Characteristics (N = 38)

Endocardial approach	35 (88.0)
Endoepicardial approach	3 (12.0)
Arterial access	23 (65.7)
Transeptal access	35 (97.2)
Agilis	20 (55.6)
Number of mapping points	2,036.14.8 ± 888.70 (718-5,725)
Number of mapping points (remap)	937.84 ± 391.70 (185-1828)
Number of VT inductions	1.81 ± 1.7 (0-9)
Number of targeted VTs	1.7 ± 1.6 (0-9)
Procedural time (minutes)	238.5 ± 50.3 (90-360)
X-ray time (minutes)	38.5 ± 12.9 (9-75)
Number of RF applications	59.2 ± 25.2 (0-105)
RF time (seconds)	1,830.2 ± 827.2 (0-3,060)
Number of remaps	
0	3 (8.3)
1	12 (33.3)
2	20 (55.6)
3	1 (2.8)
Final noninducibility	28/35 (80.0)
Abolition of DZs	29/35 (82.9)

Values are n (%) or mean ± SD (range).

DZ = deceleration zone; RF = radiofrequency; VT = ventricular tachycardia.

was 33.3 ± 7.7 assessed by echocardiogram. The baseline characteristics of the patients are shown in Table 1.

PROCEDURAL CHARACTERISTICS AND FOLLOW-UP. VT ablation was performed with an exclusively endocardial approach in 35 of 38 patients (88.0%). The average mapping points were 2,036 ± 888.70 and 937.84 ± 191.70 in remaps. Major complications occurred in 2 patients (both had cardiac tamponade after epicardial puncture, requiring pericardiocentesis). One-year VT recurrence (1 patient was excluded because he died after 3 months of ablation) was 22.9% (21.43% in ischemic patients and 28.57% in non-ischemic cardiomyopathy). One patient died due to advanced heart failure 3 months after ablation. The number of remaps during the ablation procedure was significantly associated with less VT recurrence (odds ratio [OR]: 0.35; $P = 0.043$). Other parameters, such as LAVA or LP abolition at the end of the procedure, complete DZ abolition or noninducibility, were not significantly associated with better clinical outcomes in our study. The ablation procedure parameters are detailed in Table 2.

ILAM ANALYSIS AND EVOLUTION OF DZ DURING ABLATION. Overall (including remaps), 95 DZs were found: 2.5 ± 1.11 DZs per patient. The DZs were commonly located in mid (55.8%) and basal (25.3%) AHA segments. Those located in septal segments showed a tendency to be more difficult to eliminate (OR 1.91; $P = 0.429$). The exact locations of the baseline and remap DZs are represented in Figure 3.

In the first ILAM, 75 DZs were detected. Remap was not achievable in 2 patients (3 DZs) because of complications during the procedure. After the first ablation set, 52 of 72 DZs (72.2%) disappeared. In the remap, 20 of the original DZs (27.8%) were still present in the same CMR channel, and 20 new DZs (not present in the first ILAM) were observed: Of those new DZs, 13 were DZs that changed position within the same channel as in the first map (ie, from the entrance to the middle segment), and 7 were DZs located in a new channel not visible in the first map. Of these 20 DZs (not present in the baseline map), 8 persisted after a second ablation set. Finally, 14.13% (13 of 92) of all DZs were not eliminated at the end of the procedure. In the Central Illustration, the details about the evolution of DZ are shown.

Regarding the relation of DZs and the VT isthmus (in case of VT was inducible), 67.9% (57 of 84) of DZs were associated with the VT critical site.

CORRELATION OF DZs AND CMR CHANNELS. Overall, 89 of 95 (93.68%) DZs were correlated with CMR channels: 92% (69 of 75) from the baseline map and 100% (20 of 20) from remaps. No difference was

JACC: CLINICAL ELECTROPHYSIOLOGY VOL. 9, NO. 6, 2023
JUNE 2023:779–789

FIGURE 3 Location of DZs During Ablation

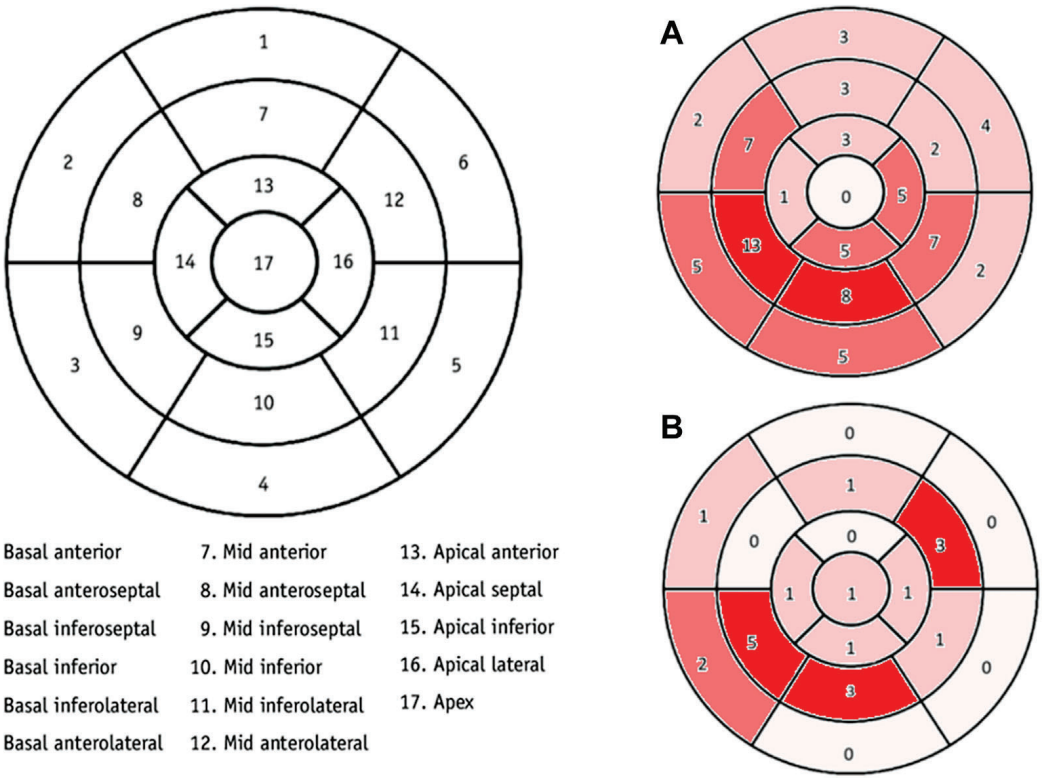

On the **left side**, a representation of the heart following the 17 American Heart Association (AHA) segments. On the **right side**, the number of DZs per segment in the first map **(A)** and in remaps **(B)**. Abbreviations as in Figure 1.

found between 3T and 1.5T CMR (92.31% vs 94.12%, $P = 0.552$) in terms of correlations with DZ areas.

Of 87 DZs correlated with the CMR channel, 39 (44.8%) were located in the middle segment and 48 (55.2%) in the entrance/exit of the channel. The location of the DZ in the entrance/exit of the CMR channel showed a trend toward greater difficulty in its elimination (OR: 3.35; $P = 0.185$).

DISCUSSION

The major findings from this study are as follows:

1. There is a high correlation between DZs detected by ILAM maps and channels detected by CMR both in the baseline map and remaps. This is the first study that correlated DZs with CCs in CMR.
2. During ablation, most DZs will disappear after the first radiofrequency lesion set, but a significant proportion of DZs can move within the same channel, or a new DZ can be detected in areas where CMR channels are present without a DZ in the first map.

ROLE OF CMR IN SUBSTRATE-BASED VT ABLATION AND RELATION WITH DZ. As stated previously, substrate-based ablation has emerged as the first-line treatment for scar-related VT. Several strategies have been used to minimize the need for extensive VT activation mapping,[1,2] such as scar homogenization, LP abolition, scar dechanneling, and LAVA ablation. The appearance of high-density mapping catheters has increased the knowledge of the VT substrate and the ability to identify the critical sites for reentry, improving the results of substrate-based approaches.[16] The most recent method has been the ablation of DZs, as they have a higher specificity for the VT isthmus than other strategies.

In parallel, imaging has been widely used to evaluate VT substrates. Our group has extensive experience in the use of CMR to identify arrhythmogenic substrates and to aid in VT ablation.[17-19] In this sense, CMR has a very high accuracy in identifying not only dense scars and BZs but also CCs.[12,20] These CMR-detected CCs have a strong correlation with EAMs in terms of detecting scars and BZs, and it has been

CENTRAL ILLUSTRATION **Evolution of Deceleration Zones During Ablation**

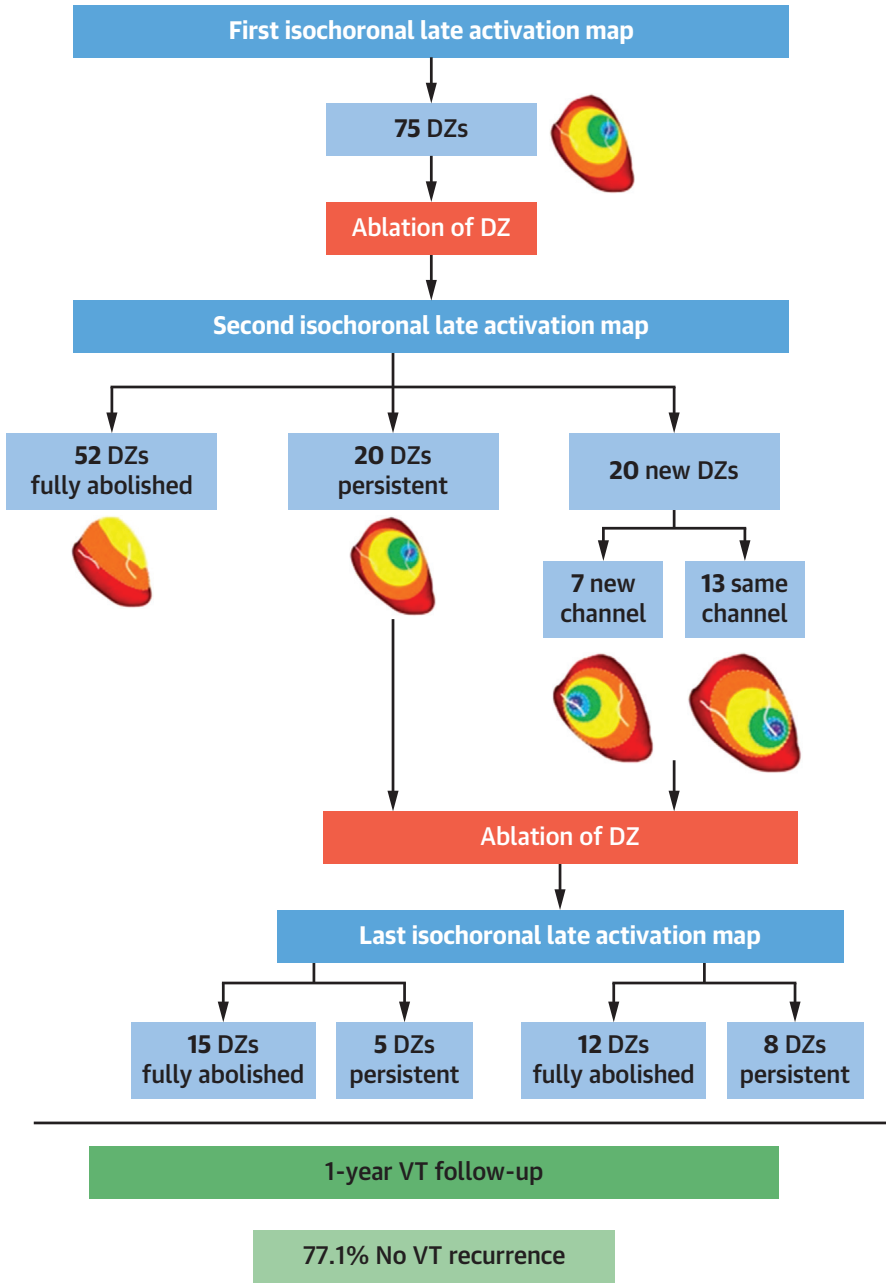

Vázquez-Calvo S, et al. J Am Coll Cardiol EP. 2023;9(6):779–789.

recently demonstrated that CCs are clearly related to scar arrhythmogenicity.[11] Some studies in this field have also shown that despite the good correlation between CMR and voltage EAMs, scars in CMR were larger than those in EAMs.[21] More importantly, some of the VT isthmuses were located in these areas of scar or BZ in CMR but with normal voltage in EAM.[22] These areas of CMR scarring not detected in EAM were also frequent areas with hidden slow conduction identified with the multiple extrastimuli technique,[21] suggesting added value of CMR for arrhythmogenic substrate characterization. The accuracy of substrate definition is similar in patients with an ICD (1.5-T scan with wideband sequence that allows enough artifact ICD-related free imaging) than in patients without ICD (3.0-T scan).[14] Indeed, in

nonrandomized trials, better outcomes have been associated with guided-CMR ablation regarding less radiofrequency delivery, lower inducibility rate at the end of the procedure and, most importantly, lower recurrence rate in the follow-up.[13] However, to our knowledge, no study has analyzed the relation of DZs and CMR-CCs.

The present study demonstrates a high correlation (93.68%) between functional DZs and CMR channels. This finding confirms, after the correlation of CMR and voltage maps,[12,14,20,23] the usefulness of CMR to noninvasively detect areas of slow conduction. Some studies have analyzed the relation of late potentials with CMR,[14,20] but as DZs have been shown to have higher specificity to detect VT isthmuses than LP areas, it seems reasonable to analyze the relation of DZs and CMR channels.

The position of the DZs related to the CMR channels was similar in terms of middle segment and entrance/exit of the channel (44.8% vs 55.2%), finding a nonsignificant higher difficulty in ablating those located in the entrance/exit of the channel (OR: 3.35; $P = 0.185$). As the entrance/exit of the CCs are closer to healthy tissue and therefore less protected by the core scar (and usually has a larger dimension), blocking conduction in those parts of the channel could be more difficult than in a protected isthmus. Regarding the location of DZs, those in septum areas also showed a nonsignificant association with difficulty of ablation (OR: 1.91; $P = 0.429$). Septal involvement has been highly associated with intramural substrate in other studies that, in addition to proximity to the conduction system, increases the difficulty of abolishing this substrate and therefore the recurrence rate after VT ablation.[24-26]

EVOLUTION OF DZs DURING ABLATION. No data are available about the evolution of DZs during ablation.[10] In our study, we systematically analyzed the evolution of DZs after every ablation set. Most of the DZs detected in the beginning disappeared after the first lesion set (70%). However, in the first remap, it is possible to continue detecting DZs in the same position (50% of total DZs in remaps), whereas some DZs (32.5% of total DZs in remaps) change their position within the same channel. This finding could argue in favor of ablation not only of DZs but also both entrance and exit of the CCs to avoid this migration after the first ablation set. On the other hand, as most of the DZs disappear after the first ablation set, one could argue that it is more efficient to address only DZs to avoid extensive ablation of the full channel. The more interesting finding, from our point of view, is the fact that 17.5% of the DZs in the remap appeared in a different region not detected in the initial ILAM, and all of them are within a channel already present in CMR since the beginning (**Figure 4**). This phenomenon confirms the added value of CMR to identify ablation targets. DZs, as mentioned previously, are based on 8 equally time distributed isochrones. With this method, the areas with the slowest conduction are detected. Hypothetically, some CMR channels not showing slow conduction in the first map could be the areas with slowest conduction after ablating the first regions. If confirmed with a larger population, it could be proposed to try to unmask slow conduction in every area with channels of the CMR despite there being no DZ in the initial map. In this sense, strategies that add short coupled extrastimuli[21,27,28] around CMR channels could unmask these hidden DZs from the beginning of the procedure.

Finally, our study confirms the usefulness of remapping after ablation (**Figure 5**). The ablation strategy guided by ILAM described by Tung et al[10] pointed out the importance of choosing the primary DZs and does not necessarily eliminate other DZs if VT is not inducible after the first ablation set. However, the rate of VT recurrence was numerically, but not statistically, lower in patients with complete elimination of DZs (11% vs 26%; $P = 0.35$), and remapping was associated with a lower rate of VT recurrence (24% vs 47%; $P = 0.01$) although this was not a standardized approach in the original ILAM protocol.[8]

Overall, our findings clearly confirm the role of CMR in defining potential areas with slow conduction and the relevance of remapping to abolish all potential areas for re-entry, especially considering that 100% of DZs in the remaps were associated with CMR channels.

STUDY LIMITATIONS. First, the benefit of our strategy with remapping and the use of CMR as key points have not been tested against a control group. Therefore, the benefit of this strategy over different approaches should be confirmed with different and probably randomized trials. However, this was not the aim of the study, as it was designed as an observational study to analyze DZ evolution and the relation with CMR channels. In this sense, in our study, the complete abolition of DZs was not related to better VT recurrence rate. The low proportion of patients without DZ abolition (18%) and the low rate of VT recurrence could justify a lack of statistical power to address this question.

Another controversial issue is the analysis of the relation of DZs with the VT isthmus. There are

FIGURE 4 Example of Evolution of DZ Within Different CMR Channels

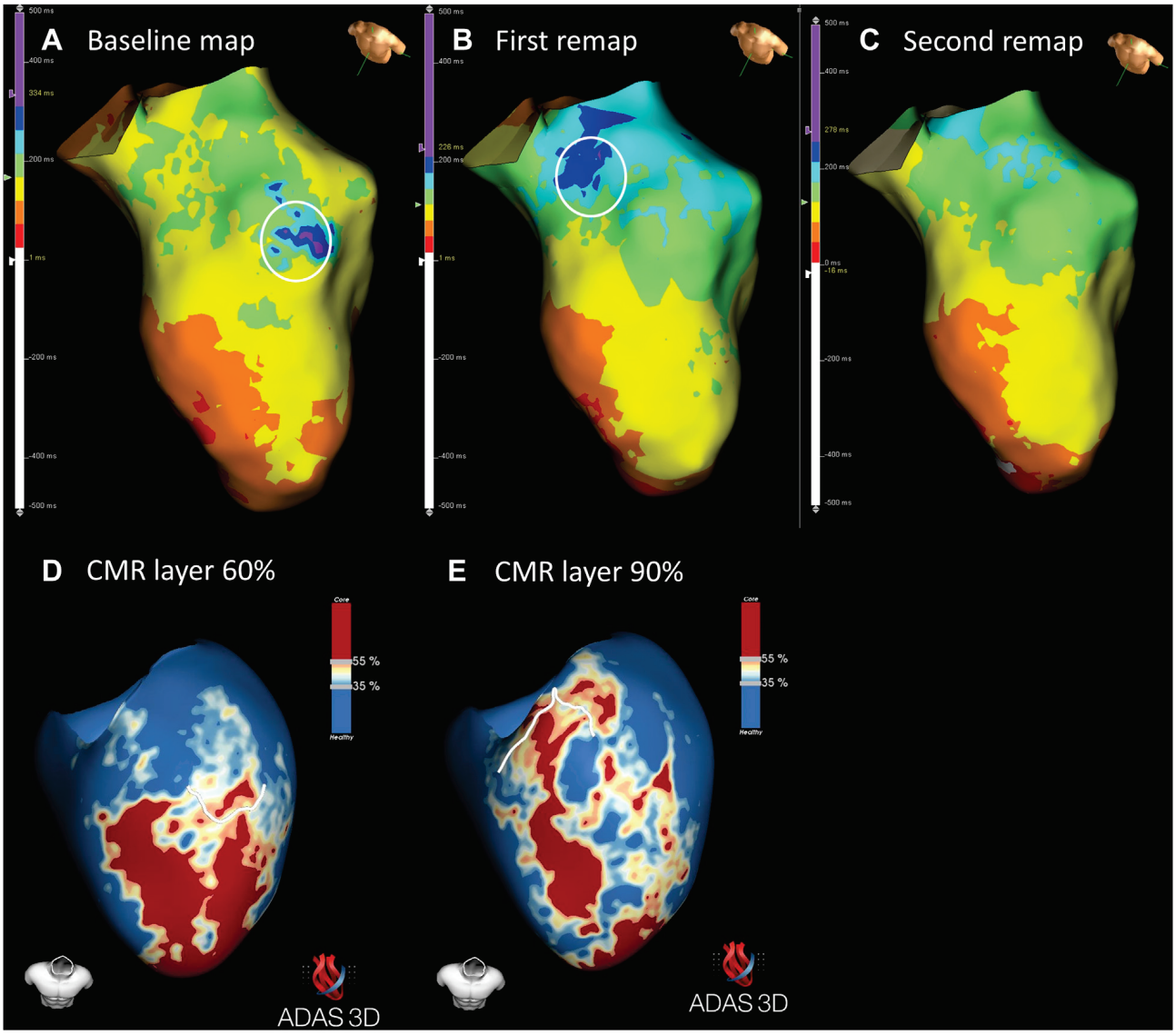

(Top) Evolution of the DZ from the baseline map to the last remap showing an initial medium-anterior DZ **(A)** that changes its position after the first ablation set to a more basal-anteroseptal position **(B)** and finally disappears in the last remap **(C)**. **(Bottom)** CMR from the same patient demonstrating a high correlation between DZs and CMR channels both in baseline map and remap. CMR from the same patient demonstrating a high correlation between DZs and CMR channels both in baseline map **(D)** and remap **(E)**. In this case, an unmasking new channel is observed in remap. Abbreviations as in Figure 1.

plenty of data suggesting that all areas with slow conduction must be ablated to avoid VT recurrences so, at the end, clinically it is more crucial to detect slow conduction regions than to determine if all of them are related to VT in this specific procedure. However, as we only induced at the beginning and at the end of the procedure, it cannot be ensured that all DZs were related to the VT isthmus and, indeed, the relation of CMR-CCs with VT isthmuses has not been studied.

Regarding mapping limitations, the number of mapping points was lower during remap compared with baseline map (Table 2). The remap was focused on the area of interest regarding baseline ILAM map and CMR images. Consequently, the presence of some other DZs very remote from initial DZs and to CMR-CCs could have potentially been missed during remaps with our strategy.

One potential limitation is the fact that correlation between DZs and CMR was performed side by

FIGURE 5 Example of Correlation Between DZs and CMR Channels

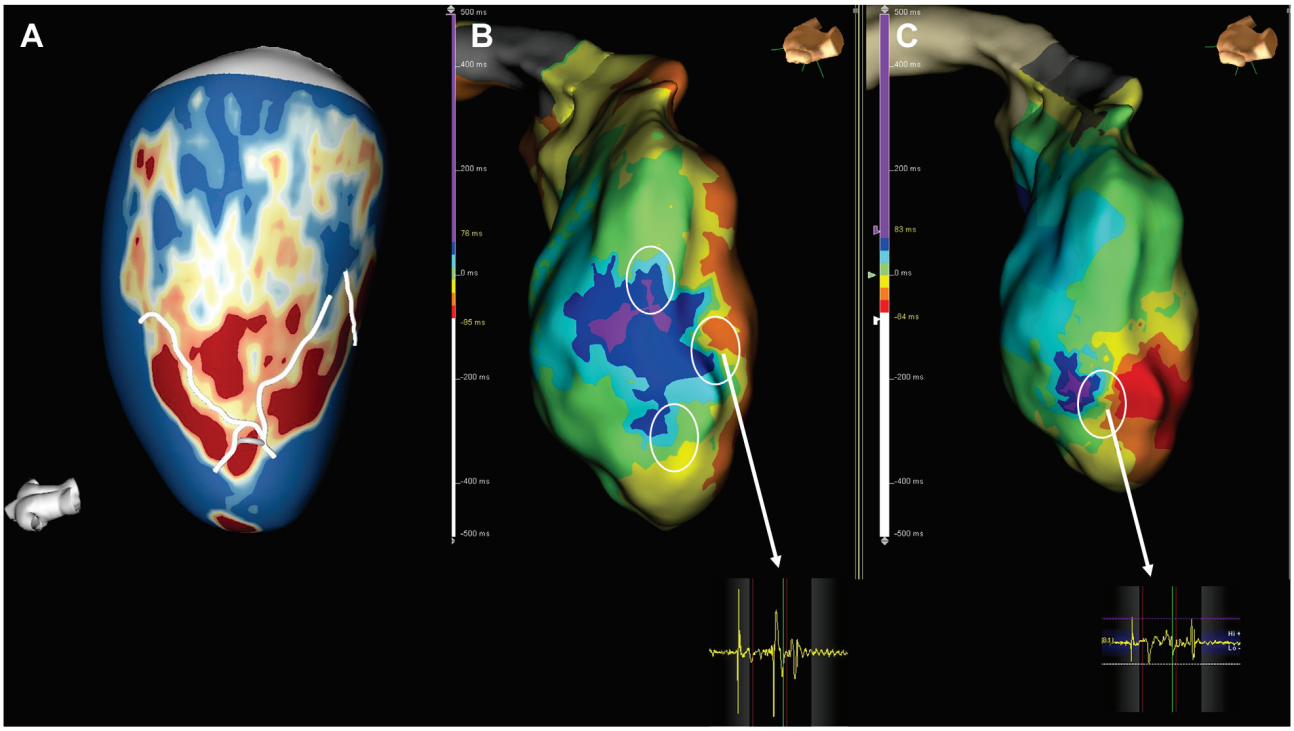

A new example of high correlation of CMR **(A)** and DZs both in baseline **(B)** and remap **(C)**. In this patient, after the first ablation set, DZs moved inside the same posterior channel. Abbreviations as in Figure 1.

side and not merging. The merging process, especially with Ensite Precision, requires a very time-consuming post-processing. Merging process should be very important to analyze quantitative data (ie, amount of scar, BZ). However, for this study, any quantitative parameter (ie, scar area) has been evaluated. In this sense, we believe that side-by-side comparison of EAM vs CMR images is an appropriate and reliable method and reproducible in clinical practice.

CONCLUSIONS

This study reports a high correlation between DZs identified by ILAM and CMR channels in both baseline and remaps. The finding that some DZs in the remaps are located in a new area but are always located in CMR channels could suggest the capability of CMR to identify all slow conduction regions even if not present at baseline. Remapping and ablating these DZs could be associated with better clinical outcomes.

ACKNOWLEDGMENTS The authors thank Dr Peng Hu (UCLA, Los Angeles, CA) for his pioneering work on wideband LGE. The authors also thank Xiaoming Bi, PhD, and Siemens Healthineers for their support with the wideband sequence work in progress collaboration.

FUNDING SUPPORT AND AUTHOR DISCLOSURES

This study was supported by Emile Letang Grand of Hospital Clinic de Barcelona/Instituto de Salud Carlos III (ISCIII) PI20/00693/CB16/11/00354, co-funded by the European Union. Drs Mont and Brugada are consultants, lecturers, and advisory board members for Abbott Medical, Boston Scientific, Biosense Webster, Medtronic, and Biotronik; and shareholders of ADAS3D Medical, S.L. Drs Roca-Luque, Tolosana, and Porta-Sanchez are consultants and lecturers for Biosense Webster, Medtronic, Boston Scientific, and Abbott Medical. Judit Mas Casanovas is currently an Abbott employee. All other authors have reported that they have no relationships relevant to the contents of this paper to disclose.

ADDRESS FOR CORRESPONDENCE: Dr Ivo Roca-Luque, Cardiovascular Institute, Arrhythmia Section, Hospital Clinic, Villarroel, 170, 08036 Barcelona, Spain. E-mail: iroca@clinic.cat.

PERSPECTIVES

COMPETENCY IN MEDICAL KNOWLEDGE: The present study constitutes the first report to analyze the evolution of DZs during ablation. Furthermore, a great correlation between DZs and CMR channels has been observed. The appearance of new DZ regions after the first ablation set reinforces the need for remapping in VT ablation with special emphasis in the regions with CCs in the CMR as all the DZs in remaps colocalized with CMR channels.

TRANSLATIONAL OUTLOOK: DZs are a dynamic concept that can change during ablation as local wavefront activation changes after elimination of first deceleration areas. Further studies with careful analysis of conduction in the areas with CMR channels could increase the knowledge about ablation targets.

REFERENCES

1. Dukkipati SR, Koruth JS, Choudry S, et al. Catheter ablation of ventricular tachycardia in structural heart disease. *J Am Coll Cardiol*. 2017;70:2924–2941.

2. Josephson ME, Anter E. Substrate mapping for ventricular tachycardia. *J Am Coll Cardiol EP*. 2015;1:341–352.

3. Roca-Luque I, Quinto L, S anchez-Somonte P, et al. Late potential abolition in ventricular tachycardia ablation. *Am J Cardiol*. 2022;1(174):53–60.

4. Anter E, Kleber AG, Rottmann M, et al. Infarct-related ventricular tachycardia: redefining the electrophysiological substrate of the isthmus during sinus rhythm. *J Am Coll Cardiol EP*. 2018;4:1033–1048.

5. Jaïs P, Maury P, Khairy P, et al. Elimination of local abnormal ventricular activities. *Circulation*. 2012;125:2184–2196.

6. Tung R, Vaseghi M, Frankel DS, et al. Freedom from recurrent ventricular tachycardia after catheter ablation is associated with improved survival in patients with structural heart disease: an International VT Ablation Center Collaborative Group study. *Heart Rhythm*. 2015;12:1997–2007.

7. Quinto L, Sanchez-Somonte P, Alarcón F, et al. Ventricular tachycardia burden reduction after substrate ablation: predictors of recurrence. *Heart Rhythm*. 2021;18:896–904.

8. Irie T, Yu R, Bradfield JS, et al. Relationship between sinus rhythm late activation zones and critical sites for scar-related ventricular tachycardia. *Circ EP*. 2015;8:390–399.

9. Ueda A, Soejima K, Nakahara S, et al. Conduction slowing area during sinus rhythm harbors ventricular tachycardia isthmus. *J Cardiovasc Electrophysiol*. 2020;31:440–449.

10. Aziz Z, Shatz D, Raiman M, et al. Targeted ablation of ventricular tachycardia guided by wavefront discontinuities during sinus rhythm: a new functional substrate mapping strategy. *Circulation*. 2019;140:1383–1397.

11. Sánchez-Somonte P, Quinto L, Garre P, et al. Scar channels in cardiac magnetic resonance to predict appropriate therapies in primary prevention. *Heart Rhythm*. 2021;18:1336–1343.

12. Andreu D, Ortiz-Pérez JT, Fernández-Armenta J, et al. 3D delayed-enhanced magnetic resonance sequences improve conducting channel delineation prior to ventricular tachycardia ablation. *Europace*. 2015;17:938–945.

13. Andreu D, Penela D, Acosta J, et al. Cardiac magnetic resonance-aided scar dechanneling: influence on acute and long-term outcomes. *Heart Rhythm*. 2017;14:1121–1128.

14. Roca-Luque I, van Breukelen A, Alarcon F, et al. Ventricular scar channel entrances identified by new wideband cardiac magnetic resonance sequence to guide ventricular tachycardia ablation in patients with cardiac defibrillators. *Europace*. 2020;22:598–606.

15. Berruezo A, Fernández-Armenta J, Andreu D, et al. *Scar dechanneling. Cir EP*. 2015;8:326–336.

16. Vázquez-Calvo S, Garre P, Sanchez-Somonte P, et al. Orthogonal high-density mapping with ventricular tachycardia isthmus analysis vs. pure substrate ventricular tachycardia ablation: a case-control study. *Front Cardiovasc Med*. 2022;9.

17. Soto-Iglesias D, Penela D, Jáuregui B, et al. Cardiac magnetic resonance-guided ventricular tachycardia substrate ablation. *J Am Coll Cardiol EP*. 2020;6:436–447.

18. Roca-Luque I, Rivas-Gándara N, Francisco-Pascual J, et al. Preprocedural imaging to guide transcoronary ethanol ablation for refractory septal ventricular tachycardia. *J Card Electrophysiol*. 2019;30:448–456.

19. Sanchez-Somonte P, Garre P, Vázquez-Calvo S, et al. Scar conducting channel characterization to predict arrhythmogenicity during ventricular tachycardia ablation. *Europace*. 2023;25(3):989–999.

20. Fernández-Armenta J, Berruezo A, Andreu D, et al. Three-dimensional architecture of scar and conducting channels based on high resolution ce-CMR: insights for ventricular tachycardia ablation. *Circ EP*. 2013;6:528–537.

21. Acosta J, Andreu D, Penela D, et al. Elucidation of hidden slow conduction by double ventricular extrastimuli:A method for further arrhythmic substrate identification in ventricular tachycardia ablation procedures. *Europace*. 2018;20:337–346.

22. Wijnmaalen AP, Van Der Geest RJ, Van Huls Van Taxis CFB, et al. Head-to-head comparison of contrast-enhanced magnetic resonance imaging and electroanatomical voltage mapping to assess post-infarct scar characteristics in patients with ventricular tachycardias: real-time image integration and reversed registration. *Eur Heart J*. 2011;32:104–114.

23. Perez-David E, Arenal Á, Rubio-Guivernau JL, et al. Noninvasive identification of ventricular tachycardia-related conducting channels using contrast-enhanced magnetic resonance imaging in patients with chronic myocardial infarction. *J Am Coll Cardiol*. 2011;57:184–194.

24. Piers SRD, Tao Q, De Riva Silva M, et al. CMR-based identification of critical isthmus sites of ischemic and nonischemic ventricular tachycardia. *J Am Coll Cardiol Img*. 2014;7:774–784.

25. Oloriz T, Silberbauer J, MacCabelli G, et al. Catheter ablation of ventricular arrhythmia in non-ischemic cardiomyopathy: anteroseptal versus inferolateral scar sub-types. *Circ EP*. 2014;7:414–423.

26. Quinto L, Sanchez P, Alarcón F, et al. Cardiac magnetic resonance to predict recurrences after ventricular tachycardia ablation: septal involvement, transmural channels, and left ventricular mass. *Europace*. 2021;23:1437–1445.

27. de Riva M, Naruse Y, Ebert M, et al. Targeting the hidden substrate unmasked by right ventricular extrastimulation improves ventricular tachycardia ablation outcome after myocardial infarction. *J Am Coll Cardiol EP*. 2018;4:316–327.

28. Porta-Sánchez A, Jackson N, Lukac P, et al. Multicenter study of ischemic ventricular tachycardia ablation with Decrement-Evoked Potential (DEEP) mapping with extra stimulus. *J Am Coll Cardiol EP*. 2018;4:307–315.

KEY WORDS cardiac magnetic resonance, deceleration zones, isochronal late activation maps, substrate mapping, ventricular tachycardia ablation

Artículo 4: Detección no invasiva de la conducción lenta con resonancia magnética cardíaca para la ablación de TV

El objetivo de este estudio fue encontrar predictores de arritmogenicidad en los canales de RMC analizando su capacidad para identificar las zonas de desaceleración (DZs) en los mapas electroanatómicos durante la ablación de TV.

Para ello, se incluyeron cuarenta y cuatro pacientes consecutivos con enfermedad cardíaca estructural y TV sometidos a ablación con realización previa de RMC en un solo centro (octubre de 2018 a julio de 2021) (edad media, 64.8 ± 11.6 años; 95.5% hombres; 70.5% con cardiopatía isquémica; fracción de eyección media de ventrículo izquierdo: 32.3 ± 7.8%). Se analizaron las características de los canales de RMC y se determinaron las correlaciones con las DZs detectadas durante el mapeo de isócronas de activación tardía tanto en el mapa basal como en remaps.

Se analizaron un total de 109 canales de RMC detectados automáticamente (2.48 ± 1.15 por paciente; longitud: 57.91 ± 63.07 mm; masa de *border zone:* 2.06 ± 2.67 gramos; *protectedness*: 21.44 ± 25.39 mm). Un 76.1% de todos los canales de RMC estaban asociados con una DZ. El análisis univariado mostró que los canales asociados con DZs eran más largos (67.81 ± 68.45 vs. 26.31 ± 21.25 mm, OR 1.03, p=0.010), con mayor masa de *border zone* (2.41 ± 2.91 vs. 0.87 ± 0.86 g, OR 2.46, p=0.011) y mayor *protectedness* (24.97 ± 27.72 vs. 10.19 ± 9.52 mm, OR 1.08, p=0.021). De todos estos parámetros, la longitud fue el que mejor se relacionó con la posibilidad de que el canal de RMC se asociara a una DZ. Así, los canales con longitud superior a 25 mm tenían un 86.7% (SE 0.04) de posibilidades de asociarse con una zona de deceleración frente a 16.7% (SE 0.15) para los canales de 10 mm o menos.

Como conclusión, la detección no invasiva de zonas funcionalmente críticas para la presencia de eventos de TV es posible con RMC. Las DZs encontradas durante el mapa electroanatómico se correlacionan con precisión con los canales de RMC, especialmente aquellos con mayor longitud, masa de zona de borde y *protectedness*.

ESC European Society of Cardiology

Europace (2024) **26**, 1–11
https://doi.org/10.1093/europace/euae025

CLINICAL RESEARCH

Non-invasive detection of slow conduction with cardiac magnetic resonance imaging for ventricular tachycardia ablation

Sara Vázquez-Calvo [1,2], Judit Mas Casanovas [1], Paz Garre [1,2], Paula Sánchez-Somonte [1,2], Pasquale Valerio Falzone [1,2], Laura Uribe [1,2], Eduard Guasch [1,2,3], José Maria Tolosana [1,2,3], Roger Borras [1,2,4], Rosa M. Figueras i Ventura [5], Elena Arbelo [1,2,3], José T. Ortiz-Pérez [1,2,3], Susana Prats[1,2], Rosario J. Perea [1,2], Josep Brugada [1,2,3], Lluís Mont [1,2,3], Andreu Porta-Sanchez [1,2], and Ivo Roca-Luque [1,2,3]*

[1]Institut Clinic Cardiovascular, Hospital Clínic, Universitat de Barcelona, Villarroel, 170, 08036 Barcelona, Spain; [2]Institut d'Investigacions Biomèdiques August Pi i Sunyer (IDIBAPS), Barcelona, Spain; [3]Centro de Investigación Biomédica en Red, Enfermedades Cardiovasculares (CIBERCV), Madrid, Spain; [4]Centro de Investigación Biomédica en Red e Salud Mental, CIBERSAM, Instituto de Salud Carlos III, Madrid, Spain; and [5]ADAS 3D Medical S.L., Barcelona, Spain

Received 27 November 2023; accepted after revision 11 January 2024; online publish-ahead-of-print 23 January 2024

Aims Non-invasive myocardial scar characterization with cardiac magnetic resonance (CMR) has been shown to accurately identify conduction channels and can be an important aid for ventricular tachycardia (VT) ablation. A new mapping method based on targeting deceleration zones (DZs) has become one of the most commonly used strategies for VT ablation procedures. The aim of the study was to analyse the capability of CMR to identify DZs and to find predictors of arrhythmogenicity in CMR channels.

Methods and results Forty-four consecutive patients with structural heart disease and VT undergoing ablation after CMR at a single centre (October 2018 to July 2021) were included (mean age, 64.8 ± 11.6 years; 95.5% male; 70.5% with ischaemic heart disease; a mean ejection fraction of 32.3 ± 7.8%). The characteristics of CMR channels were analysed, and correlations with DZs detected during isochronal late activation mapping in both baseline maps and remaps were determined. Overall, 109 automatically detected CMR channels were analysed (2.48 ± 1.15 per patient; length, 57.91 ± 63.07 mm; conducting channel mass, 2.06 ± 2.67 *g*; *protectedness*, 21.44 ± 25.39 mm). Overall, 76.1% of CMR channels were associated with a DZ. A univariate analysis showed that channels associated with DZs were longer [67.81 ± 68.45 vs. 26.31 ± 21.25 mm, odds ratio (OR) 1.03, $P = 0.010$], with a higher border zone (BZ) mass (2.41 ± 2.91 vs. 0.87 ± 0.86 *g*, OR 2.46, $P = 0.011$) and greater protectedness (24.97 ± 27.72 vs. 10.19 ± 9.52 mm, OR 1.08, $P = 0.021$).

Conclusion Non-invasive detection of targets for VT ablation is possible with CMR. Deceleration zones found during electroanatomical mapping accurately correlate with CMR channels, especially those with increased length, BZ mass, and protectedness.

* Corresponding author. Tel: +34 932 27 5400, *E-mail address*: iroca@clinic.cat

Graphical Abstract

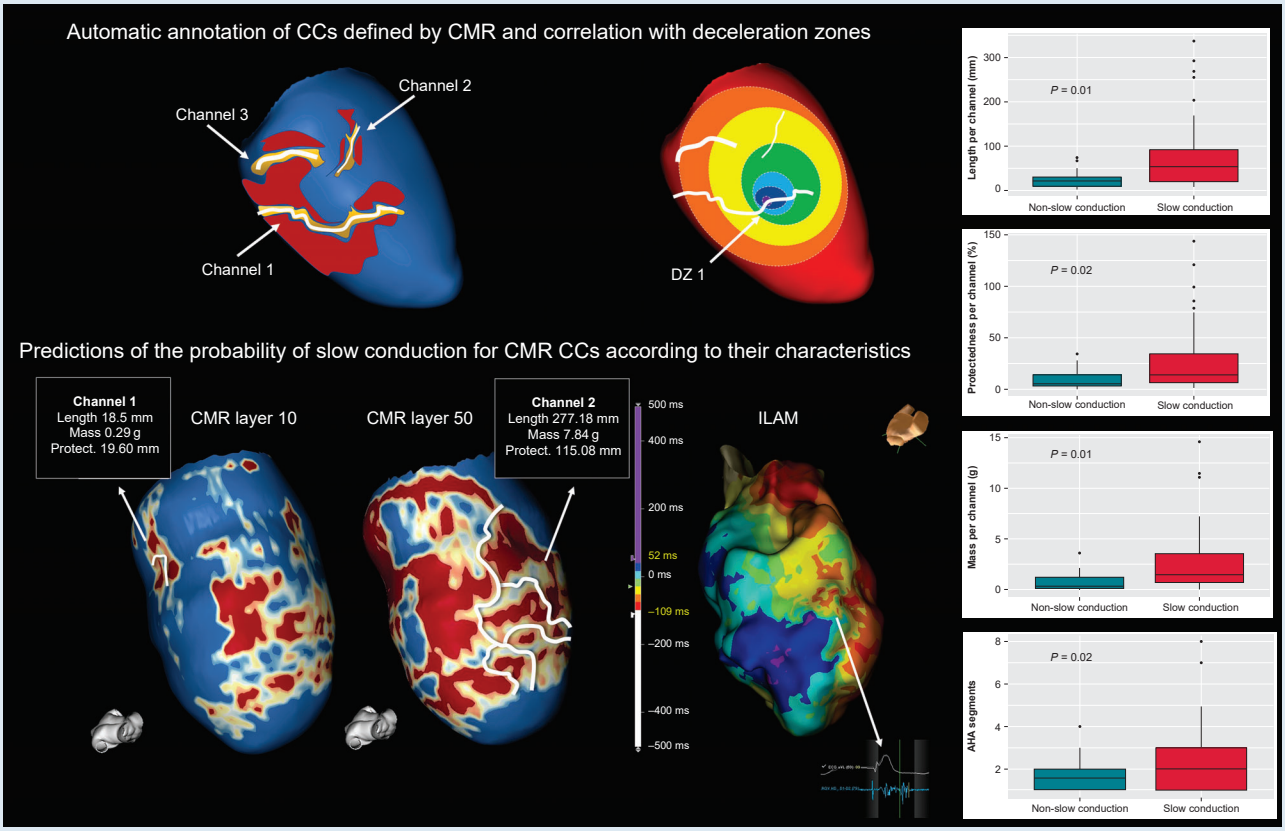

Keywords Ventricular tachycardia ablation • Cardiac magnetic resonance • Conducting channels • Isochronal late activation maps • Deceleration zones

What's new?

- This is the first study to our knowledge that analyses not only the relationship of cardiac magnetic resonance (CMR) channels with deceleration zones (DZs) but also the predictors of arrhythmogenicity.
- More than 75% of the channels of CMR were related to DZs.
- Some characteristics of the CMR channel were strongly related to arrhythmogenicity (in terms of the presence of DZ) as the length (67.81 vs. 26.31 mm, $P = 0.01$) and mass of the border zone within the channel (2.41 vs. 0.87 g, $P = 0.01$).
- These findings could have immediate clinical applications to refine CMR-aided ventricular tachycardia (VT) substrate ablation (to ablate mainly the channels with certain characteristics, thereby shortening the ablation procedures). In addition, if confirmed by other studies, the findings could also have implications for improving the specificity of CMR to stratify the risk of VT in different populations.

Introduction

Substrate-based radiofrequency catheter ablation has become a standard procedure for the treatment of scar-related ventricular tachycardia (VT).[1] The main mechanism behind scar-related VT is the re-entrant circuit. This circuit is caused by the presence of a slowly conducting area or channel (CC) usually within the border zone (BZ) tissue surrounded by the scar and connecting healthy tissue. Several strategies have been developed to identify these slow conduction areas using electroanatomical maps (EAMs) during ablation.[2] Substrate mapping focused on the analysis of abnormal electrograms after main ventricular activation—so-called late potentials (LPs)—or local abnormal ventricular activity (LAVA) within low-voltage regions is currently the principal method to define the arrhythmic substrate during stable rhythm when VT activation mapping is not possible.[3] An additional mapping tool for the detection of slow conduction areas, called isochronal late activation mapping (ILAM), was described by Irie *et al.*[4] and has recently been shown to be very specific for the VT critical zone.[5]

From a structural point of view, late gadolinium enhancement-cardiac magnetic resonance (LGE-CMR) has demonstrated to precisely identify and characterize the arrhythmogenic substrate, being able to depict the CCs with a high correlation to the EAMs[6,7] even in patients with an implantable cardioverter defibrillator (ICD) *in situ* with a dedicated LGE sequence [wideband (WB) sequence].[8] With regard to VT ablation procedures, LGE-CMR is widely used as a standard method, since it can greatly facilitate pre-procedural planning and procedural success.[9,10]

In this study, to continue improving the capability of CMR to define the arrhythmic substrate, we studied the correlation between CMR conducting channels and deceleration zones (DZs) detected during ILAM with a specific analysis of CMR channel characteristics related to the presence of DZs as a marker of the arrhythmogenicity of conducting channels.

Methods

Study population

This was a prospective observational study of all consecutive patients with structural heart disease who underwent VT ablation in a single centre (Hospital Clinic, University of Barcelona) from October 2018 to July 2021. Late gadolinium enhancement-cardiac magnetic resonance was performed within 6–12 months before ablation. The exclusion criterion of the study was the absence of pre-procedural CMR. All patients provided written informed consent. The study was carried out according to the Declaration of Helsinki guidelines and the deontological code of our institution. The study protocol was approved by the ethics committee of the hospital.

Pre-procedural cardiac magnetic resonance

A 3 T scan was performed in patients without an ICD, and a 1.5 T scan with a WB sequence was used in patients with an ICD to reduce image artefacts, as described previously.[8] The analysis of the arrhythmic substrate was performed using ADAS 3D software (ADAS 3D, Galgo Medical S.L.) following a standardized and widely validated protocol.[10] In brief, a semiautomatic segmentation of the left ventricle was performed by an expert operator. Next, ADAS 3D divided the myocardium thickness into a total of nine three-dimensional (3D) maps from the endocardium to the epicardium. The LGE pixel signal intensity maps obtained from the CMR scans were projected onto each layer with a trilinear interpolation algorithm and were colour-coded using 40 ± 5 and $60 \pm 5\%$ of the maximum intensity as thresholds. Therefore, areas with high LGE ($\geq$60%) were coded as dense scar tissue and coloured red; healthy tissue without LGE ($\leq$40%) was coloured blue; and BZs, identified as areas with an intermediate percentage of LGE (between 40 ± 5 and $60 \pm 5\%$), were coloured in an intermediate colour range from yellow to green. According to the LGE distribution from 10% (the layer closest to the endocardium) to 90% (the layer closest to the epicardium), the substrate was defined as endocardial when LGE affected 10–30% of the layer, epicardial when LGE affected 60% of the outer layer, and mid-mural when LGE was confined to the internal layer of myocardial thickness without endocardial or epicardial distribution. Areas of LGE >75% in myocardial thickness were considered transmural.

Channels and their characteristics were analysed automatically by the system. *Protectedness*, which is a parameter based on the length of the channel covered ('protected') by dense scar tissue and known to correlate with VT critical areas,[11] was also calculated. To determine protectedness, the percentage of the CMR channel perimeter containing core tissue, healthy tissue, or BZ tissue within a 3.5 mm radius was examined. Local protectedness was then determined based on these percentages: if healthy tissue was present, local protection was set to zero; if no healthy tissue was found, protection depended on the percentage of the perimeter coinciding with core tissue. A point with <15% core had 0% local protection (fully unprotected), while a point with >40% had 100% local protection (fully protected). Core values between 15 and 40% were linearly mapped to local protection values between 0 and 100%. The local protection values were integrated over the entire CMR channel.

High-density mapping: substrate and isochronal late activation mapping

Procedures were performed under general anaesthesia. Access to the left ventricle was achieved with a transseptal and/or retrograde aortic approach at the discretion of the operator. Epicardial mapping was performed in cases when an epicardial origin of VT was suspected and in cases of previously failed endocardial ablation.

The mapping approach consisted of performing ILAM of the left ventricle during right ventricular pacing with a stable cycle length of 600 ms using an HDGrid catheter and EnSite Precision system (Abbott Medical, USA). These maps were executed by annotating the latest deflection of the electrograms (EGMs) (Last Deflection algorithm, Abbott Medical) of HDGrid orthogonal signals (HD Wave algorithm, Abbot Medical) and dividing the whole activation of the chamber into eight equally distributed isochrones, with white being the earliest and purple being the latest isochrone. Deceleration zones were defined as regions with isochronal crowding, with >3 isochrones within a 1 cm radius, as previously described.[4] Late gadolinium enhancement-cardiac magnetic resonance post-processed images were carefully and systematically aligned according to the AP and LL projections in the mapping system and CMR. They were then visualized into the navigation system side by side with the EAMs.

Ablation strategy and remapping

After an analysis of the generated maps, the tagged EGMs, and the channels defined by CMR, the HDGrid catheter was positioned in the potential VT isthmus (DZ with higher isochronal crowding, especially if correlated with a channel by CMR). Ventricular tachycardia was induced by programmed electrical stimulation,[12] and if it was haemodynamically tolerated, activation mapping for diastolic and pre-systolic activity was performed. In cases in which VT was not haemodynamically tolerated, the VT critical side was defined as the area with a fast transition from good pace mapping (suggesting VT exit site) to poor pace mapping (suggesting VT entrance site). In these cases, the initial target for ablation was the central VT isthmus where diastolic EGMs were observed. After the critical areas of induced VT were targeted, substrate ablation was performed by strictly targeting the rest of the DZs. Radiofrequency was delivered using an externally irrigated 3.5 mm tip ablation catheter with 45°C temperature control (at an irrigation rate of 26–30 mL/min), at a power limit of 40–50 W. Remapping with the HDGrid catheter was performed to assess the abolition of the DZs and/or detect new DZs, especially in areas of interest according to LGE-CMR. Additional radiofrecuency (RF) lesions were delivered until complete elimination of the DZs. Acute success was defined as total abolition of DZs as well as the lack of VT inducibility at the end of the procedure.

Post hoc offline analysis

The detection and analysis of CMR channels was performed automatically by ADAS 3D software, as described in the Methods section. This analysis was done before the ablation procedure and therefore without any information related to EAM. A *post hoc* analysis of the DZs was done by an experienced operator of all maps (basal maps and remaps), blinded to CMR data. Finally, a visual correlation between each channel and the DZs was performed, not only with those observed in the baseline map but also with those observed in the remaps (*Figure 1*).

Clinical follow-up

All patients were followed routinely during a 1-year follow-up with clinical visits at 1, 6, and 12 months and with remote device monitoring when possible. Ventricular tachycardia recurrence was defined as any sustained VT episode or sudden death.

Statistical analysis

Continuous variables are presented as the mean value $\pm$ standard deviation, and minimum and maximum values were compared by using Student's *t*-test. Categorical variables are expressed as total numbers (percentages) and were compared between groups using the χ^2 test. A generalized linear mixed-effects model for binary response was used to study the effects of LGE-CMR characterization to predict slow conduction areas. Odds ratios and 95% confidence limits were calculated. A two-sided Type I error of 5% was used for all tests. A statistical analysis was performed using R software for Windows version 4.2.2 (R Project for Statistical Computing; Vienna, Austria).

Results

Study population

Between October 2018 and July 2021, 58 patients underwent ablation procedures for scar-related VT at our institution. Twelve patients were excluded due to the inability to perform CMR (arrhythmic storm, claustrophobia, etc.), and two were excluded due to poor-quality CMR. Overall, 44 patients were included in the study. The median age was 64.8 ± 11.6 years, 95.5% were male, and the median ejection fraction was $32.3 \pm 7.8\%$. A total of 70.5% had ischaemic cardiomyopathy, and 15.9% presented with a VT storm. The clinical characteristics are detailed in *Table 1*. In 73.7% of patients, 1.5 T CMR with a WB sequence was performed.

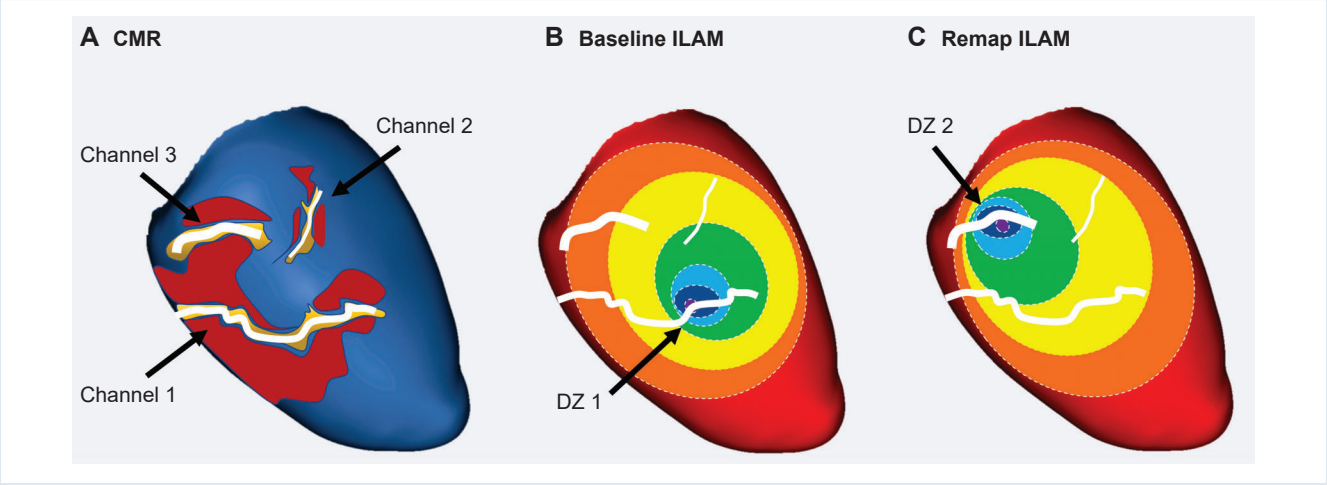

Figure 1 (*A*) A schematic of an automatic annotation of CCs defined by CMR. Different lengths, widths, and levels of protectedness can be observed for each channel. (*B*) The correlation with DZs was annotated in every map. In this case, Channel 1 is associated with a DZ in the baseline map, with Channel 3 correlated with a new DZ observed in the remap. (*C*) Channel 2 is not related to any DZ in this example. CC, conducting channel; CMR, cardiac magnetic resonance; DZ, deceleration zone; ILAM, isochronal late activation mapping.

Table 1 Clinical characteristics

	Patients studied ($n = 44$)
Age (years)	64.8 ± 11.6 (26–82)
Male sex	42 (95.5%)
Hypertension	28 (63.6%)
Diabetes	20 (46.5%)
Dyslipidaemia	27 (62.8%)
COPD	6 (15.0%)
CKD	11 (28.9%)
NYHA class	
I	7 (20.6%)
II	23 (67.6%)
III and IV	4 (11.8%)
Ischaemic cardiomyopathy	31 (70.5%)
Permanent AF	10 (23.3)
ACEIs	23 (60.5%)
Beta-blockers therapy	29 (76.3%)
Sotalol therapy	4 (10.5%)
Amiodarone therapy	31 (81.6%)
VT storm	7 (15.9%)
LVEF (%)	32.3 ± 7.8
LVEDD (mm)	61.4 ± 10.2

AF, atrial fibrillation; CKD, chronic kidney disease; COPD, chronic obstructive pulmonary disease; ACEIs, angiotensin-converting enzyme inhibitors; LVEF, left ventricular ejection fraction; LVEDD, left ventricular end-diastolic diameter; NYHA, New York Heart Association; VT, ventricular tachycardia.

Table 2 Procedural characteristics

	$n = 44$
Endocardial approach	40 (93.0%)
Endoepicardial approach	3 (7.0%)
Arterial access	26 (63.4%)
Transeptal access	41 (97.6%)
Agilis	24 (60.0%)
Number of mapping points	2199.75 ± 703.64
Number of VT inductions	1.71 ± 1.55
Number of targeted VTs	1.62 ± 1.55
Procedural time (min)	237.72 ± 48.56
X-ray time	37.97 ± 12.36
Number of RF applications	57.46 ± 24.44
RF time (s)	1883.38 ± 848.80
Final non-inducibility	33 (82.5%)
Absence of residual slow conduction	33 (82.5%)

VT, ventricular tachycardia.

Procedural characteristics

An endocardial procedure was performed in all patients, with a transeptal approach in the majority of patients (97.6%) combined with retro-aortic access in 63.6% of patients. An epicardial procedure was performed in three (6.8%) patients. During the basal electrophysiological study, 83.3% of patients were inducible for VT, with a median of 1.71 ± 1.55 VTs induced per patient (*Table 2*).

Late gadolinium enhancement-cardiac magnetic resonance characteristics and predictors of conducting channel arrhythmogenicity

A total of 109 CMR channels were studied (2.48 ± 1.15 channels per patient). The majority of channels had an endocardial location

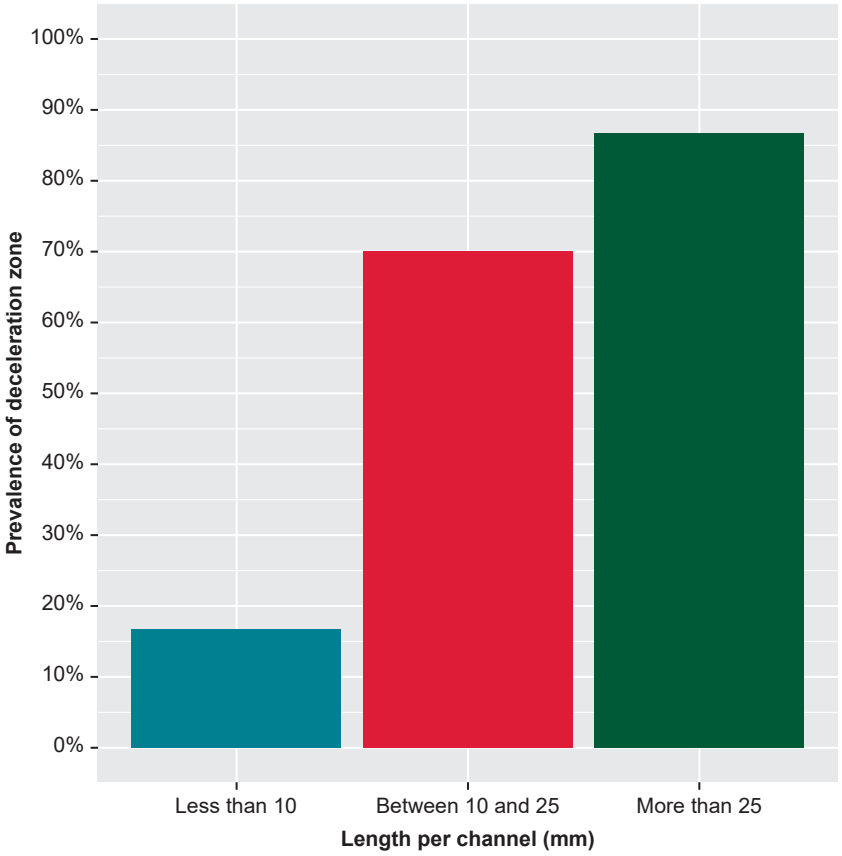

Figure 2 Probability of an association between CMR channels and DZs according to the length of the channel. CCs with a length <10 mm have a probability rate of only 16.7% to detect a DZ. In contrast, CCs that are longer than 25 mm have a probability rate as high as 86.7%. CC, conducting channel; CMR, cardiac magnetic resonance; DZ, deceleration zone.

(34.9%) or transmural location (22.0%). The median length per channel was 57.91 ± 63.07 mm, with a median mass of 2.06 ± 2.67 g. The median protectedness per channel was 21.44 ± 25.39 mm.

Overall, 76.1% of CMR channels were associated with a DZ during the procedure: 64 CMR channels (58.7%) were correlated with DZs observed in the baseline map, and 19 CMR channels (22.9%) were associated with DZs not observed in the initial map but detected during the remap after the first ablation set. Additionally, 41.8% of CMR channels correlated with a mapped VT critical site. No differences were observed between ischaemic and non-ischaemic patients in terms of the correlation between CMR channels and slow conduction areas (74.49 vs. 70.96%, $P = 0.70$).

The univariate analysis showed that channels associated with DZs were longer [67.81 ± 68.45 vs. 26.31 ± 21.25 mm, odds ratio (OR) 1.03, $P = 0.01$], with a higher mass (2.41 ± 2.91 vs. 0.87 ± 0.86 g, OR 2.46, $P = 0.01$) and greater protectedness (24.97 ± 27.72 vs. 10.19 ± 9.52 mm, OR 1.08, $P = 0.02$) compared with those not related to DZs. Regarding length and its correlation with DZs, channels over 25 mm had a probability of 86.7% (standard error [SE] 0.04) vs. only 16.7% (SE 0.15) for channels <10 mm (*Figure 2*). Other highly correlated parameters, such as the number of AHA segments or the number of layers affected, were also significantly higher in CMR channels associated with DZs (2.48 ± 1.47 vs. 1.77 ± 0.82, OR 2.09, $P = 0.02$ and 3.43 ± 2.50 vs. 2.31 ± 1.62, OR 1.44, $P = 0.02$). Channels with transmural involvement were also more likely to be associated with slow conduction areas (OR 6.42, $P = 0.04$). Cardiac magnetic resonance channel width was not a predictor of arrhythmogenicity in our study. No differences were observed between ischaemic and non-ischaemic patients. In *Table 3* and *Figure 3*, the relationship between CMR channel parameters and DZs is shown.

Radiofrequency delivery, acute success, and follow-up

The median duration of RF application was 37.97 ± 12.36 min, with a total procedural time of 237.72 ± 48.56 min. Non-inducibility at the end of the procedure was achieved in 82.5% of patients, and total elimination of DZs/LAVA/LPs was achieved in 82.5%.

Complications were observed in three patients: two patients presented cardiac tamponade, and one patient suffered an intractable VT storm during mapping of the left ventricle complicated with cardiorespiratory arrest that required advanced cardiopulmonary resuscitation manoeuvres.

After 1 year of follow-up, three patients died due to non-arrhythmic-related events. Ventricular tachycardia recurrence after 1 year of follow-up was 21.95% (19.35% in ischaemic cardiomyopathy patients and 30% in non-ischaemic cardiomyopathy patients) and 25.0% after 2 years of follow-up.

Discussion

The main findings of our study are as follows. First, three out of four CMR-detected CCs colocalized with DZs during high-density EAM. Second, CMR channels with increased length, BZ mass, and protectedness had a higher correlation with slow conduction areas.

Table 3 A univariate analysis of channel characteristics and the primary endpoint (slow conduction properties)

	Total ($n = 109$)	Slow conduction ($n = 83$)	Non-slow conduction ($n = 26$)	OR	*P*-value
Length per channel (mm)	57.91 ± 63.07 (4.16–338.10)	67.81 ± 68.45	26.31 ± 21.25	1.03 (1.01–1.06)	**0.01**
Mass per channel (g)	2.06 ± 2.67 (0.01–14.59)	2.41 ± 2.91	0.87 ± 0.86	2.46 (1.23–4.92)	**0.01**
Width per channel (mm)	5.02 ± 1.82 (0.01–9.34)	5.23 ± 1.51	4.38 ± 2.50	1.29 (0.90–1.67)	0.06
Protectedness per channel (mm)	21.44 ± 25.39 (0.01–143.51)	24.97 ± 27.72	10.19 ± 9.52	1.08 (1.01–1.2)	**0.02**
Layers affected by CMR channels					
Exclusively endocardium	38 (34.9%)	25	13	0.35 (0.11–1.07)	0.06
Exclusively mesocardium	2 (1.8%)	2	0	NA	NA
Exclusively epicardium	18 (16.5%)	15	3	1.63 (0.40–6.72)	0.50
Exclusively endo/meso	20 (18.3%)	13	7	0.56 (0.18–1.78)	0.32
Exclusively meso/epi	7 (6.4%)	6	1	NA	NA
Transmural	24 (22.0%)	22	2	6.42 (1.11–37.28)	**0.04**
Number of layers per channel	3.17 ± 2.36 (1–9)	3.43 ± 2.50	2.31 ± 1.62	1.44 (1.01–1.95)	**0.02**
Number of AHA segments per channel	2.30 ± 1.37 (1–8)	2.48 ± 1.47	1.77 ± 0.82	2.09 (1.13–3.86)	**0.02**

CMR, cardiac magnetic resonance; OR, odds ratio.
Bold values denote statistical significance ($p < 0.05$).

Tissue characterization with CMR imaging using late gadolinium enhancement has evolved in recent years, and it is currently the most commonly used non-invasive tool to assess the arrhythmic substrate in patients with structural heart disease. The use of gadolinium allows us to distinguish not only the dense scar from the healthy tissue but also the BZ where the CC is located, which in turn generates the re-entrant circuit and potentially maintains the VT.

Previous works have shown a high spatial correlation between CMR channels and voltage channels obtained during VT substrate mapping procedures.[13] However, these voltage channels have low specificity to detect VT isthmuses.[14] Notably, ablation strategies based exclusively on targeting the channel responsible for the induced/clinical VT have failed, resulting in worse clinical rates of VT recurrence in the follow-up period compared with more extensive substrate-ablation methods. One potential explanation relies on the capability of the myocardium tissue to change its properties and, therefore, its potential arrhythmogenicity according to pacing cycle length, site of pacing, etc.,[15,16] so different CCs could act as VT circuits or not under different situations. This could explain why targeting only the induced VT is not enough to avoid future VTs. For this reason, in recent years, substrate-ablation strategies have included not only ablation of the observed active VT circuit but also more extensive approaches. Several techniques have been proposed. One method based on a more detailed definition of the arrhythmic substrate is used to eliminate every LP or LAVA or even all scars (scar homogenization).[17,18] Other authors have worked on a more functional concept of arrhythmogenicity, identifying and targeting pathological EGMs unmasked after extrastimulus[19–21] or with decremental properties.[22,23] One of the more recent and successful strategies is based on ILAM,[4,5] in which the entire substrate is annotated considering not only its properties but also its relation to the surrounding tissue, defining DZs. These new strategies have been shown to improve VT ablation outcomes.

To date, CMR channels have demonstrated a great correlation with voltage channels, although the specificity of both for VT isthmuses detected during invasive VT mapping is low.[14] Recently, our group published a study analysing the evolution of the DZ during VT ablation that also showed a high correlation between DZs and CMR channels (93.68%) in both the baseline ILAM and remaps.[24] Interestingly, remapping allowed us to unmask DZs not observed in the baseline maps that were correlated with CMR channels. Our study is, to the best of our knowledge, the first to quantify and analyse the role of CMR in correctly identifying areas of slow conduction during substrate mapping performed with the ILAM technique.

Applications of cardiac magnetic resonance to evaluate arrhythmogenicity

In our study, 76.1% of CMR channels were associated with DZs in the sinus- or right ventricle (RV)-paced map. Interestingly, 22.9% of all CMR channels were related to a DZ not observed in the baseline map but detected in the remap, which highlights the potential advantage of CMR to identify arrhythmic substrates compared with a static conventional map. Two possible hypotheses could explain this phenomenon: First, the methodology of ILAM could be very helpful in identifying the primary (or more evident) DZ, especially when *very LPs* are present in the area, but not a second or third DZ, even if abnormal EGMs are present. The explanation relies on the fact that the ILAM methodology divides the total activation time into eight isochrones. In this sense, when very LPs occur, the total time activation window will be very long, so each isochrone will last a substantial amount of time, grouping isochrones with less delayed potentials and dissipating some potential DZs. After the 'primary' DZ is ablated, the 'secondary' DZs can therefore be clearly observed.

Second, as we have previously explained, the properties of the myocardium can change in different circumstances, so different DZs can be expected with different cycles, or even after changing the electrical properties of the tissue by the use of radiofrequency. *Figure 4* shows an example of these proposed mechanisms. To confirm this hypothesis, it would be interesting to perform manoeuvres during the baseline map to unmask slow conduction (for example, with extrastimulus) in those CMR channels that are initially not apparent to determine if that area had slow conduction properties that were hidden at baseline.

Improving the capability of CMR to define arrhythmogenicity can lead to a myriad of applications, from guiding faster and more effective VT ablation procedures to creating a score based on scar characteristics to predict arrhythmic events in patients with structural heart disease.[25] This last point could be particularly relevant since several studies have already shown the incremental value of scar characteristics as depicted by CMR to predict arrhythmic events when compared with

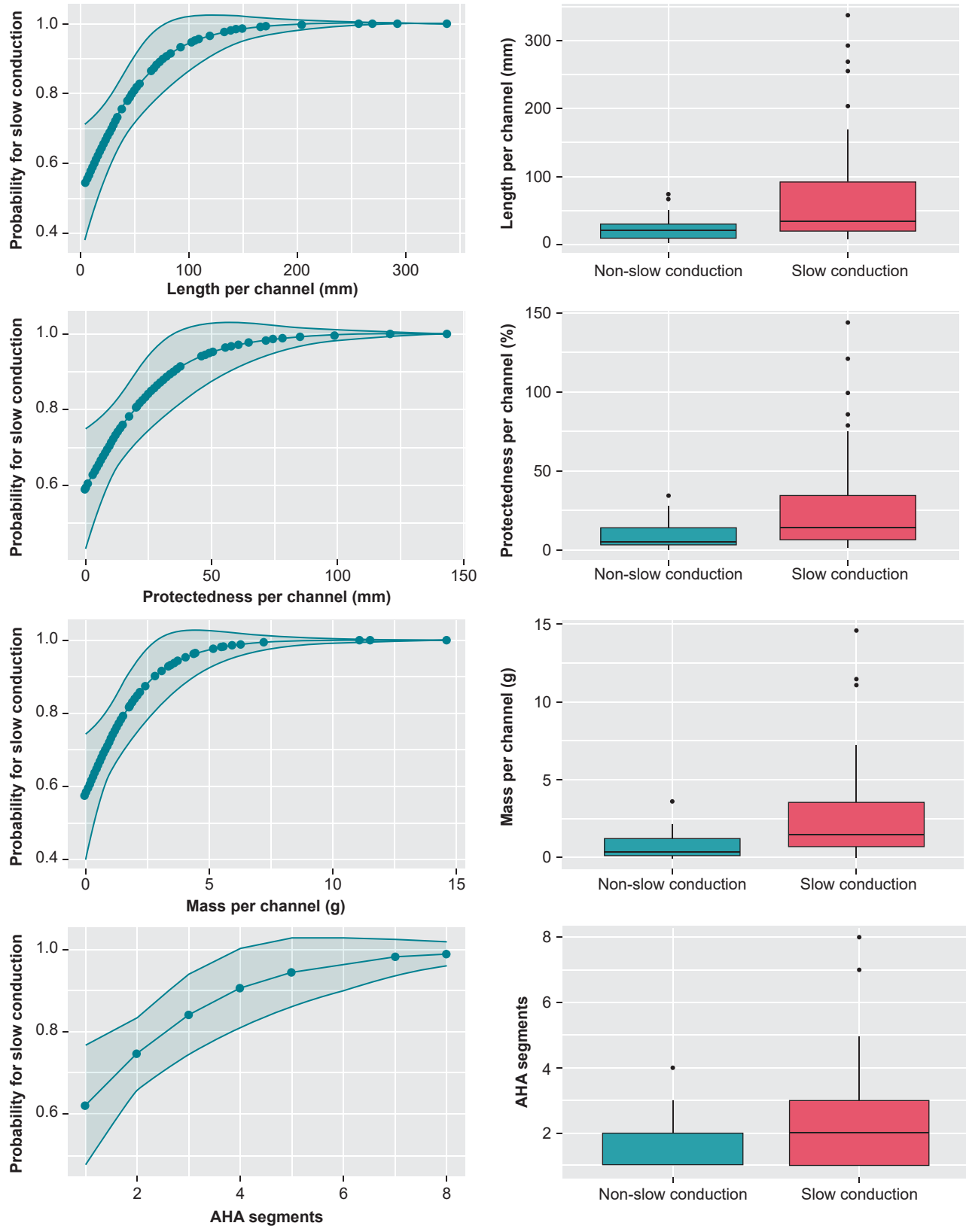

Figure 3 Predictions of the probability of slow conduction with logistic regression for length, mass, protectedness, and cumulative number of affected American Heart Association (AHA) segments.

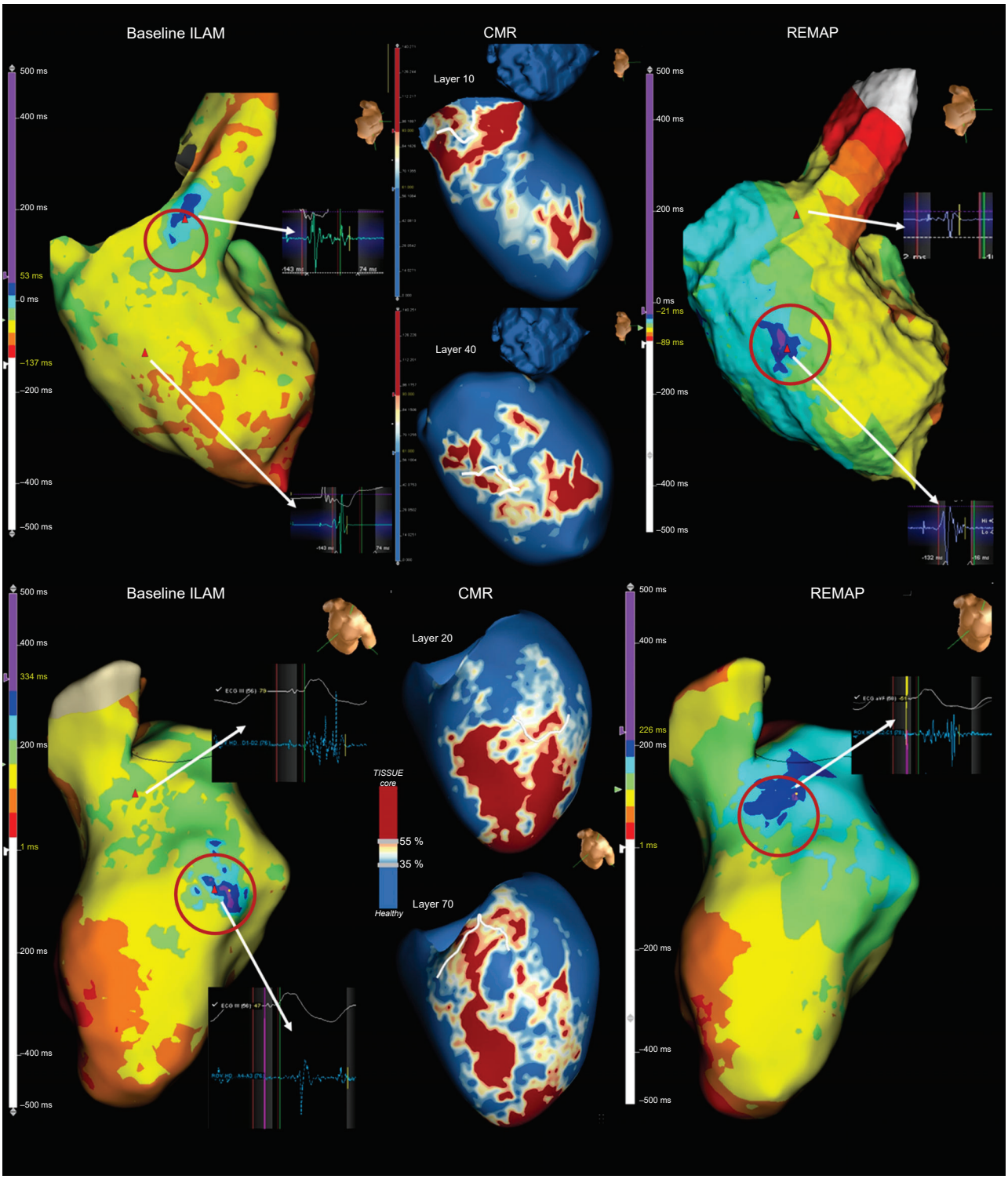

Figure 4 Examples of ILAM and CMR of two patients. In the upper panel, a basal anteroseptal endocardium channel correlated with a DZ in the baseline map. The remap shows how the primary DZ is eliminated, but a new DZ appears (not present in the baseline map), which is also correlated with CMR channels. The lower panel shows the mid-ventricle epicardial channel within the scar correlated with a DZ in the endocardial map. After ablating this primary DZ, a second DZ is shown. This area already showed LAVA in the initial map, but because of the ILAM method, it was not initially detected, and only after ablation of the DZ with the latest EGM was LAVA seen in the ILAM. Interestingly, this new DZ also correlated with CMR channels (DZs are shown in circles). CMR, cardiac magnetic resonance; DZ, deceleration zone; ILAM, isochronal late activation mapping; LAVA, local abnormal ventricular activity.

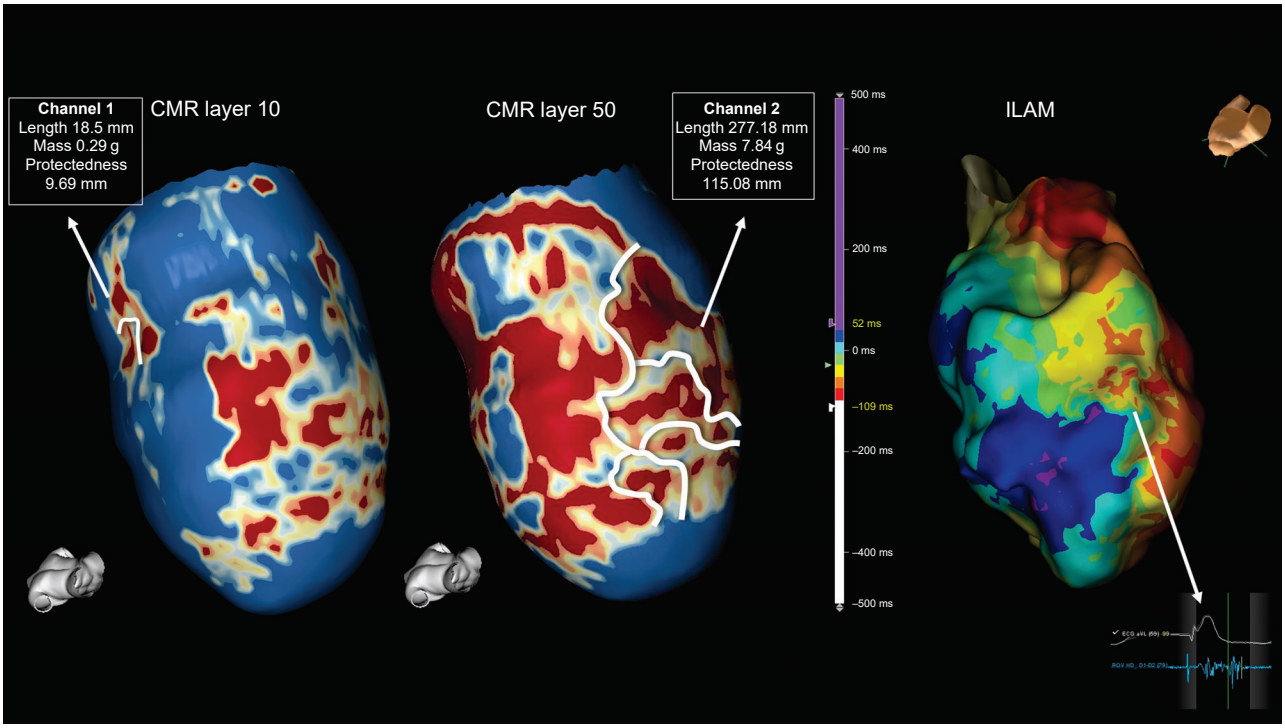

Figure 5 Cardiac magnetic resonance showing two different channels: Channel 1 located exclusively in the first endocardial layer with a shorter length, mass, and protectedness. Channel 2 observed in nine out of nine layers (transmural). ILAM shows a wide area with slow conduction properties correlated with Channel 2. CMR, cardiac magnetic resonance; ILAM, isochronal late activation mapping.

ejection fraction.[26,27] Indeed, a previous study from our group[28] in 2021 identified the absence of channels as a variable with a high negative predictive value of VT events in patients with primary prevention, suggesting that those with <10 g of scar tissue and without CCs were at very low risk of having appropriate therapies (5.26 vs. 25.31% per year, $P = 0.034$).

On the other hand, VT ablation guided by CMR has been widely developed by Berruezo *et al.* Initially, the scar dechanneling technique[17] suggested, in a non-randomized trial, that ablation of CCs based exclusively on CMR was effective with a lower need for RF delivery, higher non-inducibility rates after substrate ablation, and a higher VT recurrence-free survival.[10] However, on the one hand, it has been shown in our study that not all CMR channels have arrhythmogenic properties. On the other hand, basal EAM did not contain all the relevant information about arrhythmogenicity, due to the influence of the electrode size and interelectrode spacing and angle of the incoming wavefront on the mapping catheter[29,30] and due to the functional component of the substrate.[19,20,22] In this sense, electrophysiologica manoeuvres to unmask slow conduction could be useful in areas where LGE-CMR shows CCs, but no suspicious EGMs are seen in basal EAM. Therefore, the combination of EAM and CMR could be the best strategy to determine ablation targets. Defining which characteristics of the CMR channels turn them into arrhythmogenic channels is a priority to increase the use of CMR with all its potential applications.

Characteristics of the cardiac magnetic resonance conducting channels showing arrhythmic properties

Our work attempts to characterize CMR channels to define which channels present arrhythmic properties, showing that those with greater length, mass, and protectedness are more likely to be correlated with DZs. Aziz *et al.*[5] show that DZs had a higher correlation with the VT isthmus and were thus able to identify CMR channels that potentially correlated with these slow conduction areas before the VT ablation procedure, which could have an important role in substrate VT ablation. In addition, these results are consistent with those of Sanchez-Somonte *et al.*[11] who analysed the characteristics of CMR channels associated with VT circuits (during VT activation maps, not during sinus- or RV-paced maps) and showed a greater probability of CCs correlated with VT with the same features as we have described (*Figures 5* and *6*).

Overall, our findings confirm the usefulness of CMR to understand 3D arrhythmic substrates. Characteristics of the CMR channels, such as length, mass, and protectedness, could become useful parameters to predict arrhythmic risk and to aid VT ablation, especially with its ability to identify potential areas of slow conduction not seen with conventional maps or only seen after ablation of the first slow conduction areas.

Limitations

One potential limitation of this study is that the correlation between CMR channels and DZs was performed side by side and not merged. The merging process with Ensite Precision is technically challenging because it causes an artificial deformation of the cardiac anatomy. In addition, the merging process is very important in analysing quantitative data. However, for this study, only the correlation was assessed. In this sense, we believe that a side-by-side comparison of EAM and CMR images is an appropriate and reliable method and reproducible in clinical practice. On the other hand, 2 out of 46 CMRs were not analysed in our study due to bad quality, which is a reasonable percentage. Nevertheless, this high percentage in good-quality wideband CMR

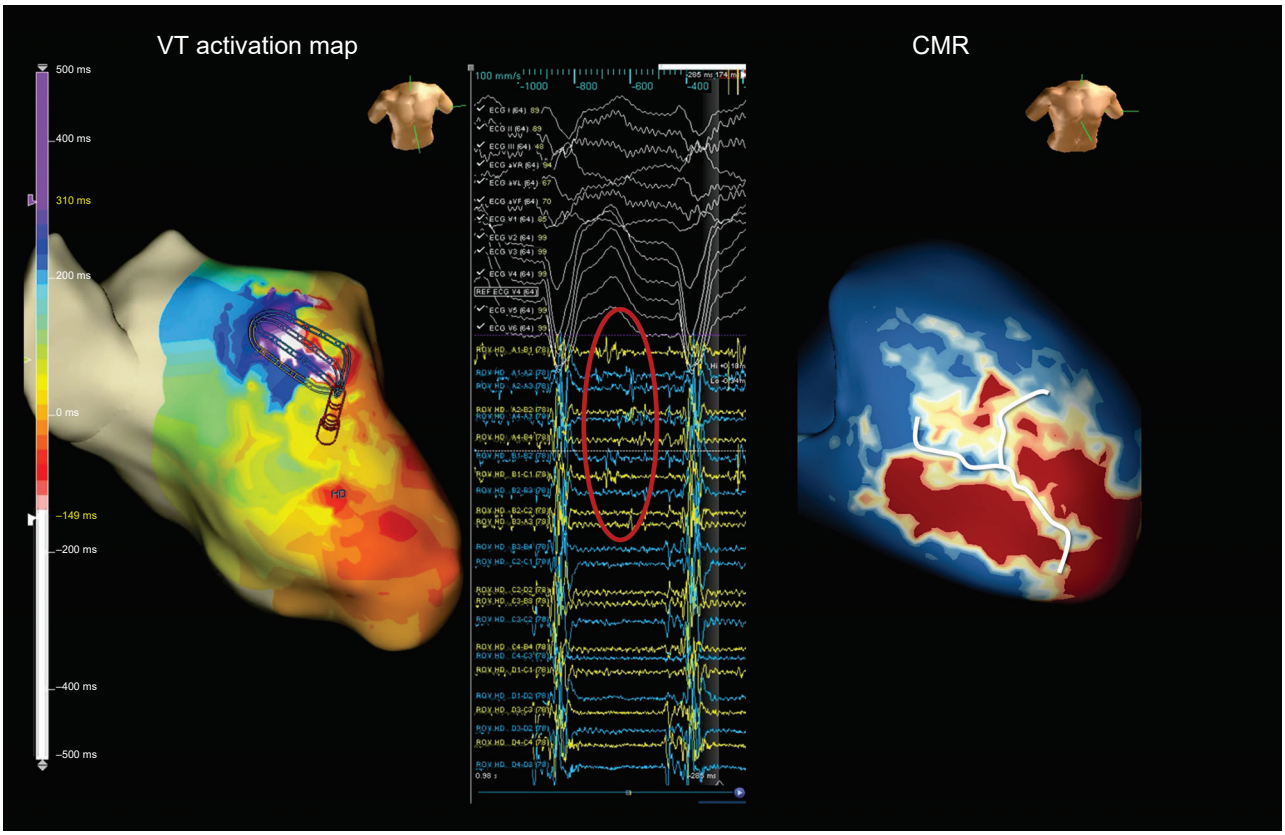

Figure 6 A ventricular tachycardia activation map showing an anterior VT circuit (left panel) with diastolic electrograms (circle) correlating with a long CMR channel (right panel). CMR, cardiac magnetic resonance; VT, ventricular tachycardia.

could be not extrapolated in centres where personnel had less experience.

Another limitation is that most of our cases were performed exclusively through endocardium access, and therefore, the epicardium surface was not mapped. This is attributed to the obvious safety concerns of a systematic endoepicardial approach. This could lead to an underestimation of the total number of detected DZs and, consequently, of the number of channels with slow conduction properties.

Conclusions

Cardiac magnetic resonance–detected conducting channels accurately colocalize with DZs, especially those with a greater length, mass, and protectedness. These findings could illustrate the capability of CMR to depict the arrhythmogenic substrate, leading to multiple potential and relevant clinical applications.

Acknowledgements

The authors thank CERCA Programme/Generalitat de Catalunya.

Funding

This study was supported in part by a grant PI20/00693, Instituto de Salud Carlos III (FEDER), co-funded by the European Union. Madrid, Spain, and the grant 2021_SGR_01350, SGR21/GENCAT, Barcelona, Catalonia, Spain.

Conflict of interest: L.M. and J.B. report activities as consultants, lecturers, and advisory board members for Abbott Medical, Boston Scientific, Biosense Webster, Medtronic, and Biotronik. They are also shareholders of Galgo Medical, S.L. I.R.-L., J.M.T., and A.P.-S. report activities as consultants and lecturers for Biosense Webster, Medtronic, Boston Scientific, and Abbott Medical. J.M.C. is currently an Abbott employee. R.M.F.V. is currently an ADAS 3D employee. All other authors report that they have no relationships relevant to the contents of this paper to disclose.

Data availability

The authors declare that the data that support the findings of this study are available from the corresponding author.

References

1. Tung R, Vaseghi M, Frankel DS, Vergara P, Di BL, Nagashima K *et al.* Freedom from recurrent ventricular tachycardia after catheter ablation is associated with improved survival in patients with structural heart disease: an International VT Ablation Center Collaborative Group study. *Heart Rhythm* 2015;**12**:1997–2007.
2. Arenal A, Glez-Torrecilla E, Ortiz M, Villacastín J, Fdez-Portales J, Sousa E *et al.* Ablation of electrograms with an isolated, delayed component as treatment of unmappable monomorphic ventricular tachycardias in patients with structural heart disease. *J Am Coll Cardiol* 2003;**41**:81–92.
3. Anter E, Kleber AG, Rottmann M, Leshem E, Barkagan M, Tschabrunn CM *et al.* Infarct-related ventricular tachycardia: redefining the electrophysiological substrate of the isthmus during sinus rhythm. *JACC Clin Electrophysiol* 2018;**4**:1033–48.
4. Irie T, Yu R, Bradfield JS, Vaseghi M, Buch EF, Ajijola O *et al.* Relationship between sinus rhythm late activation zones and critical sites for scar-related ventricular tachycardia. *Circ Arrhythm Electrophysiol* 2015;**8**:390–9.
5. Aziz Z, Shatz D, Raiman M, Upadhyay GA, Beaser AD, Besser SA *et al.* Targeted ablation of ventricular tachycardia guided by wavefront discontinuities during sinus rhythm: a new functional substrate mapping strategy. *Circulation* 2019;**140**:1383–97.

6. Andreu D, Ortiz-Pérez JT, Fernández-Armenta J, Guiu E, Acosta J, Prat-González S *et al.* 3D delayed-enhanced magnetic resonance sequences improve conducting channel delineation prior to ventricular tachycardia ablation. *Europace* 2015;**17**:938–45.
7. Fernández-Armenta J, Berruezo A, Andreu D, Camara O, Silva E, Serra L *et al.* Three-dimensional architecture of scar and conducting channels based on high resolution ce-CMR: insights for ventricular tachycardia ablation. *Circ Arrhythm Electrophysiol* 2013;**6**:528–37.
8. Roca-Luque I, van Breukelen A, Alarcon F, Garre P, Tolosana JM, Borras R *et al.* Ventricular scar channel entrances identified by new wideband cardiac magnetic resonance sequence to guide ventricular tachycardia ablation in patients with cardiac defibrillators. *Europace* 2020;**22**:598–606.
9. Soto-Iglesias D, Penela D, Jáuregui B, Acosta J, Fernández-Armenta J, Linhart M *et al.* Cardiac magnetic resonance-guided ventricular tachycardia substrate ablation. *JACC Clin Electrophysiol* 2020;**6**:436–47.
10. Andreu D, Penela D, Acosta J, Fernández-Armenta J, Perea RJ, Soto-Iglesias D *et al.* Cardiac magnetic resonance–aided scar dechanneling: influence on acute and long-term outcomes. *Heart Rhythm* 2017;**14**:1121–8.
11. Sanchez-Somonte P, Garre P, Vázquez-Calvo S, Quinto L, Borràs R, Prat S *et al.* Scar conducting channel characterization to predict arrhythmogenicity during ventricular tachycardia ablation. *Europace* 2023;**30**:989–99.
12. Brugada P, Waldecker B, Kersschot Y, Zehender M, Wellens HJJ. Ventricular arrhythmias initiated by programmed stimulation in four groups of patients with healed myocardial infarction. *J Am Coll Cardiol* 1986;**8**:1035–40.
13. Perez-David E, Arenal Á, Rubio-Guivernau JL, del Castillo R, Atea L, Arbelo E *et al.* Noninvasive identification of ventricular tachycardia-related conducting channels using contrast-enhanced magnetic resonance imaging in patients with chronic myocardial infarction. *J Am Coll Cardiol* 2011;**57**:184–94.
14. Mountantonakis SE, Park RE, Frankel DS, Hutchinson MD, Dixit S, Cooper J *et al.* Relationship between voltage map "channels" and the location of critical isthmus sites in patients with post-infarction cardiomyopathy and ventricular tachycardia. *J Am Coll Cardiol* 2013;**61**:2088–95.
15. Peters NS, Coromilas J, Hanna MS, Josephson ME, Costeas C, Wit AL. Characteristics of the temporal and spatial excitable gap in anisotropic reentrant circuits causing sustained ventricular tachycardia. *Circ Res* 1998;**82**:279–93.
16. Anter E, Neuzil P, Reddy VY, Petru J, Park KM, Sroubek J *et al.* Ablation of reentry-vulnerable zones determined by left ventricular activation from multiple directions: a novel approach for ventricular tachycardia ablation: a multicenter study (PHYSIO-VT). *Circ Arrhythm Electrophysiol* 2020;**13**:e008625.
17. Berruezo A, Fernández-Armenta J, Andreu D, Penela D, Herczku C, Evertz R *et al.* Scar dechanneling. *Circ Arrhythm Electrophysiol* 2015;**8**:326–36.
18. Di Biase L, Santangeli P, Burkhardt DJ, Bai R, Mohanty P, Carbucicchio C *et al.* Endo-epicardial homogenization of the scar versus limited substrate ablation for the treatment of electrical storms in patients with ischemic cardiomyopathy. *J Am Coll Cardiol* 2012;**60**:132–41.
19. Acosta J, Soto-Iglesias D, Jáuregui B, Armenta JF, Penela D, Frutos-López M *et al.* Long-term outcomes of ventricular tachycardia substrate ablation incorporating hidden slow conduction analysis. *Heart Rhythm* 2020;**17**:1696–703.
20. de Riva M, Naruse Y, Ebert M, Androulakis AFA, Tao Q, Watanabe M *et al.* Targeting the hidden substrate unmasked by right ventricular extrastimulation improves ventricular tachycardia ablation outcome after myocardial infarction. *JACC Clin Electrophysiol* 2018;**4**:316–27.
21. Acosta J, Andreu D, Penela D, Cabrera M, Carlosena A, Korshunov V *et al.* Elucidation of hidden slow conduction by double ventricular extrastimuli: a method for further arrhythmic substrate identification in ventricular tachycardia ablation procedures. *Europace* 2018;**20**:337–46.
22. Porta-Sánchez A, Jackson N, Lukac P, Kristiansen SB, Nielsen JM, Gizurarson S *et al.* Multicenter study of ischemic ventricular tachycardia ablation with decrement-evoked potential (DEEP) mapping with extra stimulus. *JACC Clin Electrophysiol* 2018;**4**:307–15.
23. Jackson N, Gizurarson S, Viswanathan K, King B, Massé S, Kusha M *et al.* Decrement evoked potential mapping: basis of a mechanistic strategy for ventricular tachycardia ablation. *Circ Arrhythm Electrophysiol* 2015;**8**:1433–42.
24. Vázquez-Calvo S, Casanovas JM, Garre P, Ferró E, Sánchez-Somonte P, Quinto L *et al.* Evolution of deceleration zones during ventricular tachycardia ablation and relation with cardiac magnetic resonance. *JACC Clin Electrophysiol* 2023;**9**:779–89.
25. Quinto L, Sanchez P, Alarcón F, Garre P, Zaraket F, Prat-Gonzalez S *et al.* Cardiac magnetic resonance to predict recurrences after ventricular tachycardia ablation: septal involvement, transmural channels, and left ventricular mass. *Europace* 2021;**23**:1437–45.
26. Disertori M, Rigoni M, Pace N, Casolo G, Masè M, Gonzini L *et al.* Myocardial fibrosis assessment by LGE is a powerful predictor of ventricular tachyarrhythmias in ischemic and nonischemic LV dysfunction. *JACC Cardiovasc Imaging* 2016;**9**:1046–55.
27. Acosta J, Fernández-Armenta J, Borràs R, Anguera I, Bisbal F, Martí-Almor J *et al.* Scar characterization to predict life-threatening arrhythmic events and sudden cardiac death in patients with cardiac resynchronization therapy. *JACC Cardiovasc Imaging* 2018;**11**:561–72.
28. Sánchez-Somonte P, Quinto L, Garre P, Zaraket F, Alarcón F, Borràs R *et al.* Scar channels in cardiac magnetic resonance to predict appropriate therapies in primary prevention. *Heart Rhythm* 2021;**18**:1336–43.
29. Takigawa M, Relan J, Martin R, Kim S, Kitamura T, Frontera A *et al.* Effect of bipolar electrode orientation on local electrogram properties. *Heart Rhythm* 2018;**15**:1853–61.
30. Vázquez-Calvo S, Garre P, Sánchez-Somonte P, Borras R, Quinto L, Caixal G *et al.* Orthogonal high density mapping with VT isthmus analysis vs. pure substrate VT ablation: a case-control study. *Front Cardiovasc Med* 2022;**9**:912335.

Artículo 5: Resonancia magnética cardíaca para evaluar la profundidad del sustrato ventricular en 3D: Implicaciones pronósticas para el enfoque de ablación de TV

El objetivo de este estudio fue estudiar la profundidad de los canales de RMC como predictor de recurrencia de TV tras una ablación de TV con abordaje exclusivamente endocárdico.

Se incluyeron cincuenta y un pacientes consecutivos con TV relacionada con cicatriz en ventrículo izquierdo sometidos exclusivamente a ablación endocárdica tras realización de RMC en el Hospital Clínic (octubre de 2018-junio de 2022) (72.5% miocardiopatía isquémica). La profundidad de los canales de RMC se calculó en función de las capas involucradas (sobre un total de 9 capas de mismo grosor de endocardio a epicardio) y el grosor total de la pared de los segmentos afectados. Los pacientes con sustrato en ventrículo derecho fueron excluidos por la dificultad para el cálculo detallado de la profundidad de los canales debido al marcado menor grosor de la pared.

Se analizaron 159 canales de RMC. En el análisis univariado, tanto la profundidad máxima del canal como la presencia de un canal epicárdico (definido como aquél que afecta a las 3 capas más exteriores del total de grosor de la pared) fueron los únicos predictores de recurrencia de TV en el seguimiento (OR 1.85 (1.11-3.13), p=0.02 y OR 1.22 (1.15-1.41), p=0.04, respectivamente). Mediante análisis de curva ROC, se estableció un punto de corte para la profundidad máxima del canal de RMC de 7.2 mm con una sensibilidad del 100%, especificidad del 61.36%, valor predictivo negativo (VPN) del 100% y valor predictivo positivo (VPP) del 29%, con un área bajo la curva (AUC) de 0.81 para la recurrencia de TV. La presencia de un canal epicárdico también mostró una sensibilidad y VPN del 100%, pero una menor especificidad (27.27%) y menor VPP (17.95%) que la profundidad máxima del canal. La tasa de recurrencia de TV a un año fue del 13.7%.

Como conclusión, en pacientes con TV relacionada con sustrato en ventrículo izquierdo, la profundidad máxima de los canales de RMC predice la recurrencia de TV después de una ablación endocárdica. Un punto de corte de profundidad máxima del canal de RMC de 7.2 mm podría usarse para seleccionar un enfoque endocárdico exclusivo.

Cardiac magnetic resonance to evaluate 3D ventricular substrate depth: Prognostic implications for VT ablation approach.

Sara Vázquez-Calvo, MD[1,2], Frida Eulogio-Valenzuela, MD[1,2], Pasquale Valerio Falzone, MD[1,2], Paz Garre, BEng[1,2], Till Althoff, MD, PhD [1,2,3], Jean-Baptiste Guichard MD, PhD [1,2], Eduard Guasch, MD, PhD [1,2,3], José María Tolosana, MD, PhD[1,2,3], Roger Borras[1,2], Elena Arbelo, MD, PhD[1,2,3], José T. Ortiz-Pérez, MD, PhD[1,2,3], Susana Prats, MD, PhD[1,2], Rosario J. Perea, MD, PhD[1,2], Josep Brugada, MD, PhD[1,2,3], Lluís Mont, MD, PhD[1,2,3], Andreu Porta-Sanchez, MD, PhD[1,2] and Ivo Roca-Luque, MD, PhD[1,2,3*]

[1]Institut Clinic Cardiovascular, Hospital Clínic, Universitat de Barcelona, Spain.
[2]Institut d'Investigacions Biomèdiques August Pi i Sunyer (IDIBAPS), Barcelona, Spain.
[3]Centro de Investigación Biomédica en Red Enfermedades Cardiovasculares (CIBERCV), Madrid, Spain.

* Address for correspondence:
Ivo Roca-Luque, MD, PhD
Arrhythmia Section, Cardiovascular Clinical Institute,
Hospital Clinic, Universitat de Barcelona
Villarroel, 170
08036 Barcelona, Spain.
iroca@clinic.cat

Disclosure: L.M. and J.B. report activities as consultants, lecturers, and advisory board members for Abbott Medical, Boston Scientific, Biosense Webster, Medtronic, and Biotronik. They are also shareholders of Galgo Medical, S.L.

I.R.L., J.M.T. and A.P.S. report activities as consultants and lecturers for Biosense Webster, Medtronic, Boston Scientific and Abbott Medical.

All other authors report that they have no relationships relevant to the contents of this paper to disclose.

Funding statement: This study was supported in part by a grant PI20/00693, Instituto de Salud Carlos III – FEDER, Madrid, Spain, and the grant 2021_SGR_01350, SGR21/GENCAT, Barcelona, Catalonia, Spain. We thank to CERCA Programme / Generalitat de Catalunya.

Word count: 4972

Short title: CMR channel depth to select VT ablation approach.

Abstract

Background: Substrate-based catheter ablation is an effective procedure for scar-related ventricular tachycardia (VT). Epicardial access may be considered as first strategy in cases where epicardial VT is suspected, even though this approach carries higher risk of severe complications. Cardiac magnetic resonance imaging (CMR) has demonstrated to be a valuable tool for analyzing the arrhythmic substrate and guiding ablation. The impact of CMR channel depth on the selection of the ablation approach has not been studied.

Methods: Fifty-one consecutive patients with scar-related VT undergoing exclusive endocardial ablation after CMR in Hospital Clinic (October 2018-June 2022) were included (72.5% ischemic cardiomyopathy). CMR channels depth was calculated based on the involved layers and the total wall thickness of the affected segments.

Results: Overall, 159 CMR channels were analyzed. In the univariable analysis, both the maximal depth of the channel and the presence of an epicardial channel were the only predictors of VT recurrence (OR 1.85 (1.11-3.13), p=0.02 and OR 1.22 (1.15-1.41), p=0.04, respectively). A maximal channel depth cutoff of 7.2mm showed a sensitivity of 100%, specificity of 61.36%, negative predictive value (NPV) of 100% and positive predictive value (PPV) of 29%, with an AUC=0.81 for VT recurrence. The presence of an epicardial channel also showed 100% of sensitivity and NPV but a worse specificity (27.27%) and PPV (17.95%) than the maximal channel depth. One-year VT recurrence rate was 13.7%.

Conclusions: In patients with left scar-related VT, the maximal depth of CMR channels predicts VT recurrence after endocardial ablation. A maximal CMR channel depth cutoff of 7.2mm could be used to select exclusive endocardial approach.

Keywords: Ventricular tachycardia ablation, cardiac magnetic resonance, wall thickness, channel depth, VT ablation approach, epicardial access.

Abbreviations list: VT=ventricular tachycardia, CMR=cardiac magnetic resonance, ICM= ischemic cardiomyopathy, ICD= implantable cardiac defibrillation, WB=wideband, LGE=late gadolinium enhancement, LP=late potential, LAVA=local abnormal ventricular activity, EGM=electrogram, WT=wall thickness, LVEF=left ventricular ejection fraction

Graphical Abstract

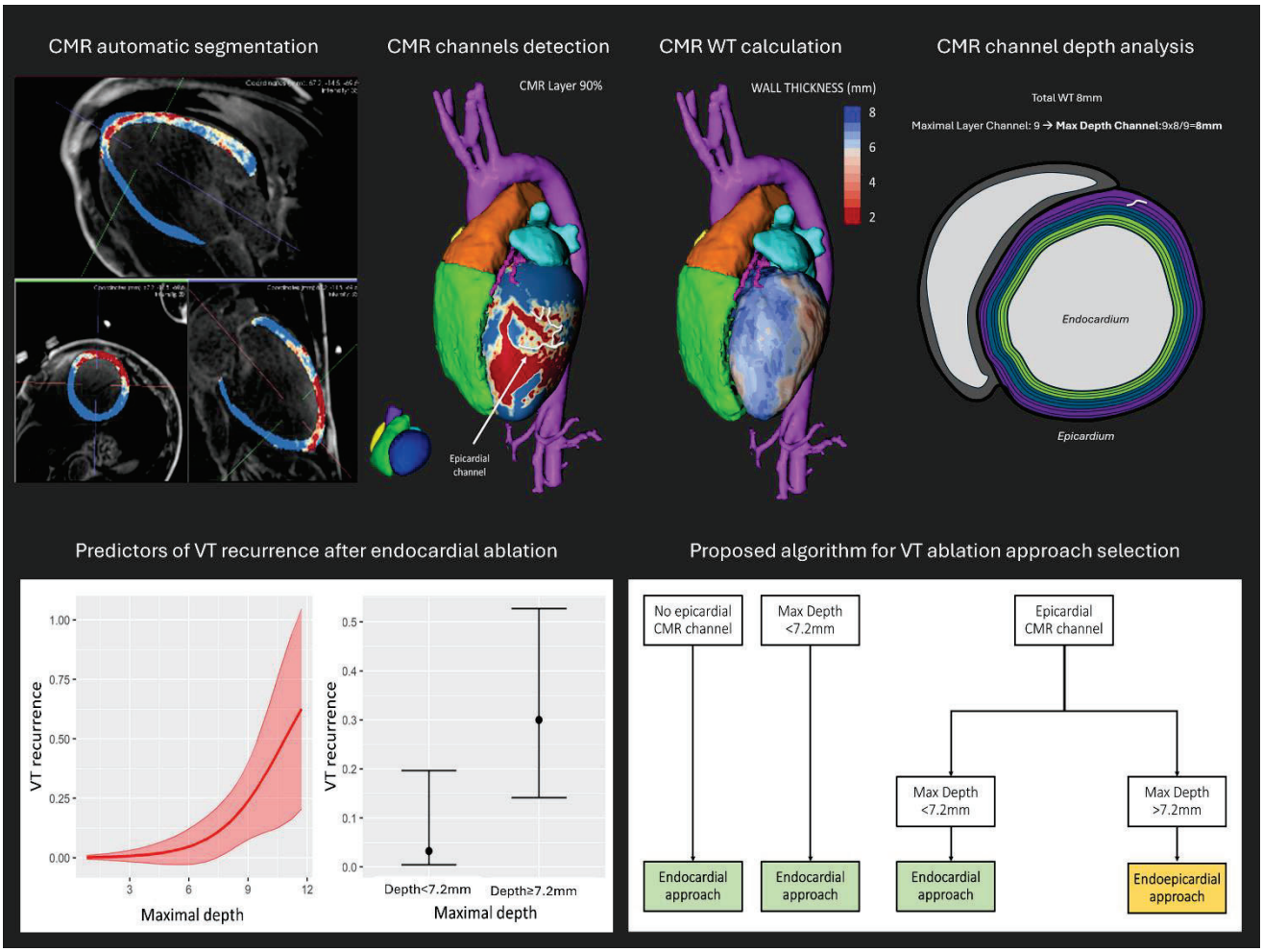

Introduction

Substrate-based catheter ablation is an effective procedure for treating scar-related ventricular tachycardia (VT). Epicardial ablation via subxiphoid access has been a useful option to target complex myocardial scars. There is a general consensus about using the epicardial approach after the initial failure of endocardial VT ablation(1), but as an initial procedure, the indications differ widely between centers(2). Epicardial ablation may be considered based on a high pretest probability of epicardial substrate based on electrocardiographic criteria(3), epicardial scar tissue detected by cardiac magnetic resonance(4) (CMR) or the underlying cardiac disease(5). In this sense, nonischemic cardiomyopathy is associated with a higher burden of epicardial scars(5) and a higher VT recurrence rate after ablation than ischemic cardiomyopathy (37% vs. 20% 1-year VT recurrence rate)(6).

In addition, some studies have shown better clinical outcomes after epicardial ablation in nonischemic patients(7), endo-epicardial ablation in ischemic cardiomyopathy (ICM) patients presenting with an electric storm(8) or demonstrating transmural involvement using cardiac magnetic resonance (CMR)(9,10). Nevertheless, epicardial access through subxiphoid puncture can result in collateral damage to several abdominal and thoracic structures, potentially requiring emergency surgery. An overall risk of 5% and 2% for major and minor complications, respectively, has been reported even in experienced centers(11). Furthemore, other limitations must be addressed, such as the difficulty of accessing the pericardial space after a prior cardiac surgery due to adhesions or the risk of damage to bypass grafts.

On the other hand, adjusting ablation parameter settings, such as an increased application duration, contact force or energy, can modify the depth of the lesion(12). In addition, different ablation strategies, which are usually used for intramural substrates, typically those affecting the septum or

papillary muscles, such as bipolar ablation(13) or the use of half-normal saline as the radiofrequency ablation cooling irrigant(14), have been demonstrated to create deeper lesions.

The correlation between histological samples and electroanatomic maps has been widely studied(15–17), but histological data analyzing the depth of the radiofrequency lesions in the ventricle are limited. Tofig et al.(18) reported that the lesion depth after radiofrequency ablation in a porcine model is smaller in scarred areas than in healthy tissue and, interestingly, found a strong correlation of the lesion depth measured in histological animal tissue samples and on postablation CMR. Glashan et al.(19) studied histological samples from 10 nonischemic cardiomyopathy patients after ablation for VT and observed a median lesion depth of 7.2mm (IQR, 6.1–8.3).

Finally, CMR has emerged as an important tool to analyze the arrhythmic substrate. Its capability to depict healthy tissue, dense scar and border zone allows to identify conducting channels (areas of border zone surrounded by scar and connected to healthy tissue). These conducting channels have not only demonstrated a high correlation with voltage channels(20) deceleration zones(21) (DZ) and VT isthmuses(22) during electroanatomic mapping but also being useful for planning and guiding ablation(23,24).

This study aimed to examine the ventricular substrate depth by CMR to better determine the need for an exclusively endocardial approach.

Methods

The data that support the findings of this study are available from corresponding author upon reasonable request.

Study population

This was a prospective observational study of all consecutive patients with structural heart disease involving the left ventricle who underwent an initial VT ablation procedure with an exclusive endocardial approach at a single center (Hospital Clinic, University of Barcelona) from October 2018 to June 2022. CMR was performed within 6-12 months before ablation. The exclusion criteria of the study were the absence of preprocedural CMR data. All patients provided written informed consent. The study was carried out according to the Declaration of Helsinki guidelines and the deontological code of our institution. The study protocol was approved by the ethics committee of the hospital.

Preprocedural CMR

LGE-CMR was performed if there were no contraindications to the 3 Tesla scan in patients without an implantable cardioverter defibrillator (ICD) or a 1.5 Tesla scan with a wideband (WB) sequence in patients with an ICD to abolish artifacts, as previously described(20,25). For 3 Tesla images, the field of view was covered by a 256 × 240 pixel matrix, and in-plane reconstruction was allowed to achieve an isotropic spatial resolution of 1.4 × 1.4 × 1.4 mm and a voxel size of 2.74 mm(20). On the other hand, WB LGE-CMR images were obtained using a WB inversion pulse sequence (3.8kHz) in serial short-axis slices (5mm slice thickness, no gap) covering the whole LV from the base to the apex(25). After manual segmentation of the left ventricle, a quantitative analysis of the substrate was executed using ADAS 3D software (ADAS 3D, Galgo Medical S.L.). This was accomplished using a standardized and well-established protocol(26). In brief, ADAS 3D created a total of 9 three-dimensional maps from the endocardium to the epicardium. By applying a trilinear interpolation algorithm, the software projected pixel signal intensity maps obtained from the late gadolinium enhancement (LGE) phase of CMR onto each layer. Color coding was

employed with intensity thresholds of 40±5% and 60±5% of the maximum signal. As a result, regions with extensive LGE (≥60%) were designated red, healthy tissue (LGE ≤40%) was indicated in blue, and the intermediate color range represented the border zone with LGE percentages between 40±5% and 60±5%. Channels (defined as areas of border zone surrounded by scar and connected to healthy tissue) and their characteristics, such as length and mass, were detected automatically by the system(26). The wall thickness (WT) of the tissue was also automatically calculated by the software. The minimal and maximal depth from the endocardial surface of each channel was manually determined by dividing the WT of the area into 9 layers and then multiplying them by the first and last layers where the channel was located, respectively (**Fig. 1**). After VT ablation, a thorough examination of all channels was conducted to analyze the correlation between channel characteristics and VT recurrence. .

VT ablation procedure strategy

Procedures were performed under general anesthesia. Access to the left ventricle was achieved with a transseptal and/or retrograde aortic approach. A substrate voltage map and an isochronal late activation map were performed utilizing an HD Grid catheter and the EnSite Precision or Ensite X system (Abbott Medical, USA). Abnormal electrograms such as local abnormal ventricular activity (LAVA) and late potentials (LPs) were manually identified and marked. Deceleration zones (DZ) were defined as regions with isochronal crowding with >3 isochrones within a 1 cm radius, as previously described(27). Postprocessed CMR images were visualized in the navigation system side by side and electroanatomic mapping focused on regions were CMR channels were observed. After delineation of the DZs, the HD Grid catheter was positioned in a potential area for a VT isthmus (slow conduction area and/or middle segment channel according

to CMR channels). VT induction was carried out through programmed electrical stimulation, employing drive cycles ranging from 600ms to 430ms, up to triple extrastimuli or refractoriness, or 200ms. (28). In cases in which induced VT permitted activation mapping, the initial target for ablation was the central VT isthmus. After the VT isthmuses were targeted, substrate ablation was performed by strictly targeting the DZs. Radiofrequency was delivered using an externally irrigated 3.5-mm-tip ablation catheter (TactiCath SE, Abbott Medical) with the following parameters: temperature limit: 45 °C; power limit: 40-50 W; irrigation rate: 26-30 mL/min; minimal contact force: >7 g; and average duration of each ablation: 60 s. The procedural endpoint was the abolition of DZs, LAVA and LPs as well as the lack of VT inducibility at the end of the procedure.

Clinical follow-up

During the one-year follow-up, we monitored patients for arrhythmic recurrence considered as any VT events detected by ICD (with or without therapies) or requiring medical attention. Throughout the follow-up period, any cases of mortality were classified as either cardiovascular or non-cardiovascular.

Statistical analysis

Continuous variables are presented as the mean±standard deviation with range, and a t test was used to compare the means of two variables. Categorical variables are expressed as the total number or percentage and were compared with the chi squared test. ROC curve analysis with Youden's index was used to define the optimal cutoff value for recurrence prediction. Predictors of VT recurrence at one year were assessed using logistic regression analyses, and odds ratios were

computed. All analyses were performed with SPSS version 26.0 (SPSS, USA) and R software version 4.3.0 (R project for Statistical Computing; Austria). All statistical tests were two-sided, and a p value <0.05 was considered statistically significant.

Results

Study population, VT ablation procedure and follow-up

Between October 2018 and June 2022, 120 patients underwent ablation procedures for scar-related VT at our institution. Thirty-eight patients were excluded due to the inability to perform CMR (arrhythmic storm, claustrophobia, etc.) or due to poor-quality CMR images (4 patients). Six patients were excluded for having right ventricular substrate assessed by CMR, 20 patients for having a previous VT ablation, 2 for complications that didn´t allow to complete the procedure and 3 for using an endo-epicardial or epicardial approach (2 for intraventricular thrombus and 1 due to operator´s preferences in a patient with Chagas disease). The flowchart of the study is shown in **Fig. 2**. Overall, 51 patients were included in the study. The median age was 65.56±11.46 years, 94.1% of patients were male, and the median ejection fraction was 31.82±8.76%. A total of 72.5% had ischemic cardiomyopathy. Among patients without ischemic cardiomyopathy, 6 patients presented with idiopathic dilated cardiomyopathy, 2 with arrhythmogenic cardiomyopathy, 3 with valvular cardiomyopathy, one with enolic cardiomyopathy, one with congenital heart disease and one with hypertrophic cardiomyopathy. A total of 19.6% presented with VT storm. Patient demographics are summarized in **Table 1**. In 70.8% of patients, 1.5 Tesla CMR with a WB sequence was performed.

An endocardial approach was performed in all patients, with a transseptal approach in the majority of patients (94.1%) combined with retro-aortic access in 62.7% of patients. During the basal

electrophysiological study, VT was inducible in 90.2% of patients, with a median of 1.86±1.2 VTs induced per patient. The ablation procedure characteristics are shown in **Table 2**.

After one year of follow-up, 2 patients died due to nonarrhythmia-related events. The rate of VT recurrence after one year of follow-up was 13.7% (7/51) [8.11% (4/37) in ischemic cardiomyopathy and 21.4% (3/14) in nonischemic cardiomyopathy patients).

LGE-CMR characteristics and predictors of VT recurrence

A total of 159 CMR channels were studied (3.10±2.01 channels per patient). The median length per channel was 61.93±8.15mm, with a median mass of 2.19±0.33g. The median WT of the channel area was 7.98±2.27mm. Considering all CMR channels, the median minimal and maximal depth per channel was 3.01±0.26mm and 4.89±0.30mm, respectively. A higher presence of endocardial channels (70.6% vs. 44.5%, p=0.02) was found in ischemic patients than in nonischemic patients, with the minimal depth of channels being lower in ischemic patients (2.65±0.29 vs. 3.93±0.46mm, p=0.02). A comparison of channel characteristics between ischemic and nonischemic patients is shown in Table 3.

After performing a univariable analysis, the presence of an epicardial channel and the maximal depth of the deepest channel per patient were the only predictors of VT recurrence in the follow-up period (OR 1.22 (0.15, 1.41), p= 0.04 and OR 1.85 (1.11, 3.13), p=0.02, respectively) **(Fig. 3).** The maximal depth cutoff of 7.2mm showed a sensitivity of 100%, specificity of 61.36%, negative predictive value (NPV) of 100% and positive predictive value (PPV) of 29%, with an area under the curve of 0.81 **(Fig. 4 and Fig. 5).** The presence of an epicardial channel also showed a sensitivity of 100% and NPV of 100% but a worse specificity (27.27%) and PPV (17.95%) than the maximal depth of the channel.

Interestingly, 75.78% (28/37) of ischemic patients presented an epicardial channel vs. 75.57% (11/14) of nonischemic patients. Only 35% (13/37) of ischemic patients presented a channel with a maximal depth greater than 7.2 mm vs. 50% (7/14) of nonischemic patients.

Nonischemic myocardiopathy was not significantly associated with a higher risk of VT recurrence after endocardial ablation in our study (OR 2.25 [0.43 to 11.66], p 0.34). Other CMR parameters, such as LV mass, BZ mas or scar mass were not predictors of VT recurrence (table 4). Moreover, we assessed the differences between ischemic and non-ischemic cardiomyopathy in terms of VT recurrence for all predictors and no statistically significative interaction was found.

Discussion

The major findings from this study are as follows:

1. In patients with structural heart disease undergoing exclusive endocardial VT ablation, the maximal depth of CMR channels could predict VT recurrence in the follow-up.
2. A maximal CMR channel depth cutoff of 7.2mm could be used to select an exclusively endocardial approach instead of an endo-epicardial approach for VT ablation procedures.

Endocardial vs. *epicardial approach for scar-related VT ablation*

The epicardial approach is attributed to an overall risk of 5% for acute and 2% for delayed major complications. In addition, challenges such as mapping difficulties arising from adhesions or bypasses, along with complexities in identifying arrhythmic substrate due to the presence of adipose tissue, limits success of epicardial ablation. Typically, the epicardial approach is reserved for selected cases, primarily those with previous unsuccessful endocardial ablation(1). Nevertheless, certain centers consider it a first-line option based on ECG(3) or imaging(4)

indications of epicardial involvement. Several attempts have been made to better stratify the need for an epicardial approach. In 2013, Andreu et al.(4) examined the relationship between the VT termination site and ablation location (endocardial vs. epicardial) in 80 patients: among ischemic cardiomyopathy patients, epicardial ablation was unnecessary in 94% of cases, whereas among nonischemic patients, epicardial ablation was needed in more than half of the patients. Other studies also reinforce the concept of greater necessity for epicardial ablation in nonischemic patients, attributed to a heightened prevalence of epicardial substrate(5) and poorer clinical outcomes postablation(6). Along these lines, our study showed a smaller number of endocardial channels in nonischemic than ischemic patients (44.5% vs 70.6%, p=0.02) and a higher minimal distance to the channel in nonischemic cardiomyopathy patients (3.93±0.46 vs 2.65±0.29, p=0.02). This underscores the need for more rigorous efforts within this population, as suggested in the literature.

Regarding the ablation approach in ICM patients, certain groups have proposed the necessity of a systematic epicardial approach in all cases(29–31). Di Biase et al.(8) conducted a nonrandomized study in 2012 involving 92 ischemic patients undergoing an initial VT ablation procedure. Patients were divided into two distinct nonrandomized cohorts: patients in one cohort underwent solely endocardial ablation, while those in the other cohort were treated via an endo-epicardial approach. The outcomes illuminated enhanced clinical efficacy in the endo-epicardial ablation group, with VT recurrence rates after a 22-month follow-up period of 19% vs. 37%. Similarly, Acosta et al.(9) pursued a deeper understanding of the necessity for epicardial access by focusing on the presence of transmural scars on CMR. In this population, improved clinical results were found in patients who underwent endo-epicardial ablation compared to those undergoing exclusively endocardial ablation (VT recurrence rate after a median follow-up of 22 months: 12.5% vs. 40.6%).

Additionally, acceptable clinical outcomes were noted in patients with subendocardial scars who exclusively underwent endocardial ablation (14.7%). However, WT data were not provided in any of these studies. Interestingly, in the Di Biase study(8), within the endo-epicardial group, epicardial RF delivery was needed in only a mere 33% of patients after epicardial substrate mapping. Remarkably, along the same line, only 35% of the ischemic population of our study would be selected for endo-epicardial ablation using the threshold of a CMR channel deeper than 7.2 mm as a criterion vs. 75.78% using the presence of an epicardial channel without considering the depth of the channel as a criterion. Therefore, the implementation of this channel depth threshold could enhance the identification of patients who could undergo ablation via endocardial approach, thereby avoiding the epicardial approach in the rest of the patients and consequently mitigating the risk of potential major complications for most of them. Yuki et al.(32) sought to address epicardial substrate elimination through endocardial ablation, using the presence of LAVA signals as the defining criterion. Their approach resulted in the successful endocardial eradication of 83% of epi-LAVA in patients with ischemic cardiomyopathy and 23% in those with nonischemic cardiomyopathy. Interestingly, they noted a clear enhancement of these percentages when targeting endocardial ablation within regions characterized by a wall thickness (WT) of less than 5 mm. The establishment of this specific threshold was suggested by a prior study by Yuki et al.(33), which showed that 100% of LAVA potentials were located within areas exhibiting a WT<5 mm, measured by CT scan, or at its border, in the context of ischemic cardiomyopathy.

Our study reinforces the importance of the WT in considering the need for an exclusively endocardial approach. Specifically, our proposal integrated data from CMR channels, which has demonstrated a strong correlation with voltage channels(4) and deceleration zones(21) in previous research (Fig 6). Among patients with structural heart disease undergoing endocardial VT ablation,

the maximal depth of CMR channels (OR 1.85, p=0.02) predicts VT recurrence in the follow-up period better than the type of cardiomyopathy (OR 2.25, p=0.34). In the same line, the use of the presence of an epicardial channel instead of the maximal depth of the CMR channel mimicking the criteria of transmural or epicardial scarring in any cardiac image would lead to many unnecessary epicardial procedures (specificity: 27.27% vs. 61.36%, respectively), with a consequent risk of major complications. Notably, a threshold of 7.2mm emerges as a potentially optimal criterion for determining the approach for VT ablation (**Figs. 7 and 8**).

Radiofrequency lesion depth

Due to the impossibility of visualizing lesion formation in real time, different surrogate measures of lesion quality have been used by combining different parameters, including the local impedance drop, contact force, supplied energy and radiofrequency application duration. These parameters have been combined to create different ablation markers, such as the Force–Time Integral or Ablation Index, which have been extensively studied in the atrium but barely in the ventricle(12,34). Tofig et al.(18) reported that the lesion depth after radiofrequency ablation was smaller in scarred areas than in healthy tissue and, interestingly, found a strong correlation of the lesion depth measured in histological animal tissue samples and measured on postablation CMR, suggesting that CMR could be a useful tool for analyzing ablation lesions. In 2020, You Mi Hwang et al.(35) studied the role of power, force and time in lesion formation in an animal model, obtaining a maximal depth of 6.98mm with 30W, 10g and 50s. Similarly, a study performed by Glashan et al.(19) in 2021 analyzed histological samples from ten patients with nonischemic cardiomyopathy who died after VT ablation (median time, 39 days). The ablation settings (irrigated tip catheter, 45-50W, 30mL/min normal saline, maximum temp of 43°C, CF>9 and 60s) were very

similar to those used in our study (irrigated tip catheter, 40-50W, irrigation 26-30mL/min with normal saline, temperature limit of 45°C, CF>7g and 60s). Under these settings, the mean depth of lesions assessed by histology in the Glashan study was 7.22mm (IQR, 6.1–8.3). In this sense, our proposed cutoff of 7.2mm fits with the results of previous studies according to lesion formation and could be useful as a criterion as long as the ablation settings remain stable. Decreasing the contact force, application duration or delivered energy could lead to the creation of shallower lesions.

Limitations

Some limitations must be addressed. First, this study was designed as a prospective study encompassing consecutively enrolled patients exhibiting left ventricular substrate and undergoing an initial endocardial VT ablation procedure following CMR assessment. It is important to note that patients with right ventricular substrate, primarily affected by arrhythmogenic cardiomyopathy, were excluded. This decision was prompted by the intricacies involved in determining the WT within the right ventricle, which is notably thinner than the left ventricle. This substantial disparity in thickness between the two chambers introduces challenges when attempting to draw meaningful comparisons between their respective structures. Furthermore, it should be acknowledged that a substantial majority of our study population exhibited ischemic cardiomyopathy (72.5%). Additionally, it should be noted that patients with non-ischemic cardiomyopathy often exhibit a higher prevalence of epicardial scars(5). Consequently, the endeavor to establish differences between ischemic and nonischemic patients or to delineate variances among diverse subcategories of nonischemic cardiomyopathy may present challenges given the relatively modest size of this particular subgroup. Another potential limitation arises

from the analysis of VT recurrence based on channel depth, whereas our ablation protocol fundamentally involves eliminating deceleration zones rather than ablating CMR channels. Nonetheless, a previous study of our group has evidenced a remarkably high correlation between deceleration zones and CMR channels (93.68%)(21).

Conclusions

In patients with left scar-related VT, the maximal depth of CMR channels is a predictor of VT recurrence after endocardial VT ablation. A maximal CMR channel depth cutoff of 7.2mm could be used to select the VT ablation approach.

Clinical perspectives

COMPETENCY IN MEDICAL KNOWLEDGE: The present study constitutes the first report on analyze the CMR channel depth after an endocardial VT ablation procedure demonstrating its role as a predictor of VT recurrence. In addition, a CMR channel depth cutoff of 7.2mm could be used to depict which patients could be ablated, using a standard VT ablation setting, exclusively with an endocardial approach.

TRANSLATIONAL OUTLOOK: CMR channel depth can be easily calculated for all patients with left-scar VT related, being a potential interesting tool to choose VT ablation approach and avoid the risk of an unnecessary epicardial puncture. Further studies using CMR channel depth are needed to validate this novel parameter.

Bibliography

1. Schmidt B., Chun KRJ., Baensch D., et al. Catheter ablation for ventricular tachycardia after failed endocardial ablation: Epicardial substrate or inappropriate endocardial ablation? Heart Rhythm 2010;7(12):1746–52. Doi: 10.1016/j.hrthm.2010.08.010.
2. Roderick Tung MD., Kalyanam Shivkumar MD, PhD. Indications for Epicardial Mapping and Ablation. 2015.
3. Berruezo A., Mont L., Nava S., Chueca E., Bartholomay E., Brugada J. Electrocardiographic Recognition of the Epicardial Origin of Ventricular Tachycardias. Circulation 2004;109(15):1842–7. Doi: 10.1161/01.CIR.0000125525.04081.4B.
4. Andreu D., Ortiz-Pérez JT., Boussy T., et al. Usefulness of contrast-enhanced cardiac magnetic resonance in identifying the ventricular arrhythmia substrate and the approach needed for ablation. Eur Heart J 2014;35(20):1316–26. Doi: 10.1093/eurheartj/eht510.
5. Mahrholdt H., Wagner A., Judd RM., Sechtem U., Kim RJ. Delayed enhancement cardiovascular magnetic resonance assessment of non-ischaemic cardiomyopathies. Eur Heart J 2005:1461–74. Doi: 10.1093/eurheartj/ehi258.
6. Aziz Z., Shatz D., Raiman M., et al. Targeted Ablation of Ventricular Tachycardia Guided by Wavefront Discontinuities during Sinus Rhythm: A New Functional Substrate Mapping Strategy. Circulation 2019;140(17):1383–97. Doi: 10.1161/CIRCULATIONAHA.119.042423.
7. Dinov B., Fiedler L., Schönbauer R., et al. Outcomes in catheter ablation of ventricular tachycardia in dilated nonischemic cardiomyopathy compared with ischemic cardiomyopathy: Results from the prospective heart centre of leipzig vt. Circulation 2014;129(7):728–36. Doi: 10.1161/CIRCULATIONAHA.113.003063.
8. Di Biase L., Santangeli P., Burkhardt DJ., et al. Endo-epicardial homogenization of the scar versus limited substrate ablation for the treatment of electrical storms in patients with ischemic cardiomyopathy. J Am Coll Cardiol 2012;60(2):132–41. Doi: 10.1016/j.jacc.2012.03.044.
9. Acosta J., Fernández-Armenta J., Penela D., et al. Infarct transmurality as a criterion for first-line endo-epicardial substrate-guided ventricular tachycardia ablation in ischemic cardiomyopathy. Heart Rhythm 2016;13(1):85–95. Doi: 10.1016/j.hrthm.2015.07.010.
10. Quinto L., Sanchez P., Alarcón F., et al. Cardiac magnetic resonance to predict recurrences after ventricular tachycardia ablation: septal involvement, transmural channels, and left ventricular mass. EP Europace 2021;23(9):1437–45. Doi: 10.1093/europace/euab127.
11. Sacher F., Roberts-Thomson K., Maury P., et al. Epicardial Ventricular Tachycardia Ablation. A Multicenter Safety Study. J Am Coll Cardiol 2010;55(21):2366–72. Doi: 10.1016/j.jacc.2009.10.084.
12. Proietti R., Lichelli L., Lellouche N., Dhanjal T. The challenge of optimising ablation lesions in catheter ablation of ventricular tachycardia. J Arrhythm 2021:140–7. Doi: 10.1002/joa3.12489.

13. Sivagangabalan G., Barry MA., Huang K., et al. Bipolar ablation of the interventricular septum is more efficient at creating a transmural line than sequential unipolar ablation. PACE - Pacing and Clinical Electrophysiology 2010;33(1):16–26. Doi: 10.1111/j.1540-8159.2009.02602.x.
14. Nguyen DT., Gerstenfeld EP., Tzou WS., et al. Radiofrequency Ablation Using an Open Irrigated Electrode Cooled With Half-Normal Saline. 2017.
15. Tung R., Nakahara S., Ramirez R., et al. Accuracy of combined endocardial and epicardial electroanatomic mapping of a reperfused porcine infarct model: A comparison of electrofield and magnetic systems with histopathologic correlation. Heart Rhythm 2011;8(3):439–47. Doi: 10.1016/j.hrthm.2010.10.044.
16. Reddy VY., Wrobleski D., Houghtaling C., Josephson ME., Ruskin JN. Combined Epicardial and Endocardial Electroanatomic Mapping in a Porcine Model of Healed Myocardial Infarction. Circulation 2003;107(25):3236–42. Doi: 10.1161/01.CIR.0000074280.62478.E1.
17. Callans DJ., Ren J-F., Michele J., Marchlinski FE., Dillon SM. Electroanatomic Left Ventricular Mapping in the Porcine Model of Healed Anterior Myocardial Infarction. Circulation 1999;100(16):1744–50. Doi: 10.1161/01.CIR.100.16.1744.
18. Tofig BJ., Lukac P., Nielsen JM., et al. Radiofrequency ablation lesions in low-, intermediate-, and normal-voltage myocardium: An in vivo study in a porcine heart model. Europace 2019;21(12):1919–27. Doi: 10.1093/europace/euz247.
19. Glashan CA., Stevenson W., Zeppenfeld K. Lesion Size and Lesion Maturation after Radiofrequency Catheter Ablation for Ventricular Tachycardia in Humans with Nonischemic Cardiomyopathy. Circ Arrhythm Electrophysiol 2021:E009808. Doi: 10.1161/CIRCEP.121.009808.
20. Andreu D., Ortiz-Pérez JT., Fernández-Armenta J., et al. 3D delayed-enhanced magnetic resonance sequences improve conducting channel delineation prior to ventricular tachycardia ablation. Europace 2015;17(6):938–45. Doi: 10.1093/europace/euu310.
21. Vázquez-Calvo S., Casanovas JM., Garre P., et al. Evolution of Deceleration Zones During Ventricular Tachycardia Ablation and Relation With Cardiac Magnetic Resonance. JACC Clin Electrophysiol 2023. Doi: 10.1016/j.jacep.2022.12.015.
22. Sanchez-Somonte P., Garre P., Vázquez-Calvo S., et al. Scar conducting channel characterization to predict arrhythmogenicity during ventricular tachycardia ablation. EP Europace 2023. Doi: 10.1093/europace/euac257.
23. Zghaib T., Ipek EG., Hansford R., et al. Standard Ablation Versus Magnetic Resonance Imaging-Guided Ablation in the Treatment of Ventricular Tachycardia. Circ Arrhythm Electrophysiol 2018;11(1):1–4. Doi: 10.1161/CIRCEP.117.005973.
24. Soto-Iglesias D., Penela D., Jáuregui B., et al. Cardiac Magnetic Resonance-Guided Ventricular Tachycardia Substrate Ablation. JACC Clin Electrophysiol 2020;6(4):436–47. Doi: 10.1016/j.jacep.2019.11.004.
25. Roca-Luque I., Van Breukelen A., Alarcon F., et al. Ventricular scar channel entrances identified by new wideband cardiac magnetic resonance sequence to guide ventricular tachycardia ablation in patients with cardiac defibrillators. EP Europace 2020;22(4):598–606. Doi: 10.1093/europace/euaa021.

26. Andreu D., Penela D., Acosta J., et al. Cardiac magnetic resonance–aided scar dechanneling: Influence on acute and long-term outcomes. Heart Rhythm 2017;14(8):1121–8. Doi: 10.1016/j.hrthm.2017.05.018.
27. Irie T., Yu R., Bradfield JS., et al. Relationship between sinus rhythm late activation zones and critical sites for scar-related ventricular tachycardia. Circ Arrhythm Electrophysiol 2015;8(2):390–9. Doi: 10.1161/CIRCEP.114.002637.
28. de Chillou C., Groben L., Magnin-Poull I., et al. Localizing the critical isthmus of postinfarct ventricular tachycardia: the value of pace-mapping during sinus rhythm. Heart Rhythm 2014;11(2):175–81. Doi: 10.1016/j.hrthm.2013.10.042.
29. Mohanty S., Trivedi C., Di Biase L., et al. Endocardial Scar-Homogenization With vs Without Epicardial Ablation in VT Patients With Ischemic Cardiomyopathy. JACC Clin Electrophysiol 2022;8(4):453–61. Doi: 10.1016/j.jacep.2021.12.011.
30. Sarkozy A., Tokuda M., Tedrow UB., et al. Epicardial Ablation of Ventricular Tachycardia in Ischemic Heart Disease. Circ Arrhythm Electrophysiol 2013;6(6):1115–22. Doi: 10.1161/CIRCEP.113.000467.
31. Izquierdo M., Sánchez-Gómez JM., Ferrero de Loma-Osorio A., et al. Endo-Epicardial Versus Only-Endocardial Ablation as a First Line Strategy for the Treatment of Ventricular Tachycardia in Patients With Ischemic Heart Disease. Circ Arrhythm Electrophysiol 2015;8(4):882–9. Doi: 10.1161/CIRCEP.115.002827.
32. Komatsu Y., Daly M., Sacher F., et al. Endocardial ablation to eliminate epicardial arrhythmia substrate in scar-related ventricular tachycardia. J Am Coll Cardiol 2014;63(14):1416–26. Doi: 10.1016/j.jacc.2013.10.087.
33. Komatsu Y., Cochet H., Jadidi A., et al. Regional myocardial wall thinning at multidetector computed tomography correlates to arrhythmogenic substrate in postinfarction ventricular tachycardia: Assessment of structural and electrical substrate. Circ Arrhythm Electrophysiol 2013;6(2):342–50. Doi: 10.1161/CIRCEP.112.000191.
34. Ikeda A., Nakagawa H., Lambert H., et al. Relationship between catheter contact force and radiofrequency lesion size and incidence of steam pop in the beating canine heart: Electrogram amplitude, impedance, and electrode temperature are poor predictors of electrode-tissue contact force and lesion size. Circ Arrhythm Electrophysiol 2014;7(6):1174–80. Doi: 10.1161/CIRCEP.113.001094.
35. Hwang YM., Lee WS., Choi KJ., Kim YR. Radiofrequency induced lesion characteristics according to force-time integral in experimental model. Medicine (United States) 2021;100(10):E25126. Doi: 10.1097/MD.0000000000025126.

Figure titles and legends

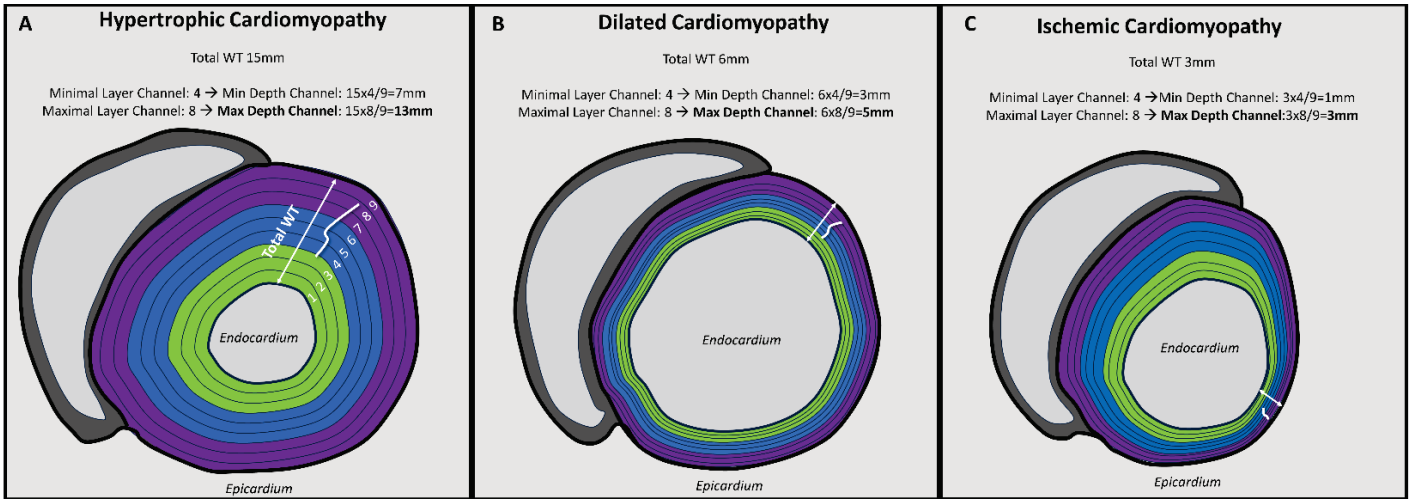

Fig. 1: Graphical representation of different arrhythmic substrates and the calculation of the minimal and maximal depth of a CMR channel based on the total WT and the channel position within the layers. Notice the presence of a mid-epicardial CMR channel that, despite affecting the same number of layers in the three examples (from 4 to 8), clearly varies in depth depending on the total WT. A) Hypertrophic cardiomyopathy with a thick wall (total WT of 15mm, minimal channel depth of 7mm, maximal depth of 13mm). B) Nonischemic dilated cardiomyopathy showing a thin myocardial wall with a smaller WT (total of 6mm, minimal channel depth of 3mm, maximal depth of 5mm). C) Ischemic cardiomyopathy with a very thin total WT (3mm) in the infero-lateral wall, a minimal channel depth of 1mm and a maximal depth of 3mm.

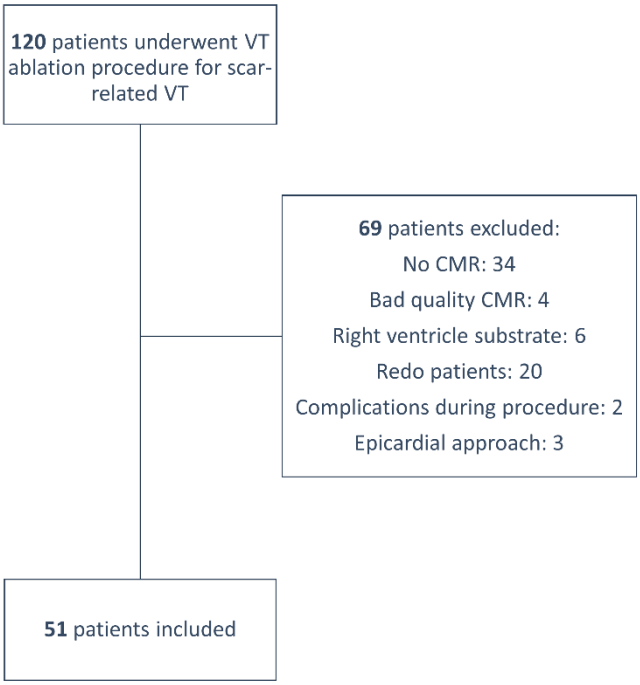

Fig. 2: Study flowchart.

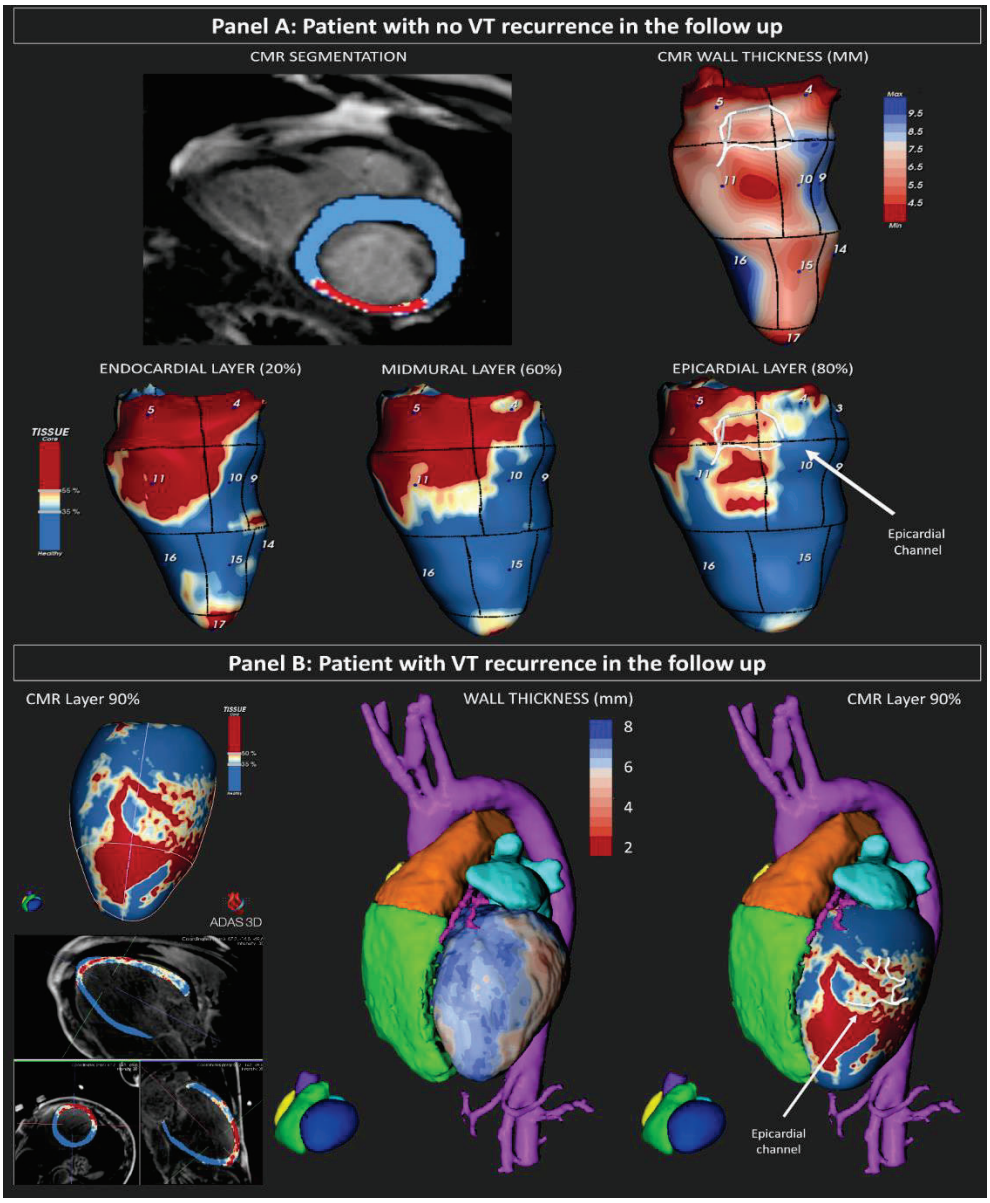

Fig. 3: Two examples of visualization of CMR channels according to layers and wall thickness. Panel A: CMR segmentation of the left ventricle in a patient with ischemic cardiomyopathy. The automatic CMR channel computation reveals an epicardial CMR channel located within an inferior transmural scar characterized by a WT<6mm. Panel 2: A similar example of an epicardial channel (affecting layer 9) in this case from a nonischemic cardiomyopathy patient. The region exhibits a notable WT>8mm. Remarkably, this patient experienced VT recurrence in the follow-up period.

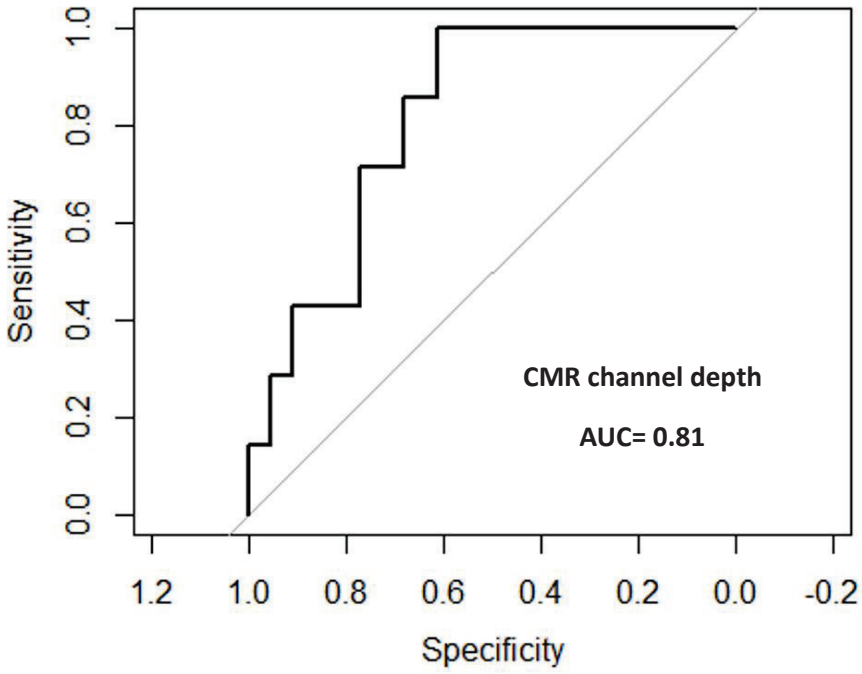

Fig. 4: ROC curve analysis of the maximal CMR channel depth in predicting VT recurrence after exclusive endocardial ablation, with an area under the curve (AUC) of 0.81.

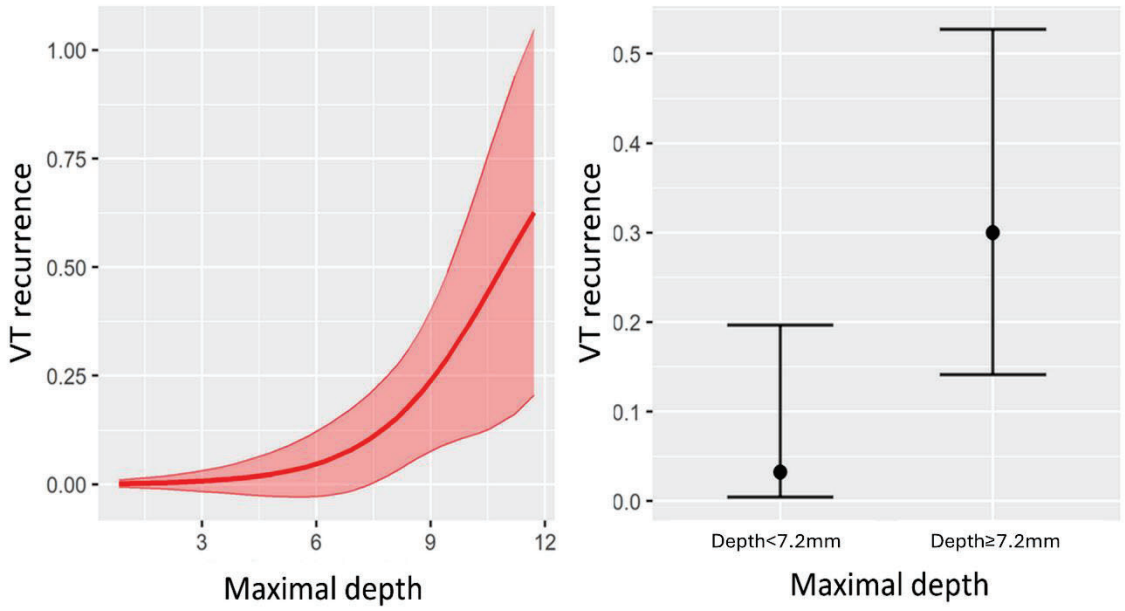

Fig. 5: Probability of VT recurrence at one year according to the maximal channel depth.

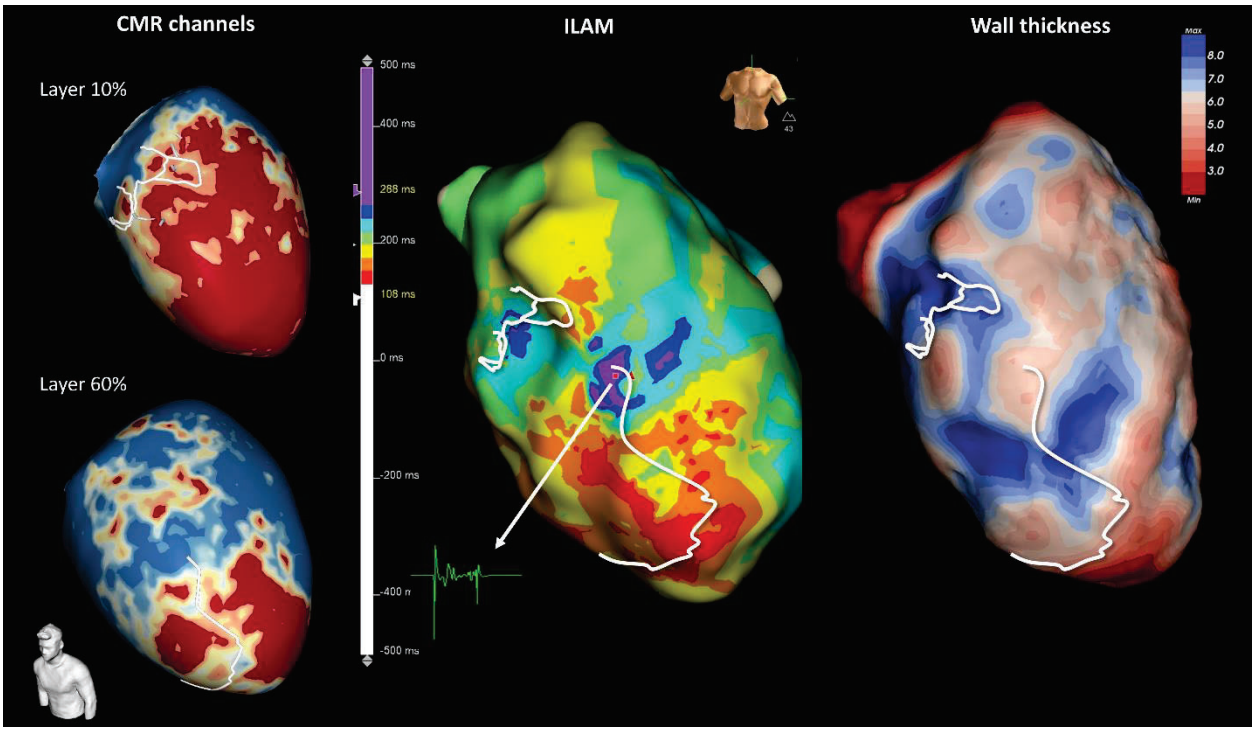

Fig. 6: CMR channels correlating with deceleration zones and WT analysis. In this example, the antero-basal CMR channel is located in an area with a WT>8mm but affecting exclusively endocardial layers (layer 10%). The antero-apical channel is midmural (layer 60%) but located in a thinner area, being the depth of both channels less than 7.2mm. In this patient, an exclusively endocardial approach could be selected.

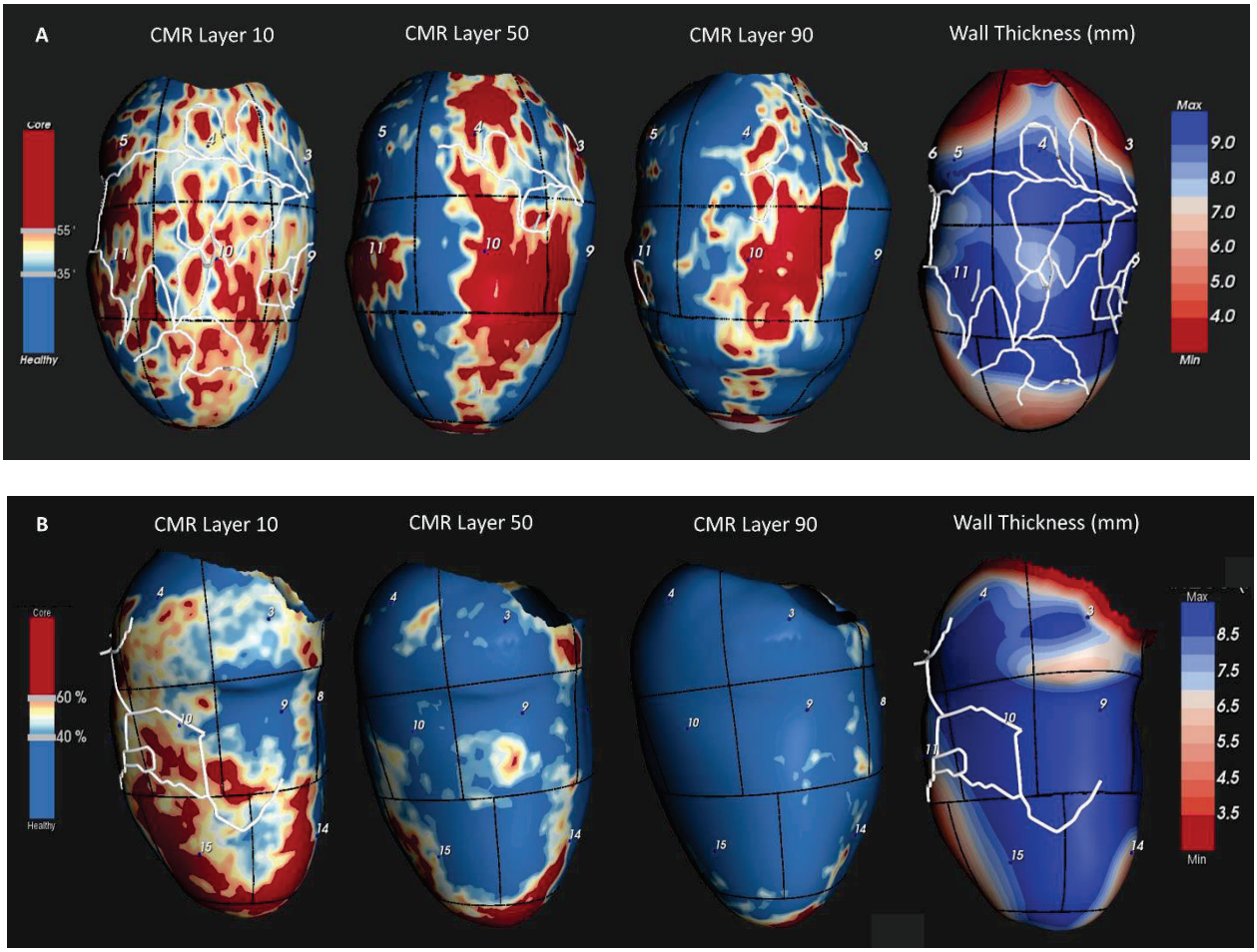

Fig. 7: Two examples of CMR channels projected in their respective layers adding information about the regional WT. Panel A: Transmural channel affecting layers from 1 to 9 in an ischemic cardiomyopathy patient with a regional WT>9mm and a maximal channel depth of 8.3mm who experienced VT recurrence during follow-up. Panel 2: Endocardial channel in an ischemic cardiomyopathy patient with a regional WT>8mm but with a maximal channel depth of 3.6mm who did not present VT recurrence in the follow-up period.

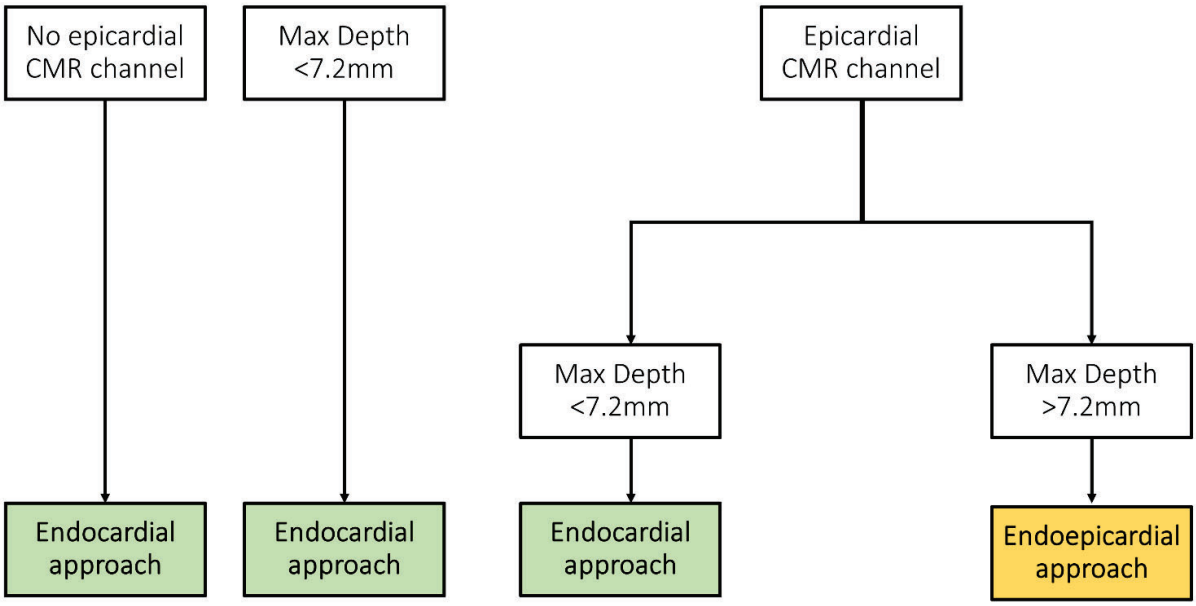

Fig. 8: Proposed algorithm for VT ablation approach selection.

Tables

Table 1: Clinical characteristics.

	Patients studied (n=51)	**Ischemic (n=37)**	**Nonischemic (n=14)**
Age (years)	65.56±11.46 (27-82)	68.22±7.28 (50-82)	58.71±16.81 (27-76)
Male sex	48 (94.1%)	37 (100%)	11 (78.6%)
Hypertension	35 (68.6%)	31 (83.8%)	4 (28.6%)
Diabetes	24 (47.1%)	17 (47.2%)	7 (50.0%)
Dyslipidemia	34 (68.0%)	30 (83.3%)	4 (28.6%)
COPD	7 (15.6%)	4 (12.9%)	3 (21.4%)
CKD	9 (20.0%)	8 (25%)	1 (7.7%)
NYHA class	I: 7 (13.7%) II: 40 (78.4%) III-IV: 4 (7.8%)	5 (13.5%) 29 (78.4%) 3 (8.1%)	2 (14.3%) 11 (78.6%) 1 (7.1%)
Permanent AF	10 (20.0%)	5 (13.5%)	5 (38.5%)
Betablocker therapy	35 (77.8%)	27 (84.4%)	8 (61.5%)
Sotalol therapy	3 (6.7%)	2 (6.3%)	1 (77.7%)

Amiodarone therapy	37 (82.2%)	25 (78.1%)	12 (92.3%)
VT storm	10 (19.6%)	6 (16.2%)	4 (28.6%)
LVEF (%)	31.82±8.76 (15-48)	31.72±8.21 (15-48)	32.35±11.36 (20-45)
LVEDD (mm)	61.68±9.09 (40-77)	61.71±8.63 (40-74)	61.57±11.10 (43-77)

Table 2: Procedural characteristics.

	n=51
Retrograde aortic approach	32 (62.7%)
Transeptal access	48 (94.1%)
Agilis	34 (66.7%)
Number of mapped points	2025±685.78 (944-3557)
Number of VT inductions	1.86±1.20 (0-5)
Number of targeted VTs	1.61±1.06 (0-5)
Procedural time (minutes)	237.48±47.45 (90-360)
X-ray time	34.21±11.01 (9-64)
Number of RF applications	60.49±24.23 (1-114)
RF time (seconds)	2051±937.92 (47-3688)
Number of remaps	1.88±1.01 (0-5)
Final noninducibility	41 (80.4%)
Abolition of DZs	37 (72.5%)

Table 3: CMR characteristics

	Channels studied (n=159)	**Ischemic (n=114)**	**Nonischemic (n=45)**	**p**
Length per channel (mm)	61.93±8.15 (45.41-78.50)	69.9±9.62 (50.31-89.52)	41.7±15.09(11.14-72.42)	0.12
Mass per channel (grams)	2.19±0.33 (1.53-2.86)	2.39±0.40 (1.59-3.19)	1.76±0.62 (0.50-3.02)	0.40
Number of layers per channel	2.83±0.20 (2.43-3.23)	2.84±0.27 (2.37-3.32)	2.80±0.37 (2.05-3.56)	0.93
Number of AHA segments per channel	2.19±0.13 (1.94-2.45)	2.25±0.15 (1.94-2.56)	2.07±0.23 (1.59-2.54)	0.52
Channel location:				
-Endocardium	**96 (60.4%)**	**70.6%**	**44.5%**	**0.02**
-Mesocardium	66 (41.5%)	39.5%	46.7%	0.41
-Epicardium	74 (47.2%)	44.7%	53.1%	0.36
-Transmural	23 (14.5%)	16.5%	8.5%	0.23
WT of the channel region (mm)	7.98±2.27 (7.43-8.52)	8.04±0.32 (7.39-8.68)	7.82±0.52 (6.77-8.87)	0.73
Mean minimal channel depth (mm)	**3.01±0.26 (2.49-3.53)**	**2.65±0.29 (2.07-3.23)**	**3.93±0.46 (3.00-4.86)**	**0.02**
Mean maximal channel depth (mm)	4.89±0.30 (4.29-5.49)	4.64±0.35 (3.94-5.34)	5.54±0.56 (4.41-6.67)	0.18

Table 4: Predictors of VT recurrence after endocardial ablation

	OR	P
Age	1.00 (0.93,1.08)	0.97
Permanent FA	2.22 (0.35,14.49)	0.39
VT storm	1.80 (0.29,11. 00)	0.52
Ejection fraction	1.06 (0.95,1.19)	0.31
Nonischemic cardiomyopathy	2.25 (0.43,11.66)	0.34
Left Ventricle Mass (gr)	1.02 (0.99,1.05)	0.19
Border Zone Mass (gr)	1.04 (0.98,1.1)	0.21
Total Scar Mass (gr)	1.04 (0.94,1.15)	0.43
Epicardial channel	**1.22 (1.05,1.41)**	**0.04**
Minimal channel depth	0.79 (0.41,1.52)	0.48
Maximal channel depth	**1.85 (1.1,3.13)**	**0.02**
Maximal depth >7.2 mm	**12.86 (1.41, 117.21)**	**0.02**

Artículo 6: Estudio de Resonancia Magnética Cardíaca Post-Ablación para Evaluar la Recurrencia de Taquicardia Ventricular (PAM-VT study)

El objetivo de este trabajo fue estudiar la capacidad de la RMC post ablación para evaluar las lesiones de ablación y definir predictores de recurrencia.

Para ello, se incluyeron prospectivamente 61 pacientes consecutivos (marzo 2019 a abril 2021) se sometieron a ablación de TV relacionada con cicatriz tras realización RMC a los que se les realizó una segunda RMC 3-6 meses después de la misma. Se compararon las características de la cicatriz de la RMC pre y post ablación. De los 61 pacientes incluidos, se excluyeron 12 pacientes (4 con RMC de baja calidad, 2 fallecieron antes de la RMC post ablación y 6 se sometieron a RMC post ablación 12 meses después de la ablación) por lo que la muestra total fue de 49 pacientes (edad: 65.5 ± 9.8 años, 97.9% hombres, fracción de eyección del ventrículo izquierdo: 34.8 ± 10.4%, 87.7% miocardiopatía isquémica). La RMC post ablación mostró una disminución en el número (3.34 ± 1.03 vs. 1.6 ± 0.2; P < 0.0001) y la masa (8.45 ± 1.3 vs. 3.5 ± 0.6 g; P < 0.001) de los canales de RMC. Los canales arritmogénicos, definidos como aquellos que se asociaban al istmo de la TV durante la ablación, desaparecieron en el 74.4% de los pacientes. La presencia de *dark core (*área hipointensa dentro de la cicatriz) fue descrita en el 75.5% de los pacientes, no relacionándose con la reducción de los canales (52.2 ± 7.4% vs. 40.8 ± 10.6%, P = 0.57). La recurrencia de TV al año de seguimiento fue del 16.3%. Respecto a los predictores de recurrencia, la presencia de dos o más canales en la RMC post ablación fue un predictor de recurrencia de TV (31.82% vs. 0%, P = 0.0038) con una sensibilidad del 100% y una especificidad del 61% (área bajo la curva 0.82). En la misma línea, una reducción de los canales <55% tuvo una sensibilidad del 100% y una especificidad del 61% (área bajo la curva 0.83) para predecir la recurrencia de TV.

Como conclusión, la RMC post ablación es factible, y una reducción en el número de canales está relacionada con un menor riesgo de recurrencia de TV. El *dark core* no está presente en todos los pacientes, no relacionándose su presencia con eventos en el seguimiento.

ESC European Society of Cardiology

European Heart Journal - Cardiovascular Imaging (2023) **00**, 1–11
https://doi.org/10.1093/ehjci/jead261

ORIGINAL PAPER

Post-Ablation cardiac Magnetic resonance to assess Ventricular Tachycardia recurrence (PAM-VT study)

Ivo Roca-Luque [1,2,3]*, Sara Vázquez-Calvo[1,2], Paz Garre[1,2], Jose T. Ortiz-Perez[1,2], Susanna Prat-Gonzalez[1,2], Paula Sanchez-Somonte[1,2], Elisenda Ferro[1,2], Levio Quinto[1,2], Francisco Alarcón[1,2,3], Till Althoff[1,2], Rosario Jesús Perea[2,4], Rosa M. Figueras i Ventura[5], Eduard Guasch [1,2,3], José Maria Tolosana[1,2,3], Daniel Lorenzatti[1,2], Carlos Igor Morr-Verenzuela[1,2], Andreu Porta-Sanchez [1,2,3], Elena Arbelo[1,2,3], Marta Sitges [1,2,3], Josep Brugada [1,2,3], and Lluís Mont [1,2,3]

[1]Arrhyhtmia Section, Institut Clinic Cardiovascular, Hospital Clínic, Universitat de Barcelona, Villarroel st. 170, Catalonia, 08036 Barcelona, Spain; [2]Institut d'Investigacions Biomèdiques August Pi i Sunyer (IDIBAPS), Barcelona, Catalonia, Spain; [3]Centro de Investigación Biomédica en Red de Enfermedades Cardiovasculares (CIBERCV), Madrid, Spain; [4]Centre de Diagnòstic per la Imatge, Hospital Clínic, Universitat de Barcelona, Catalonia, Spain; and [5]Adas3D Medical S.L., Barcelona, Spain

Received 12 May 2023; revised 4 September 2023; accepted 24 September 2023; online publish-ahead-of-print 11 October 2023

Aims Conducting channels (CCs) detected by late gadolinium enhancement cardiac magnetic resonance (LGE-CMR) are related to ventricular tachycardia (VT). The aim of this work was to study the ability of post-ablation LGE-CMR to evaluate ablation lesions.

Methods and results This is a prospective study of consecutive patients referred for a scar-related VT ablation. LGE-CMR was performed 6–12 months prior to ablation and 3–6 months after ablation. Scar characteristics of pre- and post-ablation LGE-CMR were compared. During the study period (March 2019—April 2021), 61 consecutive patients underwent scar-related VT ablation after LGE-CMR. Overall, 12 patients were excluded (4 had poor-quality LGE-CMR, 2 died before post-ablation LGE-CMR, and 6 underwent post-ablation LGE-CMR 12 months after ablation). Finally, 49 patients (age: 65.5 ± 9.8 years, 97.9% male, left ventricular ejection fraction: 34.8 ± 10.4%, 87.7% ischaemic cardiomyopathy) were included. Post-ablation LGE-CMR showed a decrease in the number (3.34 ± 1.03 vs. 1.6 ± 0.2; $P < 0.0001$) and mass (8.45 ± 1.3 vs. 3.5 ± 0.6 g; $P < 0.001$) of CCs. Arrhythmogenic CCs disappeared in 74.4% of patients. Dark core was detected in 75.5% of patients, and its presence was not related to CC reduction (52.2 ± 7.4% vs. 40.8 ± 10.6%, $P = 0.57$). VT recurrence after one year follow-up was 16.3%. The presence of two or more channels in the post-ablation LGE-CMR was a predictor of VT recurrence (31.82% vs. 0%, $P = 0.0038$) with a sensibility of 100% and specificity of 61% (area under the curve 0.82). In the same line, a reduction of CCs < 55% had sensibility of 100% and specificity of 61% (area under the curve 0.83) to predict VT recurrence.

Conclusion Post-ablation LGE-CMR is feasible, and a reduction in the number of CCs is related with lower risk of VT recurrence. The dark core was not present in all patients. A decrease in VT substrate was also observed in patients without a dark core area in the post-ablation LGE-CMR.

* Corresponding author. E-mail: iroca@clinic.cat

Graphical Abstract

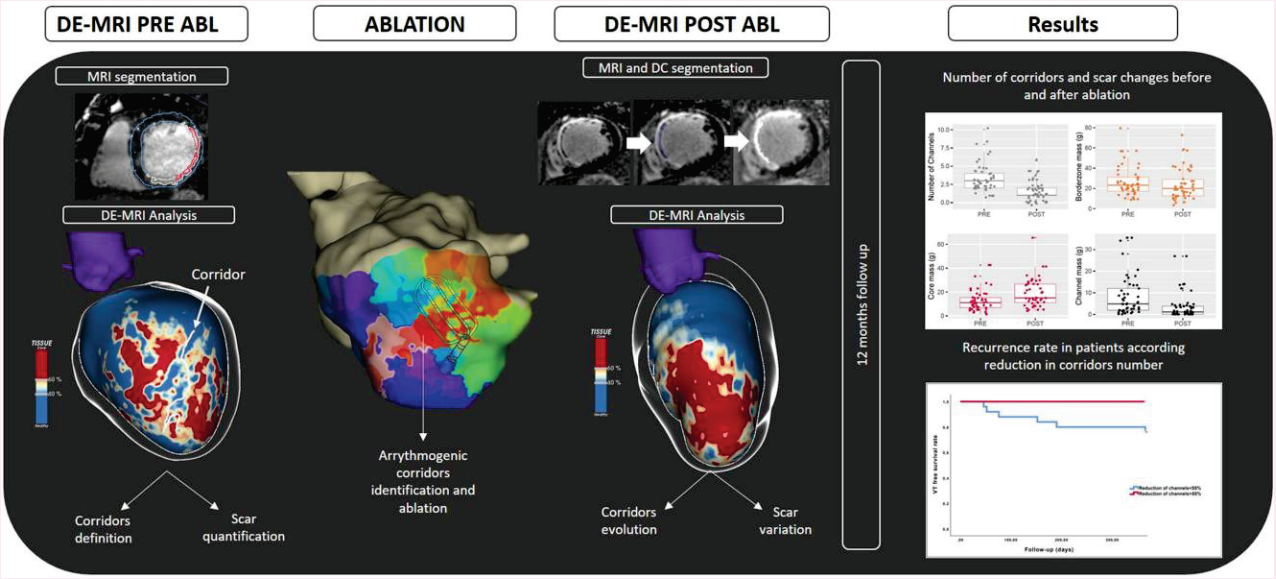

Keywords ventricular tachycardia • ventricular tachycardia ablation • cardiac magnetic resonance • scar characterization • late gadolinium enhancement

Introduction

Substrate-based radiofrequency catheter ablation has become a standard procedure for the treatment of scar-related ventricular tachycardia (VT). The main mechanism behind scar-related VT is the presence of a re-entrant circuit. This circuit is formed by the presence of a slow conduction area within the scar that connects to the healthy non-scarred myocardium, leading to re-entry. These regions are also called conducting channels (CCs) and can be accurately identified with electroanatomical maps (EAMs) during ablation.[1,2]

Likewise, late gadolinium enhancement cardiac magnetic resonance (LGE-CMR) has been demonstrated to be able to identify and characterize this arrhythmogenic substrate with unprecedented precision, being able to depict CCs[3–5] and deceleration zones (DZs).[6] Pre-procedural LGE-CMR is gaining widespread applicability as an assistance tool in ablation procedures since it can facilitate procedural planning, scar mapping and ablation,[7,8] and for the evaluation of the risk of recurrences after ablation.[9] However, the majority of patients scheduled for VT ablation has an implantable cardioverter defibrillator (ICD).[10] This issue represents a major limitation affecting image quality with conventional LGE-CMR. The use of wideband (WB) sequences can overcome this limitation by minimizing device-related artefacts, making LGE-CMR imaging robust for myocardial characterization under these conditions.[11–13] In this sense, a good correlation between WB LGE-CMR and EAM has recently been demonstrated in previous work from our group.[6,14]

Despite the use of pre-procedural LGE-CMR to aid VT ablation, clinical data on whether LGE-CMR is capable of identifying ablation lesions and its relation to VT recurrence are still lacking. A few studies, including some with pathological correlations, have reported LGE-CMR findings following catheter ablation. Based on animal models,[15,16] the appearance of ablation lesions is different in the acute phase than in the chronic phase. In the acute phase, due to haemorrhage, coagulative necrosis, and subsequent microvascular obstruction (MVO), the appearance is a dark area on post-contrast T1-weighted imaging (so-called 'dark core') surrounded by a peripheral rim of enhancement. In the chronic phase, as gadolinium contrast fills in, the ablation lesions are depicted as fully bright areas by LGE-CMR imaging, resembling the scar seen in chronic infarct patients. However, a recent retrospective observational study[17] suggests that the typical appearance in the acute state can persist during chronic follow-up, particularly when ablation lesions are produced on top of scarred tissue. That study included only patients who underwent repeated ablations for whom post-ablation LGE-CMR was not initially planned, and consequently, the elapsed time from ablation to LGE-CMR was very heterogeneous. Interestingly, dark core areas observed in post-ablation LGE-CMR were related with the ablated areas (correlation of 79 ± 15%) and more important, dark core areas were proved to be non-excitable tissue in the redo procedures (R 0.98, $P < 0.01$, Dice Score 0.84). To our knowledge, no prospective study addressing the role of post-ablation LGE-CMR in evaluating ablation results has been published. The aim of this prospective study with pre-specified control post-ablation LGE-CMR is to analyse the usefulness of this imaging test for evaluating ablation results and quantifying changes in the arrhythmogenic VT substrate.

Methods

Study population

This is a prospective observational study of all consecutive patients who underwent the first procedure of substrate-based VT ablation at a single centre (Hospital Clinic) between March 2019 and July 2020. All patients underwent LGE-CMR within the 6–12 months before and 3–6 months after the ablation procedure. Patients without LGE-CMR or those with suboptimal image quality were excluded. Patients with ventricular arrhythmias caused by reversible causes or focal VT ablation and/or without scarring on pre-procedural LGE-CMR were also excluded. All patients provided written informed consent. The study was carried out according to the Declaration of Helsinki guidelines and the deontological code of our institution. The study protocol was approved by the ethical committee of the hospital.

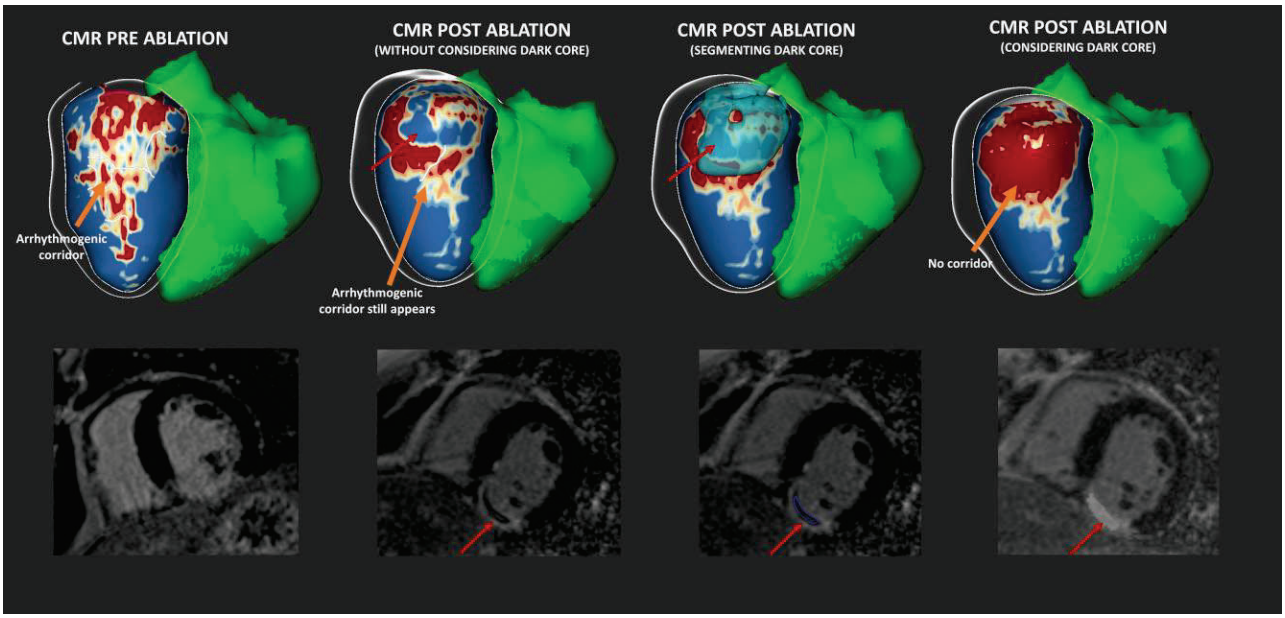

Figure 1 Cardiac magnetic resonance segmentation integrating dark core. In the bottom panels, the raw images of LGE-CMR are shown. In the upper panels, the same images in posteroanterior view after post-processing by ADAS3D are visualized. In the first panel, pre-ablation LGE-CMR reveals an arrhythmogenic channel inside the scar. In the second panel, the LGE-CMR post-ablation segmentation is shown without considering the DC (red arrow) as dense fibrosis. In this case, the software will code that area as healthy tissue because of the hypointense pixel intensity, showing the persistence of the arrhythmogenic channel and therefore, considering the ablation procedure incomplete. In the third and fourth panels, the same post-ablation LGE-CMR is shown, but the DC area has been manually delineated (light blue area, red arrow). The maximum pixel intensity threshold used to define the scar core was selected to convert the manually selected hypointense DC area into hyperenhancement scar core. Last panel shows the final LGE-CMR reconstruction, where the pre-ablation arrhythmogenic channel does not appear, so ablation can now be considered successful in terms of arrhythmogenic channel abolition.

Procedural data

Procedures were performed under general anaesthesia. After femoral venous access, a multipolar diagnostic catheter was positioned at the right ventricular (RV) apex. According to the arrhythmogenic substrate detected by LGE-CMR and VT ECG (if available), EAMs of the left ventricle (LV) and RV were obtained during RV-paced rhythm using an Ensite Precision (Abbott Medical, USA) navigation system. EAMs were created with a high-definition grid mapping catheter (Advisor HD Grid, Abbott Medical, USA). Bipolar voltage mapping was performed using established voltage settings of <0.5 mV for dense scarring and <1.5 mV for border zone (BZ).[18] Automated annotation was performed at the offset of the latest local electrogram (EGM) component using Last Deflection (Abbott Medical, USA) algorithm. Late potentials, fragmented potentials, DZs[19], and any abnormal EGM were also manually tagged during mapping to define CCs inside the scar.

After substrate mapping during paced rhythm, VT was induced by programmed electrical stimulation (drive cycles of 600 and 400 ms, up to three extrastimuli to refractoriness or 200 ms). When VT was haemodynamically tolerated, detailed activation mapping for diastolic and presystolic activity was performed. In cases in which VT was not haemodynamically tolerated, the VT isthmus was defined as the area with a fast transition of good pace mapping (suggesting the VT exit site) and poor pace mapping (suggesting the VT entrance site), as described previously by Chillou.[20] Radiofrequency was delivered using an externally irrigated 3.5 mm tip contact force sensor ablation catheter (Tacticath SE, Abbott Medical, USA) with 45°C temperature control, 40–50 W power limit, and 26–30 mL/min irrigation rate. The ablation endpoint was both non-inducibility and abolishment of late potentials, local abnormal ventricular activities, and DZs confirmed with a complete remap.

Data from LGE-CMR

LGE-CMR was performed using either a 1.5 Tesla (Magnetom Aera, Siemens Healthcare, Germany) or 3 Tesla scanner (Magnetom Trio, Siemens Healthcare, Germany) in participants with or without an ICD, respectively. For those with an ICD, a WB sequence was applied to abolish device-related artefacts.[14]

Technical details about LGE-CMR protocol are previously described by our group: wideband sequence in ICD patients[14] and 3D sequence in patients without ICD.[4]

Patients with ICD (wideband sequence)

First of all, in order to reduce possible damage to the ICD and the surrounding tissue by temperature and possible changes in thresholds and impedances, the specific absorption rate was limited to <2 W/kg. Specific workflow was performed before CMR in patients with an ICD; a trained electrophysiologist interrogated ICD parameters and all therapies and detections were disabled. Blood pressure, pulseoximetry, and heart rate were monitored during CMR. After several standard scout slices, an intravenous bolus of 0.2 mmol/kg of gadobutrol (Gadovist, BayerHispaniaSL) was injected. Seven to 10 min after the injection, WB LGE-CMR images were obtained using a WB inversion pulse sequence (3.8 kHz) in serial short-axis slices (5 mm slice thickness, no gap) covering the whole LV from the base to the apex. The inversion time was adjusted to null normal myocardium (increasing between 200 and 320 ms typically).

Patients without ICD (3D sequence)

A whole-heart, high spatial resolution, delayed-enhanced study was conducted using a commercially available free-breathing, 3D-GRE

inversion-recovery gradient echo technique (gradient echo read out). The 3D slab was acquired in the axial plane. A Cartesian trajectory was used to fill the k-space with phase-encoding (y) in the anteroposterior direction. The field of view was covered by a 256 × 240 pixel matrix, and in-plane reconstruction was allowed to achieve an isotropic spatial resolution of 1.4 × 1.4 × 1.4 mm and a voxel size of 2.74 mm^3. To compensate for the long acquisition time anticipated, we added 50 ms to the nominal value necessary to null normal myocardium, as derived from the TI scout. Other typical sequence parameters were as follows: repetition time 440 ms; echo time 1.29 ms; flip angle 158; band width 810 Hz/pixel; and 51k-space lines filled per heartbeat. In some cases, a high temporal resolution, four-chamber view cine, achieved by means of parallel imaging with an acceleration factor of 3, was used to select the optimal acquisition window and minimize cardiac motion in late-diastole. Respiratory synchronization was performed for every other heartbeat using a crossed-pair navigator approach. The data set was acquired during expiration and generalized, autocalibrating, partially parallel acquisition with an acceleration factor of 2 was used to speedup data acquisition. A set of images was reconstructed in the left ventricle (LV) short-axis orientation with 1.4 mm slice thickness (typically 50–70 images) for subsequent image processing. A new TI scout was prescribed to select an updated TI.

All LGE-CMR images were processed using a previously described protocol reported briefly here.[4,21] Full LV volume was reconstructed in the short-axis orientation, and the resulting images were processed with ADAS3D software (ADAS 3D, Barcelona, Spain). After semi-automatic delineation of the endocardium and epicardium, nine concentric equally spaced surface layers were created. A 3D shell was obtained for each layer. PSI (pixel signal intensity) maps were obtained from LGE-CMR images, projected to each of the shells following a trilinear interpolation algorithm and colour coded (core scar in red, BZ in yellow, and healthy tissue in blue). A PSI-based algorithm was applied to characterize the hyperenhanced areas using 40 ± 5% (healthy tissue) and 60 ± 5% (core scar) of the maximum intensity signal as thresholds. A CC on the LGE-CMR reconstruction was defined as a channel of BZ between two core areas, whether observed in the same layer or between consecutive layers. Depending on the LGE distribution from 10% (the layer closest to the endocardium) to 90% (the layer closest to the epicardium), the substrate was defined as subendocardial when LGE affected 10% to 30% of the layer, epicardial when LGE affected 60% of the outer layer and midmyocardial when LGE was confined to the internal layer of myocardial thickness (layer 40–60%). Areas of LGE > 75% in the myocardial thickness were considered transmural. Septal involvement was considered when more than 40% of the septal thickness presented LGE distribution in any portion. The arrhythmogenic channel was defined as the CMR channel correlated with the VT isthmus during the procedure.

Dark core definition and post-procedural LGE-CMR analysis

Because dark core (DC) lesions observed in conventional LGE imaging acquired 10 to 15 min after contrast administration appear black in post-contrast T1-weighted imaging, they can therefore be misinterpreted as healthy or BZ tissue during the segmentation process. Indeed, CCs could be incorrectly annotated if the DC area is inside the core scar. Therefore, in this study, it was considered essential to identify the presence of catheter-induced DC lesions by performing a side-by-side comparison of the pre- and post-ablation LGE-CMR studies. The coregistered short-axis slices from the pre- and post-ablation LGE studies were simultaneously presented to observers (blinded to EAM data) experienced in LGE-CMR interpretation who manually and roughly delineated DC areas. The defined criteria for DC areas was the presence, in the post-ablation LGE-CMR, of a hypointense region with signal intensity below the mean signal intensity of the non-enhanced myocardium, and surrounded by hyperenhanced myocardium not observed in the pre-ablation LGE-CMR study. Next, the maximum pixel intensity threshold used to define the scar core was selected to convert the manually selected hypointense DC areas into scar core. Therefore, those areas

Table 1 Population and procedural characteristics

Clinical characteristics	Patients studied ($n = 49$)
Age (years)	65.5 ± 9.8 (24–78)
Male sex	48 (98.0%)
Hypertension	40 (81.6%)
Diabetes	25 (51%)
Dyslipidaemia	37 (75.5%)
COPD	6 (12.2%)
CKD	13 (26.5%)
NYHA class	I–II: 33 (67.3%)
	III–IV: 13 (32.7%)
Ischaemic cardiomyopathy	43 (87.7%)
Permanent AF	6 (12.2%)
Sotalol therapy	4 (8.1%)
Amiodarone therapy	32 (65.3%)
Mexiletine therapy	3 (6.1%)
Previous ICD	42 (85.7%)
VT storm	7 (14.2%)
Incessant VT	3 (6.1%)
LVEF (%)	34.8 ± 10.5 (15–60)
LVEDD (mm)	61.4 ± 7.9 (40–75)
CMR characteristics	
Scar location	
Anterior/anterolateral	17 (34.7%)
Septal	13 (26.5%)
Inferior	19 (38.8%)
Scar transmurality	
<25%	12 (24.4%)
25–50%	20 (41.4%)
50–75%	7 (14.7%)
>75%	10 (20.4%)
Procedural characteristics	
Contact force catheter	40 (83.6%)
Transeptal access	44 (89.8%)
Epicardial access	6 (12.2%)
Number of EAM points	1358.3 ± 1103.1
Number of VT inductions	1.81 ± 1.6 (0–9)
Number of VT mapped	1.32 ± 1.6 (0–9)
Number of RF applications	58 ± 20.9 (9–99)
RF time (seconds)	1896 ± 789.4 (399–3000)
Procedural time (minutes)	228.1 ± 73.8
Final non-inducibility	44 (89.8%)
Residual slow conduction	7 (14.8%)

ICM, ischaemic cardiomyopathy; COPD, chronic obstructive pulmonary disease; CKD, chronic kidney disease; AF, atrial fibrillation; VT, ventricular tachycardia; ICD, implantable cardioverter defibrillator; NYHA, New York Heart Association; LVEDD, left ventricle end-diastolic diameter; LVEF, left ventricular ejection fraction.

Table 2 Post-ablation LGE-CMR characteristics

	Pre	Post	*P*
Number of channels detected	3.34 ± 1.03	1.61 ± 0.4	<0.0001
Channels (grams)	8.45 ± 1.3	3.5 ± 0.6	<0.0001
LV mass (grams)	165 (IQR 132 199)	155 (IQR 127 198)	0.87
Core (grams)	13.2 ± 9.21	19.3 ± 11.8	<0.0001
BZ (grams)	26.5 ± 14.8	23.7 ± 14.9	0.26
Scar heterogenicity (BZ area/total scar area)	69.1 ± 9.3%	54.7 ± 13.6%	0.002

LV, left ventricular; BZ, border zone.

Table 3 Relation of dark core with LGE-CMR and ablation parameters

	Presence of dark core (37)	Absence of dark core (12)	*P*-value
Time to ablation post-procedural LGE-CMR (days)	152.2 ± 52.3	138.1 ± 35.7	0.74
RF time (seconds)	2128.9 ± 130.6	1567.2 ± 245.3	0.06
Reduction in CCs (%)	52.2 ± 7.4%	40.8 ± 10.6	0.57
Reduction in CC mass (%)	59.1 ± 10.7%	36.6 ± 28.3	0.16
VT recurrence rate	16.2%	16.7%	0.91

LGE-CMR, late gadolinium enhancement cardiac magnetic resonance; RF, radiofrequency; CC, conducting channel; VT, ventricular tachycardia.

will appear in white in the new PSI map and coded as dense fibrosis (*Figure 1*).

Follow-up data

Patients were followed up at 3, 6, and 12 months and then yearly after ablation, and their ICDs were monitored for episodes of ventricular arrhythmia. During follow-up, a reduction or discontinuation of antiarrhythmic drugs was considered at the clinician's discretion. VT recurrence was defined as any VT episode longer than 30 s or episode that required ICD intervention. All sustained VT events, ICD therapies, and new hospitalizations were recorded.

Statistical analysis

Continuous data are reported as the means ± SDs or median and interquartile range (IQR) in case of variables without a normal distribution, and comparisons between groups were performed using Student's *t*-test or the Mann–Whitney *U* test, as appropriate. Categorical variables are expressed as the total number and percentage and were compared between groups using the χ^2 or Fisher's test or two-way ANOVA for non-dichotomous categorical variables. Receiver operating characteristic curves were calculated to estimate the predictive value of scar variables and to identify cut-off points. All analyses were performed with SPSS v18.0 (SPSS, Chicago, IL, USA) and R software for Windows version 3.6.1 (R project for Statistical Computing; Vienna, Austria). All statistical tests were two-sided, and a *P*-value < 0.05 was considered statistically significant.

Results

Study population

A total of 72 patients with structural heart disease underwent a first procedure scar-related VT ablation at a single centre from March 2019 to December 2020. In 11 patients, pre-procedural LGE-CMR was not performed because of formal contraindication (8 patients) or because they refused to LGE-CMR (3 patients). Of the 61 patients who underwent pre-procedural LGE-CMR, 4 patients had poor-quality LGE-CMR; 2 patients died before post-procedural LGE-CMR, and 6 patients underwent LGE-CMR after the designed period. Overall, the final population consisted of 49 patients (age: 65.5 ± 9.8 years; male, 98%). The most frequent underlying disease was ischaemic heart disease (87.7%). The basal characteristics of the study population (including LGE-CMR data) are shown in *Table 1*. Regarding LGE-CMR, no differences were observed in ischaemic cardiomyopathy (ICM) vs. non-ischemic cardiomyopathy (NICM) patients: BZ mass median 21 g, (IQR 17.4–32.4) vs. 25.2 (IQR 20.6–32.7) in NICM patients ($P = 0.75$), channel mass: median 5 (IQR 2.2–11.5) vs. 2.4 (IQR 1.0–8.5) ($P = 0.09$) and core mass: median 11 (IQR 7.1–18.1) in ICM vs. 7.7 (IQR 5–10.1) in NICM patients ($P = 0.16$).

Procedural data

VT ablation was performed with an exclusively endocardial approach in 44 (89.8%) patients and an endoepicardial approach in 5 patients. Major complications occurred in 4.1% (2) of the patients. VT could be induced in 34 (82.9%) patients, and an isthmus could be defined in 41 (83.6%) of these patients. Non-inducibility and complete abolition of late potentials were achieved in 44 (89.8%) and 42 (85.2%) patients. The characteristics of the procedure are summarized in *Table 1*.

LGE-CMR substrate characterization

Table 2 describes pre- and post-procedural substrate LGE-CMR-derived data. Regarding CCs, before the procedure, the mass and number of channels were 8.45 ± 1.32 g and 3.34 ± 0.32 channels, respectively.

Channels reduction after ablation

After the procedure, both mass and number of channels were reduced to 3.34 ± 1.03 g ($P < 0.001$) and 1.6 ± 0.2 channels ($P < 0.0001$), respectively. A reduction of more than 50% in CC mass was observed in 33 patients (67.3%). Accordingly, in 26 patients (53.1%), a reduction of more than 50% in the number of channels was achieved.

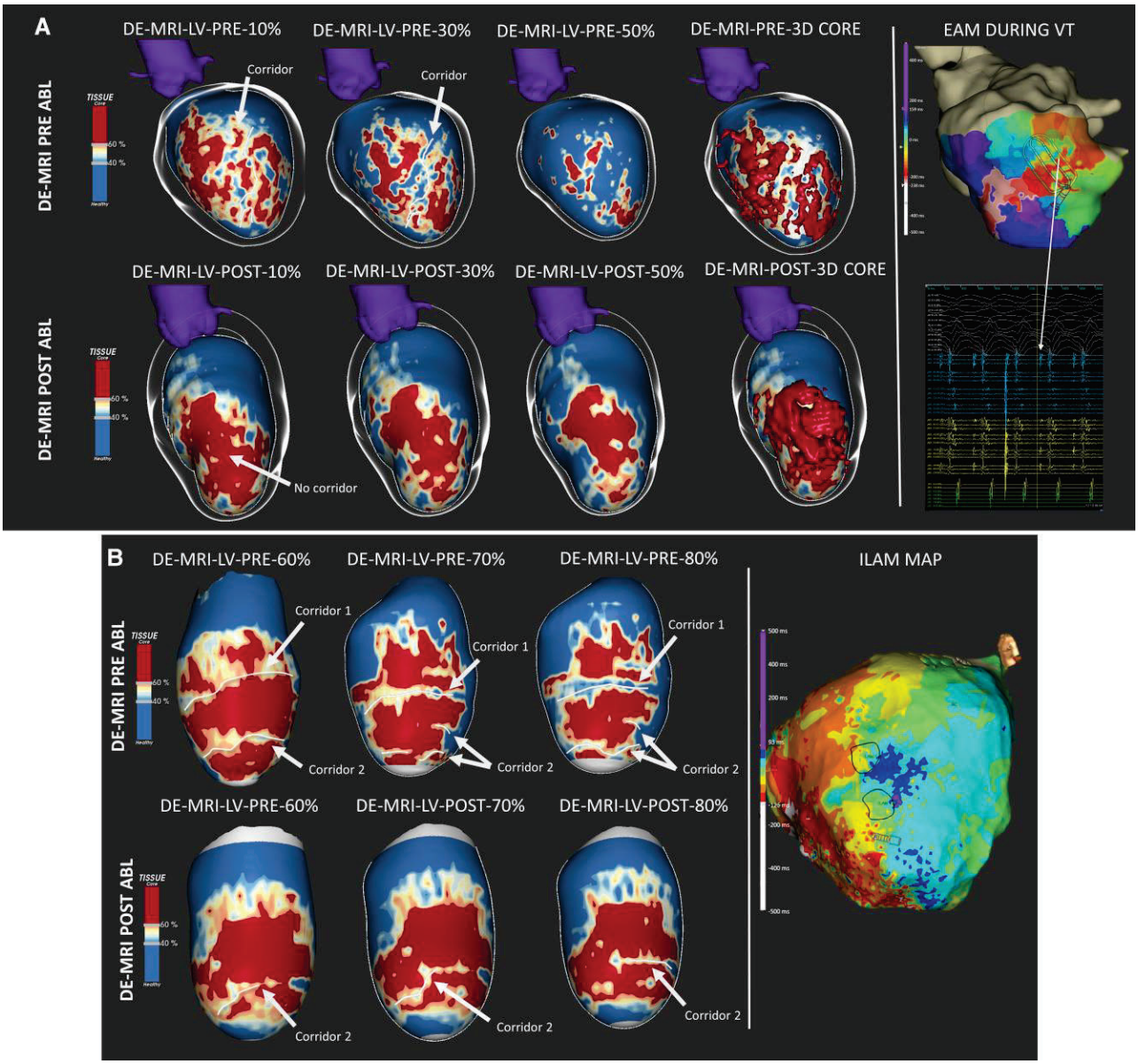

Figure 2 Arrhythmogenic channel visualization in the post-ablation LGE-CMR. Upper panel: three-dimensional reconstruction of pre-ablation LGE-CMR with the endocardial channel in the anterior wall (white arrow) from layer 10% to 30%. In the right panel activation map during VT with a clear figure-of-eight circuit using the channel shown in the LGE-CMR with diastolic potentials inside the channel. Bottom panel: three-dimensional reconstruction of LGE-CMR of the same patient 3 months after the ablation procedure. There is an increase in dense scarring produced by radiofrequency ablation that leads to the disappearance of the arrhythmogenic endocardial channel. After one year of follow-up, the patient was free of VT recurrence. Upper panel: left anterior oblique view of three-dimensional reconstruction of pre-ablation LGE-CMR with two arrhythmogenic epicardial channels. In the right panel, an isochronal late activation map during sinus rhythm is shown revealing the presence of two deceleration zones (black circles) that correspond to the entrances of both channels. Bottom panel: three-dimensional reconstruction of LGE-CMR in the same patient 3 months after the ablation procedure. There is an increase in dense scarring, but channel 1 still appears. This patient recurred presenting three VT episodes within the first 6 months after ablation.

An arrhythmogenic channel in the pre-procedural LGE-CMR was identified in 43 patients (87.7%). In 29 of these patients (67.4%), the channel disappeared in the post-ablation LGE-CMR (*Figure 2*). In the rest of the patients, the arrhythmogenic channel was still visible in the post-ablation LGE-CMR with a smaller BZ mass (pre-ablation: 8.9 ± 2.5 vs. post-ablation: 6.3 ± 2.2; $P < 0.001$) and less transmurality (number of layers affected: pre-ablation 4.7 ± 0.8 vs. post-ablation 2.8 ± 0.61; $P = 0.04$) (*Figure 3*).

Core scar, BZ, and dark core

Regarding the remaining scar characteristics, after ablation, there was an increase in core scar (19.3 ± 11.8 vs. 13.2 ± 9.21 g; $P < 0.0001$)

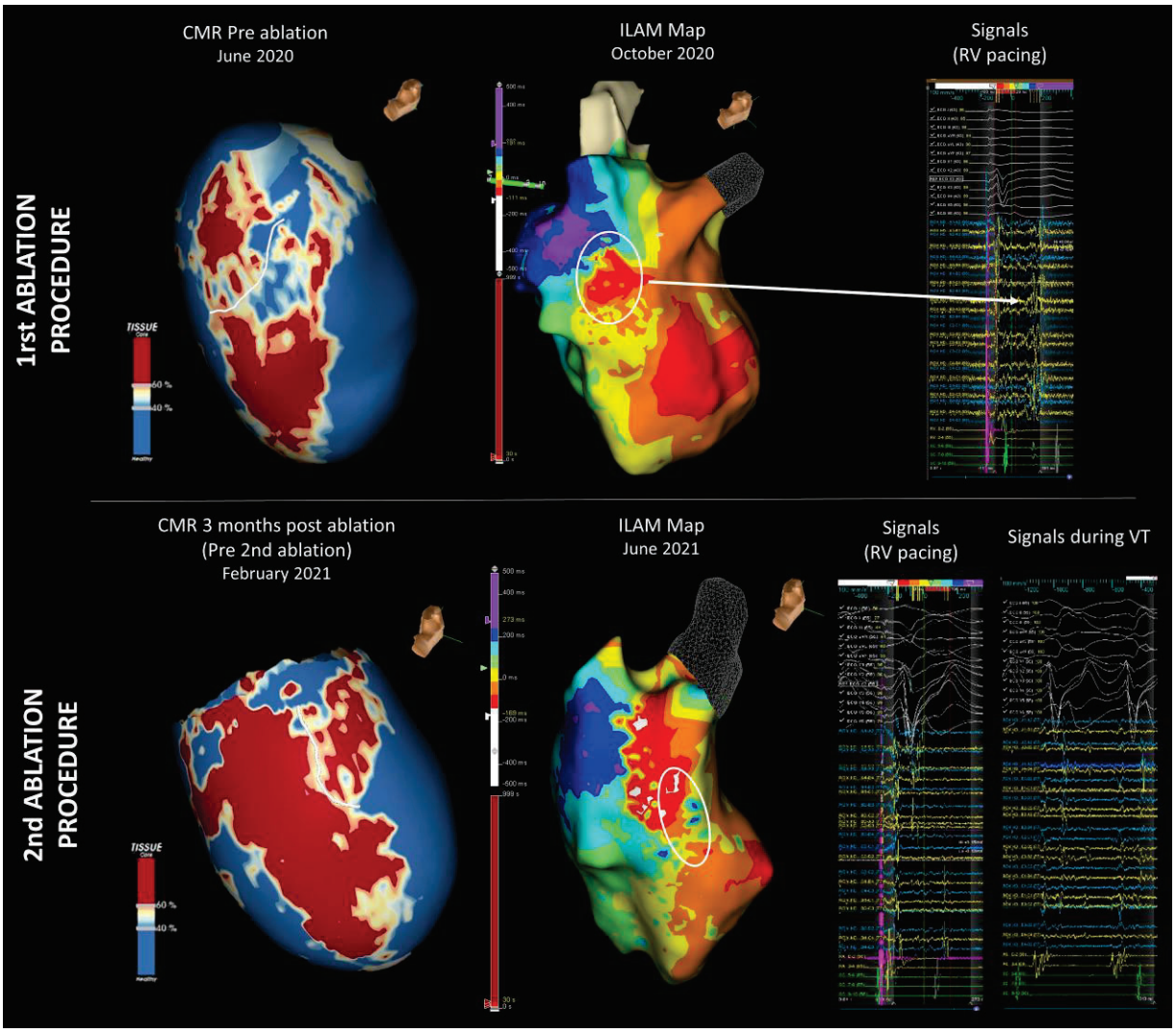

Figure 3 Channel visualization in a redo procedure. The upper panel shows LGE-CMR (before the first ablation procedure) with a clear CC in the posteroseptal scar in concordance with the DZ (white circle) in the isochronal late activation map (ILAM). Late and fragmented potentials were detected in that area (right panel). The bottom panel shows the 3-month post-ablation LGE-CMR with more homogenous scarring and disappearance of the more posterior part of the CC but a new exit in the anterior part of the scar (probably reconnection or incomplete ablation). The ILAM map shows the area of blockage in the upper part of the scar and a DZ in the new CC exit (with circle) with late potentials during RV pacing and diastolic potentials during VT.

without an increase in the area of BZ (26.5 ± ≡4.8 vs. 23.7 ± 14.9;P = 0.26). Indeed, there was a reduction in the heterogenicity of the scar in terms of the percentage of BZ over total scarring (post-ablation 54.7 ± 13.6% vs. 69.1 ± 9.3% before ablation; $P = 0.002$). Scar characteristics before and after ablation are shown in *Table 2* and *Figure 4*.

A 'dark core' area was detected in 37 patients (75.5%), but no association was found with the elapsed time between ablation and post-procedural LGE-CMR, RF time, reduction in the number of CCs, or CC mass and neither with VT recurrence rate (16.2% vs. 16.7%, $P = 0.91$). In *Table 3*, relation of DC with LGE-CMR and ablation parameters is shown.

Follow-up

After one year of follow-up, eight patients (16.2%) presented VT recurrence. Reduction of the number of CCs (49.0 ± 8.2% vs. 5 ± 3.2%; $P = 0.02$) was related with absence of VT recurrence. The presence of two or more channels in the post-ablation LGE-CMR was a predictor of VT recurrence (31.82% vs. 0%, $P = 0.0038$) with a sensibility of 100% and specificity of 61% (area under the curve 0.82). In the same line, a reduction of <55% of CCs predicts VT recurrence (28.57% vs. 0%, $P < 0.0001$, *Figure 5*) with a sensibility of 100% and specificity of 67% (area under the curve 0.83, *Figure 6*). No other post-ablation LGE-CMR -related parameter was related to VT recurrence (*Table 4*).

Discussion

Our study, to our knowledge, is the first to prospectively analyse the role of LGE-CMR in evaluating VT ablation results. The main finding is the strong relation of the degree of reduction of CCs with VT recurrence rate. A clear reduction in BZ and CCs is observed after ablation, thus resulting in an homogenization of the scar with and increased total dense scarring without an increase in the amount of BZ. These changes

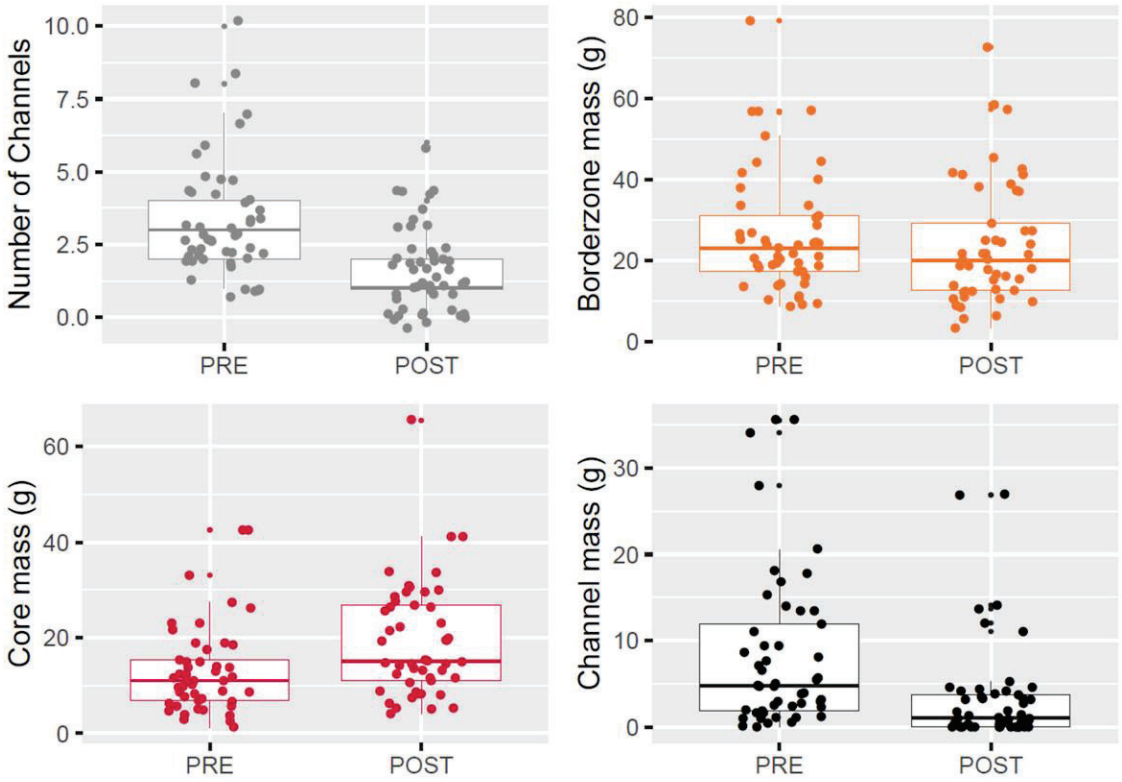

Figure 4 Scar characteristics before and after ablation. Comparison of LGE-CMR scar characteristics before and after ablation. A clear decrease in channel mass and number of channels is observed with an increase in core mass and no differences in BZ mass.

in scar can be detected by post-ablation LGE-CMR and are useful to stratify VT recurrence risk. Another important finding is the observations about the DC phenomenon in relation to MVO in the area of ablation lesions. DC has been historically related to ablation lesions and can be acutely visualized by LGE-CMR as DC even at the 3–6 months follow-up. However, in our study, its presence is neither constant nor clearly related to the percentage of CC mass reduction, so it is not a good marker of ablation lesion evaluation.

Reduction in CCs and scar changes

As stated before, CCs have been shown to be related to the VT isthmus and can be precisely detected by both EAMs and pre-procedural LGE-CMR.[1–5] The presence, extent, heterogenicity, and qualitative distribution of BZ tissue in myocardial scarring detected by LGE-CMR independently predict appropriate ICD therapies and sudden cardiac death.[22,23] In addition, CCs have also been proven to be related to appropriate therapies in patients with an ICD implanted for primary prevention.[22] In this sense, a reduction in CCs with post-procedural LGE-CMR can hypothetically be a non-invasive surrogate to evaluate the completeness of ablation. One of the main limitations of LGE-CMR in patients who have undergone VT ablation is that most of them have ICD *in situ*, so a major image artefact derived from an ICD device can minimize the post-procedural LGE-CMR quality. However, with the use of a dedicated LGE-CMR sequence (wideband sequence) to minimize ICD artefacts, LGE-CMR images have been highly improved. Indeed, the concordance of CCs in pre-ablation wideband LGE-CMR in patients with an ICD with CCs in the EAM has been proven to be as good as that in patients without ICD.[14] The use of imaging to evaluate ablation results has been shown to be useful in the field of atrial fibrillation ablation.[24] However, very little information has been published in the field of ventricular arrhythmias. In our prospective study, there was a significant reduction in the total amount of CCs and the CC mass. Changes in LGE-CMR after ablation were analysed in a small study[25]; however, the study population was different (one-third of patients did not have scarring before ablation), and there was no detailed analysis of scar characteristics, such as BZ mass, core scar mass, and CC details. Moreover, in that study, the post-ablation LGE-CMR findings were not related to ablation success. In our study, there was a reduction not only in CC number and mass but also in scar heterogenicity (percentage of BZ over total scar). In addition, we have proven that the degree of reduction of CCs was a predictor of VT recurrence after one year follow-up. Therefore, a reduction in CCs and scar heterogenicity in the post-ablation LGE-CMR could be a marker of ablation success and can lead to a tailored management of the patients after ablation.

Dark core to identify ablation lesion

The use of LGE-CMR to evaluate RF ablation lesions has been studied in the acute phase (4–8 weeks)[26] showing an area of no enhancement due to MVO also called the 'dark core' in post-contrast T1-weighted imaging. In a recent paper, these DC areas were related to the area of the ablation lesion[16] and were observed in all patients. This work included 17 non-consecutive patients who underwent post-ablation LGE-CMR before a redo VT ablation procedure. Only 10 of these patients had pre-procedural LGE-CMR. Although the delay between the index ablation procedure and the LGE-CMR study was 30 ± 29 months, a 'dark core' was observed in all patients and was related to

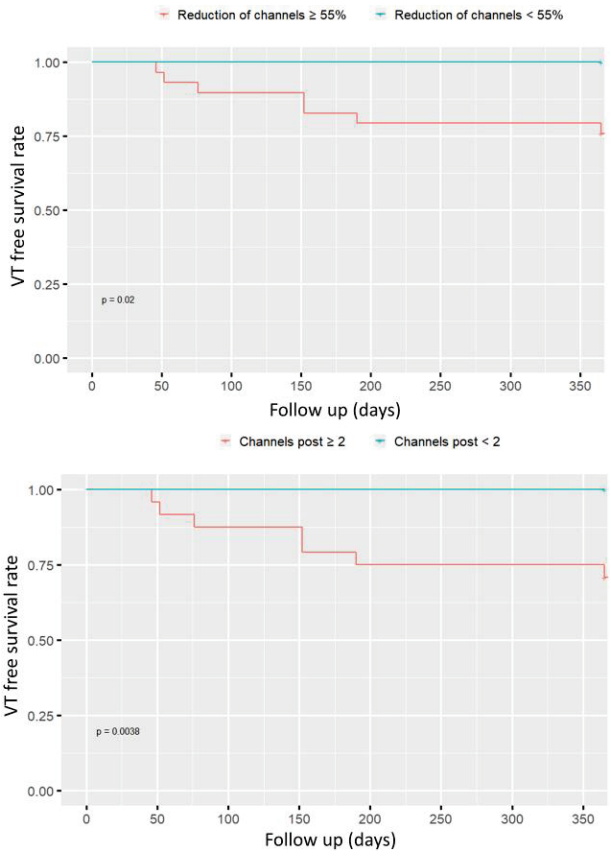

Figure 5 Kaplan–Meier VT free survival curve according to reduction of conducting channels in post-ablation CMR and the number of post-ablation LGE-CMR channels.

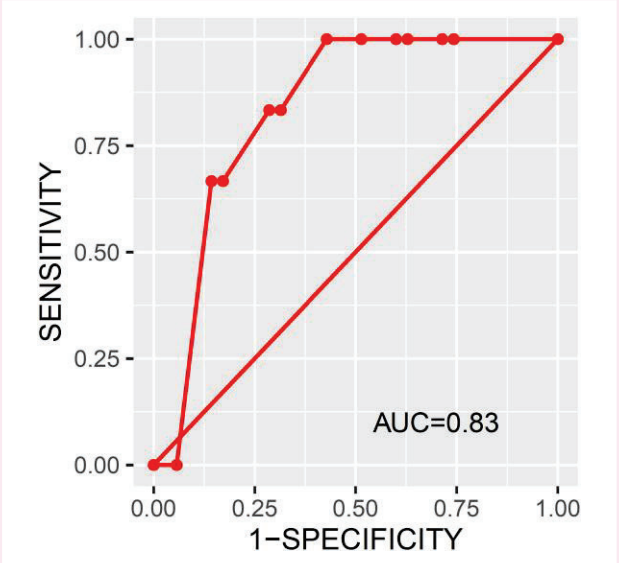

Figure 6 Receiver operating characteristic (ROC) curve of the degree of conducting channels reduction in relation to ventricular tachycardia recurrence.

the area of ablation. However, there are data in animal models[15] suggesting that visualization of 'DC' depends not only on the elapsed time between the ablation procedure and the LGE-CMR acquisition but also on the delay from contrast LGE injection to image acquisition. As the mechanism of DC is MVO, more time is required for the contrast to fill in these areas. In the mentioned study with a canine model,[15] the DC can be seen within the first 2–8 weeks after ablation, but as stated previously, the prolongation of the time to image acquisition allows the contrast to diffuse in the DC areas, resulting in a fully bright appearance of the usual scar area. At a longer follow-up (8 weeks), there was no DC detection, and the ablation lesion was typically fully bright even if image acquisition was performed 45 min after gadolinium injection, suggesting that MVO resolved in the scar core with time. In a clinical retrospective study, the typical DC appearance was not observed in cases where LGE-CMR was performed more than one month after ablation.[27] Therefore, the course of the DC and its relation to ablation lesions is still controversial. In this sense, although animal models have been used to study the time course of ablation lesions from MVO and oedema in the acute phase until its transformation to core scarring at later stages, this phenomenon is not consistent in clinical practice. Many factors can influence its occurrence, such as the presence of underlying scar tissue or local vascularization.

In our study, a DC was observed in <75% of patients, and its presence was not related to the delay between ablation and LGE-CMR (considering that all LGE-CMRs were performed between 3 and 6 months after ablation). Therefore, our study confirms that using the conventional delay of

Table 4 Association of post-ablation LGE-CMR parameters and VT recurrences

Variable	Non-recurrence	Recurrence	OR (95% CI)	*P*-value
Channels pre	2.7 ± 1.8	3.1 ± 1.7	1.13 (0.74–1.72)	0.57
Channels post	1.3 ± 1.2	3 ± 1.5	2.37 (1.19–4.72)	0.01
BZ pre (g)	24 ± 15	34 ± 14	1.04 (0.99–1.08)	0.13
BZ post (g)	22 ± 13	31 ± 24	1.03 (0.99–1.08)	0.17
Core pre (g)	12 ± 8	16 ± 10	1.05 (0.97–1.15)	0.23
Core post (g)	18 ± 10	20 ± 20	1.02 (0.95–1.08)	0.64
Channel pre (g)	8 ± 7	9 ± 4	1.00 (0.91–1.10)	0.98
Channel post (g)	3 ± 5	4 ± 4	1.03 (0.89–1.18)	0.73
% channels reduction	−49.0 ± 8.2	5 ± 3	1.02 (1.00–1.03)	0.02
% mass channels reduction	−49 ± 8.0	34 ± 7.6	1.00 (0.99–1.01)	0.65
% BZ (g) reduction	5 ± 6.6	5 ± 1.1	1.00 (0.99–1.01)	0.98
% core (g) reduction	95 ± 12.2	38 ± 1.01	1.00 (0.98–1.01)	0.26
Ischaemic (%)	81.25	100	0.56 (0.01–5.92)	0.56
Chronic kidney disease (%)	25.70	50.00	2.89 (0.49–16.97)	0.24

LGE-CMR, late gadolinium enhancement cardiac magnetic resonance; VT, ventricular tachycardia; BZ, border zone; g, grams; OR, odds ratio.

10–15 min,[14,17,22] a DC is not constant if LGE-CMR is performed out of the acute phase after ablation. More importantly, the formation of DC was not related to the acute success rate, the radiofrequency time, or the reduction in CCs (because a reduction in CCs was also observed in patients without a DC). In our opinion, this is a very important finding. There are controversial data about dark core but, considering our results, the absence of a DC does not reflect the absence of catheter-induced lesions; therefore, the changes in all scar characteristics on top of the DC must be considered to evaluate the ablation result.

Overall, our findings confirm the usefulness of LGE-CMR as a tool for evaluating VT ablation completeness. These findings, if confirmed by other studies, suggest that LGE-CMR can be useful for stratifying the risk of recurrence after ablation. Conversely, the post-ablation treatment strategy can be tailored based on the results of the ablation as assessed by LGE-CMR. In addition, post-ablation LGE-CMR is a helpful tool in cases of VT recurrence for tailoring the redo procedure based on the results of the first ablation evaluated non-invasively by LGE-CMR.

Conclusion

Post-VT ablation LGE-CMR substrate characterization can be used to evaluate ablation results in terms of CC reduction and scar homogenization. The degree of CC reduction is strongly related to VT recurrence rate. The dark core as a marker of ablation lesion is not homogeneous 3–6 months after VT ablation and is not mandatory as a marker of the ablation lesion in patients with structural heart disease.

Limitations

The main limitation of the study is that, due to the low recurrence rate, there were not enough redo procedures to ensure that scarring and CCs in the post-ablation LGE-CMR corresponded to those in the EAMs. However, the concordance of LGE-CMR with EAMs, as stated previously in the manuscript, has been proven in previous studies by our group.[14]

Regarding the LGE-CMR, a possible limitation must be addressed. The post-ablation LGE-CMR is always performed with a 1.5 Tesla scan because patients had ICD implantation, and pre-ablation LGE-CMR can be 3 Tesla in patients in whom LGE-CMR was performed before ICD implantation. It is well known that voxel size is larger in 1.5 Tesla scan, so small CCs could be underdetected. However, in most of the patients (87.5%) of patients, both pre- and post-ablation LGE-CMR was the same scan (1.5 Tesla). In addition, we have previously demonstrated that 1.5 Tesla LGE-CMR with a wideband sequence has enough accuracy to detect CCs.[14] In the same line, spatial resolution of CMR (in special 1.5 Teslas) is limited so test–retest reliability is limited. This is a common limitation of CMR technique that applies also to this study. Furthermore, within our study, four out of six patients were excluded due to artefacts or low-quality images. This decision was taken relying on the operator's criteria that presents an additional limitation.

Another limitation must be commented regarding population heterogenicity. In our study, only 6 out of 49 patients had NICM so the results must be confirmed with larger population of NICM patients. Regarding characteristics of population, only one female is included in our patients. Despite the proportion of females is always low in all VT ablation studies, is even smaller in our study so our results must be interpreted with limitations in females.

Finally, this was a single-centre study, and therefore, these results need to be confirmed in a multicentre series.

Acknowledgements

The authors want to thank Dr Peng Hu (UCLA, Los Angeles, CA) for his pioneering work on wideband LGE. We also want to thank Xiaoming Bi, PhD, and Siemens Healthineers for their support with the wideband sequence work in progress collaboration.

Conflict of interest: L.M. and J.B. report activities as a consultant, lecturer, and advisory board member for Abbott Medical, Boston Scientific, Biosense Webster, Medtronic, and Biotronik. They are also shareholders of Adas3D Medical S.L. I.R.-L. and A.P.-S. have served as a consultant for Biosense Webster, Medtronic, Boston Scientific, and Abbott Medical. M.S. reports activities as a consultant, lecturer, advisory board member, and grant recipient for Abbott Medical, Edwards Lifesciences, Sanofi, General Electric, and Medtronic. All other authors report that they have no relationships relevant to the contents of this paper to disclose.

Funding

This study was supported by Emile Letang Grand of Hospital Clinic de Barcelona/Instituto de Salud Carlos III (ISCIII) PI20/00693/CB16/11/00354, co-funded by the European Union/CIBERCV16 - CB16/11/00354 of Instituto de Salud Carlos III, Madrid and CERCA Programme/Generalitat de Catalunya. Project funded by Asociación del Ritmo SEC: SECARIT-FOR-NAC 22/008.

Data availability

No new data were generated or analysed in support of this research.

References

1. Berruezo A, Fernández-Armenta J, Andreu D, Penela D, Herczku C, Evertz R *et al.* Scar dechanneling: new method for scar-related left ventricular tachycardia substrate ablation. *Circ Arrhythm Electrophysiol* 2015;**8**:326–36.
2. Mountantonakis SE, Park RE, Frankel DS, Hutchinson MD, Dixit S, Cooper J *et al.* Relationship between voltage map "channels" and the location of critical isthmus sites in patients with post-infarction cardiomyopathy and ventricular tachycardia. *J Am Coll Cardiol* 2013;**61**:2088–95.
3. Andreu D, Ortiz-Perez JT, Boussy T, Fernandez-Armenta J, De Caralt TM, Perea RJ *et al.* Usefulness of contrast-enhanced cardiac magnetic resonance in identifying the ventricular arrhythmia substrate and the approach needed for ablation. *Eur Heart J* 2014;**35**:1316–26.
4. Andreu D, Ortiz-Perez JT, Fernandez-Armenta J, Guiu E, Acosta J, Prat-Gonzalez S *et al.* 3D delayed-enhanced magnetic resonance sequences improve conducting channel delineation prior to ventricular tachycardia ablation. *Europace* 2015;**17**:938–45.
5. Piers SRD, Tao Q, Silva M DR, Siebelink HM, Schalij MJ, Van Der Geest RJ *et al.* CMR-based identification of critical isthmus sites of ischemic and nonischemic ventricular tachycardia. *JACC Cardiovasc Imaging* 2014;**7**:774–84.
6. Vázquez-Calvo S, Casanovas JM, Garre P, Ferró E, Sánchez-Somonte P, Quinto L *et al.* Evolution of deceleration zones during ventricular tachycardia ablation and relation with cardiac magnetic resonance. *JACC Clin Electrophysiol* 2023;**9**:779–89.
7. Andreu D, Penela D, Acosta J, Perea RJ, Soto-iglesias D, De Caralt TM *et al.* Cardiac magnetic resonance–aided scar dechanneling: influence on acute and long-term outcomes. *Heart Rhythm* 2017;**14**:1121–8.
8. Roca-Luque I, Rivas-Gandara N, Francisco-Pascual J, Rodriguez-Sanchez J, Cuellar-Calabria H, Rodriguez-Palomares J *et al.* Preprocedural imaging to guide transcoronary ethanol ablation for refractory septal ventricular tachycardia. *J Cardiovasc Electrophysiol* 2019;**30**:448–56.
9. Quinto L, Sanchez-Somonte P, Alarcón F, Garre P, Castillo À, San Antonio R *et al.* Ventricular tachycardia burden reduction after substrate ablation: predictors of recurrence. *Heart Rhythm* 2021;**18**:896–904.
10. Kalin R, Stanton MS. Current clinical issues for MRI scanning of pacemaker and defibrillator patients. *Pacing Clin Electrophysiol* 2005;**28**:326–8.
11. Bhuva AN, Kellman P, Graham A, Ramlall M, Boubertakh R, Feuchter P *et al.* Clinical impact of cardiovascular magnetic resonance with optimized myocardial scar detection in patients with cardiac implantable devices. *Int J Cardiol* 2019;**279**:72–8.
12. Do DH, Eyvazian V, Bayoneta AJ, Hu P, Finn JP, Brad JS *et al.* Cardiac magnetic resonance imaging using wideband sequences in patients with nonconditional cardiac implanted electronic devices. *Heart Rhythm* 2018;**15**:218–25.
13. Hilbert S, Weber A, Nehrke K, Bornert P, Schnackenburg B, Oebel S *et al.* Artefact-free late gadolinium enhancement imaging in patients with implanted cardiac devices using a modified broadband sequence: current strategies and results from a real-world patient cohort. *Europace* 2018;**20**:801–7.
14. Roca-Luque I, Van Breukelen A, Alarcon F, Garre P, Tolosana JM, Borras R *et al.* Ventricular scar channel entrances identified by new wideband cardiac magnetic resonance sequence to guide ventricular tachycardia ablation in patients with cardiac defibrillators. *Europace* 2020;**22**:598–606.
15. Ghafoori E, Kholmovski E, Thomas S, Silvernagel J, Nathan A, Nan H *et al.* Characterization of gadolinium contrast enhancement of radiofrequency ablation lesions in predicting edema and chronic lesion size. *Circ Arrhythm Electrophysiol* 2017;**10**:1–9.
16. Celik H, Ramanan V, Barry J, Ghate S, Leber V, Oduneye S *et al.* Intrinsic contrast for characterization of acute radiofrequency ablation lesions. *Circ Arrhythm Electrophysiol* 2014;**7**:718–27.
17. Dabbagh GS, Ghannam M, Siontis KC, Attili A, Cochet H, Jais P *et al.* Magnetic resonance mapping of cathter ablation lesions after post-infarction ventricular tachycardia ablation. *JACC Cardiovasc Imaging* 2021;**14**:588–98.
18. Cronin EM, Bogun FM, Maury P, Peichl P, Vice-chair E, Chen M *et al.* 2019 HRS/EHRA/APHRS/LAHRS expert consensus statement on catheter ablation of ventricular arrhythmias. *EP Europace* 2019;**21**:1143–4.
19. Aziz Z, Shatz D, Raiman M, Upadhyay GA, Beaser AD, Besser SA *et al.* Targeted ablation of ventricular tachycardia guided by wavefront discontinuities during sinus rhythm: a new functional substrate mapping strategy. *Circulation* 2019;**140**:1383–97.
20. De Chillou C, Groben L, Magnin-poull I, Abdelaal A, Ammar S, Sellal J *et al.* Localizing the critical isthmus of postinfarct ventricular tachycardia : the value of pace-mapping during sinus rhythm. *Heart Rhythm* 2014;**11**:175–81.
21. Fernández-Armenta J, Berruezo A, Andreu D, Camara O, Silva E, Serra L *et al.* Three-dimensional architecture of scar and conducting channels based on high resolution ce-CMR insights for ventricular tachycardia ablation. *Circ Arrhythm Electrophysiol* 2013;**6**:528–37.
22. Sánchez-Somonte P, Quinto L, Garre P, Zaraket F, Alarcón F, Borràs R *et al.* Scar channels in cardiac magnetic resonance to predict appropriate therapies in primary prevention. *Heart Rhythm* 2021;**18**:1336–43.
23. van der Bijl P, Delgado V, Bax JJ. Sudden cardiac death: the role of imaging. *Int J Cardiol* 2017;**237**:15–8.
24. Linhart M, Alarcon F, Borràs R, Benito EM, Chipa F, Cozzari J *et al.* Delayed gadolinium enhancement magnetic resonance imaging detected anatomic gap length in wide circumferential pulmonary vein ablation lesions is associated with recurrence of atrial fibrillation. *Circ Arrhythm Electrophysiol* 2018;**11:e006659**:1–9.
25. Dinov B, Oebel S, Hilbert S, Loebe S, Arya A. Characteristics of the ablation lesions in cardiac magnetic resonance imaging after radiofrequency ablation of ventricular arrhythmias in relation to the procedural success. *Am Heart J* 2018;**204**:68–75.
26. Dickfeld T, Kato R, Zviman MM, Lai S, Meininger G, Lardo AC *et al.* Characterization of radiofrequency ablation lesions with gadolinium-enhanced cardiovascular magnetic resonance imaging. *J Am Coll Cardiol* 2006;**47**:370–8.
27. Vunnam R, Ghzally Y, Mbbs JBM, See V, Maheshwari V, Imanli H *et al.* Ventricular arrhythmia ablation lesions detectability. *Pacing Clin Electrophysiol* 2020;**43**:314–21.

5. DISCUSIÓN

La presente tesis doctoral busca resolver algunas de las cuestiones relacionadas con la caracterización del sustrato arrítmico mediante el uso de catéteres de alta densidad y de resonancia magnética cardíaca. Los puntos importantes de la misma son:

1. El sustrato arrítmico definido en los mapas electroanatómicos debe ser considerado con cautela debido al carácter variable del mismo (sustrato funcional) y a la dificultad para su correcta identificación debido a las limitaciones derivadas de la interacción tejido-catéter, ejemplificada en la alta variabilidad individual en los umbrales óptimos de voltaje para identificar las zonas de interés.

2. La mejor identificación del sustrato puede permitir la ablación de nuevas zonas de potencial interés. Los esfuerzos dirigidos a mejorar la identificación del mismo pueden llevar a mejores resultados clínicos. En este sentido, la realización de mapas de alta densidad mediante el uso de catéteres de alta densidad con detección de señales ortogonales se asocia a menor carga arrítmica en el seguimiento.

3. La RMC es una prueba no invasiva que se ha consolidado como herramienta fundamental para la identificación tridimensional del sustrato arrítmico con importantes implicaciones diagnósticas y pronósticas. Además de su capacidad para la representación del sustrato anatómico, es posible establecer predictores de "arritmogenicidad de sustrato" según ciertas características de los canales, en concreto, su longitud, masa y *protectedness*.

4. En términos de planificar la ablación de TV, la RMC puede ayudarnos a elegir el abordaje necesario (recomendando abordaje epicárdico si existen canales con una profundidad mayor a 7.2mm), a ajustar de forma individual los umbrales de los mapas de voltaje para

mejorar la definición del sustrato y a desenmascarar zonas de conducción lenta no aparentemente activas en el mapa electroanatómico basal.

5. Finalmente, el análisis de ciertas características de la RMC realizada 3-6 meses después de la ablación de TV, principalmente el número de canales y la reducción porcentual de los mismos respecto a la RMC realizada antes de la ablación, puede también ayudarnos a estimar la probabilidad de recurrencia y, potencialmente, individualizar el tratamiento post-ablación de los pacientes.

Mejora en la definición de los mapas electroanatómicos

Contribución de los catéteres de alta densidad

Múltiples estudios señalan que la adquisición de mapas electroanatómicos con catéteres de alta densidad permite una mejor definición del sustrato, especialmente en zonas de bajo voltaje donde se encuentran la mayor parte de los electrogramas de interés(50,51). Esto se debe no solo a la mayor adquisición de puntos con este formato de catéteres con más de un dipolo, sino también a la distribución espacial de los mismos(48,49). En este sentido, el catéter HDGrid, que presenta una distribución en forma de red y que es por tanto capaz de recibir señales al mismo tiempo en un dipolo con un ángulo de 90º y en el perpendicular con un ángulo de 180º presenta una ventaja mayor al resto de catéteres que se encuentran comercializados(53,56–58).

En el artículo 1 de esta tesis se compara una estrategia de mapeo exhaustivo con catéter de alta densidad con capacidad para detección de señales ortogonales con una estrategia de “scar dechanneling” realizada también con un catéter de alta densidad, pero con una distribución de los dipolos diferente que no es capaz de analizar señales ortogonales. La estrategia de mapeo extensivo con señales ortogonales resultó en una reducción significativa en la carga global de TVs

a un 1 año después del procedimiento, tanto en ATPs (99.47±2.29 vs. 33.94±102.46%, p<0.001) como descargas apropiadas del desfibrilador (99.00±4.47 vs. 64.67±59.87%, p = 0.02) como episodios de TV (81.69±7.79 vs. 43.46±19.97%, p < 0.05).

Como se mencionó anteriormente, estos resultados pueden estar principalmente relacionados con la mejor definición del sustrato lograda gracias a la estrategia de mapeo exhaustivo que enfatiza la recopilación de señales eléctricas para obtener mapas muy completos ya que el análisis de señales ortogonales permite disminuir parcialmente la dependencia del tipo de señal de la dirección del frente de activación. Así, este tipo de catéter permite identificar señales de interés en su máxima amplitud, lo que permite una identificación precisa del sustrato a ablacionar.

En relación a los mapas de alta densidad y a la capacidad de los catéteres de recoger la señal local en su máxima amplitud, recientemente se han desarrollado dos nuevos algoritmos que optimizan la identificación de señal: la *tecnología omnipolar* y la *tecnología near field.*

Por un lado, la **tecnología omnipolar**, que permite detectar las señales de forma prácticamente independiente a la dirección del frente de onda. Esta tecnología fue descrita inicialmente en 2016(128,129), realizándose estudios en modelos animales tanto a nivel ventricular(55) como auricular(130), mostrando una mejor definición de sustrato comparado con catéteres bipolares. Estudios muy recientes parecen demostrar que esta tecnología permite no solo la mejor identificación del sustrato en los mapas de voltaje si no una mejor identificación de las zonas de deceleración(131). De nuevo, dada la diferente identificación de la señal respecto a algoritmos previos (ya sea tecnología bipolar u ortogonal), es probable que los umbrales 0.5-1.5mV descritos en catéteres bipolares no sea aplicable para los mapas de voltaje creados con tecnología omnipolar, pudiendo ser la RMN una buena estrategia para ajustar los umbrales tal y como demostramos en el artículo 2 recogido en esta tesis.

Por otro lado, la **tecnología *near field***, que cuenta con un algoritmo basado en la frecuencia de cada uno de los componentes del EGM, que permite anotar la señal local entendida ésta como la de mayor frecuencia, evitando que la señal del *farfield* circundante impida la identificación

correcta de potenciales patológicos. Este fenómeno podría ser especialmente relevante en zonas patológicas cercanas a tejido sano, donde la señal local habitualmente es fragmentada y de menor amplitud, pero que con frecuencia queda escondida en la señal de mayor amplitud del tejido sano circundante.

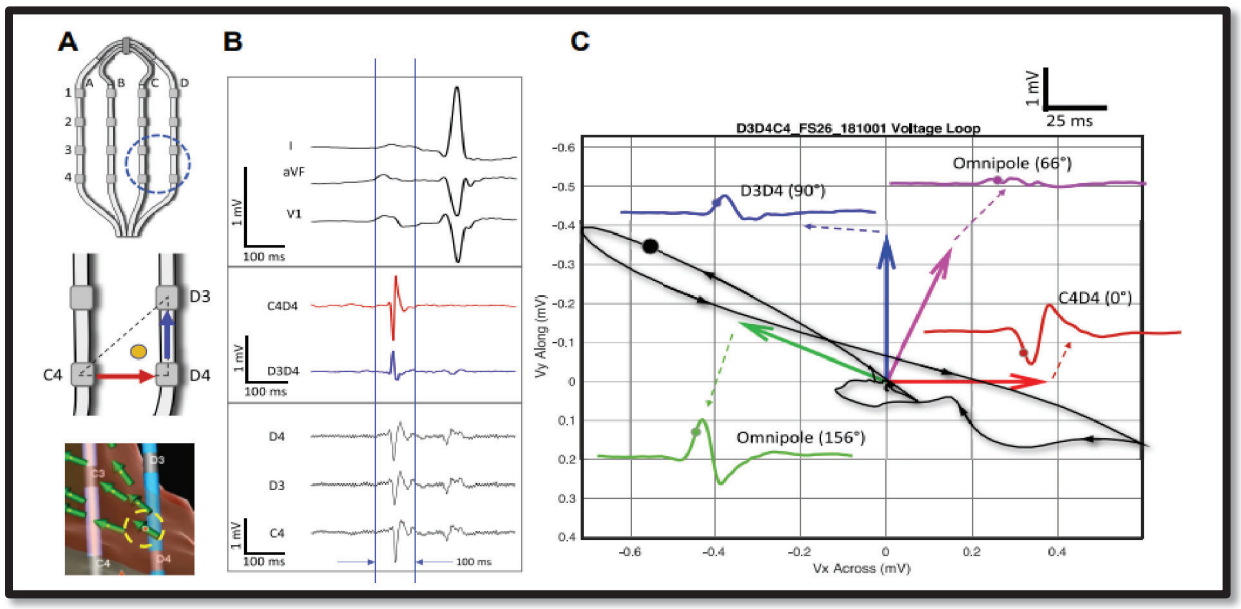

Fig 18: **Esquema representativo de la tecnología omnipolar aplicada al catéter HDGrid**. A: Catéter HDGrid formado por 36 dipolos que forman una malla 4*4. El sistema construye triángulos llamados "*Cliques*" constituidos por 3 electrodos (C4, D4 y D3 en este ejemplo). B: Representación de la señal bipolar y unipolar en dichos polos. C: Desde el centro de este *clique* se realizan *loops* que permiten identificar la zona de máxima amplitud en todas las direcciones. Imagen procedente de Deno et al. (132).

Ambas estrategias de mapeo ofrecen potenciales ventajas a la hora de analizar el sustrato y su uso forma parte actualmente de nuevas líneas de investigación.

Contribución de la RMC

- *En mapas de voltaje*

Tal y como se explicó previamente, existen distintas estrategias durante los procedimientos de ablación que nos permiten identificar el sustrato arrítmico.

Respecto a los mapas de voltaje, la mejora en la identificación de señales patológicas, ya sean potenciales tardíos o actividad ventricular anómala, ha mejorado sustancialmente gracias al uso de catéteres de alta densidad. Estos mismos catéteres han contribuido a mejorar la definición del mapa de voltaje, otro de los sistemas de mapeo usados para identificar el sustrato arrítmico, en este caso en forma de canales de voltaje. Sin embargo, una de las principales limitaciones de estos mapas, además de las ya mencionadas en relación con la correcta identificación de las señales por parte del catéter, se debe a la falta de umbrales de voltaje definidos para catéteres de alta densidad que permitan diferenciar el tejido sano de la cicatriz.

La RMC permite describir el sustrato arrítmico de una forma no invasiva, permitiéndonos disponer de una representación del mismo antes del procedimiento. Tal y como se demuestra en el artículo 2 presentado en esta tesis, la RMC puede ser usada para ajustar de forma individual los umbrales de voltaje y mejorar la capacidad del mapa de voltaje para describir el sustrato arrítmico. Los umbrales fijos que se usan habitualmente para diferenciar cicatriz, *border zone* y tejido sano (0.5mV y 1.5mV) no han demostrado una correlación fuerte con sustrato arrítmico, presentando los canales de voltaje detectados con estos umbrales una baja especificidad (30%) respecto a los circuitos de TV(60). Existe un cierto consenso en los diversos grupos acerca de la necesidad de ajustar los umbrales de voltajes de paciente a paciente para hacerlos más específicos. Sin embargo, este ajuste se hace de forma subjetiva, con todas las limitaciones que ello conlleva. Nuestro estudio es el primero que utiliza la información del mapa de sustrato no invasivo obtenido por RMC para ajustar de forma personalizada los umbrales, siendo la media similar a la descrita (0.51±0.32 y 1.79±0.71mV) pero encontrando una importante variabilidad de paciente a paciente (desde 0.14-1.68mV hasta 0.7-3.21mV). Estos mapas de voltaje personalizados mejoran de forma muy relevante la capacidad para identificar correctamente el sustrato arrítmico, tanto en lo que concierne a la detección de zonas de deceleración como a los istmos de TV.

Cabe preguntarse, de todos modos, cuál es la necesidad de ajustar los umbrales del mapa de voltaje usando la RMC cuando ésta misma puede ser directamente usada como un mapa sobre el que realizar la ablación, identificando correctamente tejido sano y cicatricial, así como los canales arrítmicos, pudiendo potencialmente sustituir al mapa de voltaje. Sin embargo, dado que

independientemente de la estrategia de ablación, los métodos actuales consiguen únicamente una tasa de recurrencia no inferior al 20-30%(133), tiene sentido pensar que toda la información que podamos obtener puede ayudar a mejorar la eficacia de los procedimientos. El sustrato arrítmico esconde una importante complejidad dada su tridimensionalidad, su funcionalidad, etc. por lo que probablemente no puede ser completamente entendido utilizando una única estrategia de mapeo. La combinación de diferentes estrategias puede ser la respuesta a la específica eliminación total del sustrato arrítmico.

- *En la descripción del sustrato funcional*

Siguiendo la evolución en el conocimiento en el sustrato arrítmico y la mejora en los sistemas de mapeo para identificar el mismo nace el concepto de sustrato funcional. En este sentido, las zonas de deceleración halladas en los mapas de isócronas definidas por el grupo del Dr. Tung(73,74) han constituido una revolución gracias a la facilidad para generar mapas reproducibles y automáticos en ritmo sinusal, de fácil interpretación, y, lo que es más importante, con una gran correlación de las zonas de deceleración con las zonas críticas del circuito de TV. Sin embargo, este modelo de fácil identificación de zonas críticas, basado inicialmente en ablacionar solo la zona de deceleración principal en caso de que el paciente sea no inducible para TV, presenta igualmente tasas de recidiva altas, lo que obliga a continuar mejorando las estrategias de ablación.

En esta tesis se analiza la capacidad de la RMC primero para identificar de forma no invasiva las zonas de deceleración, y segundo, para desenmascararlas durante los procedimientos, ambas funciones con importantes aplicaciones.

Por una parte, en el artículo 4 de la presente tesis se muestra que no todos los canales detectados por RMC se asocian con propiedades de conducción lenta (76.1%). En concreto, parecen ser aquellos canales con mayor longitud, gramos y *protectedness* los que presentan propiedades funcionales críticas para el desarrollo de TVs. Estos hallazgos implican por una parte que, una técnica de ablación basada únicamente en eliminar canales detectados por RMC podría llevarnos

a aplicar radiofrecuencia en zonas sin potencial capacidad de generar taquicardias, pudiendo esta modificación del sustrato generar nuevas zonas potencialmente responsables de arritmias en el futuro. El máximo exponente de esta técnica son los estudios liderados por el grupo del Dr. Berruezo(95), que utiliza la descanalización como estrategia de ablación. Incorporar la información sobre longitud, masa y *protectedness* a la ténica *scar dechanneling* podría llevar a mejores resultados clínicos.

De forma muy interesante, en el artículo 3 de esta tesis demostramos también que un 93.68% de las zonas de deceleración detectadas mediante mapas de isócronas se correlacionan con un canal de RMC. No solo ello, si no que tras ablacionar las zonas detectadas en el mapa basal, solo un 72.2% de las mismas desaparece, lo que implica casi un tercio persiste en la misma localización, siendo aquellas de localización septal y las que se encuentran en la zona intermedia del canal (no la entrada ni la salida) las que presentan mayor dificultad para ser eliminadas. Poder disponer de esta información previa al procedimiento podría llevar a una mejor planificación de la estrategia de ablación, de lo que hablaremos extensamente en el siguiente apartado.

Además, si cabe más interesante, durante los mapas sucesivos realizados después del primer set de ablación, se observan un 17.5% de nuevas zonas de deceleración que no eran visibles en el mapa inicial pero que coinciden igualmente con canales de resonancia. Es decir, zonas de deceleración asociadas a un sustrato anatómico que aparentemente no eran activas pero que se manifiestan como tal tras eliminar la zona de deceleración principal. En el artículo 3 dos hipótesis son planteadas al respecto: la primera referida a que estas zonas cuenten ya con potenciales patológicos desde el principio, pero, debido a la metodología de ILAM, no sea visible como zona de deceleración. Esto se debe a que la ventana se divide en 8 isocronas basándose en la duración del potencial más retrasado. Podría por tanto ocurrir que, si la primera zona de deceleración cuenta con señales muy muy atrasadas, cada uno de los 8 fragmentos de la ventana dure una cantidad importante de tiempo, dificultando la identificación de otra potencial zona patológica sin tanto retraso local. Sin embargo, al eliminar los primeros electrogramas más retrasados, la "nueva ventana" se acortaría, permitiendo la visualización de otras zonas de deceleración. La segunda hipótesis se basa en que realmente no se observen señales patológicas en las zonas aparentemente normales en el mapa basal debido a los cambios en funcionalidad del sustrato,

que pueden hacer que un área sea aparentemente normal, pero muestre signos de "funcionalidad" cuando se realizan maniobras de desenmascaramiento, principalmente con extraestímulos. Ambas hipótesis constituyen posibles futuras líneas de investigación que podrían ayudar a lograr una mejor definición del sustrato mediante mapas de isócronas.

De todos modos, independientemente del motivo por el que esto ocurre, el hecho de que la RMC permita identificar en dichas localizaciones, aparentemente sanas en el mapa basal, un canal le otorga un valorar esencial en el desenmascaramiento de zonas potencialmente responsables de arritmias en el procedimiento, o bien para intentar desenmascararlas en el mapa basal (mediante estrategia de extraestímulos por ejemplo) o bien para insistir en el *remap* en dichas zonas. De hecho, en nuestro estudio, así como en el estudio original de Aziz et al.(74), el número de *remaps* se asoció con menos recurrencia de TV en el seguimiento, dando a entender que este sustrato desenmascarado en los *remaps* es relevante y debe ser eliminado. Sería interesante valorar la realización sistemática de un protocolo de extraestímulos S1-S2-S3 que potencialmente pueda desenmascarar todas las zonas de deceleración ya en el mapa basal, reduciendo la necesidad de múltiples *remaps*. Del mismo modo, podría ser interesante valorar a partir de que duración de ventana debería plantearse modificar el número de isocronas en las que se divide la señal, hipotetizando que podrían ser necesarias más de 8 cuando la duración de la ventana es muy amplia, para evitar la infradetección de zonas de deceleración. Existen, por tanto, múltiples campos de mejora a explorar que pueden constituir futuras líneas de investigación en las que la RMC ejerza como herramienta central para guiar la correcta identificación del sustrato durante los procedimientos de ablación.

Planificación de los procedimientos de ablación de TV mediante RMC

Otro de los aspectos relevantes en la alta tasa de recurrencias tras una ablación de TV guarda relación con la elección del abordaje; dado que algunos pacientes pueden requerir un abordaje epicárdico para la completa eliminación del sustrato. Sin embargo, este acceso se asocia con tasas de complicaciones superior al abordaje exclusivo endocárdico, principalmente en relación

con la punción, pero también con aplicar radiofrecuencia en arterias coronarias, etc. (120). Por este motivo se intenta seleccionar de forma muy cuidadosa a los pacientes en los que la ablación epicárdica va a ser imprescindible, ya sea porque la morfología del electrocardiograma (ECG) en TV sugiere un origen a dicho nivel o porque el sustrato sea claramente epicárdico (lo que se puede inferir por el tipo de cardiopatía o visualizar directamente mediante RMC). De todos modos, existe una fuerte controversia entre diferentes grupos acerca de cuándo elegir un acceso epicárdico, especialmente en pacientes isquémicos en los que conceptualmente el sustrato es mayoritariamente endocárdico. Así, algunos estudios(119) sugieren que, en esta población, el istmo de la TV se origina en capas endocárdicas en el 94% de los pacientes. Sin embargo, como ya hemos comentado, el istmo de la TV no representa la totalidad del sustrato, por lo que podría ser necesario realizar aplicaciones adicionales en otras localizaciones para la total abolición del sustrato. Otros grupos(45) sugieren realizar sistemáticamente mapas endo y epicárdicos en pacientes isquémicos y para la eliminación no sólo de la TV sino también de todo el sustrato.

En esta tesis se incluye un estudio (artículo 5) que intenta aclarar cuándo es necesario acceder al epicardio basándose en la profundidad del sustrato, analizada mediante RMC, estableciendo un punto de corte de 7.2mm a partir del cual el acceso exclusivo desde el endocardio utilizando un patrón standard de parámetros de ablación (40W, 60segundos) es insuficiente para la eliminación del sustrato. Es importante señalar que este punto de corte podría variar utilizando otros protocolos de ablación que impliquen aumentar la potencia o la duración de las aplicaciones(111), si bien la utilizada en el estudio es comparable a la práctica clínica habitual en la mayoría de los centros. En este trabajo, la presencia de sustrato epicárdico también constituye de por si un predictor de recurrencia, si bien con una especificidad mucho más baja (27.27% vs 61.36%). En este sentido, de forma interesante, solo un solo el 35% de la población isquémica cumpliría con los criterios para la ablación endoepicárdica utilizando el umbral de un canal de RMC más profundo que 7.2 mm, lo que coincide con el estudio de Di Biase(45) en el que, pese a sugerir abordaje endoepicárdico en todos los pacientes, sólo en un porcentaje bajo de pacientes (alrededor de un 33%) se requiere realizar aplicaciones en el epicardio. Además, el uso de la profundidad del canal (7.2 mm) limita mucho la necesidad de abordaje epicárdico en comparación con el uso de la presencia de un canal epicárdico sin considerar la profundidad del

canal como criterio ya que, en este caso, el 75.78% de los pacientes requeriría abordaje epicárdico. Es por ello que la profundidad de canal evaluado mediante RMC puede constituir un nuevo método para seleccionar de forma más específica a los pacientes que van a requerir un abordaje epicárdico. Para comprobar dicha hipótesis, sería necesario realizar estudios prospectivos multicéntricos en los que se utilice este punto de corte de 7.2mm para seleccionar el acceso.

Además de la contribución de la RMC pre-procedimiento en la elección del abordaje, la RMC puede ayudarnos a planificar el procedimiento en muchas otras perspectivas. En la presente tesis se profundiza (mediante los artículos 3 y 4) en la capacidad de la RMC para definir el sustrato arrítmico, gracias a la comparación tanto con mapas de voltaje como con mapas funcionales, encontrando predictores de arritmogenicidad no solo en las características de la cicatriz, tal y como han descrito otros grupos, si no en las características de los canales. Aquellos canales con mayor masa, longitud y *protectedness* se asocian con mayor probabilidad con zonas de deceleración durante los mapas electroanatómicos. Además, tal y como se comentaba previamente, casi un tercio de las zonas de deceleración persisten en la misma localización después de aplicar radiofrecuencia, siendo aquellas de localización septal y las que se encuentran en la zona intermedia del canal las que presentan mayor dificultad para ser ablacionadas.

De nuevo, el uso de esta información procedente de RMC podría ser campo de nuevas líneas de investigación que incluyan, por ejemplo, elegir una estrategia de ablación u otra según la localización del sustrato evaluado mediante la RMC realizada antes del procedimiento (ablación standard o ablación bipolar o con suero salino para alcanzar lesiones más profundas en el septo por ejemplo o ablaciones más extensas en las zonas intermedias del canal con respecto a entrada/salida del mismo).

Estimación de riesgo arrítmico mediante RMC

La mejora en el conocimiento no invasivo del sustrato arrítmico mediante RMC tiene implicaciones no solo en relación a la ablación de TV, si no a la estimación del riesgo arrítmico,

ya sea en pacientes que ya han presentado un primer evento arrítmico como en aquellos potencialmente en riesgo.

Múltiples esfuerzos han sido realizados en la línea de mejorar la identificación de pacientes en riesgo de eventos arrítmicos, no solo para decidir el implante o no de un DAI sino también para plantear ablaciones de sustrato precoces o incluso profilácticas. SMASH-VT(134) fue el primer ensayo aleatorizado (2007) que evaluó el papel de la ablación "profiláctica" de TV en pacientes con miocardiopatía isquémica e indicación de DAI en prevención secundaria, demostrando una reducción en la incidencia de terapias de DAI en los grupos de ablación en comparación con el tratamiento convencional. En 2010, el estudio VTACH(135) fue diseñado de manera similar, pero se centró no solo en la incidencia de terapias de DAI sino también en el tiempo hasta la recurrencia de TV, observando también que la ablación de TV parecía prolongar el tiempo hasta la recurrencia de TV en la población estudiada (pacientes con TV estable, infarto de miocardio previo y FEVI reducida). En 2017, el estudio SMS(136), sin embargo, no logró confirmar estos resultados en una población muy similar. Willems et al., en 2020, realizaron un nuevo estudio (BERLIN VT(136)), también en pacientes isquémicos, comparando una ablación inmediata después de un episodio de TV vs. una ablación diferida con un *endpoint* diferente: un compuesto de muerte y hospitalización por TV/FV o empeoramiento de la insuficiencia cardíaca. El estudio se detuvo temprano por futilidad, no encontrando diferencias entre los grupos. El último estudio se realizó en 2022 por Della Bella et al.: El estudio PARTITA(137) donde 517 pacientes (78% isquémicos) con un DAI fueron seguidos hasta que se detectó el primer choque y luego se asignaron al azar a ablación o continuación de la terapia estándar. El *endpoint* primario también fue un compuesto de muerte por cualquier causa u hospitalización por empeoramiento de la insuficiencia cardíaca (la recurrencia de TV no se incluyó en el punto final primario). Los resultados fueron absolutamente favorables para la estrategia de ablación, demostrando un riesgo reducido del punto final combinado de muerte o hospitalización por empeoramiento de la insuficiencia cardíaca, pero también una menor mortalidad y menos choques de DAI.

En ninguno de estos estudios se evaluaron las características de la cicatriz mediante RMC para decidir una estrategia de ablación precoz o no, pese a que se ha demostrado que las características del sustrato evaluadas mediante esta técnica son predictoras de eventos(127).

En esta tesis se presentan resultados (artículo 3) que otorgan todavía más poder predictor a la RMC en dicho sentido, encontrando diferencias significativas entre unos canales y otros, siendo aquellos con más masa, longitud y *protectedness* los más arritmogénicos.

Este trabajo constituye es el inicio de una futura línea de investigación con numerosas aplicaciones clínicas de alto impacto, incluyendo cómo incorporar los hallazgos del sustrato por RMC para la mejor selección de pacientes que van a someterse a un implante de DAI o a un procedimiento de ablación precoz.

Predictores de recurrencia post ablación de TV

Tal como se ha comentado anteriormente, la tasa de recurrencia de taquicardia ventricular (TV) tras un procedimiento de ablación varía entre el 30% y el 40%, siendo más elevada en pacientes no isquémicos(133). Aunque parte de este porcentaje puede atribuirse, especialmente en esta segunda población, a la progresión de la enfermedad que resulta en nuevas TV originadas en áreas previamente no patológica, la mayor parte de las recurrencias se deben a un fracaso del procedimiento de ablación(121). En este sentido, múltiples grupos han descrito que, tanto la eliminación completa de señales patológicas como la no inducibilidad de taquicardia ventricular al final del procedimiento, constituyen predictores de recurrencia(42,138–140). Sin embargo, la no identificación de potenciales tardíos al final del procedimiento podría deberse a la falta de un correcto mapeo en una zona de interés no detectada durante el procedimiento o que pasa desapercibida por una mala detección por parte del catéter. Del mismo modo, la no inducibilidad de la TV como criterio de éxito de procedimiento es un *endpoint* insuficiente ya que, sin acompañarse de la eliminación de todo el sustrato se relaciona con tasa de recurrencia muy elevada(140). Esto ocurre por varios motivos, principalmente el hecho de que la inducibilidad de TV no es estática si no que depende también de otros factores como la carga adrenérgica, pudiendo un paciente ser no inducible para TV durante el procedimiento y presentar TV a los pocos días en otro contexto. De hecho, un tercio de los pacientes en los que se realiza una ablación programada de TV son no inducibles para TV ya al inicio del procedimiento pese a haber

presentado eventos previos a la ablación. Algunos grupos intentan compensar esta situación realizando una estimulación programada no invasiva (NIPS) unos días después del procedimiento a través del DAI, aplicando terapia antitaquicardia con la intención de inducir TV(141) siendo la inducibilidad por este método un predictor de recurrencia de TV. Sin embargo, este método no permite identificar los motivos de fracaso de la ablación ni aporta información sobre el origen del circuito arrítmico no eliminado, además de asociarse a la posible necesidad de choque del DAI de la TV inducida.

En esta tesis, mediante el artículo 6, se presenta un nuevo método para entender los cambios en el sustrato arrítmico con la intención no solo de identificar qué pacientes van a recurrir después del procedimiento si no de conocer cómo la ablación modifica el sustrato arrítmico y cómo son los circuitos arrítmicos responsables de las recurrencias. La RMC, respecto a los *endpoints* clásicos de ablación, tiene la ventaja de que no depende del contacto del catéter con el tejido ni se ve afectada por la funcionalidad del sustrato en un momento determinado. De este modo, la presencia de dos o más canales en la RMC 3-6 meses post ablación constituye un predictor de recurrencia de TV a los 12 meses (31.82% vs. 0%, P = 0.0038) con una sensibilidad del 100% y una especificidad del 61% (área bajo la curva 0.82). Esto implica que ninguno de los pacientes sin canales en la RMC post ablación presentó recurrencia durante el seguimiento. En la misma línea, una reducción de los canales menor al 55% tuvo una sensibilidad del 100% y una especificidad del 61% (área bajo la curva 0.83) para predecir la recurrencia de TV.

Este trabajo es sólo el inicio de una línea de investigación que se continuará con el análisis de una segunda RMC a los 18-24 meses que permitirá conocer mejor la evolución del sustrato a medio-largo plazo. Correlacionar esta información con la presencia de recurrencia y especialmente con la información obtenida en los mapas electroanatómicos de aquellos pacientes que se sometan a un segundo procedimiento tras una recurrencia de la primera ablación será crucial para entender toda la información que nos aporta la RMC. El objetivo final es doble. Por un lado, identificar precozmente a pacientes en riesgo alto de recurrencia, pudiendo esto cambiar el manejo clínico o bien manteniendo antiarrítmicos durante más tiempo o proponiendo una segunda ablación precozmente. En segundo lugar, entender mecanismos que expliquen la recidiva. Este segundo aspecto es fundamental para mejorar los resultados de un procedimiento

con una alta tasa de recurrencias. Además, el análisis particular de la evolución de los canales detectados por RMC permitirá observar cómo se comportan los mismos ante la ablación (si se mantienen en la RMC post ablación, si se fragmentan, si desaparecen completamente, etc), pudiendo generar predictores específicos de dificultad de eliminación de canales según sus características y localización, lo que podría llevar a aplicar diferente energía de forma diferente durante el primer procedimiento, etc. Nuestro estudio describe también la presencia de *dark core* no en todos los pacientes, no estando éste relacionado con recurrencia en el seguimiento.

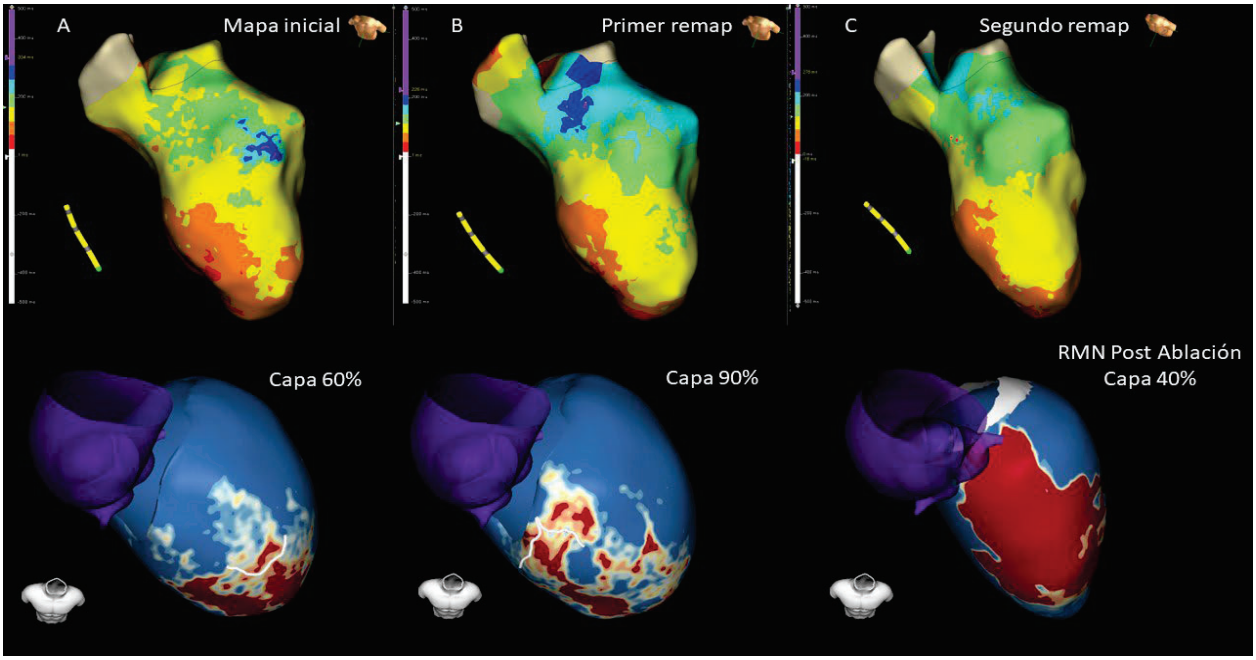

Fig. 19: **Correlación de mapas electroanatómicos y RMC**. Se observa una zona de deceleración en el mapa basal (A) que coincide con un canal de RMC en la capa 6 (D), apareciendo una nueva zona de deceleración en el primer *remap* (B) no presente en el mapa basal pero que coincide a su vez con un canal de la RMC preablación, esta vez en la capa 9 (E). En el último *remap* (C) se observa la total desaparición de zonas de deceleración, mostrándose en la RMC post ablación una cicatriz densa, sin presencia de canales. Este paciente no presentó recurrencia de TV un año post ablación. Imagen propia.

6. CONCLUSIONES

1. El uso de un método basado en un mapeo extenso con catéteres de alta densidad con capacidad de detectar señales ortogonales permite una mejor discriminación del sustrato arrítmico y podría estar asociado con mejores resultados del procedimiento de ablación de TV
2. Los mapas de voltaje personalizados basados en imágenes de RMC permiten una identificación más clara del sustrato con una mayor correlación tanto con las DZ como con los istmos de TV comparado con los mapas de voltaje convencionales que utilizan umbrales fijos.
3. Las DZs están altamente correlacionadas con los canales de RMC. Además, el remap puede conducir a la identificación de sustrato oculto inicialmente no identificado por el mapeo electroanatómico, pero sí detectado por RMC.
4. La detección no invasiva de zonas funcionalmente críticas para la presencia de eventos de TV es posible con RMC. Las DZs encontradas durante el mapa electroanatómico se correlacionan con precisión con los canales de RMN, especialmente aquellos con mayor longitud, masa de zona de borde y *protectedness*.
5. En pacientes con TV relacionada con sustrato izquierdo, la profundidad máxima de los canales de RMC predice la recurrencia de TV después de una ablación endocárdica. Un punto de corte de profundidad máxima del canal de RMC de 7.2 mm podría usarse para seleccionar un enfoque endocárdico exclusivo.
6. La RMC post ablación es factible, y una reducción en el número de canales está relacionada con un menor riesgo de recurrencia de TV. El *dark core* no está presente en todos los pacientes, no relacionándose su presencia con eventos en el seguimiento.

7. BIBLIOGRAFÍA

1. Brugada J. La muerte súbita cardiaca. La necesidad de una estrategia integral para combatirla. Revista Española de Cardiología Suplementos 2013;13:1. Doi: 10.1016/S1131-3587(13)70059-1.

2. Moss AJ., Hall WJ., Cannom DS., et al. Improved Survival with an Implanted Defibrillator in Patients with Coronary Disease at High Risk for Ventricular Arrhythmia. New England Journal of Medicine 1996;335(26):1933–40. Doi: 10.1056/NEJM199612263352601.

3. Fernández Lozano I., Osca Asensi J., Alzueta Rodríguez J. Registro español de desfibrilador automático implantable. XIX informe oficial de la Asociación del Ritmo Cardiaco de la Sociedad Española de Cardiología (2022). Rev Esp Cardiol 2023;76(11):922–35. Doi: 10.1016/j.recesp.2023.06.018.

4. Echt DS., Liebson PR., Mitchell LB., et al. Mortality and Morbidity in Patients Receiving Encainide, Flecainide, or Placebo. New England Journal of Medicine 1991;324(12):781–8. Doi: 10.1056/NEJM199103213241201.

5. Hamilton D., Nandkeolyar S., Lan H., et al. Amiodarone: A Comprehensive Guide for Clinicians. American Journal of Cardiovascular Drugs 2020;20(6):549–58. Doi: 10.1007/s40256-020-00401-5.

6. Hii JT., Wyse DG., Gillis AM., Duff HJ., Solylo MA., Mitchell LB. Precordial QT interval dispersion as a marker of torsade de pointes. Disparate effects of class Ia antiarrhythmic drugs and amiodarone. Circulation 1992;86(5):1376–82. Doi: 10.1161/01.CIR.86.5.1376.

7. Sapp JL., Wells GA., Parkash R., et al. Ventricular Tachycardia Ablation versus Escalation of Antiarrhythmic Drugs. New England Journal of Medicine 2016;375(2):111–21. Doi: 10.1056/nejmoa1513614.

8. Arenal Á., Ávila P., Jiménez-Candil J., et al. Substrate Ablation vs Antiarrhythmic Drug Therapy for Symptomatic Ventricular Tachycardia. J Am Coll Cardiol 2022;79(15):1441–53. Doi: 10.1016/j.jacc.2022.01.050.

9. E WASSERMAN., J YULES. CARDIAC ANEURYSM WITH VENTRICULAR TACHYCARDIA: CASE REPORT AND BRIEF REVIEW OF THE LITERATURE. Ann Intern Med 1953;39(4):948. Doi: 10.7326/0003-4819-39-4-948.

10. COUCH OA. Cardiac Aneurysm with Ventricular Tachycardia and Subsequent Excision of Aneurysm. Circulation 1959;20(2):251–3. Doi: 10.1161/01.CIR.20.2.251.

11. Josephson ME., Harken AH., Horowitz LN. Endocardial excision: a new surgical technique for the treatment of recurrent ventricular tachycardia. Circulation 1979;60(7):1430–9. Doi: 10.1161/01.CIR.60.7.1430.

12. Calkins H., Sousa J., El-Atassi R., et al. Diagnosis and Cure of the Wolff–Parkinson–White Syndrome or Paroxysmal Supraventricular Tachycardias during a Single Electrophysiologic Test. New England Journal of Medicine 1991;324(23):1612–8. Doi: 10.1056/NEJM199106063242302.

13. Jackman WM., Wang X., Friday KJ., et al. Catheter Ablation of Accessory Atrioventricular Pathways (Wolff–Parkinson–White Syndrome) by Radiofrequency Current. New England Journal of Medicine 1991;324(23):1605–11. Doi: 10.1056/NEJM199106063242301.

14. Morady F., Harvey M., Kalbfleisch SJ., el-Atassi R., Calkins H., Langberg JJ. Radiofrequency catheter ablation of ventricular tachycardia in patients with coronary artery disease. Circulation 1993;87(2):363–72. Doi: 10.1161/01.CIR.87.2.363.

15. WELLENS HJ., SCHUILENBURG RM., DURRER D. Electrical Stimulation of the Heart in Patients with Ventricular Tachycardia. Circulation 1972;46(2):216–26. Doi: 10.1161/01.CIR.46.2.216.

16. Spurrell RA., Sowton E., Deuchar DC. Ventricular tachycardia in 4 patients evaluated by programmed electrical stimulation of heart and treated in 2 patients by surgical division of anterior radiation of left bundle-branch. Heart 1973;35(10):1014–25. Doi: 10.1136/hrt.35.10.1014.

17. WELLENS HJJ., LIE KI., DURRER D. Further Observations on Ventricular Tachycardia As Studied by Electrical Stimulation of the Heart. Circulation 1974;49(4):647–53. Doi: 10.1161/01.CIR.49.4.647.

18. DURRER D., SCHOO L., SCHUILENBURG RM., WELLENS HJJ. The Role of Premature Beats in the Initiation and the Termination of Supraventricular Tachycardia in the Wolff-Parkinson-White Syndrome. Circulation 1967;36(5):644–62. Doi: 10.1161/01.CIR.36.5.644.

19. SASYNIUK BI., MENDEZ C. A Mechanism for Reentry in Canine Ventricular Tissue. Circ Res 1971;28(1):3–15. Doi: 10.1161/01.RES.28.1.3.

20. Cox JL., Daniel TM., Sabiston DC., Boineau JP. Desynchronized activation in myocardial infarction a re-entry basis for ventricular arrhythmias. Circulation 1969;Suppl. 3,63.:39-t.

21. El-Sherif N., Scherlag BJ., Lazzara R., Hope RR. Re-entrant ventricular arrhythmias in the late myocardial infarction period. 1. Conduction characteristics in the infarction zone. Circulation 1977;55(5):686–702. Doi: 10.1161/01.CIR.55.5.686.

22. Josephson ME., Horowitz LN., Farshidi A. Continuous local electrical activity. A mechanism of recurrent ventricular tachycardia. Circulation 1978;57(4):659–65. Doi: 10.1161/01.CIR.57.4.659.

23. Josephson ME., Horowitz LN., Farshidi A., Spielman SR., Michelson EL., Greenspan AM. Sustained ventricular tachycardia: Evidence for protected localized reentry. Am J Cardiol 1978;42(3):416–24. Doi: 10.1016/0002-9149(78)90936-0.

24. Dillon SM., Allessie MA., Ursell PC., Wit AL. Influences of anisotropic tissue structure on reentrant circuits in the epicardial border zone of subacute canine infarcts. Circ Res 1988;63(1):182–206. Doi: 10.1161/01.RES.63.1.182.

25. Peters NS., Coromilas J., Severs NJ., Wit AL. Disturbed Connexin43 Gap Junction Distribution Correlates With the Location of Reentrant Circuits in the Epicardial Border Zone of Healing Canine Infarcts That Cause Ventricular Tachycardia. Circulation 1997;95(4):988–96. Doi: 10.1161/01.CIR.95.4.988.

26. Costeas C., Peters NS., Waldecker B., Ciaccio EJ., Wit AL., Coromilas J. Mechanisms Causing Sustained Ventricular Tachycardia With Multiple QRS Morphologies. Circulation 1997;96(10):3721–31. Doi: 10.1161/01.CIR.96.10.3721.

27. de Bakker JM., van Capelle FJ., Janse MJ., et al. Reentry as a cause of ventricular tachycardia in patients with chronic ischemic heart disease: electrophysiologic and anatomic correlation. Circulation 1988;77(3):589–606. Doi: 10.1161/01.CIR.77.3.589.

28. de Bakker JM., van Capelle FJ., Janse MJ., et al. Slow conduction in the infarcted human heart. “Zigzag” course of activation. Circulation 1993;88(3):915–26. Doi: 10.1161/01.CIR.88.3.915.

29. Ajijola OA., Tung R., Shivkumar K. Ventricular tachycardia in ischemic heart disease substrates. Indian Heart J 2014;66:S24–34. Doi: 10.1016/j.ihj.2013.12.039.

30. Stevenson WG., Khan H., Sager P., et al. Identification of reentry circuit sites during catheter mapping and radiofrequency ablation of ventricular tachycardia late after myocardial infarction. Circulation 1993;88(4):1647–70. Doi: 10.1161/01.CIR.88.4.1647.

31. Delasnerie H., Biendel C., Elbaz M., et al. Hemodynamical consequences and tolerance of sustained ventricular tachycardia. PLoS One 2023;18(5):e0285802. Doi: 10.1371/journal.pone.0285802.

32. Josephson ME., Waxman HL., Cain ME., Gardner MJ., Buxton AE. Ventricular activation during ventricular endocardial pacing. II. Role of pace-mapping to localize origin of ventricular tachycardia. Am J Cardiol 1982;50(1):11–22. Doi: 10.1016/0002-9149(82)90003-0.

33. Sacher F., Tedrow UB., Field ME., et al. Ventricular Tachycardia Ablation. Circ Arrhythm Electrophysiol 2008;1(3):153–61. Doi: 10.1161/CIRCEP.108.769471.

34. Cassidy DM., Vassallo JA., Marchlinski FE., Buxton AE., Untereker WJ., Josephson ME. Endocardial mapping in humans in sinus rhythm with normal left ventricles: activation patterns and characteristics of electrograms. vol. 70. 1984.

35. Cassidy DM., Vassallo JA., Buxton AE., Doherty JU., Marchlinski FE., Josephson ME. The value of catheter mapping during sinus rhythm to localize site of origin of ventricular tachycardia. 1984.

36. Gepstein L., Hayam G., Ben-Haim SA. A Novel Method for Nonfluoroscopic Catheter-Based Electroanatomical Mapping of the Heart. Circulation 1997;95(6):1611–22. Doi: 10.1161/01.CIR.95.6.1611.

37. Shpun S., Gepstein L., Hayam G., Ben-Haim SA. Guidance of Radiofrequency Endocardial Ablation With Real-time Three-dimensional Magnetic Navigation System. Circulation 1997;96(6):2016–21. Doi: 10.1161/01.CIR.96.6.2016.

38. Tung R., Nakahara S., Ramirez R., et al. Accuracy of combined endocardial and epicardial electroanatomic mapping of a reperfused porcine infarct model: A comparison of electrofield and magnetic systems with histopathologic correlation. Heart Rhythm 2011;8(3):439–47. Doi: 10.1016/j.hrthm.2010.10.044.

39. Reddy VY., Wrobleski D., Houghtaling C., Josephson ME., Ruskin JN. Combined Epicardial and Endocardial Electroanatomic Mapping in a Porcine Model of Healed Myocardial Infarction. Circulation 2003;107(25):3236–42. Doi: 10.1161/01.CIR.0000074280.62478.E1.

40. Callans DJ., Ren J-F., Michele J., Marchlinski FE., Dillon SM. Electroanatomic Left Ventricular Mapping in the Porcine Model of Healed Anterior Myocardial Infarction. Circulation 1999;100(16):1744–50. Doi: 10.1161/01.CIR.100.16.1744.

41. Arenal A., Glez-Torrecilla E., Ortiz M., et al. Ablation of electrograms with an isolated, delayed component as treatment of unmappable monomorphic ventricular tachycardias in patients with structural heart disease. J Am Coll Cardiol 2003;41(1):81–92. Doi: 10.1016/S0735-1097(02)02623-2.

42. Jaïs P., Maury P., Khairy P., et al. Elimination of Local Abnormal Ventricular Activities. Circulation 2012;125(18):2184–96. Doi: 10.1161/CIRCULATIONAHA.111.043216.

43. Arenal A., del Castillo S., Gonzalez-Torrecilla E., et al. Tachycardia-Related Channel in the Scar Tissue in Patients With Sustained Monomorphic Ventricular Tachycardias. Circulation 2004;110(17):2568–74. Doi: 10.1161/01.CIR.0000145544.35565.47.

44. Tzou WS., Frankel DS., Hegeman T., et al. Core Isolation of Critical Arrhythmia Elements for Treatment of Multiple Scar-Based Ventricular Tachycardias. Circ Arrhythm Electrophysiol 2015;8(2):353–61. Doi: 10.1161/CIRCEP.114.002310.

45. Di Biase L., Santangeli P., Burkhardt DJ., et al. Endo-epicardial homogenization of the scar versus limited substrate ablation for the treatment of electrical storms in patients with ischemic cardiomyopathy. J Am Coll Cardiol 2012;60(2):132–41. Doi: 10.1016/j.jacc.2012.03.044.

46. Di Biase L., Burkhardt JD., Lakkireddy D., et al. Ablation of Stable VTs Versus Substrate Ablation in Ischemic Cardiomyopathy. J Am Coll Cardiol 2015;66(25):2872–82. Doi: 10.1016/j.jacc.2015.10.026.

47. Sánchez Muñoz JJ., Peñafiel Verdú P., Martínez Sánchez J., Salar Alcaraz M., Valdés Chavarri M., García Alberola A. Usefulness of the Contact Force Sensing Catheter to Assess the Areas of Myocardial Scar in Patients With Ventricular Tachycardia. Revista Española de Cardiología (English Edition) 2015;68(2):159–60. Doi: 10.1016/j.rec.2014.09.011.

48. Takigawa M., Relan J., Martin R., et al. Effect of bipolar electrode orientation on local electrogram properties. Heart Rhythm 2018;15(12):1853–61. Doi: 10.1016/j.hrthm.2018.07.020.

49. Anter E., Josephson ME. Bipolar voltage amplitude: What does it really mean? Heart Rhythm 2016;13(1):326–7. Doi: 10.1016/j.hrthm.2015.09.033.

50. Acosta J., Penela D., Andreu D., et al. Multielectrode vs. point-by-point mapping for ventricular tachycardia substrate ablation: a randomized study. EP Europace 2018;20(3):512–9. Doi: 10.1093/europace/euw406.

51. Tschabrunn CM., Roujol S., Dorman NC., Nezafat R., Josephson ME., Anter E. High-Resolution Mapping of Ventricular Scar. Circ Arrhythm Electrophysiol 2016;9(6). Doi: 10.1161/CIRCEP.115.003841.

52. Leshem E., Tschabrunn CM., Jang J., et al. High-Resolution Mapping of Ventricular Scar. JACC Clin Electrophysiol 2017;3(3):220–31. Doi: 10.1016/j.jacep.2016.12.016.

53. Okubo K., Frontera A., Bisceglia C., et al. Grid Mapping Catheter for Ventricular Tachycardia Ablation. Circ Arrhythm Electrophysiol 2019;12(9). Doi: 10.1161/CIRCEP.119.007500.

54. Papageorgiou N., Karim N., Williams J., et al. Initial experience of the High-Density Grid catheter in patients undergoing catheter ablation for atrial fibrillation. Journal of Interventional Cardiac Electrophysiology 2022;63(2):259–66. Doi: 10.1007/s10840-021-00950-y.

55. Porta-Sánchez A., Magtibay K., Nayyar S., et al. Omnipolarity applied to equi-spaced electrode array for ventricular tachycardia substrate mapping. EP Europace 2019;21(5):813–21. Doi: 10.1093/europace/euy304.

56. Proietti R., Adlan AM., Dowd R., et al. Enhanced ventricular tachycardia substrate resolution with a novel omnipolar high-density mapping catheter: the omnimapping study. Journal of Interventional Cardiac Electrophysiology 2020;58(3):355–62. Doi: 10.1007/s10840-019-00625-9.

57. Jiang R., Beaser AD., Aziz Z., Upadhyay GA., Nayak HM., Tung R. High-Density Grid Catheter for Detailed Mapping of Sinus Rhythm and Scar-Related Ventricular Tachycardia. JACC Clin Electrophysiol 2020;6(3):311–23. Doi: 10.1016/j.jacep.2019.11.007.

58. Proietti R., Dowd R., Gee LV., et al. Impact of a high-density grid catheter on long-term outcomes for structural heart disease ventricular tachycardia ablation. Journal of Interventional Cardiac Electrophysiology 2021;62(3):519–29. Doi: 10.1007/s10840-020-00918-4.

59. Roca-Luque I., Zaraket F., Garre P., et al. Accuracy of standard bipolar amplitude voltage thresholds to identify late potential channels in ventricular tachycardia ablation. Journal of Interventional Cardiac Electrophysiology 2022. Doi: 10.1007/s10840-022-01148-6.

60. Mountantonakis SE., Park RE., Frankel DS., et al. Relationship Between Voltage Map "Channels" and the Location of Critical Isthmus Sites in Patients With Post-Infarction Cardiomyopathy and Ventricular Tachycardia. J Am Coll Cardiol 2013;61(20):2088–95. Doi: 10.1016/j.jacc.2013.02.031.

61. Glashan CA., Androulakis AFA., Tao Q., et al. Whole human heart histology to validate electroanatomical voltage mapping in patients with non-ischaemic cardiomyopathy and ventricular tachycardia. Eur Heart J 2018;39(31):2867–75. Doi: 10.1093/eurheartj/ehy168.

62. Arenal A., del Castillo S., Gonzalez-Torrecilla E., et al. Tachycardia-Related Channel in the Scar Tissue in Patients With Sustained Monomorphic Ventricular Tachycardias. Circulation 2004;110(17):2568–74. Doi: 10.1161/01.CIR.0000145544.35565.47.

63. Hsia HH., Lin D., Sauer WH., Callans DJ., Marchlinski FE. Anatomic characterization of endocardial substrate for hemodynamically stable reentrant ventricular tachycardia: Identification of endocardial conducting channels. Heart Rhythm 2006;3(5):503–12. Doi: 10.1016/j.hrthm.2006.01.015.

64. Lammers WJ., Kirchhof C., Bonke FI., Allessie MA. Vulnerability of rabbit atrium to reentry by hypoxia. Role of inhomogeneity in conduction and wavelength. American Journal of Physiology-Heart and Circulatory Physiology 1992;262(1):H47–55. Doi: 10.1152/ajpheart.1992.262.1.H47.

65. Segal OR., Chow AWC., Peters NS., Davies DW. Mechanisms that initiate ventricular tachycardia in the infarcted human heart. Heart Rhythm 2010;7(1):57–64. Doi: 10.1016/j.hrthm.2009.09.025.

66. Roelke M., Garan H., McGovern BA., Ruskin JN. Analysis of the initiation of spontaneous monomorphic ventricular tachycardia by stored intracardiac electrograms. J Am Coll Cardiol 1994;23(1):117–22. Doi: 10.1016/0735-1097(94)90509-6.

67. Saeed M., Link MS., Mahapatra S., et al. Analysis of intracardiac electrograms showing monomorphic ventricular tachycardia in patients with implantable cardioverter-defibrillators. Am J Cardiol 2000;85(5):580–7. Doi: 10.1016/S0002-9149(99)00815-2.

68. Jackson N., Gizurarson S., Viswanathan K., et al. Decrement Evoked Potential Mapping: Basis of a Mechanistic Strategy for Ventricular Tachycardia Ablation. Circ Arrhythm Electrophysiol 2015;8(6):1433–42. Doi: 10.1161/CIRCEP.115.003083.

69. Porta-Sánchez A., Jackson N., Lukac P., et al. Multicenter Study of Ischemic Ventricular Tachycardia Ablation With Decrement-Evoked Potential (DEEP) Mapping With Extra Stimulus. JACC Clin Electrophysiol 2018;4(3):307–15. Doi: 10.1016/j.jacep.2017.12.005.

70. Acosta J., Andreu D., Penela D., et al. Elucidation of hidden slow conduction by double ventricular extrastimuli: A method for further arrhythmic substrate identification in ventricular tachycardia ablation procedures. Europace 2018;20(2):337–46. Doi: 10.1093/europace/euw325.

71. de Riva M., Naruse Y., Ebert M., et al. Targeting the Hidden Substrate Unmasked by Right Ventricular Extrastimulation Improves Ventricular Tachycardia Ablation Outcome After Myocardial Infarction. JACC Clin Electrophysiol 2018;4(3):316–27. Doi: 10.1016/j.jacep.2018.01.013.

72. Srinivasan NT., Garcia J., Schilling RJ., et al. Multicenter Study of Dynamic High-Density Functional Substrate Mapping Improves Identification of Substrate Targets for Ischemic Ventricular Tachycardia Ablation. JACC Clin Electrophysiol 2020;6(14):1783–93. Doi: 10.1016/j.jacep.2020.06.037.

73. Irie T., Yu R., Bradfield JS., et al. Relationship between sinus rhythm late activation zones and critical sites for scar-related ventricular tachycardia. Circ Arrhythm Electrophysiol 2015;8(2):390–9. Doi: 10.1161/CIRCEP.114.002637.

74. Aziz Z., Shatz D., Raiman M., et al. Targeted Ablation of Ventricular Tachycardia Guided by Wavefront Discontinuities during Sinus Rhythm: A New Functional Substrate Mapping Strategy. Circulation 2019;140(17):1383–97. Doi: 10.1161/CIRCULATIONAHA.119.042423.

75. Peshock RM., Malloy CR., Buja LM., Nunnally RL., Parkey RW., Willerson JT. Magnetic resonance imaging of acute myocardial infarction: gadolinium diethylenetriamine pentaacetic acid as a marker of reperfusion. Circulation 1986;74(6):1434–40. Doi: 10.1161/01.CIR.74.6.1434.

76. Rehr RB., Peshock RM., Malloy CR., et al. Improved in vivo magnetic resonance imaging of acute myocardial infarction after intravenous paramagnetic contrast agent administration. Am J Cardiol 1986;57(10):864–8. Doi: 10.1016/0002-9149(86)90628-4.

77. Mewton N., Liu CY., Croisille P., Bluemke D., Lima JAC. Assessment of Myocardial Fibrosis With Cardiovascular Magnetic Resonance. J Am Coll Cardiol 2011;57(8):891–903. Doi: 10.1016/j.jacc.2010.11.013.

78. Kim RJ., Fieno DS., Parrish TB., et al. Relationship of MRI delayed contrast enhancement to irreversible injury, infarct age, and contractile function. Circulation 1999;100(19):1992–2002. Doi: 10.1161/01.cir.100.19.1992.

79. Lima JAC., Judd RM., Bazille A., Schulman SP., Atalar E., Zerhouni EA. Regional Heterogeneity of Human Myocardial Infarcts Demonstrated by Contrast-Enhanced MRI. Circulation 1995;92(5):1117–25. Doi: 10.1161/01.CIR.92.5.1117.

80. McCrohon JA., Moon JCC., Prasad SK., et al. Differentiation of Heart Failure Related to Dilated Cardiomyopathy and Coronary Artery Disease Using Gadolinium-Enhanced Cardiovascular Magnetic Resonance. Circulation 2003;108(1):54–9. Doi: 10.1161/01.CIR.0000078641.19365.4C.

81. Mahrholdt H., Wagner A., Judd RM., Sechtem U., Kim RJ. Delayed enhancement cardiovascular magnetic resonance assessment of non-ischaemic cardiomyopathies. Eur Heart J 2005;26(15):1461–74. Doi: 10.1093/eurheartj/ehi258.

82. Tandri H., Friedrich M., Calkins H., Bluemke D. MRI of Arrhythmogenic Right Ventricular Cardiomyopathy/Dysplasia. Journal of Cardiovascular Magnetic Resonance 2004;6(2):557–63. Doi: 10.1081/JCMR-120030583.

83. Patel MR., Cawley PJ., Heitner JF., et al. Detection of Myocardial Damage in Patients With Sarcoidosis. Circulation 2009;120(20):1969–77. Doi: 10.1161/CIRCULATIONAHA.109.851352.

84. De Cobelli F., Pieroni M., Esposito A., et al. Delayed Gadolinium-Enhanced Cardiac Magnetic Resonance in Patients With Chronic Myocarditis Presenting With Heart Failure or Recurrent Arrhythmias. J Am Coll Cardiol 2006;47(8):1649–54. Doi: 10.1016/j.jacc.2005.11.067.

85. Holmström M., Kivistö S., Heliö T., et al. Late gadolinium enhanced cardiovascular magnetic resonance of lamin A/C gene mutation related dilated cardiomyopathy. Journal of Cardiovascular Magnetic Resonance 2011;13(1):30. Doi: 10.1186/1532-429X-13-30.

86. Arbelo E., Protonotarios A., Gimeno JR., et al. 2023 ESC Guidelines for the management of cardiomyopathies. Eur Heart J 2023;44(37):3503–626. Doi: 10.1093/eurheartj/ehad194.

87. Andreu D., Berruezo A., Ortiz-Pérez JT., et al. Integration of 3D Electroanatomic Maps and Magnetic Resonance Scar Characterization Into the Navigation System to Guide Ventricular Tachycardia Ablation. Circ Arrhythm Electrophysiol 2011;4(5):674–83. Doi: 10.1161/CIRCEP.111.961946.

88. Ashikaga H., Sasano T., Dong J., et al. Magnetic Resonance–Based Anatomical Analysis of Scar-Related Ventricular Tachycardia. Circ Res 2007;101(9):939–47. Doi: 10.1161/CIRCRESAHA.107.158980.

89. Piers SRD., Tao Q., De Riva Silva M., et al. CMR-based identification of critical isthmus sites of ischemic and nonischemic ventricular tachycardia. JACC Cardiovasc Imaging 2014;7(8):774–84. Doi: 10.1016/j.jcmg.2014.03.013.

90. Desjardins B., Crawford T., Good E., et al. Infarct architecture and characteristics on delayed enhanced magnetic resonance imaging and electroanatomic mapping in patients with postinfarction ventricular arrhythmia. Heart Rhythm 2009;6(5):644–51. Doi: 10.1016/j.hrthm.2009.02.018.

91. Andreu D., Ortiz-Pérez JT., Boussy T., et al. Usefulness of contrast-enhanced cardiac magnetic resonance in identifying the ventricular arrhythmia substrate and the approach needed for ablation. Eur Heart J 2014;35(20):1316–26. Doi: 10.1093/eurheartj/eht510.

92. Andreu D., Ortiz-Pérez JT., Fernández-Armenta J., et al. 3D delayed-enhanced magnetic resonance sequences improve conducting channel delineation prior to ventricular tachycardia ablation. Europace 2015;17(6):938–45. Doi: 10.1093/europace/euu310.

93. Perez-David E., Arenal Á., Rubio-Guivernau JL., et al. Noninvasive Identification of Ventricular Tachycardia-Related Conducting Channels Using Contrast-Enhanced Magnetic Resonance Imaging in Patients With Chronic Myocardial Infarction. J Am Coll Cardiol 2011;57(2):184–94. Doi: 10.1016/j.jacc.2010.07.043.

94. Andreu D., Penela D., Acosta J., et al. Cardiac magnetic resonance–aided scar dechanneling: Influence on acute and long-term outcomes. Heart Rhythm 2017;14(8):1121–8. Doi: 10.1016/j.hrthm.2017.05.018.

95. Berruezo A., Fernández-Armenta J., Andreu D., et al. Scar dechanneling. Circ Arrhythm Electrophysiol 2015;8(2):326–36. Doi: 10.1161/CIRCEP.114.002386.

96. Soto-Iglesias D., Penela D., Jáuregui B., et al. Cardiac Magnetic Resonance-Guided Ventricular Tachycardia Substrate Ablation. JACC Clin Electrophysiol 2020;6(4):436–47. Doi: 10.1016/j.jacep.2019.11.004.

97. Martin ET., Coman JA., Shellock FG., Pulling CC., Fair R., Jenkins K. Magnetic resonance imaging and cardiac pacemaker safety at 1.5-Tesla. J Am Coll Cardiol 2004;43(7):1315–24. Doi: 10.1016/j.jacc.2003.12.016.

98. Nazarian S., Hansford R., Rahsepar AA., et al. Safety of Magnetic Resonance Imaging in Patients with Cardiac Devices. New England Journal of Medicine 2017;377(26):2555–64. Doi: 10.1056/NEJMoa1604267.

99. Schaller RD., Brunker T., Riley MP., Marchlinski FE., Nazarian S., Litt H. Magnetic Resonance Imaging in Patients With Cardiac Implantable Electronic Devices With Abandoned Leads. JAMA Cardiol 2021;6(5):549. Doi: 10.1001/jamacardio.2020.7572.

100. Dickfeld T., Tian J., Ahmad G., et al. MRI-Guided Ventricular Tachycardia Ablation. Circ Arrhythm Electrophysiol 2011;4(2):172–84. Doi: 10.1161/CIRCEP.110.958744.

101. Sasaki T., Hansford R., Zviman MM., et al. Quantitative Assessment of Artifacts on Cardiac Magnetic Resonance Imaging of Patients With Pacemakers and Implantable Cardioverter-Defibrillators. Circ Cardiovasc Imaging 2011;4(6):662–70. Doi: 10.1161/CIRCIMAGING.111.965764.

102. Rashid S., Rapacchi S., Vaseghi M., et al. Improved Late Gadolinium Enhancement MR Imaging for Patients with Implanted Cardiac Devices. Radiology 2014;270(1):269–74. Doi: 10.1148/radiol.13130942.

103. Stevens SM., Tung R., Rashid S., et al. Device artifact reduction for magnetic resonance imaging of patients with implantable cardioverter-defibrillators and ventricular tachycardia: Late gadolinium enhancement correlation with electroanatomic mapping. Heart Rhythm 2014;11(2):289–98. Doi: 10.1016/j.hrthm.2013.10.032.

104. Roca-Luque I., Van Breukelen A., Alarcon F., et al. Ventricular scar channel entrances identified by new wideband cardiac magnetic resonance sequence to guide ventricular tachycardia ablation in patients with cardiac defibrillators. EP Europace 2020;22(4):598–606. Doi: 10.1093/europace/euaa021.

105. Sanchez-Somonte P., Garre P., Vázquez-Calvo S., et al. Scar conducting channel characterization to predict arrhythmogenicity during ventricular tachycardia ablation. EP Europace 2023. Doi: 10.1093/europace/euac257.

106. de Riva M., Piers SRD., Kapel GFL., et al. Reassessing Noninducibility as Ablation Endpoint of Post-Infarction Ventricular Tachycardia. Circ Arrhythm Electrophysiol 2015;8(4):853–62. Doi: 10.1161/CIRCEP.114.002702.

107. Quinto L., Sanchez P., Alarcón F., et al. Cardiac magnetic resonance to predict recurrences after ventricular tachycardia ablation: septal involvement, transmural channels, and left ventricular mass. EP Europace 2021;23(9):1437–45. Doi: 10.1093/europace/euab127.

108. Oloriz T., Silberbauer J., Maccabelli G., et al. Catheter Ablation of Ventricular Arrhythmia in Nonischemic Cardiomyopathy. Circ Arrhythm Electrophysiol 2014;7(3):414–23. Doi: 10.1161/CIRCEP.114.001568.

109. Glashan CA., Stevenson W., Zeppenfeld K. Lesion Size and Lesion Maturation after Radiofrequency Catheter Ablation for Ventricular Tachycardia in Humans with Nonischemic Cardiomyopathy. Circ Arrhythm Electrophysiol 2021:E009808. Doi: 10.1161/CIRCEP.121.009808.

110. Tofig BJ., Lukac P., Nielsen JM., et al. Radiofrequency ablation lesions in low-, intermediate-, and normal-voltage myocardium: An in vivo study in a porcine heart model. Europace 2019;21(12):1919–27. Doi: 10.1093/europace/euz247.

111. Proietti R., Lichelli L., Lellouche N., Dhanjal T. The challenge of optimising ablation lesions in catheter ablation of ventricular tachycardia. J Arrhythm 2021:140–7. Doi: 10.1002/joa3.12489.

112. Sivagangabalan G., Barry MA., Huang K., et al. Bipolar ablation of the interventricular septum is more efficient at creating a transmural line than sequential unipolar ablation. PACE - Pacing and Clinical Electrophysiology 2010;33(1):16–26. Doi: 10.1111/j.1540-8159.2009.02602.x.

113. Bennett R., Campbell T., Byth K., Turnbull S., Kumar S. Catheter Ablation Using Half-Normal Saline and Dextrose Irrigation in an Ovine Ventricular Model. JACC Clin Electrophysiol 2021;7(10):1229–39. Doi: 10.1016/j.jacep.2021.05.002.

114. Schmidt B., Chun KRJ., Baensch D., et al. Catheter ablation for ventricular tachycardia after failed endocardial ablation: Epicardial substrate or inappropriate endocardial ablation? Heart Rhythm 2010;7(12):1746–52. Doi: 10.1016/j.hrthm.2010.08.010.

115. Roderick Tung MD., Kalyanam Shivkumar MD, PhD. Indications for Epicardial Mapping and Ablation. 2015.

116. Berruezo A., Mont L., Nava S., Chueca E., Bartholomay E., Brugada J. Electrocardiographic Recognition of the Epicardial Origin of Ventricular Tachycardias. Circulation 2004;109(15):1842–7. Doi: 10.1161/01.CIR.0000125525.04081.4B.

117. Mahrholdt H., Wagner A., Judd RM., Sechtem U., Kim RJ. Delayed enhancement cardiovascular magnetic resonance assessment of non-ischaemic cardiomyopathies. Eur Heart J 2005:1461–74. Doi: 10.1093/eurheartj/ehi258.

118. Dinov B., Fiedler L., Schönbauer R., et al. Outcomes in catheter ablation of ventricular tachycardia in dilated nonischemic cardiomyopathy compared with ischemic cardiomyopathy: Results from the prospective heart centre of leipzig vt. Circulation 2014;129(7):728–36. Doi: 10.1161/CIRCULATIONAHA.113.003063.

119. Acosta J., Fernández-Armenta J., Penela D., et al. Infarct transmurality as a criterion for first-line endo-epicardial substrate-guided ventricular tachycardia ablation in ischemic cardiomyopathy. Heart Rhythm 2016;13(1):85–95. Doi: 10.1016/j.hrthm.2015.07.010.

120. Sacher F., Roberts-Thomson K., Maury P., et al. Epicardial Ventricular Tachycardia Ablation. A Multicenter Safety Study. J Am Coll Cardiol 2010;55(21):2366–72. Doi: 10.1016/j.jacc.2009.10.084.

121. BERTE B., SACHER F., VENLET J., et al. VT Recurrence After Ablation: Incomplete Ablation or Disease Progression? A Multicentric European Study. J Cardiovasc Electrophysiol 2016;27(1):80–7. Doi: 10.1111/jce.12858.

122. Ghafoori E., Kholmovski EG., Thomas S., et al. Characterization of Gadolinium Contrast Enhancement of Radiofrequency Ablation Lesions in Predicting Edema and Chronic Lesion Size. Circ Arrhythm Electrophysiol 2017;10(11). Doi: 10.1161/CIRCEP.117.005599.

123. Celik H., Ramanan V., Barry J., et al. Intrinsic Contrast for Characterization of Acute Radiofrequency Ablation Lesions. Circ Arrhythm Electrophysiol 2014;7(4):718–27. Doi: 10.1161/CIRCEP.113.001163.

124. Dabbagh GS., Ghannam M., Siontis KC., et al. Magnetic Resonance Mapping of Catheter Ablation Lesions After Post-Infarction Ventricular Tachycardia Ablation. JACC Cardiovasc Imaging 2021;14(3):588–98. Doi: 10.1016/j.jcmg.2020.08.041.

125. Disertori M., Rigoni M., Pace N., et al. Myocardial Fibrosis Assessment by LGE Is a Powerful Predictor of Ventricular Tachyarrhythmias in Ischemic and Nonischemic LV Dysfunction. JACC Cardiovasc Imaging 2016;9(9):1046–55. Doi: 10.1016/j.jcmg.2016.01.033.

126. Acosta J., Fernández-Armenta J., Borràs R., et al. Scar Characterization to Predict Life-Threatening Arrhythmic Events and Sudden Cardiac Death in Patients With Cardiac Resynchronization Therapy. JACC Cardiovasc Imaging 2018;11(4):561–72. Doi: 10.1016/j.jcmg.2017.04.021.

127. Sánchez-Somonte P., Quinto L., Garre P., et al. Scar channels in cardiac magnetic resonance to predict appropriate therapies in primary prevention. Heart Rhythm 2021;18(8):1336–43. Doi: 10.1016/j.hrthm.2021.04.017.

128. Massé S., Magtibay K., Jackson N., et al. Resolving Myocardial Activation With Novel Omnipolar Electrograms. Circ Arrhythm Electrophysiol 2016;9(7). Doi: 10.1161/CIRCEP.116.004107.

129. Deno DC., Balachandran R., Morgan D., Ahmad F., Masse S., Nanthakumar K. Orientation-Independent Catheter-Based Characterization of Myocardial Activation. IEEE Trans Biomed Eng 2017;64(5):1067–77. Doi: 10.1109/TBME.2016.2589158.

130. Liang JJ., Tschabrunn CM., Marchlinski FE. Omnipolar Mapping. Circ Arrhythm Electrophysiol 2017;10(9). Doi: 10.1161/CIRCEP.117.005700.

131. Ascione C., Kowalewski C., Bergonti M., et al. Omnipolar versus bipolar mapping to guide ventricular tachycardia ablation. Heart Rhythm 2023;20(10):1370–7. Doi: 10.1016/j.hrthm.2023.06.022.

132. Deno DC., Bhaskaran A., Morgan DJ., et al. High-resolution, live, directional mapping. Heart Rhythm 2020;17(9):1621–8. Doi: 10.1016/j.hrthm.2020.04.039.

133. Tung R., Vaseghi M., Frankel DS., et al. Freedom from recurrent ventricular tachycardia after catheter ablation is associated with improved survival in patients with structural heart disease: An International VT Ablation Center Collaborative Group study. Heart Rhythm 2015;12(9):1997–2007. Doi: 10.1016/j.hrthm.2015.05.036.

134. Reddy VY., Reynolds MR., Neuzil P., et al. Prophylactic Catheter Ablation for the Prevention of Defibrillator Therapy. New England Journal of Medicine 2007;357(26):2657–65. Doi: 10.1056/NEJMoa065457.

135. Kuck KH., Schaumann A., Eckardt L., et al. Catheter ablation of stable ventricular tachycardia before defibrillator implantation in patients with coronary heart disease (VTACH): a multicentre

randomised controlled trial. The Lancet 2010;375(9708):31–40. Doi: 10.1016/S0140-6736(09)61755-4.

136. Kuck KH., Tilz RR., Deneke T., et al. Impact of substrate modification by catheter ablation on implantable cardioverter-defibrillator interventions in patients with unstable ventricular arrhythmias and coronary artery disease: Results from the multicenter randomized controlled SMS (Substrate Modification Study). Circ Arrhythm Electrophysiol 2017;10(3). Doi: 10.1161/CIRCEP.116.004422.

137. Della Bella P., Baratto F., Vergara P., et al. Does Timing of Ventricular Tachycardia Ablation Affect Prognosis in Patients With an Implantable Cardioverter Defibrillator? Results From the Multicenter Randomized PARTITA Trial. Circulation 2022;145(25):1829–38. Doi: 10.1161/CIRCULATIONAHA.122.059598.

138. Quinto L., Sanchez-Somonte P., Alarcón F., et al. Ventricular tachycardia burden reduction after substrate ablation: Predictors of recurrence. Heart Rhythm 2021;18(6):896–904. Doi: 10.1016/j.hrthm.2021.02.016.

139. Ghanbari H., Baser K., Yokokawa M., et al. Noninducibility in Postinfarction Ventricular Tachycardia as an End Point for Ventricular Tachycardia Ablation and Its Effects on Outcomes. Circ Arrhythm Electrophysiol 2014;7(4):677–83. Doi: 10.1161/CIRCEP.113.001404.

140. Silberbauer J., Oloriz T., Maccabelli G., et al. Noninducibility and Late Potential Abolition. Circ Arrhythm Electrophysiol 2014;7(3):424–35. Doi: 10.1161/CIRCEP.113.001239.

141. Frankel DS., Mountantonakis SE., Zado ES., et al. Noninvasive Programmed Ventricular Stimulation Early After Ventricular Tachycardia Ablation to Predict Risk of Late Recurrence. J Am Coll Cardiol 2012;59(17):1529–35. Doi: 10.1016/j.jacc.2012.01.026.